Aus dem Departement für Geowissenschaften - Geographie
Universität Freiburg (Schweiz)

Spatio-temporal variations of rockfall activity into forests - results from tree-ring and tree analysis

INAUGURAL - DISSERTATION

zur Erlangung der Würde eines *Doctor rerum naturalium* der Mathematisch - Naturwissenschaftlichen Fakultät der Universität Freiburg in der Schweiz

Markus STOFFEL

aus
Visperterminen (VS, Schweiz)

Dissertation Nr. 1480

Multiprint, Fribourg, 2005

Die vorliegende Arbeit wurde an der Mathematisch - Naturwissenschaftlichen Fakultät der Universität Freiburg, Schweiz, im Juni 2005 aufgrund der Gutachten von Prof. Michel Monbaron, Prof. Hans Kienholz, Prof. Horst Strunk und Dr. Hugo Raetzo angenommen.
Als Jurypräsident waltete Prof. Martin Beniston.

The Faculty of Science of the University of Fribourg, Switzerland, accepted the present work as dissertation in June 2005 based on the experts' reports of Prof. Michel Monbaron, Prof. Hans Kienholz, Prof. Horst Strunk and Dr. Hugo Raetzo.
President of the Jury: Prof. Martin Beniston

Fribourg, 27 June 2005

The PhD thesis' director:

Prof. Michel Monbaron

The Dean:

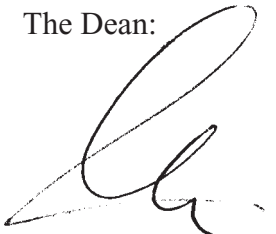

Prof. Marco Celio

Zitierung (Citation):
Stoffel M., 2005: Spatio-temporal variations of rockfall activity into forests – results from tree-ring and tree analysis. PhD thesis No. 1480, University of Fribourg. GeoFocus 12, 188 pp.

GeoFocus is the publication series of the Dept. of Geosciences, University of Fribourg, Switzerland, and can be ordered at

Department of Geosciences - Geology
University of Fribourg
1700 Fribourg

TABLE OF CONTENTS

TABLE OF CONTENTS 1
ZUSAMMENFASSUNG 5
ABSTRACT 7
ABBREVIATIONS 9
ACKNOWLEDGEMENTS 11

CHAPTER A: OVERALL INTRODUCTION

1 ROCKFALL

1.1 UNDERSTANDING THE PROCESS 17
1.1.1 What is rockfall - some definitions 17
1.1.2 Triggers of rockfall activity 18
1.1.3 Departure, transit and deposition zone of rockfall 19
1.1.4 Rocks and boulders 'traveling downslope' 20
1.2 ROCKFALL INTO FORESTS 21
1.2.1 Influence of forest stands on rockfall propagation 21
1.2.2 Reactions of trees to rockfall 22
1.2.3 Protection forests - dreams and reality 23
1.3 FREQUENCY AND VOLUMES OF PAST ROCKFALL ACTIVITY 24
1.4 MODELING ROCKFALL IN LABORATORY TESTS, ON SLOPES AND IN FORESTS 25
1.4.1 Empirical rockfall models 25
1.4.2 Process-based rockfall models 25
1.4.3 GIS-based rockfall models 26
1.4.4 Combined modeling approaches and the integration of trees 26
1.5 HAZARD ANALYSIS AND RISK ASSESSMENT IN ROCKFALL RESEARCH 27

2 DENDROGEOMORPHOLOGY

2.1 A GENERAL INTRODUCTION TO TREE-RING ANALYSIS IN THE FIELD OF GEOMORPHOLOGY 29
2.2 STUDIES DEALING WITH TREE RINGS AND PAST ROCKFALL ACTIVITY - A STATE OF THE ART 31

3 AIMS AND STRUCTURE OF THIS THESIS

4 STUDY SITES

4.1 INTRODUCTORY COMMENTS AND LOCALIZATION OF STUDY SITES 35
4.2 TÄSCHGUFER (TÄSCH, VS) 35
4.2.1 Geology 35
4.2.2 Topography 37
4.2.3 Temperature, precipitation and permafrost 37
4.2.4 Forest cover 38
4.2.5 Rockslides, large rockfalls and rockfall processes 38
4.2.6 Other processes 42
4.3 ALTDORFER BANNWALD (ALTDORF, UR) 42

CHAPTER B: ASSESSING PAST ROCKFALL ACTIVITY WITH TREE RINGS

1 THE SEASONAL TIMING OF ROCKFALL ACTIVITY

ABSTRACT 47
ZUSAMMENFASSUNG 48
RÉSUMÉ 48
1.1 INTRODUCTION 49
1.2 STUDY SITES 49
1.3 MATERIAL AND METHODS 51
1.3.1 Dendrochronological analysis of rockfall activity 51
1.3.2 Seasonal timing of rockfall 52
1.4 RESULTS 53
1.4.1 Rockfall activity and construction works 54
1.4.2 Natural rockfall activity 55

1.5 Discussion 57
1.6 Conclusion 58
Acknowledgements 58

2 Spatio-temporal fluctuations in rockfall activity (1600-2002)

Abstract 59
2.1 Introduction 60
2.2 Study area 60
2.3 Material and methods 63
2.3.1 Sampling strategy 63
2.3.2 Tree-ring analysis and rockfall 63
2.3.3 Spatial visualization of single tree data 65
2.4 Results 66
2.4.1 Age structure of the forest stand 66
2.4.2 Visible defects and growth reactions to rockfall impacts 67
2.4.3 Spatial distribution of growth disturbances 68
2.4.4 Rockfall magnitudes and frequencies 69
2.4.5 Decadal variations in rockfall activities 70
2.5 Discussion 74
2.6 Conclusion 76
Acknowledgements 76

Chapter C: Height distribution and the persistence of rockfall scars on stem surfaces

Summary 79
Zusammenfassung 79
Résumé 80
1.1 Introduction 80
1.2 Study site 80
1.3 Methods 81
1.4 Results 81
1.4.1 Tree data and rockfall scars 81
1.4.2 Vertical distribution of scars on stems 82
1.4.3 Visible and hidden scars 83
1.5 Discussion and conclusions 84
Acknowledgements 85

Chapter D: Some limitations of tree-ring analysis in rockfall research

Summary 89
1.1 Introduction 90
1.2 Material and methods 91
1.3 Results 92
1.3.1 Height distribution of scars on stems 92
1.3.2 Radial distribution of scars on stems 93
1.3.3 Visible injuries vs. overgrown scars 94
1.3.4 Scars at 'test height' vs. injuries to the entire tree 95
1.3.5 Growth disturbances at 'test height' vs. injuries to the entire tree 96
1.4 Overall discussion and conclusions 96
Acknowledgements 99

Chapter E: Overall conclusions

1.1 Summary of main results and overall conclusions 103
1.2 Outlook and further research needs 104
1.2.1 Traumatic rows of resin ducts: where do they occur? 104
1.2.2 Vertical distribution of scars on trees: Did we largely underestimate bounce heights so far? 105
1.2.3 Does seismic activity in Valais trigger rockfall(s) at Täschgufer? 105
1.2.4 Are there correlations between rockfall and climate at Täschgufer? 105

Chapter F: Appendices

1 A review of studies dealing with tree rings and rockfall activity

Abstract 109
1.1 Introduction 109
1.2 dendrogeomorphological applications and methods 110
1.3 Case studies focusing on tree rings and past rockfall activity 112
1.3.1 The beginnings 112
1.3.2 Later works 113
1.3.3 Studies on the spatial distribution of rockfall activity 115
1.3.4 Studies on the seasonal timing of rockfall activity 116
1.4 Discussion and conclusions 118
Acknowledgements 118

2 Spatial and temporal rockfall activity in a forest stand in the Swiss Prealps - a dendrogeomorphological case study

Abstract 119
2.1 Introduction 120
2.2 Material and methods 120
2.2.1 Study site and sampling 120

2.2.2 Recording past rockfall events — 121
2.2.3 Spatial and temporal data analysis — 122
2.3 Results — 123
2.3.1 Characteristics of trees and their rockfall injuries — 123
2.3.2 Spatial rockfall distribution — 124
2.3.3 Temporal rockfall activity — 124
2.4 Discussion — 127
2.5 Conclusions — 129
Acknowledgement — 130

3 Quantifying the protective effect of mountain forests using a 3D simulation model

Abstract — 131
3.1 Introduction — 132
3.2 Methods — 133
3.2.1 The Rockyfor model — 133
3.2.2 Study sites — 133
3.2.3 Model input data — 135
3.2.4 Simulation set-up — 135
3.2.5 Assessment of model accuracy — 135
3.2.6 Assessment of the protective effect of the different stands — 137
3.3 Results — 137
3.3.1 Model accuracy — 137
3.3.2 Protective effect — 139
3.4 Discussion — 141
3.4.1 Model accuracy — 141
3.4.2 Protective effect — 142
3.5 Conclusions — 142
Acknowledgements — 143

4 Täschgufer - a 'picturesque' journey

Plate 1: Bedrock — 146
Plate 2: Discontinuietes and fissures — 148
Plate 3: Loose debris and remobilization of rocks and boulders — 150
Plate 4: Talus slope and forest fringe — 152
Plate 5: Protection dams — 154
Plate 6: Injuries caused to trees growing at Täschgufer — 156
Plate 7: Cross-sections and micro-cuts — 158

5 Methods used to study past rockfall activity

5.1 Sampling trees and sample preparation — 161
5.2 Counting tree rings, skeleton plots and tree-ring measurement — 163
5.3 Building a reference chronology with undisturbed trees — 164
5.4 Assessing past events in increment rings of disturbed trees — 165
5.5 Preparing micro-cuts from cross-sections — 169

Bibliography — 171
Curriculum vitae — 187

*****

ZUSAMMENFASSUNG

Steinschlag stellt einen der am häufigsten in Gebirgsregionen auftretenden geomorphologischen Prozesse dar und wurde daher in der Vergangenheit ausgiebig studiert. Trotzdem bleiben detaillierte Kenntnisse zur Steinschlagfrequenz (*wie häufig*), zu Steinschlagvolumen (*wie gross*), zu räumlichen Mustern (*wo*) oder zur Jahreszeitlichkeit (*wann*) der Steinschlagaktivität die Ausnahme und Angaben zumeist nur sehr fragmentarisch. Ebenso wurden Jahrringanalysen bislang nur in wenigen Ausnahmen herangezogen, um die vergangene Steinschlagaktivität zu untersuchen. Es ist daher das Ziel dieser Arbeit, (i) saisonale Unterschiede in der Steinschlagaktivität festzulegen und (ii) räumlich-zeitliche Variationen in der Steinschlagaktivität mit dendrochronologischen Untersuchungen zu durchleuchten. Daneben wurden die vertikale Verteilung und die Sichtbarkeit von Steinschlagverletzungen auf der Stammoberfläche betrachtet, bevor Stärken und Schwächen der Dendrochronologie im Bereich der Steinschlagforschung mit zahlreichen Datensätzen existierender Studien evaluiert wurden.

In einer ersten Untersuchung wurden 270 Stammscheiben von 18 juvenilen Lärchen (*Larix decidua*) aufbereitet, um saisonale Unterschiede in der Steinschlagaktivität auf einem bewaldeten Hang im Täschgufer (Täsch, Schweizer Alpen) zu studieren. Basierend auf einem Ansatz, der bislang nur in der Waldbrandforschung zur Anwendung kam, wurde die Position von Kallusgewebe und traumatischer Harzkanalreihen innerhalb des Jahrrings bestimmt und daraus die Jahreszeitlichkeit der Ereignisse abgeleitet. Die Ergebnisse zeigen deutliche saisonale Unterschiede bezüglich der Steinschlagaktivität, wobei Verletzungen während der Vegetationsperiode (Anfang Juni bis Mitte Oktober) eindeutig die Ausnahme bilden (12%). Im Gegensatz dazu können 88% der Verletzungen der winterlichen Wachstumspause zugeordnet werden, welche lokal von Mitte Oktober bis Ende Mai andauert. Direkte Beobachtungen am Hang bestätigen diese Resultate und deuten überdies darauf hin, dass die Aktivität im April und Mai am ausgeprägtesten sein dürfte. Während dieser Periode nimmt die globale Sonneneinstrahlung am westexponierten Hang des Täschgufer kontinuierlich zu und vermag so die Eislinsen aufzutauen, die durch das Gefrieren von Schmelzwasser in den Spalten und Rissen der Anrisszonen gebildet werden konnten. Im Gegensatz dazu scheint die Steinschlagaktivität im Täschgufer weder durch Sommergewitter noch durch anhaltende Niederschläge im Herbst beeinflusst zu werden.

In einer zweiten Untersuchung wurden im Täschgufer an 135 stark verletzten Lärchen 564 Bohrkerne gezogen, um langfristige Veränderungen in räumlich-zeitlichen Steinschlagmustern festzustellen. Die Untersuchungen umfassten vier Jahrhunderte (1600–2002) und ermöglichten die jahrgenaue Rekonstruktion von 741 Wachstumsstörungen in der Form von Verletzungen, traumatischen Harzkanalreihen, Reaktionsholz oder abrupten Wachstumsänderungen. Räumliche Analysen zeigten klar auf, dass Steinschlag während der letzten 400 Jahre immer wieder auftrat, wobei die Bäume in der südlichen Hälfte des Hanges regelmässiger von Steinschlag beeinflusst wurden, teils sogar mehr als einmal pro Jahrzehnt. Im Gegensatz dazu wurden die Bäume in der nördlichen Hälfte des Untersuchungsgebiets weniger häufig durch Steinschlag gestört, was die Wiederkehrdauer zwischen zwei Steinschlagereignissen lokal auf mehr als 150 Jahre anwachsen liess. Des weiteren fällt auf, dass sich Steinschlag in der Vergangenheit vorab mittels kleinvolumiger aber hochfrequenter Ereignisse manifestierte. Die Ausnahme bildet das Jahr 1720, als durch ein

grossvolumiges Ereignis der Waldrand im südlichen Bereich des Hanges umgeschlagen und der Waldbestand weitestgehend eliminiert wurde. Der aufwachsende Wald hat sich im Anschluss an das Ereignis jedoch wieder erholt und konnte dadurch seine Schutzfunktion je länger je besser wieder wahrnehmen, was sich unter anderem auch in einer Reduktion der rekonstruierten Steinschlagrate im Südsektor zwischen 1740 und 1990 um den Faktor 13 auswirkt.

Danach wurden im Altdorfer Bannwald (Altdorf, Schweizer Voralpen) drei ausgewachsene Bäume (*Abies alba*, *Fagus sylvatica*, *Picea abies*) gefällt und die vertikale Verteilung sowie die Sichtbarkeit von Steinschlagschäden am Baum untersucht. Für die Analyse vergangener Schäden wurden zwischen dem Stammanlauf und der Krone alle paar Zentimeter Stammscheiben gesägt, insgesamt 307. Aus den Resultaten der Untersuchung geht hervor, dass die Höhenverteilung der Schäden in Zusammenhang stehen dürfte mit der Grösse der Steine und Blöcke, der Hangneigung und dem Waldbestand. Infolgedessen lassen sich Schäden sowohl in Bodennähe wie auch auf über neun Metern Höhe erkennen.

Schliesslich wurden – basierend auf den Resultaten aus dem Altdorfer Bannwald – Schwachpunkte, Möglichkeiten und Grenzen der Rekonstruktion von Steinschlagereignissen mit Jahrringanalysen unter die Lupe genommen. Die Untersuchung ging davon aus, dass Steinschlagschäden sehr viel zufälliger auf verschiedene Bäume verteilt sind und in sehr viel stärker variierenden Höhen auftreten als etwa Wunden, die durch das Auftreten von Fliessprozessen wie Überschwemmung, Nassschneelawine oder Murgang entstehen können. Nebst der vertikalen Verteilung der Schäden wurde anhand bestehender Daten aus den Schweizer Voralpen und Alpen unter anderem auch der Anteil der von aussen sichtbaren Schäden mit der Gesamtzahl der im Jahrringbild rekonstruierbaren Wunden verglichen. In ähnlicher Weise wurde danach versucht, den Prozentsatz der Verletzungen festzulegen, der erfasst werden kann, falls anstelle des ganzen Baumes nur eine einzelne Stammscheibe untersucht wird. Die Resultate der Untersuchungen deuten darauf hin, dass der Prozentsatz 'unsichtbarer' Schäden im wesentlichen von artspezifischen Borkeneigenschaften, jährlichen Zuwachsraten, dem Baumalter und dem Baumdurchmesser sowie von der Grösse des Steinschlags abhängen. Dies hat zur Folge, dass in einzelnen Baumarten nur 15% der Schäden von aussen nicht mehr sichtbar sind, während in anderen 90% nur mehr durch Jahrringanalysen festgestellt werden können. Das Studium einzelner Scheiben auf einer durch das äussere Erscheinungsbild des Stammes vorgegebenen 'Testhöhe' zeigt zudem auf, dass mit nur einer Scheibe pro Baum im besten Fall 13 bis 35% aller Wunden erfasst werden können. Eine wesentliche Verbesserung der Resultate kann jedoch erreicht werden, wenn weitere Indikatoren für die Präsenz von vergangener Steinschlagaktivität herangezogen werden, wie etwa Reaktionsholz, abrupte Wachstumseinbrüche oder – falls vorhanden – traumatische Harzkanalreihen.

Zusammenfassend kann festgehalten werden, dass die vorliegende Arbeit Einblicke zu Möglichkeiten und Grenzen der Jahrring-Steinschlag-Forschung schuf und umfassende Daten zur Jahreszeitlichkeit, Frequenz und Magnitude der Steinschlagaktivität sowie der Sichtbarkeit und vertikalen Verteilung von Steinschlagschäden auf der Stammoberfläche lieferte. Die im Rahmen dieser Arbeit entwickelten Methoden konnten seither auf einem anderen Standort erfolgreich angewandt. Trotzdem sind weitere Untersuchungen zur Jahrring-Steinschlag-Forschung im Allgemeinen und zur vergangenen Aktivität im Täschgufer im Speziellen unerlässlich, da die gewählten Analysemethoden weiter ausgebaut und nicht zuletzt auch der Einfluss von Erdbeben oder Klimafluktuationen auf die Steinschlagaktivität im Detail untersucht werden sollten.

Schlüsselwörter: *Steinschlag, Jahrring, Dendrogeomorphologie, Wachstumsstörungen, Jahreszeitlichkeit, Frequenz, Magnitude, räumliche Muster, Trefferhöhen, Sichtbarkeit von Schäden, Schutzwald*

*****

Abstract

Rockfall represents one of the most common geomorphological processes in mountain regions and has extensively been studied in the past. Nonetheless, detailed data on frequencies (*how often*), volumes (*how large*), spatial distributions (*where*) or the seasonality (*when*) of rockfall activity remain scarce and most of the time fragmentary. Similarly, tree-ring analysis has only exceptionally been used to investigate past rockfall activity. It was therefore the aim of this study to (i) assess intra-annual differences in rockfall activity and (ii) to investigate spatial and decadal fluctuations of rockfall activity on forested slopes with dendrochronological analysis. Furthermore, the vertical distribution of scars was investigated and the visibility of scars determined, before other strengths and weaknesses of dendrochronology in rockfall research were evaluated with extensive datasets from existing studies.

Firstly, 270 stem discs from 18 juvenile *Larix decidua* trees were prepared to study 25 years of intra-seasonal differences in rockfall activity on a forested slope at Täschgufer (Täsch, Swiss Alps). Based on approaches used to date past forest fires, the position of callous tissue and resin ducts has been assessed within the tree ring as to determine the intra-seasonal timing of events. Results show distinct differences in rockfall activity, indicating that rockfall is scarce during the vegetation period (12%), which locally lasts from early June through mid October. In contrast, 88% of the impacts occur during the winter dormancy of trees between mid October and the end of May. Direct observations on the slope confirm the results, indicating that rockfall activity would be highest around April and May, when global insolation on the west-facing slope gradually rises and ice lenses formed from meltwater slowly disappear in the joints and fissures of the rockfall source areas. In contrast, rockfall seems to be neither influenced by thunderstorms in summer nor abundant rainfall in autumn.

Secondly, 564 increment cores from 135 severely injured *Larix decidua* trees have been sampled at Täschgufer to investigate long-term spatial and temporal variations of rockfall activity. The analysis covers four centuries (1600–2002) and allowed reconstruction of 741 growth disturbances such as scars, traumatic rows of resin ducts, reaction wood and abrupt growth changes. Spatial analysis clearly shows that evidence from past rockfall events can commonly be found in trees located in the southern part of the slope, where they recurred more than once per decade. In contrast, trees in the northern part were less frequently disturbed by rockfall and locally define recurrence intervals of more than 150 years. Throughout the last four centuries, rockfall has caused growth disturbances to the trees sampled on the slope, most frequently in the form of low magnitude-high frequency events. In addition, analysis allowed identification of one high magnitude-low frequency event in 1720, which displaced the forest fringe of the northern sector a considerable distance downslope and eliminated an entire forest stand. Data further show that the forest recolonizing the southern sector after the 1720 event gradually improved its protective function, reducing the rate of reconstructed rockfall activity by a factor of 13 between the 1740s and the 1990s.

Thirdly, three adult trees (*Abies alba*, *Fagus sylvatica*, *Picea abies*) have been felled in the Altdorfer Bannwald (Altdorf, Swiss Prealps) as to investigate the height distribution and visibility of impacts (scars) on trees. Past impacts on trees were analyzed with 307 cross-sections taken every few centimeters between the stem's base and its crown. Results demonstrate that impact heights of rockfall fragments on trees lar-

gely vary depending on the diameter of rockfall fragments, the slope gradient as well as the forest cover. As a consequence, scars were identified at heights ranging from almost 0 to more than 900 cm above ground.

Lastly and based on the results obtained from the three adult trees gathered at Altdorfer Bannwald, methodological difficulties, possibilities and limits of tree-ring analysis in rockfall research have been investigated. The study has been based on the idea that – in contrast to other hazardous processes such as debris flows, floods or wet snow avalanches – scars caused by rockfall activity are more randomly distributed on trees and may occur at largely varying heights. As a consequence, data gathered from nine different datasets in the Swiss Alps and Prealps have been analyzed in order to determine inter alia the percentage of scars remaining visible on the stem surface. Similarly, the number of scars reconstructed on entire trees has been compared to the events identified on only one cross-section or a series of increment cores taken at the height with a maximum number of wounds (i.e. test height) visible on the stem. Data indicate that the amount of overgrown scars would much depend on the bark properties of the species, yearly increment rates, the age of the tree, tree diameter as well as the size of rockfall fragments, resulting in an amount of 'blurred evidence' ranging from 15 to 90%. Analysis of single cross-sections at a given 'test height' indicates that, at best, 13 to 35% of the scars occurring on the entire tree can be detected. Data further suggest that the amount of events reconstructed at this 'test height' can be considerably improved as soon as other growth disturbances such as reaction wood, abrupt growth reductions or – if existing – traumatic rows of resin ducts are considered as well.

In conclusion, new insights about possibilities and limitations of tree ring-rockfall research have been gained in this thesis and comprehensive data obtained on the seasonality, frequency or magnitude of rockfall activity as well as the vertical distribution and visibility of scars on stem surfaces. Replicate studies have since proved the general applicability of the approaches developed. Nonetheless, further research is needed in general and at Täschgufer in particular, as there is potential for improvements and further research, namely on earthquake-rockfall or climate-rockfall interactions.

Keywords: *rockfall, tree rings, dendrogeomorphology, growth disturbances, seasonality, frequency, magnitude, spatial patterns, impact heights, visibility of scars, protection forest*

*****

ABBREVIATIONS

AD	anno Domini
age BH	pith age at breast height
a.s.l.	above sea level
BE	Canton of Berne
BP	years before «present» (i.e. 1950)
BUWAL	Bundesamt für Umwelt, Wald und Landschaft
CS	cross-section
D	dormancy, dormant season of trees
DBH	diameter at breast beight (in cm)
DEM	Digital Elevation Model
E	East
ED	exposed diameter, tree diameter exposed to rockfall
EE	early earlywood
EL	early latewood
e.g.	exempli gratia (for example)
GD	growth disturbance (e.g., scars, traumatic rows of resin ducts, reaction wood, abrupt growth reduction or growth release)
GIS	Geographical Information System
GrPh	growth phase of earlywood (E) and latewood (L) cells
H_{max}, H_{mean}	maximum / mean impact heights of rockfall fragments on trees
IC	increment core

i.e.	id est (that is)
inc. yr^{-1}	averaged yearly increment of trees (in cm)
LE	late earlywood
LL	late latewood
ME	middle earlywood
ML	middle latewood
MSK	Medvedev-Sponheuer-Karnik scale of seismic intensity (GEOLOGY 2005)
M_W	seismic-moment magnitude scale as defined by HANKS & KANAMORI (1979)
N	North
NNE	North-Northeast
sensu lato	in the broad sense
SMI	Swiss Meteorological Institute
SP1, SP2	study plots 1 and 2
SSW	South-Southwest
UR	Canton of Uri
VS	Canton of Valais
WNW	West-Northwest
yr, yrs	year(s)
Ø	diameter (in cm)
° , ‘	degree, minute

Important remark

Within this Philosopher’s Degree thesis, the term ‘**rockfall**’ will exclusively be used to describe the **falling, rolling and bouncing** of **isolated rocks** (= *Steinschlag*; Ø < 50 cm) and **boulders** (= *Blockschlag*; Ø > 50 cm) sensu BUWAL *et al.* (1997).

*****

Acknowledgements

On my journey of exploration through the world of rockfall and dendrogeomorphology, I was accompanied, encouraged and supported by many people.

First, I would like to express my sincere gratitude to Prof. Dr. Michel Monbaron, director of this PhD thesis, for financially supporting my research and for his complete confidence in my plans, projects and personality. In addition, I am inately grateful to him for giving me the unique possibility to initiate and coordinate a Dendrogeomorphology Lab at the University of Fribourg. Thank you!

Many thanks also go to Prof. Dr. Hans Kienholz, Prof. Dr. Horst Strunk and Dr. Hugo Raetzo for their willingness to act as members of the PhD Jury, for carefully reading the present thesis and for their constructive and helpful comments. I am also thankful to Prof. Dr. Martin Beniston for presiding over the Jury during my PhD defense.

Next, I would like to thank "my" diploma students, Michelle Bollschweiler, Vendelin Cabernard, Delphine Conus, Melanie Ehmisch, Michael Armand Grichting, Gion-Reto Hassler, Igor Lièvre, Gilles Maître, Frédéric Schlatter and Dominique Schneuwly for the extremely pleasant and stimulating ambiance in the lab as well as during the many days spent in the field. I will never forget my repeated "Hearts" defeats on Friday afternoons or the first timid attempts to launch a solo music career during the many endless – and sleepless – nights spent in Grächen.

In particular, I feel deeply indebted to Dominique, who analyzed many thousands of tree rings for my PhD research, always with exemplary accuracy and precision, allowing me to progress rapidly in my work. Igor merits particular acknowledgement as well. I cannot thank you enough for your never-ending help, your patience and for the thousand and one tricks you taught me about computers in general and Adobe Illustrator in particular. Last but not least, I would like to give my special thanks to Michelle for the many highly enriching discussions, critical remarks and for helping me to measure samples. All the best for your thesis and always keep a stiff upper lip!

Working is so much easier if you have plenty of fun at your office. I therefore would like to thank my colleagues Oliver M. Hitz and Nicole Gaillard for the good times spent together and for continuously reminding me that coffee breaks form an important constituent of a good working day. Thanks for every little thing, good luck for your own projects and vill Gschpass bim "Gumpu"!

I am also especially grateful to Dr. Reynald Delaloye for the many discussions on rockfall, permafrost and statistics as well as for the time spent on reading several drafts of my papers.

Particular thanks also go to Dr. Maung Moe Myint for introducing me to the miracles of ESRI Geostatistical Analyst, for the many long and interesting conversations held on science, philosophy and Buddhism as well as for giving us the unique opportunity to work as GIS volunteers in the marvelous Himalayan Kingdom of Bhutan. Thank you so much and "tashi delek", Moe!

I would also like to address my gratitude to Prof. Dr. Martin Beniston for giving me the possibility to attend many meetings and congresses abroad and for bearing every kind of publication-related costs. Sylvie

Bovel-Yerly merits particular acknowledgement as well for the eternal encouragement, for all the little things she discretely did in the background and for the many last-minute solutions she presented in times of menacing financial hard times. Finally, all my thoughts are with Danièle Yerly, who had to leave this world years too early. I will never ever forget your smile, the way you lived your life and how you accepted to give it back to God. Many, many thanks to all of you!

Eddie Graham (IGUF), Heather Murray (*Institute for Applied Linguistics, Berne*) and Fran E. King (*Eastbourne College, UK*) merit particular thanks for proof-reading the different texts of this publication.

Further, I would like to address my thanks to all the other (current and past) members working at the Department of Geosciences, Geography, for being there, the good times spent together and for every little encouragement: Khalid Al Ghamdi, François Bavaud, Claude Béguin, Louis Boyer, Paula Casals, Claude Collet, Marie Descloux, Evariste Faye, Samuel Fierz, Holger Willi Gärtner, Vincent Grandgirard, Joëlle et Stéphane Goyette, Thomas Hammer, Philipp Häuselmann, Ingo Heinrich, Dominik Jungo, Patricia Jungo, Francisco Klauser, Franziska Keller, Brigitte Koffi-Lefeivre, Ernest Koffi, Gregor Kozlowski, Sylvie Lehmann, Walter Leimgruber, Claire Matti-Gallice, Thierry Menoud, Valérie November, Luc Perritaz, Ivo Raemy, Emmanuel Reynard, Jean Ruegg, Christian Savary, Verena Schäffer, Christian Schubarth, Yi Shi, Michel Spicher, Trudy Stadelmann, Ignaz Strebel, Pierre Terretaz and Stefan Winter.

Another important source of information were the lectures and the introduction to tree-ring analysis given by Prof. Dr. Fritz Hans Schweingruber. The extremely instructive field week spent in the forests around Mašun (Slovenia; July 2000), the discussions and analyses realized with my charming Italian friends Dr. Rosanna Fantucci and Dr. Maria Cleofe Stefanini constituted further important "bricks" for the "construction" of the Dendrogeomorphology Lab in Fribourg. Mille grazie!

Similarly, I would like to express my gratitude to several persons working at the *Swiss Federal Research Institute for Forest, Snow and Landscape Research (WSL, Birmensdorf)*, namely Dr. Andreas Rigling for providing me with hints for the intra-seasonal analysis of rockfall, Werner Schoch for showing me how to prepare and photograph microcuts, Dr. Jan Esper and Werner Gerber for transporting three entire trees from the Altdorfer Bannwald back to Birmensdorf, Rolf Räber for believing in my craftsman skills while using a circular saw and the fire fighters for extinguishing the fire as soon as I had proved that this machine wasn't really made for me…

I would also like to address my gratitude to the members of the *"Applied Geomorphology and Natural Risks"* group at the *Dept. of Geography, University of Bern (GIUB)* for the excellent collaboration and the different joint projects. My special thanks go to Dr. Simone Perret for making me familiar with the secrets of scientific writing, for the innumerous enriching discussions, for her detailed reviews of several papers and for involving me in her research.

I am also extremely grateful to all those who, through their financial support, made life so much easier and gave me the possibility to participate in a series of interesting projects covering different research domains. In this way, my thanks are also expressed to: the *Federal Office for Water and Geology* (Dr. Andreas Götz, Dr. Armin Petrascheck, Dr. Hugo Raetzo), the *Service des routes et des cours d'eau du Valais* (SRCE, Dr. Dominique Bérod), the *Service des forêts et du paysage du Valais* (SFP, Charly Wuilloud), the *Etablissement Cantonal d'Assurance des Bâtiments* (ECAB, Dr. h.c. Pierre Ecoffey).

Many thanks also go to the community president of Täsch, Kilian Imboden, for his interest in the tree ring–rockfall research as well as for his assistance in finding data and reports on past events. Similarly, I am also grateful to the forest engineers Leo Jörger (*Forstrevier Inneres Nikolaital*) and Göran Gfeller (*Forstbetrieb, Korporations-Bürgergemeinde Altdorf*) for their repeated help, for felling adult trees and for coring permissions. Beat Annen and Hans Grossmann (*Amt für Wald und Jagd, Kanton Uri*) are most kindly acknowledged for their data on stand structure and plant sociology for the forest stand at Altdorf.

I also address my thanks to Patrick Amoos (*Büro für beratende Geologie Odilo Schmid & Partner, Brig-Glis*), Reinhold Bumann (*dipl. Forst-Ing. ETH/SIA, Naters*), Dr. Theo Lauber (*Gehytec AG, Naters*) and Bernhard Dräyer (*Rovina + Partner AG, Varen*) for providing me with geological advisory opinions, engineering plans, data on past rockfall events and numerous photographs. Last but not least, I acknowledge the anonymous helicopter pilot who transported an adult tree studied within this PhD out of the Altdorfer Bannwald.

My thanks also include Prof. Dr. André Strasser and Prof. Dr. Christian Caron from the Department of

Geosciences, Geology for inviting me to publish this PhD thesis in the *GeoFocus* series.

In this kind of research work, moral support plays a crucial role, and this was perfectly exemplified by my companion Nicole. Thank you for all your love, your tenderness, for being proud of me in the time of success and for giving me the strength and confidence to continue even at times when difficulties seemed overwhelming. I also love you for showing me that there are not only debris flows, rockfall and trees in the mountains, but also biking, hiking and climbing trails in summer as well as on the marvelous virgin powder slopes in winter.

My very special thanks go to my parents and my sister Sabine. My mum and my dad made it possible for me to study and they always lent me their continuing moral support. If I reach my goal, it is mainly due to that, and for this reason I would like to dedicate this PhD thesis to them.

I finally would like to thank all my friends and also those I did involuntarily neglect!

*****

CHAPTER A

OVERALL INTRODUCTION

This first chapter gives an overview on the current knowledge of rockfall as well as its interaction with trees. In addition, studies focusing on rockfall and simulation modeling, hazard analysis and risk assessment are presented. Thereafter, the methods used in dendrogeomorphology are described briefly before the goals of this PhD study are illustrated. Chapter A ends with an extensive description of the principle study sites used within this thesis, *Täschgufer* and *Altdorf*.

1 Rockfall

1.1 Understanding the process

1.1.1 What is rockfall - some definitions

Rockfall is one of the most widespread geomorphic processes in mountainous regions (Whalley 1984, Erismann & Abele 2001), where its continuous occurrence regularly forms accumulations of rock fragments at the base of talus slopes (Rapp 1960a, b, Church *et al.* 1979, Evans & Hungr 1993). Rockfall is generally considered as one of the various 'landslide' processes *sensu lato*, which also include e.g., soil slips, deep-seated slides, debris flows, large rockfalls or rockslides (Varnes 1978, Cruden & Varnes 1996, Hungr *et al.* 2001). Within this assemblage of 'landslide' processes *sensu lato*, rockfall would – together with debris flows – belong to the category of 'fast-moving landslides' (Guzzetti *et al.* 2004).

While processes of slope stability (flows and slides) control other types of 'landslide' processes *sensu lato*, Malamud *et al.* (2004) pertinently emphasize that processes of fragmentation primarily control rockfall. Other definitions specify similar peculiarities of rockfall, describing it as:

- "a fragment of rock detached by sliding, toppling or falling from a vertical or subvertical cliff, before proceeding downslope by bouncing and flying along parabolic trajectories or by rolling on talus or debris slopes" (Varnes 1978);
- "a relatively small landslide confined to the removal of individual and superficial rock fragments from cliff faces" (Selby 1993);
- "a displacement of a single fragment or several pieces […] with an episode of free fall during the movement" (Evans & Hungr 1993);
- "a single mass that travels as a freely falling body with little or no interaction with other solids. Movement is normally through the air, although occasional bouncing or rolling may be considered as part of the motion" (Ritter *et al.* 2002).

As a result of these vague definitions, rockfall may range from tiniest pebbles to very large boulders and topples hundreds of cubic meters in size (Guzzetti *et al.* 2004). Evans & Hungr (1993) even use the term 'fragmental rockfall' for volumes of up to 10^5 m^3 (!) and emphasize that the volume of single fragments can also change within the fall, as "more or less coherent blocks can disintegrate during the course of movement". Berger *et al.* (2002), in contrast, note that rockfall generally involves volumes < 5 m^3.

In Switzerland, rockfall processes are primarily classed depending on their kinetics and kinematics (Buwal *et al.* 1997, Perret *et al.* 2004a): The term 'rockfall' is used to describe the falling, rolling and bouncing of isolated rocks (= *Steinschlag*; Ø < 50 cm) and boulders (= *Blockschlag*; Ø > 50 cm). The detachment of single rockfall fragments occurs abruptly and may either consist of one single or repeated events. Maximum speed of falling rocks and boulders normally remains < 30 m/s.

As soon as a fragmented portion of a cliff starts moving downslope in the form of a more or less collective mass, Buwal *et al.* (1997) designate the process as 'large rockfalls' (= *Felssturz*). In the course of the downslope movement, the mass is generally further fragmented. Single *Felssturz* events may mobilize volumes between 100 and 100'000 m^3 and velocities ranging from 10 to 40 m/s may occur.

In contrast, 'very large rockfalls', 'fast rockslides' or 'rock avalanches' (= *Bergsturz*) result from the simultaneous detachment of huge volumes of rocks,

ranging from one to several millions of cubic-meters (Buwal *et al.*, 1997). The type of movement largely depends on topographical factors, the fragmentation of the material as well as the interaction between rock fragments. This interaction is characteristic for 'very large rockfalls' (*Sturzstrom*), where the material can be milled to fine powder or even melt (Abele 1971, 1994, Erismann & Abele 2001). Velocities of *Bergsturz* processes exceed 40 m/s and runout distances are known to be considerably long, even on comparably flat slopes.

The three main groups of 'rockfall' processes described by Buwal *et al.* (1997) are illustrated in Figure A1.1 with characteristic examples. Within this Philosopher's Degree thesis, the term 'rockfall' will be exclusively used for the motion of isolated rocks and boulders *sensu* Buwal *et al.* (1997).

1.1.2 Triggers of rockfall activity

Rockfall starts with the detachment of rocks from bedrock slopes, which are subject to various degrees of weathering, fracturing, opening of joints and, as a result, promotion of rockfall. Dorren (2003) further indicates that rockfall activity strongly depends on environmental factors causing physical and chemical weathering, on the type of bedrock (Day 1997) or on geotechnical properties (Douglas 1980). In addition to the given morphological, geological or geotechnical properties of slopes, a large number of trigger mechanisms are described in rockfall literature: So far, research repeatedly focused on the role of alternating freeze–thaw cycles in bedrock (Gardner 1983, Porter & Orombelli 1980, 1981, Coutard & Francou 1989, McCarroll *et al.* 1998, 2001). Matsuoka & Sakai (1999) highlight that, on average, maximum rockfall activity occurs ~10 days after meltout of cirque walls. Interestingly, intense rockfall activity is rarely triggered by diurnal frost cycles on rock faces, but rather by the thawing of seasonal frost and the infiltration of meltwater into rock joints that are still at a subfreezing temperature (Matsuoka 2001, Matsuoka *et al.* 2003). As a consequence, this meltwater can refreeze, causing permanent opening of the joints and favor low magnitude–high frequency events, which are widely considered the typical form of rockfall occurrence in alpine areas (e.g., Matsuoka & Sakai 1999, Jomelli & Francou 2000). This theory somewhat contradicts Gardner (1983), whose pluri-seasonal field observations of rockfall indicate that rockfall forcing factors operate within confines of a diurnal period and not across it.

Earthquakes represent another important trigger of rockfall – and sometimes even rockslide – activity

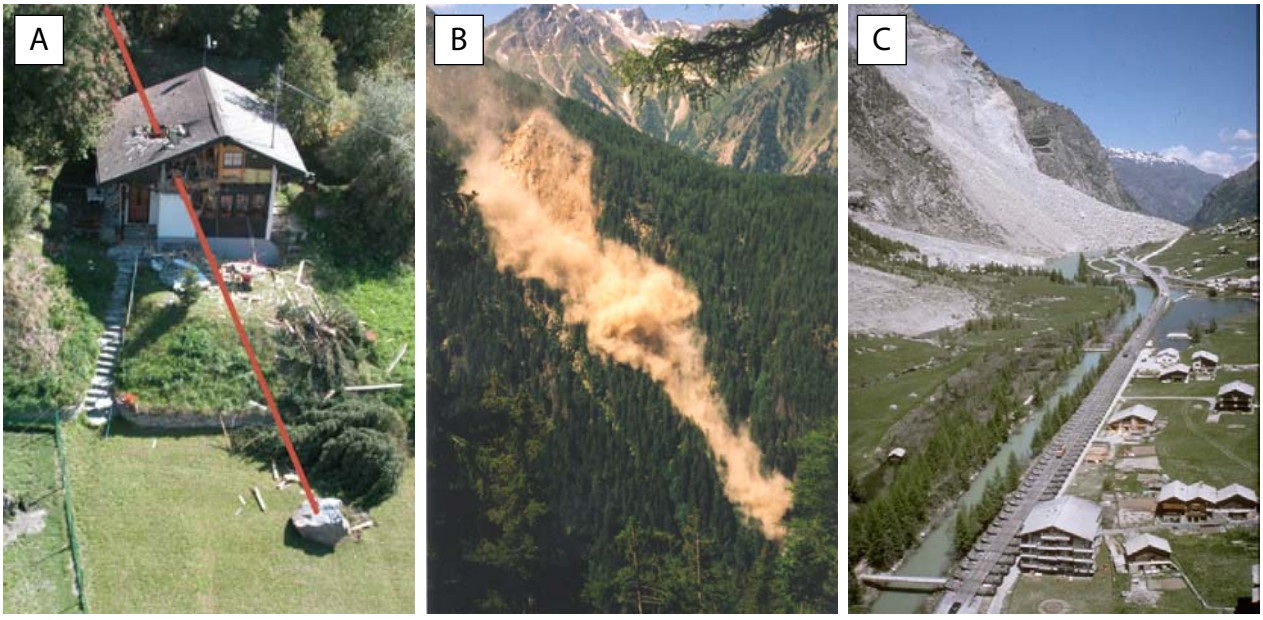

Fig. A1.1 *(a) Large boulder damaging a holiday home during a rockfall event near Evolène (Valais Alps, Switzerland) in 2003; (b) Some 150'000 m³ of unstable gneiss layers were released during the Wassergraben 'rockfalls' (Felssturz) near the Simplonpass (Valais Alps) on July 22 and 23, 1995 (*Stoffel 1996*); (c) During several 'very large rockfalls' (Felssturzserie) occurring between April 18 and May 9, 1991, some 30 million cubic-meters of gneisses were released from the Grossgufer cliff near Randa (Valais Alps). (Photo courtesy by CREALP/Jean-Daniel Rouiller [a, c] and Charles-Louis Joris and [b], used with permission)*

(Kobayashi *et al.* 1990, Harp & Wilson 1995, Bull *et al.* 1994, Keefer 2000, Vidrih *et al.* 2001, Marzorati *et al.* 2002, Jibson *et al.* 2004, Eberhart-Phillips *et al.* 2003). According to Bull & Brandon (1998), the magnitude of the earthquake determines the area in which rockfall might be expected as a result: Moment magnitudes (M_w) greater than 7.0 can provoke rockfall events or rockfalls at distances of up to 400 km from the epicenter (e.g., Keefer 1984, 1994, Wieczorek *et al.* 1995, Wieczorek & Jäger 1996), whilst the effects of moderate earthquakes (M_w = 5.5 to 7.0) would only trigger rockfall(s) within 15 km of the epicenter (Bull & Brandon 1998).

Case studies repeatedly emphasized that rockfall may be released through the interaction of different causes and triggers along with pre-existing morphological features: In this sense, Luckman (1976) concludes that rockfall depends on morphological and geological factors of the cliffs together with fluctuations in rock surface temperatures. Studies from the *Yosemite Valley* (California, USA; Wieczorek *et al.* 1995, 2000) indicate that rockfall events may be provoked by a large array of factors such as e.g., earthquakes, rainstorms, rapid snowmelt, freeze–thaw cycles of water in joints, root penetration or wedging. Interestingly, important winter rainstorms, rapid snowmelt and earthquakes apparently triggered more rockfall events in the *Yosemite Valley* than did freeze–thaw cycles or anthropogenic activity (Wieczorek & Jäger 1996). Nonetheless, the authors also admit that for more than half of the inventoried rockfall events, no trigger could be identified.

In addition to the triggers favoring destabilization of single rocks and boulders, long-term changes in climatic conditions became an intensely debated issue in the heat of the summer 2003: Based on simulations predicting mean annual air temperatures to rise (Knutti *et al*. 2002, Schär *et al*. 2004) and snow distribution and duration to change (Harris *et al.* 2001), discussions have more and more focused on the influence of thawing permafrost on rockfall rates (Schiermeier 2003). With data on the transient subsurface temperature fields in rock walls and modeling approaches, Gruber *et al.* (2004) determined the progression of summer thaw or winter freezing. Results indicate that the modeled thaw of summer 2003 exceeded the maximum of all previous years. The authors, thus, believe that the 'exceptional rockfall activity' observed in 2003 might represent a direct and unexpectedly fast impact of climate change. Gruber *et al.* (2004) stress that effects of temperature rise on rockfall activity would be most obvious on northern slopes, where the depth of permafrost thaw is mainly controlled through air temperatures (long-wave radiation). In contrast, southern slopes receive short-wave radiation as well and thus showed less important anomalies in 2003. These field data from the Swiss Alps also seem to confirm the assumptions of Davies *et al.* (2001) or Gude & Barsch (2005), emphasizing that the warming of bedrock could reduce the strength of ice-bonded open joints and thus favor destabilization in the *Zugspitze* area (*Bavarian Alps*, Germany). In a similar way, Harris *et al*. (2001) believe that such warming-induced permafrost degradation would be likely to lead to increasing size and frequency of slope failures such as creep-related processes, rockfall, rockslides, mudslides or debris flows. However, the reduction in snow cover could also lead to greater winter cooling in certain areas (Wegmann *et al.* 1998) and therefore favor stabilization. Instead of analyzing the warming tendency in summer temperatures, Beniston (2005) focused on exceedances of maximum winter temperatures beyond particular thresholds, emphasizing that so-called 'warm winter spells' have substantially increased in the Swiss Alps since the late 1960s and, thus, have significant impacts on environmental systems as well.

1.1.3 Departure, transit and deposition zone of rockfall

As illustrated in Figure A1.2, rockfall slopes normally consist of a departure (*Ablösungs*-), a transit (*Transit*-) and a deposition zone (*Ablagerungsbereich*). In the departure zone, factors such as the slope morphology, the direct surroundings or the form of the potentially unstable rock (Fig. A1.3) strongly determine whether a rock fragment (i) will start its journey downslope, (ii) will be remobilized after deposition (secondary rockfall) or (iii) will remain where it is (Descoeudres 1990, Goodman & Kiefer 2000, Dorren 2003). As for the release of rocks and boulders, studies widely agree that rockfall can only be triggered on slopes with gradients > 31° (e.g., Jahn 1988, Gsteiger 1993, Schwitter 2000).

Moreover, rockfall fragments generally come to a stop as soon as slope gradients drop < 30° (Buwal *et al.* 1997). This area is called the deposition zone and is regularly characterized by the accumulation of rockfall scree. Exceptionally, boulders may reach areas located beyond the base of the slope in the so-called 'shadow of talus slopes'. In southwestern *British Columbia* (Canada), Evans & Hungr (1993) investigated geomorphic evidence ('silent witnesses') in the field, empirical methods, physical modeling and computer-based analytical models as to examine return

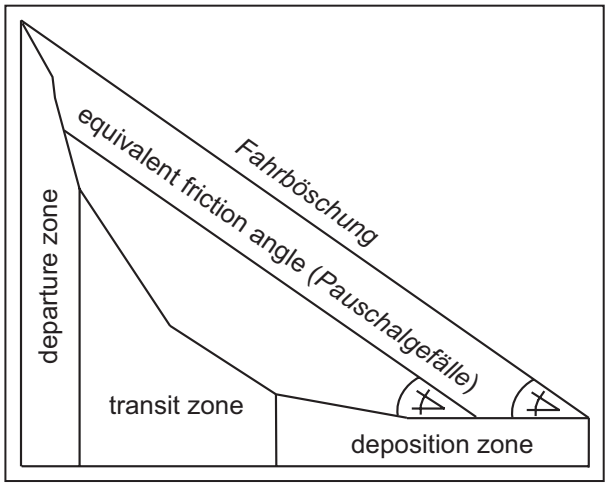

Fig. A1.2 *Rockfall slopes are generally subdivided into a departure, a transit and a deposition zone. The line described by the uppermost point of departure and the farthermost point of deposition is called 'Fahrböschung'. In contrast, the Pauschalgefälle takes account of the center of gravity of the departing mass with that of the deposited mass. (modified after* Heim 1932, Körner 1980, Gerber 1998, Kienholz 1998, *and* Schneuwly 2003*)*

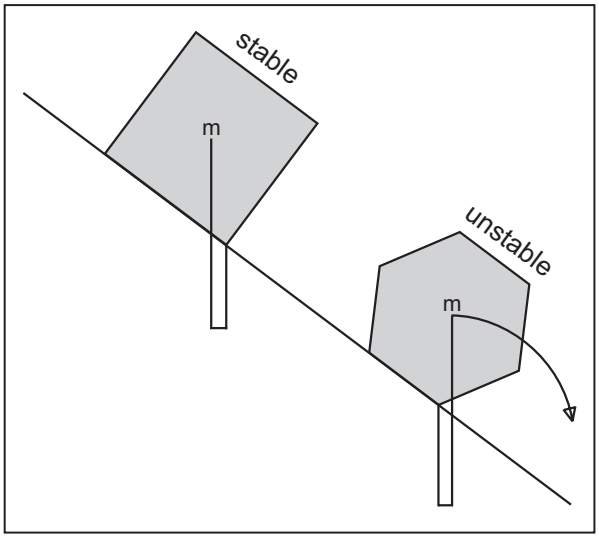

Fig. A1.3 *The stability of a rock depends inter alia on its shape: As the center of gravity lies within the zone of contact between the rockfall fragment and the surface in example A, the rock will probably remain where it is, whereas the completely different shape and the change in the position of the center of gravity will favor instability in example B (modified after* Descoeudres 1990*)*

periods for such exceptional rockfall events. Results indicate that return periods of the order of 1000 years are typical for specific sites. Analysis also yielded a 'minimum shadow angle' of 27.5°, which is thought to correspond to the rolling-friction angle for the slope surfaces in question. As illustrated in Figure A1.2, the 'minimum shadow angle' suggested by Evans & Hungr (1993) considers the highest point of the talus slope as well as the farthest deposition point and can therefore be compared to the *Fahrböschung* as defined by Heim (1932). Figure A1.2 also shows that, in contrast, the equivalent friction angle (*Pauschalgefälle*) takes account of the angle formed by a line connecting the center of gravity of the departing mass with that of the deposited mass (Kienholz 1998). In any case, all of these methods should only be used as a first approximation of the length of the runout zone.

In between the two zones highlighted above, the transit zone can be found. Here, rocks and boulders commonly pass through on their way to the deposition zone. Due to the lower slope gradients, rockfall fragments may be temporarily stopped and remobilized. In addition, passing fragments become more and more influenced by the soil, scree and vegetation (i.e. surface roughness, damping effects).

1.1.4 Rocks and boulders 'traveling downslope'

After being triggered, the motion of rockfall strongly depends on the mean slope gradient. Generally, three different modes of motion are described in literature: falling (also freefall), bouncing and rolling: The freefall of rocks is limited to very steep slopes. According to Ritchie (1963), slope gradients need to exceed 76° to allow the falling motion of rockfall fragments, whereas Dorren (2003) believes that the limit between the bouncing and falling motion would oscillate around 70° (Fig. A1.4a). As illustrated in Figure A1.4b, Schweigl *et al.* (2003) indicate that freefall occurs as soon as the vertical distance traveled by the rockfall fragment excels the horizontal distance by at least four times. As the air friction during freefall may be neglected (Bozzolo & Pamini 1986, Erismann & Abele 2001), rockfall is exclusively influenced through collisions with other falling rocks during freefall (Azzoni *et al.* 1995).

As soon as the mean slope gradient decreases, rockfall fragments start to collide with the slope surface and, thus, initiate the bouncing motion. Through the first impact, some 75–86% of the total energy accumulated during the freefall is lost at once (Broilli 1974, Evans & Hungr 1993, Dorren 2003) and incompetent rockfall fragments tend to fall apart (Bozzolo & Pamini 1986). Azzoni *et al.* (1995) suggest that the bouncing motion will continue as long as the irregularities within the rockfall fragment remain less

important than the unevenness of the slope surface. Erismann & Abele (2001) argue that an ellipsoid starts to bounce as soon as a certain velocity is reached. As can be seen from Figures A1.4a and A1.4b, Dorren (2003) and Schweigl *et al.* (2003) suggest that the slope gradient has to be > 45° to allow a bouncing motion of rockfall fragments. In opposition, Schwitter (2000) believes that the limit between rolling and bouncing is rather be located at 35°.

As soon as mean slope gradients become < 45°, the bouncing motion of rockfall fragments is gradually transformed to rolling, as rocks and boulders gather rotational momentum (Dorren 2003). Rather than using indications of the slope gradient, Azzoni *et al.* (1995) emphasize that a rolling motion will set in as soon as the irregularities in the rockfall fragment become more important than those on the slope surface, the reason why rolling rockfall fragments start to almost constantly remain in contact with the slope surface (Hungr & Evans 1988). In combination with short bounces, rolling represents one of the most economic displacement mechanisms (Erismann 1986).

Stopping of rockfall fragments occurs through an abrupt rather than a gradual process and may be the result of energy loss through collision and friction forces (Dorren 2003).

After the above description of the different modes of motion, we shall now give some information on velocities, jump distances, bounce heights or kinetic energies associated with rockfall activity: Velocities of rockfall fragments vary widely and range from a few to even tens of meters per second (m/s). In Switzerland, federal authorities (Buwal *et al.* 1997) consider 30 m/s (108 km/h) to be the maximum velocities reached by rockfall fragments (see Chapter A1.1). In the field, data gathered from impact craters and jump parabola caused by a large rockfall boulder (10 t) suggest maximum speeds of 88 km/h (Rickli *et al.* 2004), thus excelling the velocities of small rocks (25 kg) by almost four times. According to Rickli *et al.* (2004), the mass of rockfall fragments would also influence jump distances and jump heights: Based on a relatively small number of observations in the field, maximum jump distances of small rocks (25 kg) oscillate around 2.2 m, whereas large boulders (10 t) are able to perform jumps of up to 33.6 m. In a similar way, maximum bounce heights range from 0.3 to 4.2 m. However, the most important differences arise from the maximum kinetic energies, differing by a factor of 6000 between small rocks (0.5 kJ) and large boulders (3000 kJ; Rickli *et al.* 2004).

1.2 Rockfall into forests

1.2.1 Influence of forest stands on rockfall propagation

Protection forests may provide passive protection against rockfall by absorbing rockfall fragments or reducing their speed and bounce heights in the transit or deposition zones (Brang 2001, Brang *et al.* 2001, Rickli *et al.* 2004). In addition, trees may also stabilize or anchor rocks, prevent the release of rockfall fragments (Berger & Rey 2004, Hurand & Berger 2002) or even protect their sites by limiting excessive soil erosion (Rey & Chauvin 2001, Badoux *et al.* 2002, Gertsch & Kienholz 2004). However, quantitative data on the effect of forest cover on rockfall propagation remains minimal (Meissl 1998, Stoffel *et al.* 2005d). An investigation from *Liechtenstein* indicates

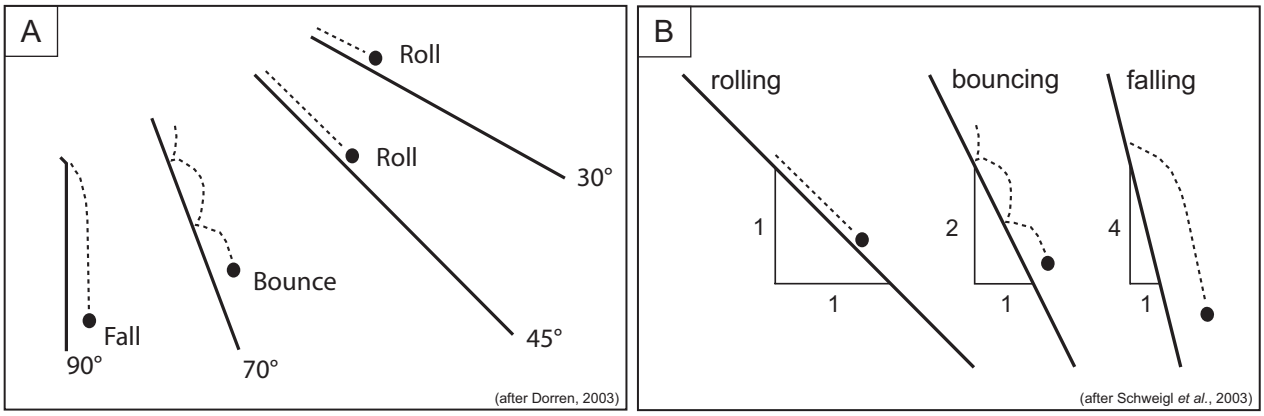

Fig. A1.4 *Thresholds for the falling, bouncing and rolling motion of rockfall fragments as given (a) in minimum slope gradient by* Dorren (2003) *and (b) proportions between the horizontal and vertical distance by* Schweigl *et al.* (2003).

that rockfall is stopped three to ten times more frequently on densely forested slopes than on comparable slopes without forest cover (Jahn 1988). Studies from the *French Alps* emphasize that 60–95% of all rocks starting from the top of a slope would reach roads if the forest stands were absent, whereas with an existing forest cover, only 10–15% would do so (Cattiau *et al.* 1995, in Dorren *et al.* 2004a). Such a protective effect even exists in wind-thrown forest stands: Schönenberger *et al.* (2005) demonstrate that fallen trees, snags, stumps, boles or mounds remaining on the slope efficiently prevent rock releases and stop falling rocks and boulders for at least a decade, whereas the removal of trees from these areas, in contrast, results in increased rockfall releases and decreased protection. In a GIS-based approach, Brauner *et al.* (2005) tried to quantify protection effects provided by forest stands against rockfall. Examples of rocks and boulders that were effectively stopped in forests are illustrated in Figures A1.5, A1.6 and A1.7.

Similarly, data from the *Gaspé Peninsula* (Canada; Lafortune *et al.* 1997, Hétu & Gray 2000) state that forested slopes do have the potential to efficiently absorb rockfall if the event is of low magnitude and high frequency. According to Leibundgut (1986), a 100 m large strip of protection forest should be sufficient to almost completely prevent rockfall from reaching lower areas. In contrast to these results, Wullschleger (1982) believes that concentrated and frequently occurring rockfall of low magnitude would rather exhaust the healing potential of single trees and hence reduce the protective potential of a forest.

In the case of 'large rockfalls' – i.e. high magnitude, but low frequency events – the protection forest can in no way avoid the devastating effects of the events and the stand will be eliminated or at least its fringe (temporarily) displaced downslope (Hétu & Gray 2000, Stoffel *et al.* 2005c). Studies also indicate that the forest cover influences the velocity, bounce height and jump distance of rock-fall: For instance, results obtained from 132 rocks (25–30 kg) artificially released on a 35° steep slope indicate that the repeated contacts with trees would considerably slow down rockfall and thus preventing velocities > 15 km/h (Jahn 1988). On slopes without a forest cover, (small) rocks may, in contrast, reach maximum velocities of up to 25 km/h only 40 m after being triggered (Gsteiger 1993).

1.2.2 Reactions of trees to rockfall

Along with tree-specific parameters such as e.g., the DBH, the mass and velocity of rockfall fragments or the impact height on the stem determine whether a tree is only shaken or broken through the impinging rocks and boulders (Fig. A1.8). The type of wood species exposed to rockfall further influences the resulting reaction, as different species possess different breaking strengths (*Bruchfestigkeiten*; Gerber 1998, Dorren & Berger 2005). Krummenacher (1995) emphasizes that trees are able to provide sufficient protection against rockfall as long as the diameter of boulders remains < 2 m. Rickli *et al.* (2004) state that efficient protection can only be provided by the forest stand if both the mass and the velocity of the rockfall component would remain below the critical values of 10 t and 20 m/s. Otherwise, the stand would not be able to effectively influence the gravitational process and, as a further

Fig. A1.5 *This large boulder (2.4 m³) passed the uppermost rockfall dam before it was stopped by a dense stand of juvenile Larix decidua trees on the Täschgufer slope.*

Fig. A1.6 *Small rockfall fragments lodged in a pine stem in Ticino, Switzerland. (Photo courtesy by Fritz Hans Schweingruber, used with permission).*

Fig. A1.7 *'Wheel-shaped' rockfall fragment stopped by a larch tree at Täschgufer. (Photo courtesy by Dominique Schneuwly, used with permission)*

result, trees are eliminated along the fall path (Fig. A1.9). Additional results on the interaction of rock-fall and trees can be expected from the analyses conducted by Berger *et al.* (2002) and Le Hir *et al.* (2004), who are currently studying the effect of trees on rock-fall (and vice-versa!) with real size experiments and modeling approaches on forested slopes near *Grenoble* (*French Alps*; Dorren *et al.* subm. a, subm. b).

Similarly, Foetzki *et al.* (2004) are actually analyzing the mechanical behavior of adult Norway spruce trees (*Picea abies*) during impacts in a forest near *Davos* (*Grisons*, Switzerland): First results indicate that the root system and the soil may absorb 50% or more of the impact energy during rockfall events, depending on the impact height as well as the mass and the velocity of the impinging body.

Quantitative results on the number of rockfall scars in stands have been gathered during the 'Sanasilva' program, where visible defects have been searched for in a forest of the central *Swiss Alps* (*Altdorf* UR). Results indicated that 36% of all trees exhibited visible defects (after Jahn 1988). In Austria, the analysis of the *Ausserbacher* mountain forest stand indicated that 84% of all trees were damaged by rockfall activity (Stand Montafon 1990, Dorren *et al.* 2005).

More recently, visible defects have been inventoried in the *Diemtigtal* (*Bernese Oberland*, Switzerland) and a pluri-annual monitoring project initiated in order to perform yearly follow ups of rockfall impacts on trees of a mixed forest stand (Baumgartner 2002, Perret *et al.* 2004b, 2005a). Examples of scars visible on the stem surface are given in Figures A1.10 and A1.11.

Fig. A1.8 *While the large stem of this Larix decidua (60 cm DBH) was broken through the impact of a large boulder (5 t), the remaining stump was nonetheless able to stop the rockfall fragment. (Photo courtesy by Werner Gerber, used with permission)*

Fig. A1.9 *This large boulder (8.5 m^3; 23 t) travelled for more than 130 m in a 30° steep forest near Flüelen (UR, Switzerland), eliminating several stems within the stand (850 trees ha^{-1}). (Photo courtesy by Werner Gerber, used with permission)*

Fig. A1.10 *Fresh rockfall scar (spring 2002) at the stem of a tree growing in the protection forests at Brünigpass BE. (Photo courtesy by Simone Perret, used with permission)*

Fig A1.11 *The partly overgrown scar on the stem surface of this century-old Larix from the Täschgufer VS stand testifies for the occurrence of rockfall processes on the slope. (Photo courtesy by Dominique Schneuwly, used with permission)*

1.2.3 Protection forests – dreams and reality

The Mountain Forest Protocol of the Alpine Convention underlines the important role of mountain forests, indicating that they would provide the most effective, least expensive and most aesthetic protection against different types of natural hazards. In order to maintain or improve these protective functions provided by the mountain forests, approximately 50 million Euros are spent in Switzerland and Austria alone each year (Cipra 2005).

Simultaneously, studies started to deal with the effects of forest composition, tree species, number and DBH of trees or the natural regeneration on the

efficiency or sustainability of protection forests (e.g., Chauvin *et al.* 1994, Wasser & Frehner 1996, Frehner *et al.* 2005).

As for the tree species, Schweingruber (1996) indicates that rockfall gullies are only settled by those species best able to compartmentalize scars and with the best growing capacity: For higher elevation alpine stands, these would either be conifers or Sycamore maple trees (*Acer pseudoplatanus*), while in the angiosperm forest level, beech trees (*Fagus sylvatica*) and various bush species would generally predominate. Dorren *et al.* (2004a) emphasize that mixed protection forests would be more resistant to and more resilient after disturbances caused by rockfall than monocultures. While Wasser & Frehner (1996) believe that a protection forest stand should consist of a large number of trees with preferably thick stems near the rockfall source area, data from the *French Alps* imply that the number of trees would be more important than the diameter (Dorren *et al.* 2004a). In the accumulation zone, forests composed of dense bushes and shrubs seem to be best suited to reduce the effects of rockfall further downslope (Mani & Kläy 1992, Gsteiger 1993, Gerber & Elsener 1998). Dorren *et al.* (2004a) summarize results from recent studies on the efficiency and the management of protection forests (Kräuchi *et al.* 2000, Motta & Haudemand 2000, Bebi *et al.* 2001) by defining the best-suited protection forest as an "uneven multilayered stand with a mosaic of all tree sizes and age classes".

As part of the Second National Forest Inventory of Switzerland (*Landesforstinventar*), Duc *et al.* (2004) quantified the efficacy of the currently existing (rockfall) protection forests using a "stand density index" (*Bestandesdichteindex*) based on the mean number of stems per hectare and the mean diameter of trees. Their results indicate that only 20% of the currently existing protection forests are able to provide good or even very good protection, while 30% are able to provide medium and 50% only low protection of values at risk from rockfall activity. Last but not least, NaiS (2005) currently prepares guidelines for the composition of sustainable protection forests in Switzerland (Frehner *et al.* 2005).

1.3 Frequency and volumes of past rockfall activity

An extensive database with sufficient descriptions on the size and the frequency of past rockfall events represents a compulsory prerequisite for hazard assessment or risk analysis (see Chapter A1.5). But so far, only little information exists on how rockfall frequencies and magnitudes vary over time. Former studies focusing on frequencies and volumes have repeatedly been based on short-term observations of rockfall activity in the field (Luckman 1976, Douglas 1980, Gardner, 1980, 1983, Matsuoka & Sakai 1999), rendering estimates of long-term accretion rates very difficult, if not impossible: For instance, Luckman (1976) studied rockfall in the *Surprise Valley* (*Jasper National Park*, Canada) and derived an average rockfall frequency of 0.66 events per hour of observation. Data gathered near *Lake Louise* (Canada; Gardner 1970) furnished comparable results, indicating an hourly frequency of 0.70. Even a higher frequency was obtained after 993 hours of observation on slopes southwest of *Calgary* (Canada; Gardner 1980), indicating a frequency of 0.83. However, values significantly dropped with time of observation being extended to 2181 hours, resulting in a frequency of 0.49 (Gardner 1983). The only analysis of this type performed outside Canada was realized in *Co. Antrim*, Northern Ireland (Douglas 1980). Antonini *et al.* (2002) *a posteriori* inventoried the deposits of 200 rockfalls triggered during a series of earthquakes in Central Italy in September and October 1997. Field-based approaches focusing on long-term changes and evolutions in rockfall frequencies have, in contrast, commonly been based on estimates of accumulation rates derived from accumulated talus volumes (Rapp 1960a).

Other studies analyzed archival data in order to get hints of past rockfall activities. In Central Italy, for instance, this approach allowed identification and dating of 111 'landslide events' for the period 1918–2002 (Guzzetti *et al.* 2004). Others focused on roadway damage reports (Bunce *et al.* 1997) or railroad and highway records (Rapp 1960b) as to assess past rockfall activity. Similarly, Hungr *et al.* (1999) analyzed maintenance reports to study rockfall activity along transportation corridors. In their case, data covered four decades and contained 3500 records, half of which included information on the size of events.

On slopes composed of siliceous lithologies, lichenometry has repeatedly been used to evaluate the mean age or to roughly estimate 50-yr and long-term rates of rockfall accretion (Luckman & Fiske 1995). As the maximum 50-year accretion rates determined in *British Columbia* appear to be at least an order of magnitude too small to have produced the entire talus slopes over the Holocene, it is concluded that rockfall accumulation rates must have been considerably greater at

some earlier period of the Holocene, possibly a period of unloading immediately after deglaciation (Grove 1988).

André (1986, 1997), in contrast, believes that the talus surfaces in Northern Europe would mainly have been built during two distinct periods of the Little Ice Age. Enhanced rockfall activity during the Little Ice Age was also observed in Norway, where McCarroll *et al.* (1998, 2001) combined a lichen-based analysis of spatial and temporal patterns of past rockfall activity with a modeling approach. Bull & Brandon (1998), finally, used lichenometric methods to date earthquake-generated regional rockfall events in the *Southern Alps* of New Zealand.

Based on the results gathered from archives, road and railway reports, frequency–volume relationships and statistics have repeatedly been applied to derive rockfall frequencies or magnitudes. Hungr *et al.* (1999), for instance, used 3500 rockfall events inventoried along the main transportation corridors of *British Colombia* (Canada) as to determine 'magnitude–*cumulative* frequency relationships'. In contrast, Dussauge-Peisser *et al.* (2002) and Dussauge *et al.* (2003) used '*cumulative* frequency–volume statistics' to study rockfall(s) originating from sub-vertical cliffs in the *Grenoble* and *Yosemite Valley* areas. Guzzetti *et al.* (2003a) applied an approach based on a '*non-cumulative* frequency–volume distribution'. Lastly, Malamud *et al.* (2004) focused on rockfall inventories as to determine a '*frequency density f*' of rockfalls as a function of the rockfall volume V_R.

1.4 Modeling rockfall in laboratory tests, on slopes and in forests

There are many different ways to simulate the motion, trajectories or runout zones of rockfall activity. Dorren (2003) gives an excellent review of approaches, and this is the reason why the next three paragraphs on (i) empirical, (ii) process-based and (iii) GIS-based models follow accordingly his literature review and are only completed with some literature sources published since.

1.4.1 Empirical rockfall models

Empirical rockfall models are generally based on relationships between topographical factors and the length of the runout zone of single or multiple rockfall events. In the past, this kind of model has sometimes been referred to as statistical model (Keylock & Domaas 1999). Empirical models e.g., investigated logarithmic correlations to determine the influence of rockfall volume on the maximum horizontal distance traveled and the area covered with rockfall fragments (Tianchi 1983, Moriwaki 1987).

Other studies focused on the *Fahrböschung* principle or 'minimum shadow angles' in order to predict the runout zones of rockfall (Toppe 1987, Evans & Hungr 1993). More recently, Keylock & Domaas (1999) used simple topographic parameters and tested three empirical models on their ability to predict the maximum length of runout zones, namely a *height function*, an α–β and a *runout ratio* model.

1.4.2 Process-based rockfall models

The second group of rockfall simulation approaches can be described as process-based models. They describe or simulate the different modes of motion of rocks over slope surfaces. At first, the motion of rockfall fragments was considered a sliding motion over talus slopes and results obtained compared with data gained from laboratory experiments (Kirkby & Statham 1975, Statham 1976). Based on the approach of Kirkby & Statham (1975), Keylock & Domaas (1999) developed a *simple dynamics rockfall model*. There are plenty of similar process-based approaches, all of them designed as two-dimensional slope-scale models and restricted to the motion of rocks and boulders within a vertical plane without lateral movement (Bozzolo & Pamini 1986, Hungr & Evans 1988, Bozzolo *et al.* 1988, Pfeiffer & Bowen 1989, Kobayashi *et al.* 1990, Evans & Hungr 1993, Budetta & Santo 1994, Chen *et al.* 1994, Azzoni *et al.* 1995, Chau *et al.* 1998).

In addition, a few three-dimensional process-based models have been designed for the use at slope scale (Descoeudres & Zimmermann 1987, Gascuel *et al.* 1998). Descoeudres & Zimmermann (1987) developed their model in order to analyze a rockfall involving large rocks and boulders (1–10 m^3) in *Valais (Switzerland)*. The model was based on a high resolution DEM and integrated friction coefficients as well as coefficients for the plasticity and elasticity of the soil. More recently, process-based approaches gradually integrated the possibility of simulating multiple falling rockfall fragments and interactions or providing data on coordinates, velocity and angular velocity of multiple rockfall fragments on a three-dimensional slope with *Discrete Element Methods* (Donzé *et al.* 1999, Okura *et al.* 2000a, b) or *Discontinuous Deformation Analysis* (Koo & Chern 1998).

1.4.3 GIS-based rockfall models

GIS-based rockfall models can be subdivided into two groups, namely those running within a GIS environment and those using input data gathered from GIS analysis to run their raster-based models. GIS-based rockfall models consist of three procedures, including (i) the identification of rockfall source areas, (ii) the determination of the fall track and (iii) the calculation of the length of runout zones.

Within her GIS-based simulation approach, Meissl (1998, 2001) used two different empirical models (i.e., *Schattenwinkel*, *geometrisches Gefälle*) to calculate runout zones of rockfall fragments. The fall track was assessed with a raster neighborhood analysis and the motion of rocks simulated as either freefall or sliding. Other models rather focused on hazard assessment at a regional scale (van Dijke & van Westen 1990, Meissl 2001, Menéndez Duarte & Marquínez 2002, Ayala-Carcedo *et al.* 2003, Baillifard *et al.* 2003, Dorren & Seijmonsbergen 2003, Marquínez *et al.* 2003, Chau *et al.* 2004).

1.4.4 Combined modeling approaches and the integration of trees

In the last few years, process- and GIS-based approaches have regularly been combined in order to realistically model rockfall, resulting in the *Zinggeler-Geotest* (Zinggeler 1989, Zinggeler et al. 1991, Krummenacher 1995, Krummenacher & Keusen 1996, Utelli 1999, Liniger 2000, Perret *et al.* 2004a, Stoffel *et al.* in prep.), *Stone* (Agliardi *et al.* 2001, Guzzetti *et al.* 2002, Agliardi & Crosta 2002a, b, 2003, Crosta & Agliardi 2003, 2004, Crosta *et al.* 2004) or *Rockyfor* models (Dorren 2002, Dorren & Seijmonsbergen 2003, Dorren & Heuvelink 2004, Dorren *et al.* 2004b, 2005, Kühne 2005, Stoffel *et al.* 2005d).

The *Zinggeler-Geotest* model considers forest and terrain characteristics (e.g., topography, vegetation, surface roughness, damping effects), but also calculates contact reactions with single trees or the slope surface as to determine rotational effects of stones and boulders. The model is process-based and runs in a GIS environment. The fall direction of rockfall is determined from each raster cell, whereas stand density or DBH distributions are randomly chosen using stochastic models. In opposition to the two simulation approaches introduced further down, the *Zinggeler-Geotest* model has, by now, almost been in use for two decades and is commonly applied throughout Switzerland for hazard analysis or risk assessment. *Stone* uses kinematic algorithms, treating the falling rock as a lumped mass in freefall, bouncing or rolling motion and produces raster files in a GIS environment as output data.

Rockyfor, in contrast, uses raster maps as input data and models trajectories of falling, rolling and bouncing rocks within raster cells. In addition, the model calculates the energy loss due to impacts of rocks and boulders against trees. The model therefore includes the position of the rock with respect to the position of the tree, the diameter of the tree and the kinetic energy of the rock before the impact. The *Rockyfor* model has been extensively corroborated with data gathered from 218 real-size rockfall experiments on a forested slope in the *French Alps* (Le Hir *et al.* 2004; A1.12).

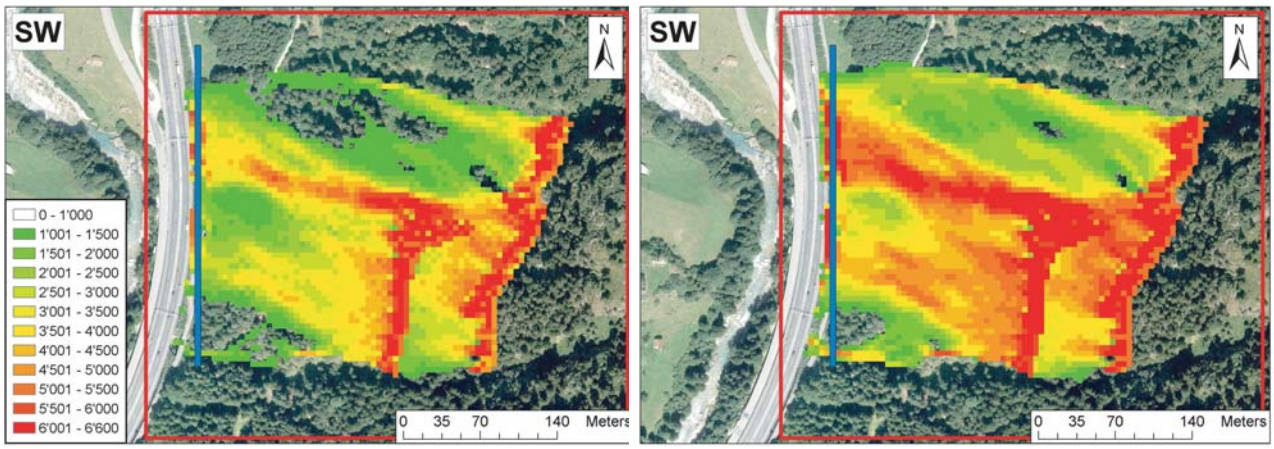

Fig. A1.12 *Simulation of rockfall trajectories in the Stotzigwald (Gurtnellen UR, Switzerland) realized with the currently existing forest stand and on a non-forested slope* (modified after Kühne 2005, Stoffel *et al.* 2005d).

1.5 Hazard analysis and risk assessment in rockfall research

There is wide agreement that rockfall(s) belong to the most destructive mass movements in mountain environments (e.g., Evans & Hungr 1993, Evans 1997, Guzzetti 2000). In the recent past, rockfall repeatedly reached inhabited areas (Bloetzer & Stoffel 1998) or traffic routes (Kienholz *et al.* 1988, Budetta 2004), where it destroyed infrastructure or even caused fatalities (Porter & Orombelli 1980, Agliardi & Crosta 2003, Baillifard *et al.* 2003, Dorren *et al.* 2004a). In Italy, rockfall activity even represents the primary cause of landslide fatalities (Guzzetti 2000), e.g., eight fatalities during the *'Monte San Martino'* rockfall in 1969 (Eisbacher & Clague 1984).

Casualties have also been caused on transportation corridors: On May 10, 1939, six people were killed along the railway connecting *Terni* to *Rome*. Accident statistics are also available for Canada. Here, data indicates that from the 13 persons were killed during 20th century rockfall incidences, four casualties occurred in houses and nine on transportation routes (Hungr & Evans 1989). The comparably low number of fatalities in Canada is supposedly due to development pressure being – in contrast to most parts of the *European Alps* – much less important and damages to houses quite infrequent (Evans & Hungr 1993). Nonetheless, indirect costs of land alienation as a result of rockfall hazard seem to be very significant in Canada as well! Finally, Hungr *et al.* (1999) indicate that the major part of the risk to life would result from 'intermediate-magnitude rockfall events' (1–10 m^3) in southwestern *British Columbia* (Canada).

Hazard assessment should determine *where* (spatial location), *how large* (magnitude or intensity), *when* and *how frequently* (temporal prediction) slope failures will occur in the future (Guzzetti *et al.* 1999, Cardinali *et al.* 2002). Due to the peculiar characteristics of rockfall, investigations should also include information on the travel distance (Guzzetti *et al.* 2004).

One of the first studies focusing on rockfall hazards in inhabited areas was realized by Evans & Hungr (1993), who assessed the 'landing probability' of boulders in the shadow of talus slopes (i.e. beyond the base of the slope; cf. Chapter A1.1.3). In the *Umbrian* region (Central Italy), Cardinali *et al.* (2002) used a geomorphological approach to estimate the landslide hazards and risks in urban and rural areas. Finally, Guzzetti *et al.* (2003a) investigated rockfall hazard and risk assessment in the *Yosemite Valley* (California, USA).

Hazards and risks have repeatedly been assessed for transportation corridors as well, where rockfall causes delays, damage, injury and death to users (A1.13): After a fatal rockfall incidence, Bunce *et al.* (1997) developed a risk analysis methodology to determine the probability of loss of life due to rockfall on *British Columbia Highway 99*. The calculations of probabilities of death were based on rockfall frequencies and risks compared with accepted societal risks commonly used in industries and large engineering projects. Results indicate that the chance of a one time user and a daily commuter to die on the highway were 6×10^{-8} and 3×10^{-5} per year, respectively. The annual probability of a rockfall causing a death in the exposed

Fig. A1.13 *In mountainous areas, transportation corridors are regularly subject to rockfall activity: (a) In November 2003, rockfall obstructed the cantonal road connecting Stalden with Saas-Almagell (Eisten, Valais Alps); (b) On May 1, 2003, a small rock (Ø 30 cm) crashed through the roof of a car passing the Stägjitschuggen rock cliff near St. Niklaus (Valais Alps), killing the passenger (20min 2003). (Photo courtesy by Kantonspolizei Wallis [a, b], used with permission)*

population was 8 x 10^{-2} and thus higher than the level of commonly accepted risk. Other studies assessing the hazard from rockfall on a highway or along transportation corridors in Canada have been realized by Hungr & Beckie (1998) or Hungr *et al.* (1999). In Central Italy, rockfall hazard and risks have been investigated along transportation corridors as well (Guzzetti *et al.* 2004). Here, the approach is based on the recurrence of rockfall, 'frequency–volume statistics' obtained from inventories of recent rockfalls (see Chapter A1.3) and the results of a physically based, spatially distributed rockfall simulation model. Results indicate a frequency of 0.12 events per year on the 32 km of roads investigated.

Occasionally, rockfall hazard and risk have also been studied in connection with earthquake activity. The coupling of earthquake with rockfall analysis was e.g., performed by Jibson *et al.* (1998), who created digital probabilistic maps of 'landslide' hazards in relation to seismic activity in the *Los Angeles* area. Marzorati *et al.* (2002) used a similar approach to determine predictive rules for the 'hazard estimation' of rockfall triggered by earthquakes. Their GIS-based approach primarily considered strong ground motion parameters of past earthquakes, locations of mass movements, slope angles and geology. Relations existing among environmental, seismic factors and rockfall occurrence were conducted with a multiple regression analysis. Even though the resulting 'rockfall susceptibility maps' do not, as such, present risk maps, they nonetheless represent a valuable tool for earthquake–rockfall hazard mitigation and emergency planning.

However, while assessing the 'landing probability', these studies did not necessarily consider the 'failure probability', which has, so far, been commonly investigated with probabilistic methods, e.g., *'Monte Carlo'* simulations or a combination of historical, geomechanical and probabilistic approaches (Cancelli & Crosta 1993, Hoek 1998a, b, Rouiller *et al.* 1998, Mazzoccola & Sciesa 2000, Nilsen 2000, Dussauge-Peisser *et al.* 2002, Hantz *et al.* 2003a, b).

*****

2 DENDROGEOMORPHOLOGY

2.1 A GENERAL INTRODUCTION TO TREE-RING ANALYSIS IN THE FIELD OF GEOMORPHOLOGY [1]

Over the past few decades, tree-ring research has gradually evolved from the dating of wood (dendrochronology, dendroarcheology) to the much broader field of dendroecology, including all areas of science involved in drawing some type of environmental information from tree-ring sequences (SCHWEINGRUBER 1996). In this sense, 'dendrogeomorphology' represents one of the many subfields of dendroecology and has repeatedly been used to study and date past geomorphic processes. The approach, developed by ALESTALO (1971) and refined by SHRODER (1978), takes advantage of the fact that trees form yearly increment rings and that they immediately react to external disturbances. Figure A2.1 illustrates that as a reaction to the impacts caused by snow avalanche, landslide, debris flow or rockfall activity, trees (i) gradually redress their

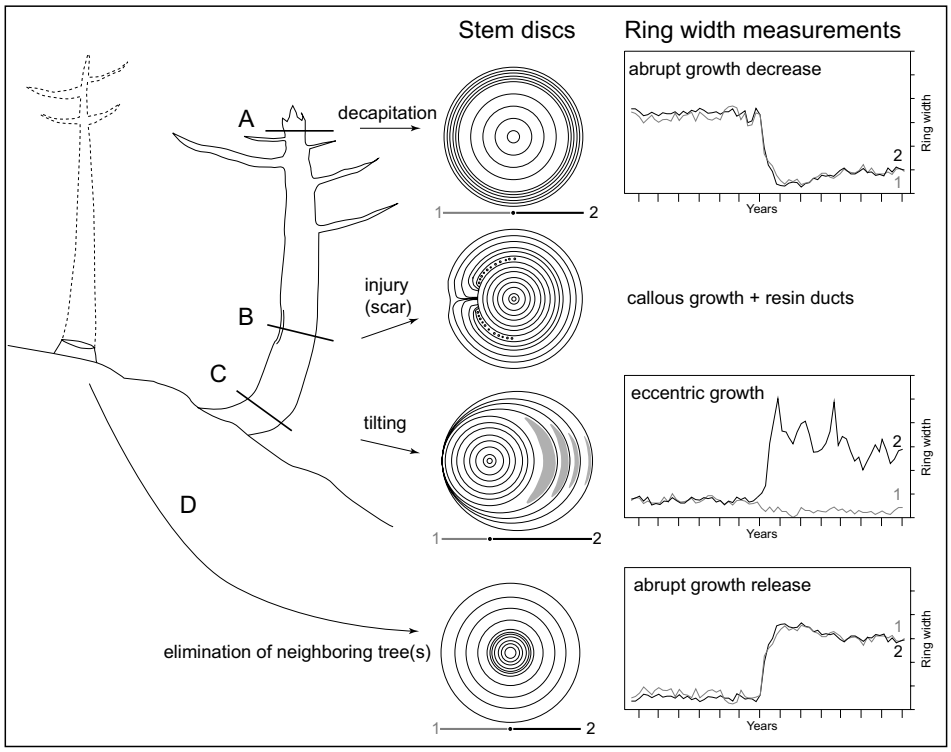

Fig. A2.1 *Evidence used to infer rockfall events from tree-ring sequences: Visual analysis of the samples (left) and the measurement of tree-ring widths (right) allows identification of sudden growth releases, growth suppressions, reaction wood, callous tissue or traumatic rows of resin ducts.*

[1] Major parts of the chapter 'Dendrogeomorphology' have been adapted from a paper accepted for publication in «Natural Hazards». The complete article - entitled 'A review of studies dealing with tree rings and past rockfall activity: The role of dendrogeomorphology in natural hazard research' is reproduced in Chapter F (Appendix 1).

stems with the formation of reaction wood after tilting through instability or unilateral pressure, (ii) overgrow their scars after injury or even (c) concentrate cell formation to areas vital for survival after decapitation and the loss of important branches or roots. Sudden reductions in tree-ring growth also occur as a reaction to the partial burying of the tree stem with subsequent shortage in nutrient supply (Strunk 1997) or the exposure of roots through erosional processes.

In addition, the elimination of trees through geomorphic events can result in growth releases in undamaged neighboring trees, as they can suddenly take advantage of improved environmental conditions (e.g., light, nutrients, water). Finally, certain conifer species even form traumatic rows of resin ducts after cambial damage.

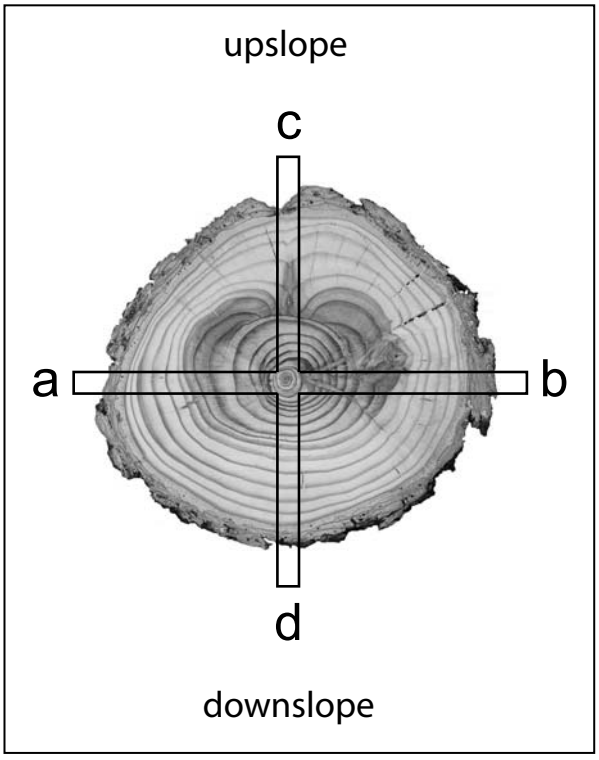

Fig. A2.2 *Cross-section of a scarred Larix decidua with indication of the sampling positions a, b, c and d for increment cores.*

Figure A2.1 summarizes the different reactions of trees to geomorphic events and how the responses may look in tree-ring sequences. Further details on the principles of dendrogeomorphology or tree reactions to external processes can be *inter alia* found in Shroder (1980), Shroder & Butler (1987), Bräuning (1995) or Wiles *et al.* (1996).

Dendrogeomorphological analyses comprise both investigations in the field and work in the laboratory: In the field, detailed geomorphic investigations and process analyses must precede the sampling of trees. Only when the geomorphic process and its area of influence have been determined, should cores either be extracted from trees with increment borers or, ideally, stem discs (cross-sections) sawn. As illustrated in Figure A2.2, increment cores are normally taken in the fall line of the process in question, i.e. one core upslope (core c) and one core downslope (core d). In addition and because rockfall may also injure trees laterally, further samples should be taken perpendicular to the slope (cores a, b) along with cores extracted from the visible wound and the overgrowing callous.

Samples are then prepared in the laboratory (Phipps 1985, Krusic *et al.* 1987) and analyzed visually, with obvious growth anomalies such as abrupt growth changes, the onset of reaction wood, resin ducts or scars noted on skeleton plots (Schweingruber *et al.* 1990). This graphic method assists in cross-dating samples and aims at identifying and locating missing or false rings through comparison of one tree-ring sequence with the next sequential record (Wiles *et al.* 1996). In a further step, ring-widths are measured using digital positioning tables. Thereafter, data are processed following the procedures described by Bräker (2002). As growth reactions can be caused by factors other than geomorphic ones, increment curves of disturbed trees then need to be cross-dated with a reference chronology. This chronology, built with undisturbed samples from a nearby forest stand, reflects growth conditions driven by exclusively environmental factors such as altitude, slope exposure, temperature, precipitation or occasional insect outbreaks (Fritts 1976, Graybill 1982, Cook & Kairiukstis 1990, Schweingruber 1996). A comparison of the reference chronology with the tree-ring sequences of disturbed trees allows (a) distinguishing locally predominant growth patterns from disturbances induced by geomorphic processes and (b) accurately dating them with, at least, yearly resolution.

Results from the different trees sampled within the study area can then be compared and, sample depth permitting, frequencies or volumes for the slope in question derived. In addition, data on e.g., the lateral dispersion or the maximum reach of single events can be analyzed and represented with interpolations. A detailed illustration of dendrochronological approaches (i.e., methods as well as single working steps) used to study past rockfall activity is given in Chapter F (Appendix 5).

Over the last few years, tree rings have been extensively used to analyze processes such as landslides (Jacoby *et al.* 1992, Lateltin *et al.* 1997, Raetzo-Brülhart 1997, Fantucci & Sorriso-Valvo 1999, Stefanini 2004), debris flows (Strunk 1995, Baumann & Kaiser 1999, Stoffel *et al.* 2004, 2005a), flooding (Hupp 1988, LePage & Bégin 1996, St. George & Nielson 2003), snow avalanches (Butler *et al.* 1992, Patten & Knight 1994, Rayback 1998, Hebertson & Jenkins 2003), earthquakes (Jacoby *et al.* 1988, 1992, Jacoby 1997, Lin & Lin 1998, Van Arsdale *et al.* 1998, Allen *et al.* 1999, Vittoz *et al.* 2001, Fantucci 2002), volcanic eruptions (Kaiser & Kaiser-Bernhard 1987, Baillie 1994, Biondo *et al*. 2003) or movements of rock glaciers (Carter *et al.* 1999, Bachrach *et al.* 2004).

the scars was in all cases of rockfall origin, the process responsible for the damage to the trees was not rockfall. While in the studies presented by Moore & Mathews (1978) and Butler *et al.* (1986), the process was described as a downslope displacement of rock particles in a 'rapid flow-like movement' (also see Chapter A1.1), different debris transfer processes (e.g., frost-coated clast flows, niveo-aeolian sedimentation, debris flows, snow avalanches) seem to be responsible for the remobilization of small rockfall clast (Ø 2,36 cm) on the slopes of the *Gaspé Peninsula*.

The first dendrogeomorphological analysis purely focusing on rockfall activity was performed on different slopes at *Brienzergrat* (*Bernese Oberland*, Switzerland), where Gsteiger (1989) analyzed three beech (*Fagus sylvatica*) and four Norway spruce trees (*Picea abies*). Trees were felled for analysis and 25 stem discs prepared. In total, analysis allowed identification of 56 rockfall scars, 37 in the beech and 19 in the spruce samples. Even though the century-old trees were entirely felled for analysis, only the lowermost section of the trunks was analyzed. Scars occurring higher up on the stem were disregarded. Moreover, Gsteiger (1993) realized a first attempt to illustrate spatial variations in rockfall activity by analyzing the number and distribution of scars visible on the stem surface to derive rockfall activity maps (*Aktivitätskartierung*).

Another study using stem discs to determine past rockfall activity was performed at the foot of a slope near *Bourg St. Pierre* (*Valais*, Switzerland), where a "rockfall chronology" (1890–1987) was built with 30 cross-sections sampled at the base of previously felled Norway spruce trees (Schweingruber 1996). A

Fig. A2.3 *Sawing of cross-sections from previously felled Picea abies stumps at the foot of the Schwarzenberg rockwall (Diemtigtal, Bernese Prealps). (Photo courtesy by Simone Perret, used with permission)*

2.2 Studies dealing with tree rings and past rockfall activity – a state of the art

Surprisingly, and despite the potential of dendrogeomorphological methods, rockfall activity has only rarely been studied through the analysis of tree-ring sequences. The work of Moore & Mathews (1978) seems to represent the first (published) attempt to date the impacts of rocks on trees with dendrogeomorphological methods, resulting in the reconstruction of the historical *'Rubble Creek'* rockfall avalanche in southwestern *British Columbia* (Canada). Similarly, Butler *et al.* (1986) dated two recent 'rockfall avalanches' located in *Glacier National Park* (*Montana*, USA). On the *Gaspé Peninsula* (Canada), cross-sections were analyzed to determine annual sedimentation rates and recent displacements of forest edges on active scree slopes (Hétu 1990, Lafortune *et al.* 1997, Hétu & Gray 2000). Even though the material causing

total of 66 scars could be identified and periods with abundant (1953–1960) or infrequent rockfall activity (1941–1949) determined. The study also indicates that the construction of a road across the slope prevented rockfall from reaching the lowermost part of the slope after 1970. Schweingruber (1996) concludes that his "rockfall frequency" would most likely be correlated with the frequency of precipitation. The study finally illustrates the spatial distribution of injured and non-injured trees with dots of different color. On a slope in the *Val Calanca* (*Grisons*, Switzerland), Hopfmüller (1997) sampled 52 stem discs at the base of previously felled and 66 increment cores from 33 living Norway spruce trees. While 42 injuries were found on the cross-sections, the increment cores allowed identification of 52 scars. Nonetheless, only two thirds of the scars could be precisely dated, as the wood of 22 samples proved to be rotten. In contrast, the age of the injuries in the decaying samples was given with an error margin ranging from ±1 to ±10 years. Results indicate increased rockfall activity during the 1940s and after 1955 (until 1965). In addition to the high frequency–low magnitude activity, two large 'rockfalls' (*Felsstürze*) were identified, causing 12 scars in the winter of 1938/39 and even 30 wounds in the subsequent winter (1939/40).

*****

3 Aims and structure of this study

In their totality, the previously mentioned studies contributed considerably to a better understanding of the rockfall process as well as of interactions between rockfall, trees and tree-rings in mountain forests in particular.

Nonetheless, studies focusing on the seasonal timing, the frequency or volumes of (past) rockfall events, impact heights of rocks on trees, the visibility of (overgrown) scars on stem surfaces as well as strengths, weaknesses or methodological uncertainties of tree ring–rockfall analyses remain too scarce or even non-existent.

As a consequence, very essential – not to say basic – knowledge on the behavior of rocks and boulders in forests and the reaction of trees and tree-rings to impinging rockfall fragments continues to be lacking as soon as rockfall hazards are assessed, risks analyzed, rockfall processes modeled, the protective effect of mountain forests assessed or countermeasures against rockfall planned.

It is therefore the aim of this interdisciplinary PhD thesis to study (past) rockfall activity on forested slopes with dendrogeomorphological methods in order to assess the seasonal timing, the frequency and the volumes of rockfall occurring on a forested slope within the southern *Swiss Alps*.

In addition, this thesis focuses on the vertical distribution and the visibility of scars on stem surfaces of trees, before some strengths and weaknesses of dendrogeomorphological methods are addressed. In summary, the specific issues of this thesis are

- to determine the seasonal timing of rockfall activity on cross-sections and thincuts of juvenile trees (Chapter B1)
- to investigate long-term fluctuations, spatial distributions and recurrence intervals of rockfall with increment cores taken from century-old trees (Chapter B2)
- to study the vertical distribution and the visibility of scars on the stem surface of adult trees (Chapter C)
- to point out methodological problems occurring when trees and tree-rings are used to assess (past) rockfall activity as well as to illustrate strengths and weaknesses of tree-ring analyses in the field of rockfall research (Chapter D)

Each of these issues is addressed in one of the four papers which form the core of this thesis and which are either published, in press or submitted for publication. Each paper is accompanied by its own introduction where the specific issues under consideration are addressed in more detail. Even though short descriptions of the study sites are given in Chapters B1, B2, C and D, the principle study sites *Täschgufer* (*Täsch*, VS) and *Altdorfer Bannwald* (*Altdorf*, UR) are described and illustrated in Chapter A4 as well.

An overall conclusion (Chapter E) and five appendices (Chapter F) complement this work. The appendix includes three papers (co-)written by the author of the PhD thesis, a first one giving a literature review of tree-ring analysis dealing with rockfall (Stoffel 2005a), a second one focusing on spatio-temporal variations of rockfall activity on a slope in the *Diemtigtal* (Perret *et al.* 2005b; *Bernese Prealps*, Switzerland) and a third one assessing the accuracy of the 3D process-based rockfall model *Rockyfor* and the protective effect of forest stands on several sites within Switzerland (Stoffel *et al.* 2005d). In addition, the study

site *Täschgufer* is illustrated with a series of photographs in Chapter F4 and a detailed description given on how increment cores and cross-section have been sampled and raw tree-ring data processed within this thesis (Chapter F5). An overall bibliography and curriculum vitae complete the thesis. [2]

*****

[2] In all papers, the spelling is left as it was submitted for publication, meaning that in contrast to the rest of the PhD thesis written in American English, Chapter F2 (Perret *et al.* 2005b) was left in British English.

4 STUDY SITES

4.1 INTRODUCTORY COMMENTS AND LOCALIZATION OF STUDY SITES

Analyses related to this PhD study have been realized within Switzerland. A majority of results were gathered from trees growing on the forested slope *Täschgufer* (*Täsch*, VS, Chapters B1, B2, and D). Consequently, the site description will primarily focus on this area. In addition, a short description is given for the *Altdorfer Bannwald* (*Altdorf*, UR), even though the analysis of three adult trees felled in this stand primarily followed theoretical goals and not the reconstruction of frequencies or volumes (Chapter C). In contrast, no site description will be provided for *Brienzergrat* (GSTEIGER 1989, 1993) and *Schwarzenberg* (PERRET *et al.* 2004b, 2005a, b), as data on rockfall activity have not been gathered by the author of this PhD study and were exclusively used for comparison of impact heights and the visibility of scars on stem surfaces (Chapter D). All the study sites mentioned in this paragraph are illustrated in Figure A4.1.

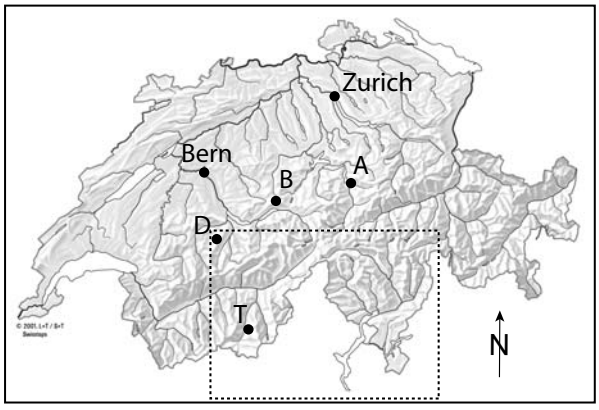

Fig. A4.1 *Localization of the principle study sites Altdorfer Bannwald (Altdorf, UR), indicated with A, and Täschgufer (Täsch, VS), marked with T. In addition, data from existing studies have been used for comparison, namely from sites B for Brienzergrat (Brienz, BE) and D for Diemtigtal (Entschwil, BE). The dashed rectangle refers to the map reproduced in Figure A4.9. All sites are located in Switzerland.*

4.2 TÄSCHGUFER (TÄSCH, VS)

Täschgufer is a west-facing rockfall slope descending from the *Leiterspitzen* summit (46°4'N, 7°47'E, 3214 m a.s.l.; cf. Fig. A4.2). The area lays in the *Nikolaital* (VS) and NE of the village of *Täsch*, a small settlement with a mere 850 permanent inhabitants. Figure A4.2 shows the village and shows the overall situation on the *Täschgufer* slope.[3]

4.2.1 Geology

The bedrock at *Täschgufer* is built of eruptive rocks. The unit is of pre-Triassic age and was probably formed before the Upper Carboniferous (> 300 million years BP). Polymethamorphic processes have since remodeled the crystalline rocks and gave birth to a garnet-bearing paragneiss containing lenses of amphibolites and prasinites. The paragneiss units at *Täschgufer* belong – geologically speaking – to a contact zone (= *Schuppenzone*) between the *Siviez-Mischabel* and the *Monte Rosa* nappes (BEARTH 1964, WICHT & JORIS 1985, MARRO 1994, LAUBER 1995).

The rockwalls underneath the *Leiterspitzen* summit are heavily disintegrated. Layers of this weak bedrock

[3] Further pictures illustrating the summit area, the departure zones, the forest at *Täschgufer* as well as the rockfall dams can be found in Chapter F (Appendix 4).

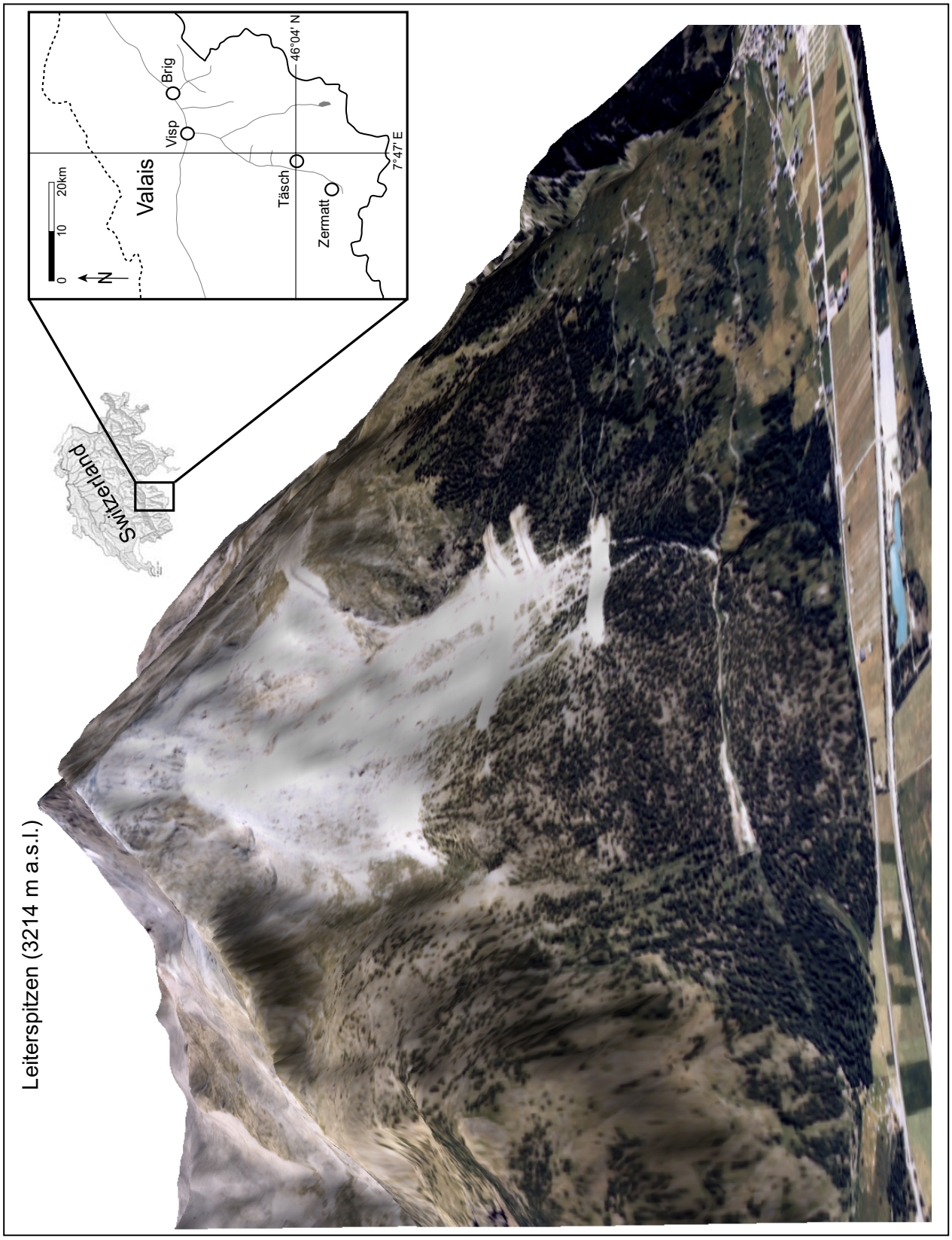

Fig. A4.2 *Three-dimensional view from NNE towards Täschgufer and the Leiterspitzen summit. In the upper part of the slope, bedrock and vegetation-free talus slopes prevail, while sparsely forested deposits of an ancient rockslide characterize the landscape in the lower half of the slope. In the late 1980s and until 1998, seven rockfall protection dams have been built at Täschgufer as to protect the village and the cantonal road from rocks and boulders. (Aerial photographs arranged in* ERDAS IMAGINE (2005)*; copyright of aerial photographs by* SWISSPHOTO (2000)*; used with permission)*

Fig. A4.3 *In the summit area, several layers of the heavily fissured and disintegrated bedrock of paragneissic origin are protruding out from the slope. (Photo courtesy by Theo Lauber; used with permission)*

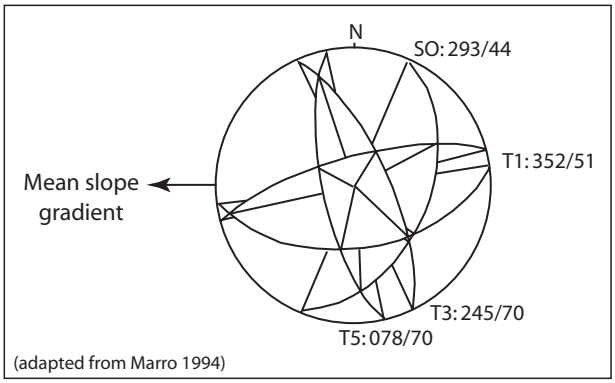

Fig. A4.4 *Schmidt-Lambert projection of the discontinuity plains and the schistosity as observed in the summit area of the Täschgufer slope (adapted after* Marro 1994*).*

generally strike SSW and dip WNW with angles of 40–80°, thus containing joints dipping out of the slope (Lauber 1995; Fig. A4.3). Luckily, structural and geomechanical analysis of the discontinuity plains (Marro 1994) indicate that the schistosity would only allow the release of superficial rockfall events with volumes remaining limited to – in the worst case – some hundreds of cubic-meters. The different discontinuity plains as well as the predominant schistosity occurring in the summit areas are illustrated with a Schmidt-Lambert projection in Figure A4.4. Pictures illustrating the discontinuities and joints occurring on the slope are reproduced in Chapter F (Appendix 4).

4.2.2 Topography

The rockfall slope at *Täschgufer* has a considerable length (2300 m), an important difference in elevation (1670 m) and a *Fahrböschung* of 35°. Maximum slope gradients occur near the summit area (3000 to 2900 m a.s.l.), where they reach 48°. Thereafter, the slope gets generally flatter and slope gradients gradually decrease to reach 20° next to the valley floor. Figure A4.5 gives an overall impression on the horizontal distance, the difference in elevation and the *Fahrböschung sensu* Heim (1932) as observed at *Täschgufer*.

4.2.3 Temperature, precipitation and permafrost

Meteorological data are not available for the study area. Mean annual air temperatures therefore need to be derived from meteorological data registered at the *Zermatt* station (Smi 2003). Consequently, mean annual air temperatures of +4.5° C for *Täsch* and –4.5° C for the *Leiterspitzen* summit were determined using a local temperature lapse of 5.1° C km $^{-1}$ as suggested by King (1996). Precipitation is most frequent between August and November, including persistent rain from low-pressure masses located in the *Mediterranean Sea* (Grebner 1994). On the sparsely wooded surfaces at around 1800 m a.s.l., annual average precipitation is estimated to 660 mm. Here, snow usually covers the slope in early winter, reaching an averaged maximum depth of around 70 cm in early March (Smi 2000). Snowmelt generally starts in mid March. In contrast, snow accumulation is modest on the steep slopes above 2000 m a.s.l. and surfaces remain largely snow-free during the winter months.

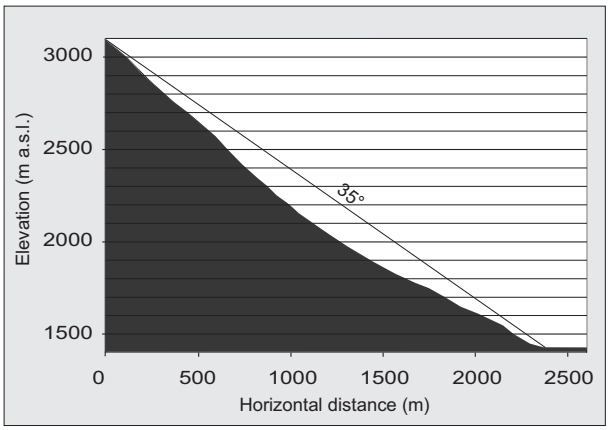

Fig. A4.5 *Difference in elevation, horizontal distance and Fahrböschung between the uppermost point of departure and the farthermost point of deposition at Täschgufer (adapted from* Schneuwly 2003*).*

Fig. A4.6 *The stand at Täschgufer has a density of only 150 trees ha $^{-1}$, leaving lots of space for rockfall fragments traveling downslope.*

Fig. A4.7 *In the areas most heavily affected by rockfall, the forest cover reaches 1780 m a.s.l.. (Photo courtesy by Dominique Schneuwly; used with permission)*

A locally calibrated permafrost distribution model suggests the presence of permafrost in the upper part of the slope and seasonal frost below (Gruber & Hoelzle 2001). The existence of contemporary permafrost has been confirmed on the southern edge of the slope between 2400 and 2500 m a.s.l., where ground ice was encountered during construction work (Haeberli 1992, 1995).

4.2.4 Forest cover

The forest at *Täschgufer* predominantly consists of European larch (*Larix decidua* Mill.), accompanied by single Norway spruce (*Picea abies* (L.) Karst.) and Swiss stone pine (*Pinus cembra* ssp. *sibirica*). Tree densities oscillate around 150 trees ha $^{-1}$ and the mean DBH is 30 cm (Fig. A4.6). The European larches also form the regional timberline, reaching approximately 2300 m a.s.l. in the immediate neighborhood of the rockfall slope. In the areas that are most heavily affected by rockfall, continuous forest cover reaches only 1780 m a.s.l. As shown in Figure A4.7, surfaces are sparsely wooded in this part of the slope and large sectors remain free of vegetation.

4.2.5 Rockslides, large rockfalls and rockfall processes

Both landscape and topography at *Täschgufer* are clearly marked by the deposits of a large postglacial 'rockslide' (*Bergsturz;* Figs. A4.8). In contrast, the event did apparently not leave many traces in written sources: According to Zurbriggen (1952), the *Bergsturz* would have destroyed the first settlement of *Täsch* and occurred before 1423 AD, when the church rebuilt after the event was – for the first time – mentioned in local chronicles. Similarly, Joris (1995) states that lichen growth on 'rockslide' boulders indicates an age of 600–1500 years BP for the event. The deposits at *Täschgufer* are only one testimony of important Holocene rockslide activity within the *Nikolaital*, where several dozen rockslides and *sackung* processes can be

Fig. A4.8 *The deposits of an ancient rockslide chiefly characterize the landscape of the west-facing slope at Täschgufer. (Photo courtesy (left) by CREALP/Christian Marro; used with permission)*

identified (e.g., Eisbacher & Clague 1984, Joris 1995). These events were predominantly triggered from west-facing slopes, where the western dipping of geological layers favored instability. East-facing slopes would be, in contrast and although heavily fissured, less prone to produce large rockslides (Bearth 1964). In April and May 1991, however, a series of very 'large rock-falls' (*Felssturzserie*; 30 million m^3) collapsed from the *Grossgufer* rockwall northwest of *Randa* (e.g., Götz & Zimmermann 1993, Schindler *et al.* 1993, Eberhardt

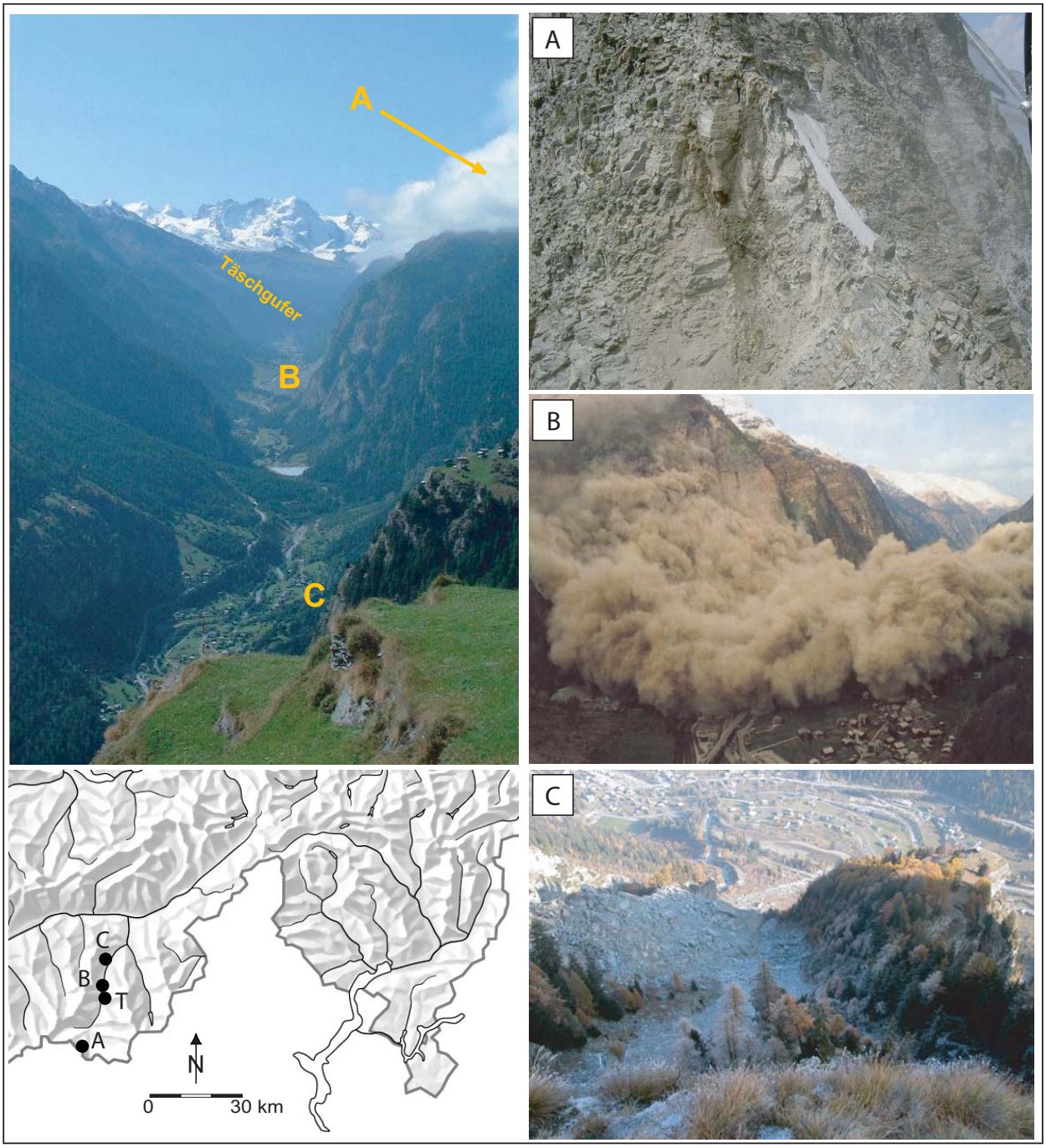

Fig. A4.9 *(a) In July 2003, 'rockfalls' affected a section of the normal route leading to the summit of the Matterhorn (Zermatt); (b) Huge volumes of dust temporarily covered the village of Randa during and in the days after the 'very large rockfalls' at Grossgufer in 1991; (c) In October 2003, 'rockfalls' were artificially triggered at Medji, as they threatened several buildings in the southern parts of the village of St. Niklaus. The three sites are shown on the map as well as on the overview photo of the Nikolaital. (Photo courtesy by* Air Zermatt (2003) *[a], CREALP/Jean-Daniel Rouiller [b] and Rovina + Partner AG [c], used with permission)*

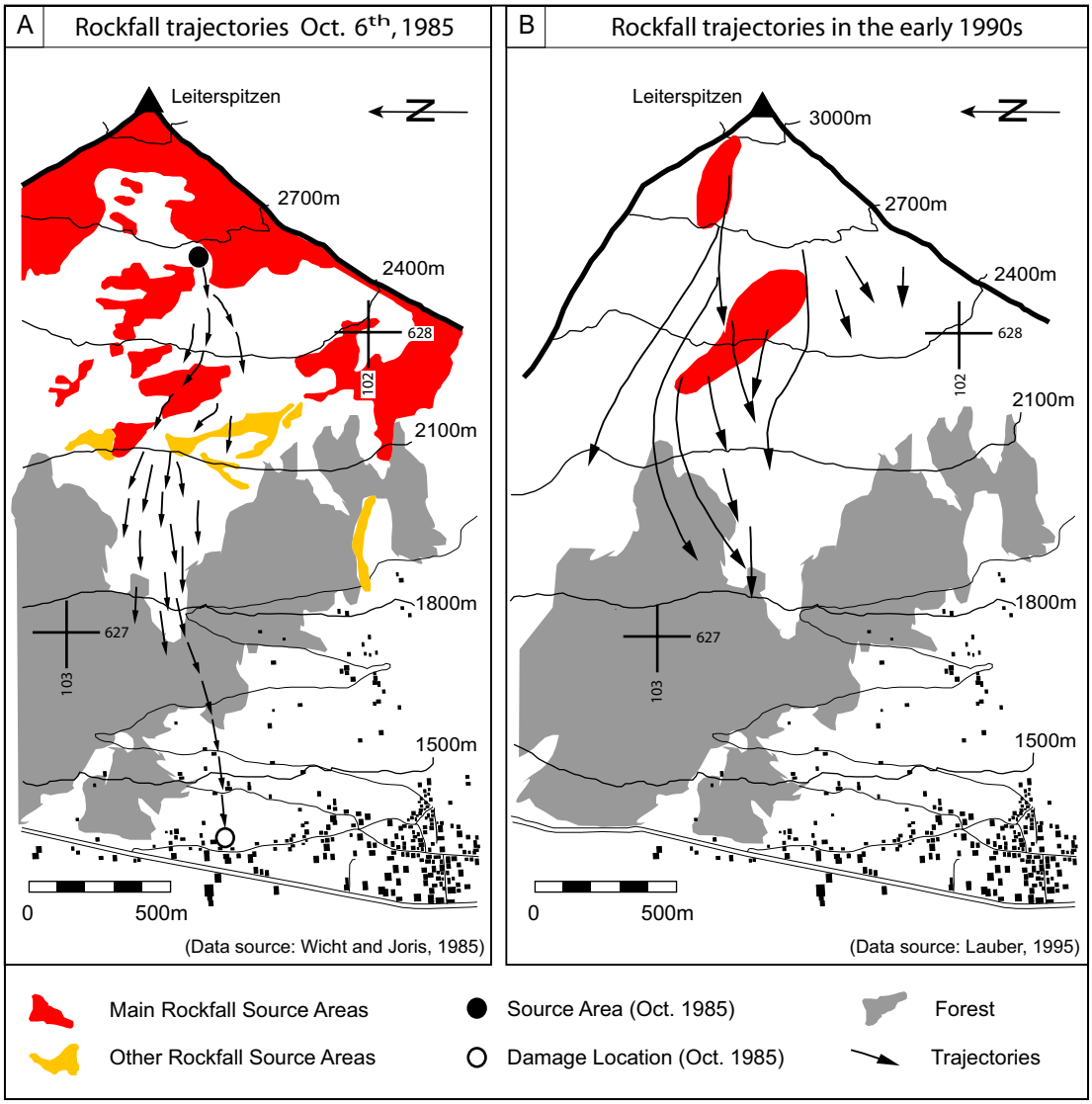

Fig. A4.10 *Rockfall source areas at Täschgufer and trajectories of past rockfall activity as identified by (a)* Wicht & Joris (1985) *as well as (b)* Lauber (1995). *(A) The first graphic gives all the potential departure zones of rockfall along with the trajectories of rocks and boulders as observed during the October 6, 1985 event, when a stable was destroyed in the building zone of Täsch. (B)* Lauber (1995)*, in contrast, focuses on the active rockfall departure zones as observed in the late 1980s and the early 1990s.*

et al. 2001, 2004, Sartori *et al.* 2003, Jaboyedoff *et al.* 2004, Segalini & Giani 2004). In July 2003, a comparably tiny *Felssturz* of only a few 1000 m^3 gained worldwide media interest (Faz 2003), as it affected a section of the normal route leading to the summit of the *Matterhorn* (*Zermatt*). Only a few months later, another *Felssturz* threatened several buildings in the southern parts of the village of *St. Niklaus* (*Medji*; Jaboyedoff *et al.* 2003a, b, Ladner *et al.* 2004). The location of the different sites mentioned in this paragraph is given, along with some illustrations, in Figure A4.9.

In addition, small 'rockfall' events very frequently take place in the *Nikolaital*. At *Täschgufer*, rockfall regularly occurs on the slope, originating from various rockfall source areas (Fig. A4.10). In addition, the remobilization of rocks is common from the steep slopes of loose rockfall debris located above 2100 m a.s.l., as shown in Chapter F (Appendix 4). While Wicht & Joris (1985) classified almost all paragneissic rockwalls as potential rockfall source areas (Fig. A4.10a), Lauber (1995) rather gives an idea on the departure zones of rockfall fragments as observed in the late 1980s and early 1990s. As can be seen from Figure A4.10b, a first source area would be located

between 2300 and 2600 m a.s.l., another one above 2700 m a.s.l.

The size of single rockfall events at *Täschgufer* normally does not exceed 1–2 m^3. Some characteristic types of rockfall fragments are illustrated in Figure A4.11. However, rockfall sometimes also involves larger volumes. For instance, an estimated 100 m^3 of rockfall fragments was released on October 6, 1985, destroying an agricultural building (i.e. stable) within the construction zone of *Täsch* (Fig. A4.10a). According to Wicht & Joris (1985), the rockfall mass was disintegrated during the fall. Furthermore, the falling mass triggered secondary rockfall by remobilizing material from the talus. Most of the rocks and boulders would have come to a stop on the talus slope or within the adjacent forest, while one 'wheel-shaped' boulder (1–2 m^3) was able to pass the protection forest. Impact craters identified in the field indicate considerable jump distances and only very few contacts with the ground (Fig. A4.12). The departure zone – located at 2650 m a.s.l., the location of the damaged site in the valley floor as well as the approximate position of rockfall trajectories are given in Figure A4.13a. Lauber (1995) further indicates that rockfall activity apparently increased on the slope and repeatedly caused damage to transportation corridors (roads, hiking trails) in the mid-1980s and again after 1993. As a response, the construction of an unhitched road for construction traffic and an earth-fill deflection dam initiated the realization of major protection measures on the slope in 1988 (cf. Fig. B1.1 and Chapter F, Appendix 4 for details). Further earth fill deflection dams were built in the succeeding year. Finally, two large protection dams were erected north of the existing constructions in 1996/97 (400 m in length) and 1998 (260 m in length).

Fig. A4.11 *Due to the schistosity and the fissures present in the bedrock, rockfall fragments at Täschgufer are quite often 'wheel-shaped' and of limited volume (< 1 m^3), but large boulders occur as well: (a) Medium-sized (70 × 70 × 6 cm, 0.03 m^3), (b) large (160 × 90 × 30 cm, 0.43 m^3); (c) very large boulder (220 × 120 × 90 cm, 2.38 m^3).*

Fig. A4.12 *Large impact craters can regularly be observed in the field (crater illustrated on the right image: 150 × 230 cm, depth: 60 cm). (Photo courtesy (left) by Theo Lauber, used with permission)*

4.2.6 Other processes

Other processes occur in the surroundings of *Täsch* as well. For instance, small debris flows regularly cause damage at the foot of the *Täschgufer* slope. Single events generally amount to only a few cubic-meters and move downslope in well-defined channels (Bollschweiler *et al.* 2005). Much larger debris flows are reported for the *Täschbach* located south of the study area (Huggel *et al.* 2002, 2003) and floods repeatedly occurred in the *Mattervispa* (Bonnard & Gardel 1997). While large and destructive snow avalanches repeatedly affected transportation corridors (i.e. railway, road) and infrastructure on adjacent slopes and in the valley floor (Schneebeli *et al.* 1998, Bloetzer *et al.* 1998, Stoffel 1999), they have never been witnessed at *Täschgufer*.

4.3 Altdorfer Bannwald (Altdorf, UR)

The *Altdorfer Bannwald* is located NNE of the village of *Altdorf* (UR, Switzerland; 46°54'N, 8°39'E; also see Fig. A4.13), extends from 440 to 1600 m a.s.l. and covers more than 300 hectares (Annen & Redmann 1993). Mean slope gradients in the forest average 70 to 80% and the forest mainly consists of *Fagus sylvatica* in the lower parts of the slope (< 1200 m a.s.l.), whereas *Picea abies* pre-

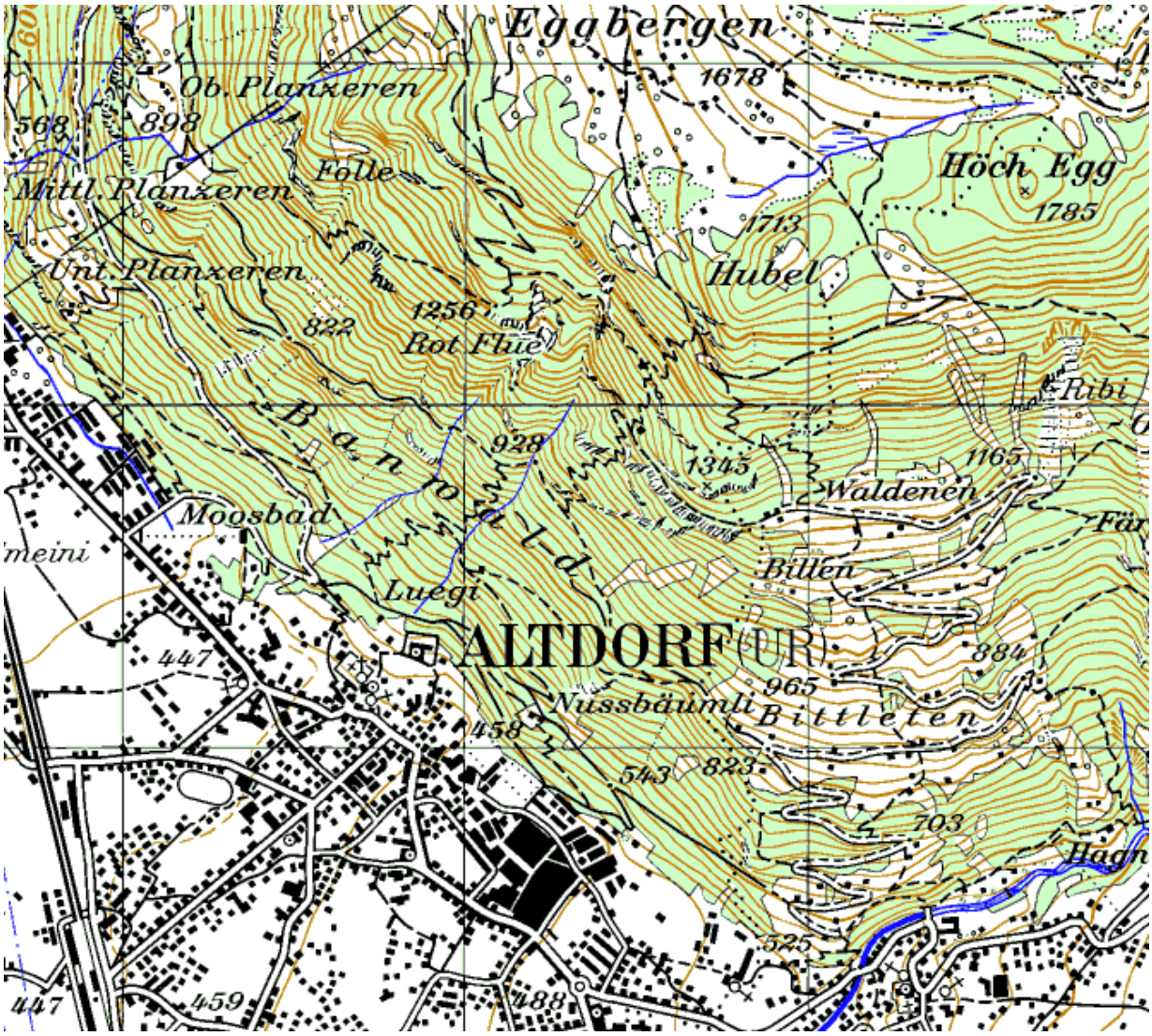

Fig. A4.13 *Topographic map indicating the study site Altdorfer Bannwald, the village of Altdorf, Eggberge and the Rot Flüe. Extract of the national map 246 (Klausenpass) in a scale of 1:50'000. Reproduced with the permission of Swisstopo (BA057233).*

Fig. A4.14 *Scars visible on the stem surface of a century-old Picea abies tree from the Altdorfer Bannwald UR...*

Fig. A4.15 *... and on a Fagus sylvatica tree.*

dominates in the subalpine forest, which is locally shifted to > 1600 m a.s.l. through the presence of frequent foehn winds. In addition, the dry soils covering bedrock and exposed cliffs are locally colonized by *Pinus sylvestris*.

Bedrock on the slope is part of the *Schächental Flysch* unit, forming a compilation of sandstone and clay layers. Rockfall is frequently triggered from these heavily fissured formations. Individual rocks are commonly quite small, but boulders of up to 10 m^3 (> 30 tons) have been observed as well. On 16 August 1973, rockfalls even triggered 8000 m^3 from the 100 m high cliff at *'Rot Flue'* (Niederberger 2002). Evidence of other large rockfalls can be identified in the field and in local chronicles, indicating that major activity occurred in 1268 or 1886. The latter event would have caused severe damage to the church and adjacent buildings in the valley floor (Annen & Redmann 1993). Today, rockfall is most frequently triggered from the rock cliff at *'Rot Flue'*, but other source areas exist on the slope as well. Niederberger (2002) indicates that rockfall activity would locally be favored through frequent freeze–thaw cycles or periods with intense precipitation. Signs of rockfall activity are also preserved in the stems of the trees colonizing the *Altdorfer Bannwald*. According to field data gathered during the 'Sanasilva' program, 36% of the trees growing on the slope would show visible signs of past rockfall impacts (Jahn 1988; Figs. A4.14 and A4.15). In addition, debris flows repeatedly occurred in the *Kapuzinertal*, where they caused human losses and the destruction of buildings in e.g., 1910 (Niederberger 2002).

As a result of rockfall and debris-flow activity, the *Altdorfer Bannwald* was first declared "protected" (*gebannt*) in 1387 AD. Over the centuries, private needs and economic pressure lead, however, to a considerable overuse of the forest, hindering sustainable development and the rise of seedlings. In the 19th century, the miserable state of the protection forest necessitated reaction and some 100,000 trees

have been planted between 1878 and 1885. Similarly, the construction of protection dams was initiated around 1890. These dams are still in use today, together with protection nets installed along forest roads in the last decades. In addition, appropriate forest management more and more allowed sustainable development of the protection forest. Today, the forest service of the *Korporations-Bürgergemeinde Altdorf* fells approximately 1000 m^3 of wood and invests ca. CHF 220'000 every year to guarantee desirable forest structures and sufficient long-term protection for the village of *Altdorf*. In late 2002, a guided walk has been opened in the *Altdorfer Bannwald* between *Altdorf* and *Eggberge* (*"schutz.wald.mensch", Lernpfad Altdorf*; Niederberger 2002), illustrating some of the aspects described above.

*****

CHAPTER B

ASSESSING PAST ROCKFALL ACTIVITY WITH TREE RINGS

Tree rings have been used to investigate the seasonality, frequency and magnitude of past rockfall activity at *Täschgufer*. The seasonal timing of rockfall activity was assessed with 270 stem discs taken from 18 juvenile *Larix decidua* trees. The onset of callous tissue and the formation of traumatic rows of resin duct were assessed with an approach previously used in forest fire reconstructions. In contrast, the frequency and magnitude of past rockfall activity was studied using 564 increment cores from 135 severely injured *Larix decidua* trees and events primarily dated through the presence of traumatic rows of resin ducts. The papers reproduced in Chapters B1 and B2 have been published in the journals *"Zeitschrift für Geomorphologie"* and *"Geomorphology"*.

1. The seasonal timing of rockfall activity

Markus Stoffel [1], Igor Lièvre [1], Michel Monbaron [1] and Simone Perret [2]

"Seasonal timing of rockfall activity on a forested slope at Täschgufer (Swiss Alps) – a dendrochronological approach"

[1] *Groupe de Recherches en Géomorphologie (GReG), Department of Geosciences, Geography, University of Fribourg*
[2] *Applied Geomorphology and Natural Risks, Department of Geography, University of Berne*

published in Zeitschrift für Geomorphologie 2005, Vol. 49, No.1, 89–106
revised: 8 October 2004, accepted: 8 December 2004

Abstract

Dendrochronology was used to study 25 years of rockfall activity on a forested slope at Täschgufer, Täsch (Swiss Alps). We introduce a new approach by evaluating the initiation of callous tissue and resin duct formation after rockfall occurrence to determine the seasonal timing of events. Results from 270 stem discs of 18 *Larix decidua* Mill. trees show distinct seasonal differences in rockfall activity and indicate that, except for the years with anthropogenic activity on the slope, the occurrence of rockfall proves to be mostly restricted to the dormancy and is rather uncommon during the vegetation period. Only 12% of the injuries occur within the vegetation period, which locally lasts from early June through mid October. In contrast, some 88% of the scars occur in the dormant season between mid October and end of May. Direct observations on the slope confirm these findings, indicating that rockfall activity is highest in April and May, when global insolation on the west-facing Täschgufer slope gradually rises and ice lenses formed from meltwater slowly disappear in the joints and fissures of the rockfall source areas. According to nearby meteorological data, rockfall at Täschgufer seems to be neither influenced by thunderstorms in summer nor abundant rainfall in autumn.

The approach used for this investigation proves to be a useful tool for analyzing differences in intra-annual rockfall activity on forested slopes. In the case of data available on the different growth phases within the vegetation period of the selected tree species at the study site, results on the seasonal timing of rockfall activity can even be given with almost monthly resolution. However, for rockfall occurring within the dormant season, tree-ring analysis needs to be completed with direct observations on the site.

Zusammenfassung

Saisonale Steinschlagverteilung auf einem bewaldeten Hang im Täschgufer (Schweizer Alpen) – ein dendrochronologischer Ansatz. Mit Hilfe dendrochronologischer Methoden wurde auf einem bewaldeten Hang im Täschgufer, Täsch (Schweizer Alpen) die Steinschlagaktivität während der letzten 25 Jahre untersucht. Um die saisonale Verteilung des Steinschlags zu bestimmen, wurde ein neuer Ansatz gewählt, welcher das Einsetzen von Kallusgewebe und Harzkanälen im geschädigten Holz untersucht. Die Ergebnisse von 270 Stammscheiben von 18 Lärchen (*Larix decidua* Mill.) zeigen deutliche saisonale Unterschiede bezüglich der Steinschlagaktivität. Mit Ausnahme der Jahre, in denen am Hang bauliche Massnahmen vorgenommen wurden, trat Steinschlag im Untersuchungsgebiet praktisch ausschliesslich während der winterlichen Wachstumspause zwischen Mitte Oktober und Ende Mai auf (88%) – Verletzungen während der Vegetationsperiode bildeten die Ausnahme (12%). Direkte Beobachtungen am Hang bestätigen diese Resultate und deuten überdies darauf hin, dass die Aktivität im April und Mai am ausgeprägtesten sein dürfte. Während dieser Periode nimmt die globale Sonneneinstrahlung am westexponierten Hang des Täschgufer kontinuierlich zu und vermag so die Eislinsen aufzutauen, die durch das Gefrieren von Schmelzwasser in den Spalten und Rissen der Anrisszonen gebildet werden konnten. Im Gegensatz dazu zeigt ein Vergleich mit Daten einer nahegelegenen Wetterstation, dass die Steinschlagaktivität im Täschgufer weder durch Sommergewitter noch durch anhaltende Niederschläge im Herbst beeinflusst wird.

Der im Rahmen dieser Untersuchung verwendete Ansatz erwies sich als geeignetes Werkzeug für die Analyse intra-annueller Variationen in der Steinschlagaktivität. Unter Einbezug der Wachstumsdaten der Baumart am untersuchten Standort lassen sich Steinschlagereignisse innerhalb der Vegetationsperiode mit nahezu monatsgenauer Auflösung wiedergeben. Jedoch werden für die Analyse von Steinschlagereignissen während der Wachstumspause zusätzliche Informationen aus direkten Beobachtungen benötigt.

Résumé

Répartition temporelle des chutes de pierre sur un versant boisé du Täschgufer (Alpes suisses) – une approche dendrochronologique. La dendrochronologie a été utilisée pour étudier 25 ans d'activités de chutes de pierres sur le versant boisé de Täschgufer, à Täsch (Alpes suisses). Une nouvelle approche, basée sur l'apparition de tissu calleux et de canaux résinifères résultant d'impacts dus à des chutes de pierres, permet de déterminer la saison des événements. Les résultats issus de l'analyse de 270 échantillons prélevés sur les troncs de 18 mélèzes (*Larix decidua* Mill.) montrent des différences saisonnières dans l'activité des chutes de pierres. A l'exception des années influencées par l'activité humaine sur le versant, la majorité des événements sont survenus durant la période de dormance et peu durant la période de végétation. Seuls 12% des blessures sont produits durant la période de végétation (début juin à mi-octobre), alors que 88% sont déterminés durant la période de dormance (mi-octobre à fin mai). Les observations directes sur le versant confirment ces résultats, indiquant que l'activité de chutes de pierres est plus importante en avril et en mai. À ce moment, l'ensoleillement global sur ce versant orienté vers l'Ouest augmente graduellement, alors que les lentilles de glace formées par l'eau de fonte disparaissent lentement des joints et fissures des roches situées dans les zones de départ des chutes de pierres. Selon les données météorologiques régionales, les chutes de pierres ne semblent ni influencées par les orages d'été, ni par les abondantes précipitations d'automne.

L'approche utilisée dans cette étude prouve qu'elle est un outil utile pour analyser les différences intra-annuelles de chutes de pierres sur un versant boisé. Si l'espèce sélectionnée sur le terrain d'étude (*Larix decidua* Mill.) montre bien les différentes phases de croissance durant la période de végétation, les résultats de l'analyse peuvent indiquer l'occurrence des chutes de pierres quasi au mois près. En revanche, pour celles survenues durant la période de dormance, l'analyse des cernes de croissance doit être complétée par des observations directes sur le site.

1.1 Introduction

Rockfall is a widespread phenomenon in mountain environments (e.g., Whalley 1984, Selby 1993, Erismann & Abele 2001). It consists of free falling, bouncing or rolling stones of different size, with volumes of single components smaller than 5m^3 (Berger *et al.* 2002). As rockfall frequently endangers inhabited areas or traffic routes in mountainous regions (Bloetzer & Stoffel 1998), it became one of the most intensely studied geomorphic process of the cliff zone (Luckman & Fiske 1995).

Previous studies have addressed the initiation and kinetics of the process (Fahey & Lefebure 1988) as well as the rates of cliff retreat (Rapp 1960a, André 1986, 1997). Recent advances focus on rockwall instability (Košták *et al.* 1998), the time prediction of rockfall (Glawe *et al.* 1993) or interacting rockfall triggers (André 2003). Perennial monitoring of rockfall activity, the measurement of near-surface rock temperatures and moisture content further allowed evaluation of freeze-thaw cycles in rockfall triggering (Hall 1997, Matsuoka & Sakai 1999). Studies on past rockfall frequency are mainly based on short-term observations in the field (Luckman 1976, Douglas 1980, Gardner 1983). Historical approaches concentrate on lichenometry, allowing evaluation of long-term changes in rockfall accretion rates as well as spatial and temporal patterns of rockfall activity (Luckman & Fiske 1995, McCarroll *et al.* 1998).

In mountain forest stands, geomorphic processes injure trees by tilting, scaring, or breaking their stems (Alestalo 1971). Affected coniferous trees react upon such impacts with reaction wood, callous tissue or resin ducts (Schweingruber 1996), allowing one to precisely date geomorphic disturbances. So far, dendrogeomorphology has mainly been applied to the analysis of mass movements (Shroder 1980, Strunk 1992, Wiles *et al.* 1996, Baumann & Kaiser 1999, Fantucci & Sorriso-Valvo 1999, Solomina 2002, Stoffel *et al.* 2004). In rockfall research, tree-ring analyses concentrated on the determination of sedimentation rates and the dynamics of forest edges on scree slopes (Lafortune *et al.* 1997, Hétu & Gray 2000). Studies on forest – rockfall interactions dealt with the analysis of rockfall scars in individual trees (Gsteiger 1993), biogeomorphology of visible scars (Perret *et al.* 2005a) or the effectiveness of mountain forests as a protection against rockfall (Bebi *et al.* 2001, Dorren *et al.* 2004a). However, the previously mentioned studies on rock-fall in mountain forests did not explore the precise information that tree-rings may furnish on intra- and inter-annual fluctuations of rockfall activity. It is therefore the purpose of the present study to analyze the frequency and the seasonal timing of rockfall using dendrochronological methods. We report on results obtained from 270 stem discs of 18 heavily injured European larch trees (*Larix decidua* Mill.). Based on methods used in fire scar analyses (Brown & Swetnam 1994, Ortloff *et al.* 1995), we introduce a new approach evaluating the initiation of callous tissue and resin ducts to analyze the seasonal timing of rockfall. Results show distinct seasonal differences in rockfall activity and indicate that, except for the years with anthropogenic activity on the slope, the occurrence of rockfall is restricted to the dormancy of trees and rather uncommon during the vegetation period. The discussion is focused on the seasonal timing and the driving factors of rockfall triggering.

1.2 Study area

The analysis is conducted on the west-facing *Täschgufer* slope descending from the *Leiterspitzen* summit (46°4'N, 7°47'E, 3214 m a.s.l.) in the *Siviez-Mischabel Range* (Valais), southern Swiss Alps (Fig. B1.1). As illustrated in Figures B1.1b and B1.2, rockfall frequently occurs on the slope, originating from the heavily disintegrated gneissic rockwalls underneath the *Leiterspitzen* summit. The figures also show that the main rockfall source areas are located between 2300 and 2600 m a.s.l. (Rockfall Source Area 1) and above 2700 m a.s.l. (Rockfall Source Area 2) as well as the main rockfall trajectories. Remobilization of rocks is common from the steep slopes of loose rockfall debris located above 2100 m a.s.l. Here mean slope gradients locally rise up to 48°. Below, slope gradients gradually decrease to reach 20° next to the valley floor. Maximum sizes of single rocks at *Täschgufer* do normally not trespass 1-2 m^3.

Besides frequent rockfall activity, one major rockslide on the *Täschgufer* slope is noted in local chronicles (Zurbriggen 1952). Its age was estimated with lichenometry to at least 600 years BP (Joris 1995). Furthermore, small debris flows occur on the *Täschgufer* slope. Single surges generally count a few cubic meters and pass the slope in well-defined channels. Avalanches have not been witnessed on the slope. Next to the rockfall slope, the local timberline is formed by European larch (*Larix decidua* Mill.) at about 2300 m a.s.l.. In the part heavily affected by rockfall, the surface is sparsely wooded with small individual trees and large areas remaining free of vegetation. Mean annual air temperatures at *Täschgufer* are derived from meteoro-

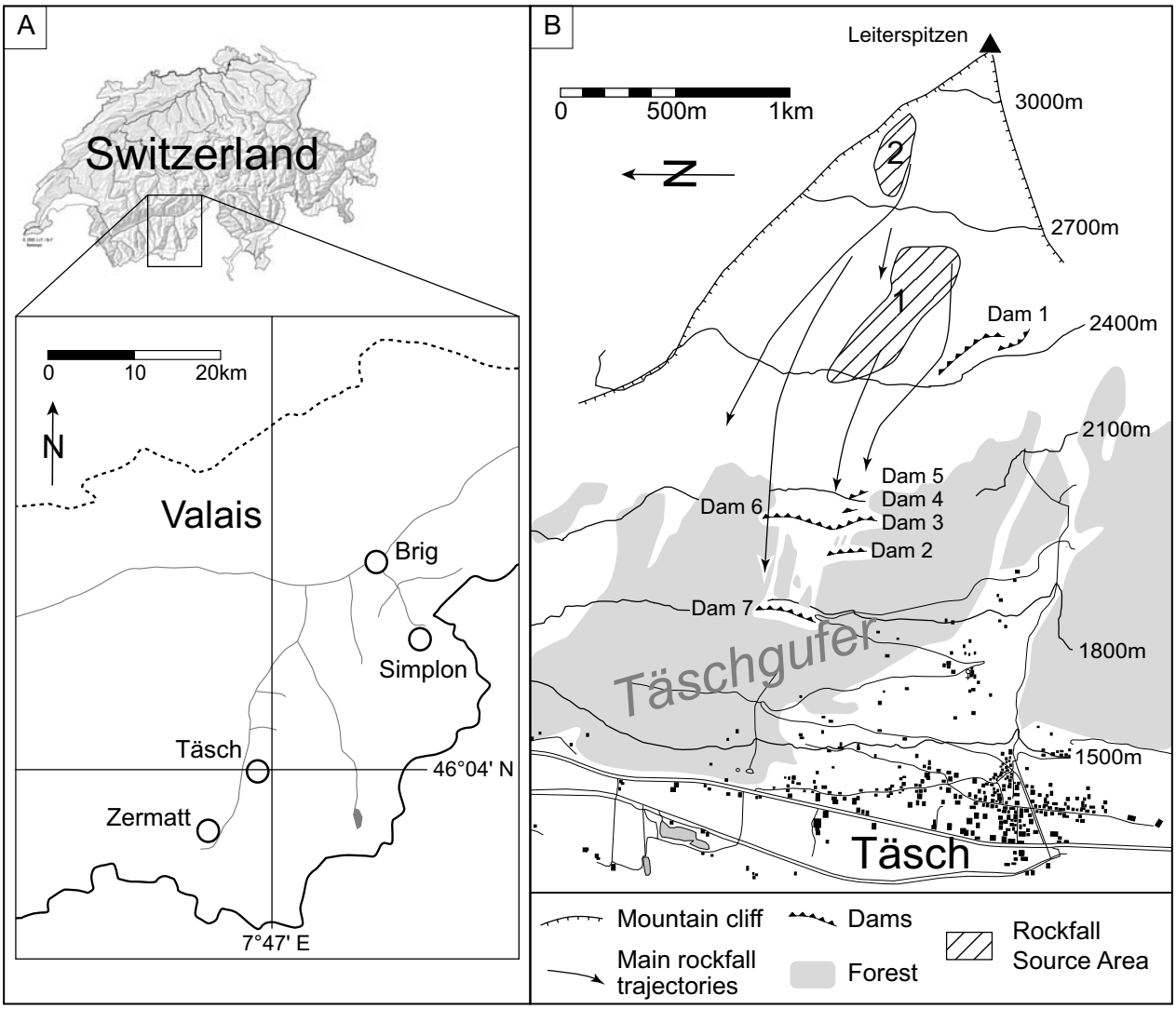

Fig. B1.1 *(a) The Täschgufer slope is located in the southern Swiss Alps north-east of Täsch. (b) Sketch map of the rockfall slope with the main Rockfall Source Areas, the main trajectories and the dams built after 1988.*

logical data at *Zermatt* (SMI 2003). Using a local temperature lapse of 5.1°C km^{-1} (King 1996), mean annual air temperature reaches +4.5°C at *Täsch* and –4.5°C at the *Leiterspitzen* summit. Precipitation most frequently occurs between August and November, including persistent rain from low-pressure masses located in the *Mediterranean Sea* (Grebner 1994). On the sparsely wooded surfaces around 1800m a.s.l., annual average precipitation is estimated to 660 mm. Here, snow usually covers the slope in early winter, reaching a maximum depth of around 70 cm in early March (Smi 2000). Snowmelt generally starts in mid March. In contrast, snow accumulation is modest around the Rockfall Source Areas 1 and 2 and surfaces remain largely snow-free during the winter months. The Rockfall Source Areas at *Täschgufer* are situated on the borderline between seasonal frost and permafrost environments, as suggested by a locally calibrated permafrost distribution model (Gruber & Hoelzle 2001). As illustrated in Figure B1.2, the presence of permafrost is namely proofed at the southern edge of the slope between 2400 m and 2500 m a.s.l., where massive ground ice was encountered during construction works (Haeberli 1992).

In the mid-1980s and again after 1993 (Lauber 1995), rockfall activity apparently increased on the slope and rocks repeatedly caused damage to infrastructure (roads, hiking trails) on the valley floor. On October 6, 1985, single blocks damaged an agricultural building in *Täsch*. As a consequence, in 1988 an unhitched road for construction traffic and an earth-fill deflection dam (Dam 1; see Fig. B1.1b) initiated the realization of major protection measures on the

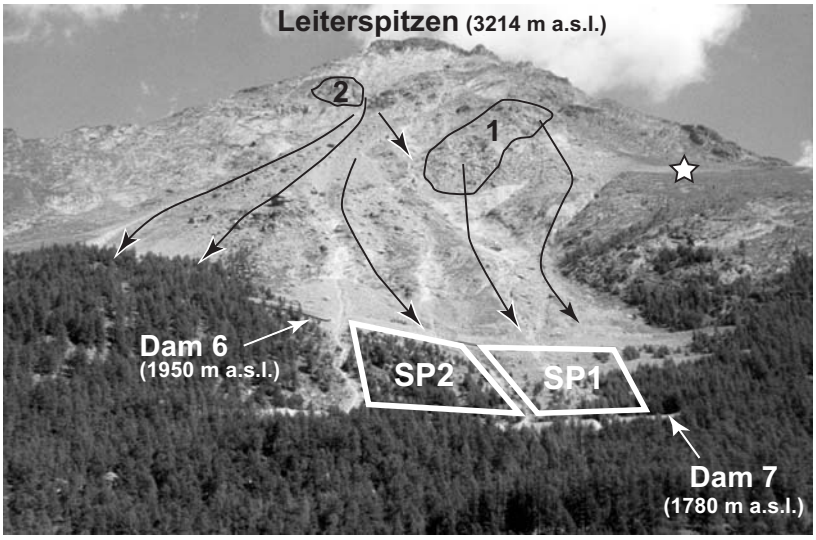

Fig. B1.2 *View of the Täschgufer slope and the Leiterspitzen summit (3214 m a.s.l.): Note the main Rockfall Source Areas (1, 2), the main rockfall trajectories (arrows) and the zone where massive ground ice was encountered (star) during construction works. (Photo courtesy by Dominique Schneuwly, used with permission).*

slope. Further earth fill deflection dams were built in the succeeding year (Dams 2 to 5). Finally, two large protection dams were erected north of the existing constructions in 1996/97 (Dam 6, 400 m in length) and 1998 (Dam 7, 260 m in length).

For the investigation described in this paper, two study plots (SP1, SP2) are selected in the heavily injured forest stand between Dams 6 and 7 (1780 to 1900 m a.s.l.). Figure B1.3 shows the two neighboring plots, which cover a surface of 0.06 km^2. At SP1, the slope surface is vegetation-free and alpine pioneer formations exceptionally occur in the southern part. European larch trees (< 50 yrs) have recolonized the plot, forming relatively dense forest patches. At SP2, the slope surface is mostly covered with alpine pioneer formations. Trees are generally older than 50 yrs and the recolonization rate is weak. While rockfall at SP1 widely originates from Rockfall Source Area 1, rockfall activity in SP2 is influenced by both zones, but predominantly by blocks provided from Rockfall Source Area 2.

1.3 Material and methods

The investigation on the frequency and the seasonal timing of rockfall activity at *Täschgufer* is based on a dendrochronological analysis of scars and resin ducts in stem discs of European larch trees. The position of callous tissue and scars within the tree-ring is used to determine the moment of the impact.

1.3.1 Dendrochronological analysis of rockfall activity

For the analysis of intra-annual rockfall activity at *Täschgufer*, 18 European larch trees (*Larix decidua* Mill.) were selected on the slope and felled at ground level. Criteria for the selection of trees included a high number of visual injuries and a diameter at breast height (DBH) ranging from 15 to 25 cm. The locations of the selected trees (trees 1, 3-10 in SP1; trees 2, 11-18 in SP2) are given in Figure B1.3. From the sampled trees, 270 stem discs were sawn and polished. Ring-widths were measured and data processed following the procedure described in Bräker (2002). Yearly increments were then crossdated with undisturbed trees growing next to the rockfall slope and disturbed samples age-corrected, where applicable.

Rockfall injuries (scars) were used to date past events. After the destruction of dividing cambium cell layers by the impact, tree-ring formation fails to appear in the injured area (Schweingruber 1996). At the lateral edges of the injury, cambium cells start to continuously overgrow the wound producing callous tissue (Sachs 1991, Larson 1994). For this investigation, the position of the first layer of callous tissue within the tree-ring was used to determine the seasonal timing of rockfall activity. Traumatic rows of resin ducts (Larson 1994, Schweingruber 1996, 2001) occurring next to the injury were used as a further indicator to analyze the distribution of intra-annual rockfall activity (Stoffel 2002).

1.3.2 Seasonal timing of rockfall

In temperate climates, coniferous trees are characterized by a vegetation period in summer and a dormant season (dormancy) in winter. As illustrated in Figure B1.4, cambium starts to produce thin-walled earlywood cells (E) at the beginning of the growth period. In summer, cell formation gradually merges to thick-walled latewood cells (L), before cell growth slowly ceases in fall. As callous tissue and resin ducts appear at once after mechanical impact (Baumann & Kaiser 1999), injuries can be attributed to these different segments of the vegetation period.

In the case of rockfall injuries occurring outside the preceding or within the first days of the vegetation period, callous tissue and resin ducts instantaneously substitute earlywood cells at the beginning of the new growth period. In both cases, rockfall is attributed to the dormant season (D). Growth reactions within earlywood cells are furthermore subdivided into early (EE), middle (ME) and late (LE) earlywood, those in latewood into early (EL) and late (LL) latewood. Knowing the species' growth data at the study site, the intra-annual distribution of rockfall activity can be dated, as demonstrated by forest fire and fire scar analyses (Brown & Swetnam 1994, Ortloff *et al.* 1995).

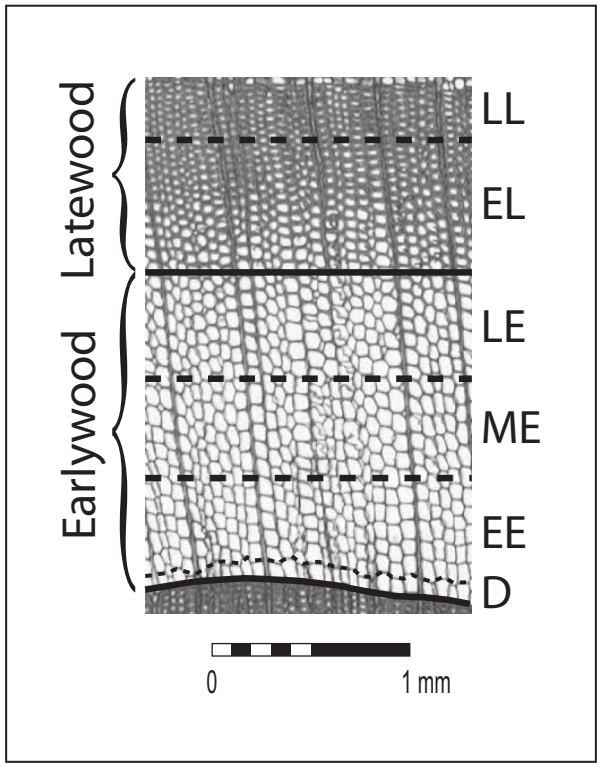

Fig. B1.4 *Tree-rings are subdivided into thin-walled earlywood (E) and thick-walled latewood (L) cell layers. At the end of the vegetation period, cell formation ceases and the dormancy (D) occurs. E is furthermore subdivided into early (EE), middle (ME) and late (LE) earlywood, L into early (EL) and late (LL) latewood.*

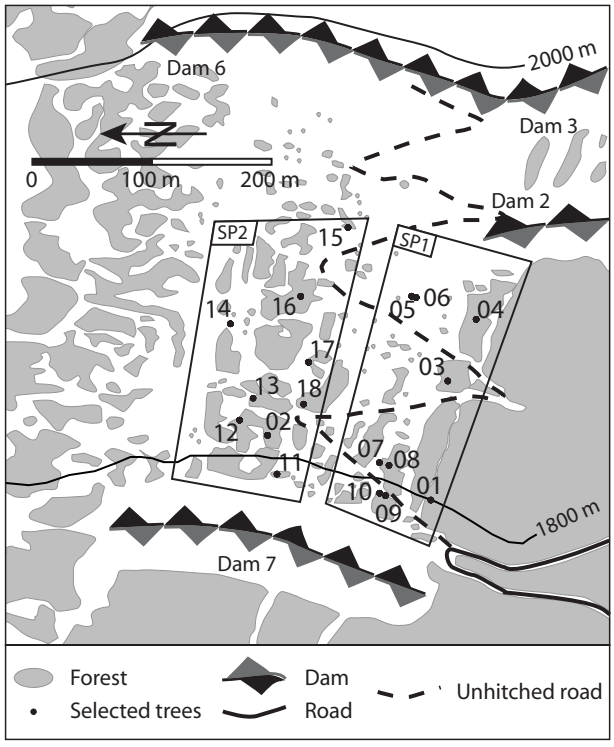

Fig. B1.3 *Location of the study site and the investigated study plots (SP1, SP2). For this study, nine Larix decidua trees have been selected in each plot (trees 1 to 18).*

In the Valais region, growth data exists for several conifer stands (*Larix decidua, Picea abies, Pinus montana*) with different slope orientations at *Simplon* (1800 m a.s.l.). Table B1.1 provides details on the timing of radial growth for the conifer stands at *Simplon*. According to Müller (1980), who studied the stands in 1976, radial growth (earlywood cells) is initiated in late May. Formation of latewood cells starts by mid July and cell formation ceases in early October.

The table further shows that this growth data perfectly coincide with the results of Camarero *et al.* (1998), who analyzed a *Pinus uncinata* stand at *Sahún* (1790 m a.s.l.), *Spanish Pyrenees*, in 1993/94. By virtue of the similarity of the results, growth data of *Larix decidua* trees at *Simplon* (Müller 1980) are used to correlate the intra-annual position of injuries within the tree-ring with calendar data at *Täschgufer*.

Table B1.1 *Onset of the different growth phases (GrPh) in coniferous trees (Larix decidua, Pinus montana and Pinus uncinata) at sites comparable to the Täschgufer slope. Data at Simplon (1, 2) represent the situation in 1976 (*Müller 1980*), those at Sahún (3) the situation in 1993/94 (*Camarero *et al.* 1998*). Based on these data, an approximate date for the onset of growth phases is derived for the study site (4).*

GrPh	*Larix decidua* (1) Simplon, 1800 m	*Pinus montana* (2) Simplon, 1800 m	*Pinus uncinata* (3) Sahún (E), 1790 m	*Larix decidua* (4) Täschgufer, 1800 m
E	May, 29	May, 29	June, 10	late May – early June
L	July, 17	July, 17	July, 18	mid July
D	October, 9	October, 9	October, 11	early October

1.4 Results

Dendrochronological analysis of the 18 *Larix decidua* trees allowed identification of 180 rockfall scars between 1977-2001, representing a mean of more than 7 hits yr^{-1}. From Figure B1.5 it can be seen that rockfall activity at *Täschgufer* both varied between single years as well as within the growth period.

As for the inter-annual variations in rockfall activity, Figure B1.5 shows an increased number of rockfall scars in 1990 and from 1994 to 1997. While in 1990 and 1995, 26 and 29 scars occurred respectively in the selected trees, none of the trees were scarred in 1978, 1979, 1981 and 1986. As the selected trees only record rockfall signals at 18 specific points within the study site, these results represent a rough tendency of rockfall activity on the slope by showing a minimum frequency of events for the last 25 yrs. Concerning the intra-annual distribution of rockfall activity, scars attributed to the dormant season (D) largely predominate: about 79% of all scars were generated outside the vegetation period or immediately at its beginning. In both cases, growth reactions occurred within the first layer of earlywood cells and are hence attributed to the dormant season (D). In contrast, only 6% of the scars belong to the earlywood cell layers, whereas 15% of the injuries are located in the latewood. Over the last 25 years, abundant rockfall activity during latewood formation was mostly restricted to the years 1985, 1989, 1996 and 1997. Figure B1.6 displays characteristic examples (microsections) of callous tissue and resin ducts in dormancy, earlywood and latewood.

1.4.1 Rockfall activity and construction works

Distinct differences in the number of scars and the seasonal timing of rockfall exist both between the years with construction activity on the slope (Dams 1 to 6) and the years without anthropogenic interventions. As indicated in Table B1.2, the above-average number of injuries in 1990, 1996 and 1997 coincide with major anthropogenic interventions on the slope. In total, 65 scars were supposedly related to the construction of dams.

During the construction works of Dams 2 to 5, 30 injuries are noted in the latewood cell layers (EL) of

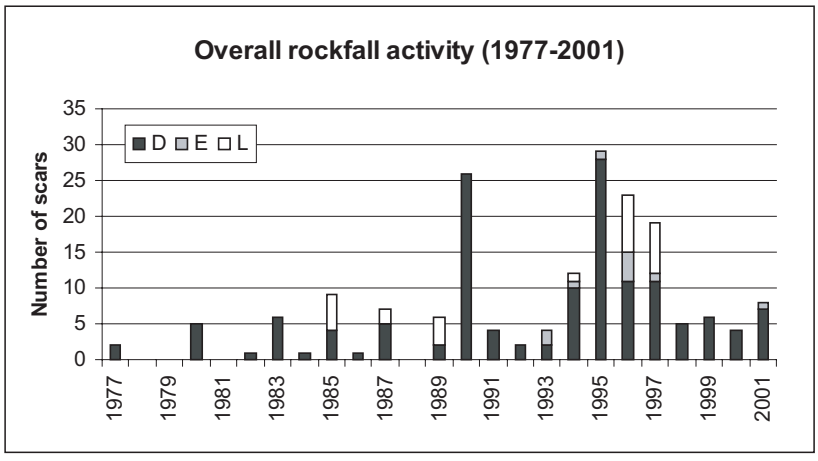

Fig. B1.5 *Reconstructed minimum frequency of rockfall activity on the Täschgufer slope (1977-2001; D = dormancy, E = earlywood, L = latewood).*

1989 and the succeeding dormant season (D 1990). The spatial distribution of injuries attributed to the construction of these dams is represented in Figure B1.7a. While rocks released during construction works caused injuries to all trees in SP1, several individuals remained unaffected in SP2. Repeatedly affected trees are restricted to SP1 (trees 4, 5, 8 and 10) and located close to the construction sites of Dams 2 to 5. Within the period of construction works, the first scars are noted in EL 1989, when injuries were restricted to Tree 5. Rockfall activity apparently increased during the dormancy of 1990 (26 scars). During this time, rocks were most probably released by final aggradations in late fall 1989. Moreover, some rocks may have been mobilized during the thawing in spring 1990 as a result of the destabilization by the preceding building activities.

Trees with scars occurring during the constitution of Dam 6 (1996/97) are displayed in Figure B1.7b. In this period, 35 injuries were recorded in all 18 trees. In contrast to the relatively homogenous spatial distribution of scars in 1989 and 1990 (Dams 2 to 5), injuries caused by the constitution of Dam 6 are dispersed throughout the study plots. While anthropogenic rockfall apparently caused major damage in SP1, scars are again missing in several trees of SP2. While the first scars occur in Tree 7 within the last layers of earlywood cell layers (LE) in 1996, most injuries occur within the latewood cell layers (EL and LL) of 1996 (8 scars). In the succeeding dormant season (1997), 11 scars are counted in the samples. Similarly to the scars attributed to the dormancy (D) of 1990, rockfall activity in D 1997 is supposedly linked to construction works in late fall 1996 or the release of formerly destabilized rocks in spring 1997. In the second year of construction works, anthropogenic interventions caused 7 injuries within the latewood cell layers (EL) and in the dormant season of 1998 (5 injuries). Again, these scars are assessed the result of final aggradations of Dam 6 in fall 1997.

Contrary to expectations, the 18 selected trees obviously remained unaffected during the first year of construction works on the slope in 1988, when the unhitched road for construction traffic and Dam 1 were built. As the construction site of Dam 7 was located below the study plots, trees also remained unaffected during these anthropogenic interventions on the slope.

As for the intra-annual distribution of rockfall activity during construction works on the slope, it can be seen from Table B1.2 that rockfall injuries outside the dormant season are mostly restricted to the periods with anthropogenic interventions on the slope. In this sense, 19 out of 27 injuries attributed to the latewood

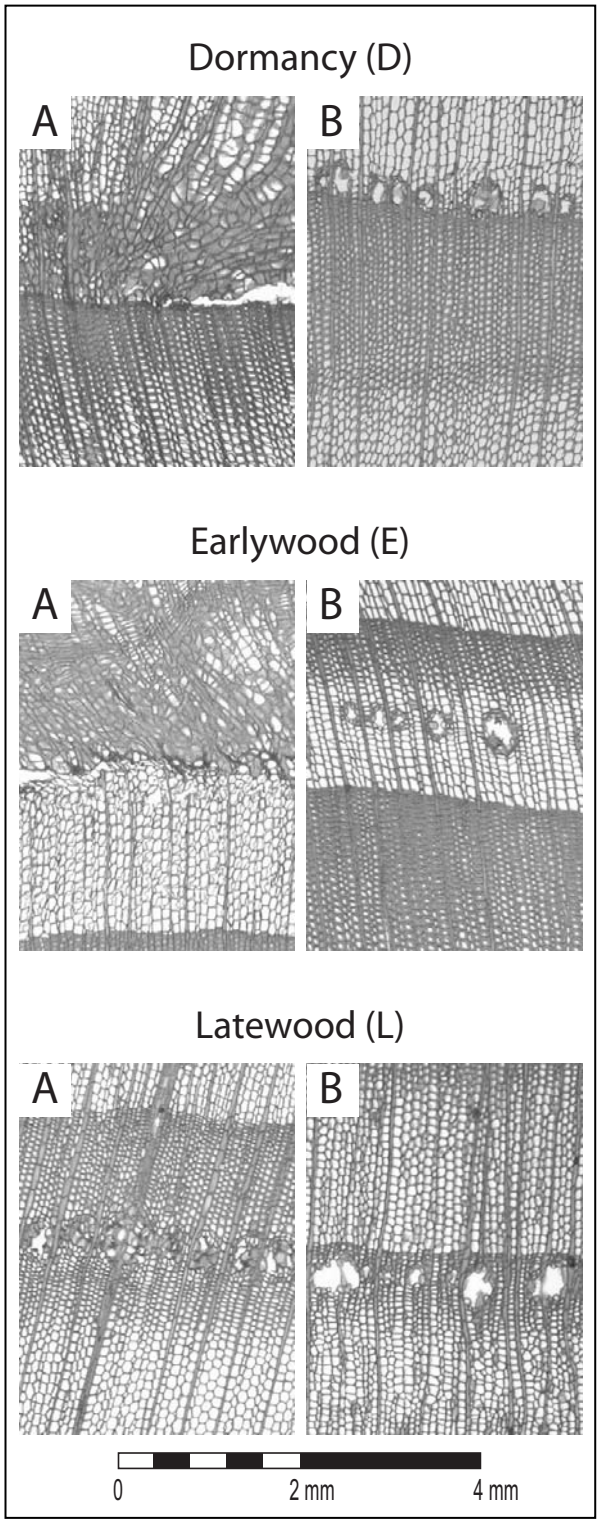

Fig. B1.6 *Microsections of characteristic callous tissue (A) and traumatic rows of resin ducts (B) as a result of rockfall activity in the dormant season (D), earlywood (E) or latewood (L).*

Table B1.2 *Seasonal timing of rockfall activity on the slope between 1977 and 2001. Gray surfaces represent the periods of construction works influencing the study plots (i.e. Dams 2 to 6). Accordingly, numbers in italics designate rockfall scars that have most probably been caused by anthropogenic interventions on the slope.*

Year	Dormancy (D)	Earlywood cells (E)			Latewood cells (L)		Total
		EE	ME	LE	EL	LL	
1977	2						2
1978							0
1979							0
1980	5						5
1981							0
1982	1						1
1983	6						6
1984	1						1
1985	4				5		9
1986	1						1
1987	5				1	1	7
1988							0
1989	2				***4***		6
1990	***26***						26
1991	4						4
1992	2						2
1993	2		2				4
1994	10			1	1		12
1995	28		1				29
1996	11			***4***	***3***	***5***	23
1997	***11***		1		***7***		19
1998	***5***						5
1999	6						6
2000	4						4
2001	7		1				8
TOTAL	143		5	5	21	6	180

cell layers between 1977 and 2001 were most likely released by construction works. Similarly, four out of five scars attributed to the last layers of earlywood cells are supposedly linked to construction works on the slope.

1.4.2 Natural rockfall activity

By excluding the rockfall activity attributed to construction works, the number of scars observed in the 18 trees over the past 25 years is reduced from 180 to 115, which means that naturally driven rockfall activity accounts for almost 5 hits yr^{-1} on an average.

Figure B1.8 shows the variations of rockfall activity between individual years and within the different growth periods. Again, rockfall activity greatly varies between the individual years. While no scars can be discerned in 1978, 1979, 1981 and 1988, above-average numbers of scars are recorded in 1985, 1994, 1995, 1999 and 2001. In this sense, reconstructed rockfall activity appears to coincide with direct observations on the Täschgufer slope, indicating increased rockfall activity in 1985 and after 1993 (see Chapter B1.2). Above-average numbers of scars are mainly recorded after 1993. During the dormant season of 1994, rockfall activity caused 10 scars.

A comparable number of injuries can be discerned in the dormancy of 1996 (11 scars). Massive rockfall in the dormant season of 1995 caused important damage to the selected trees, leaving 28 injuries. During the dormant season of 2001, rockfall activity caused 7 scars. As for the intra-annual distribution of rockfall scars, events attributed to the dormant season are even more predominant (88%). It can clearly be seen from

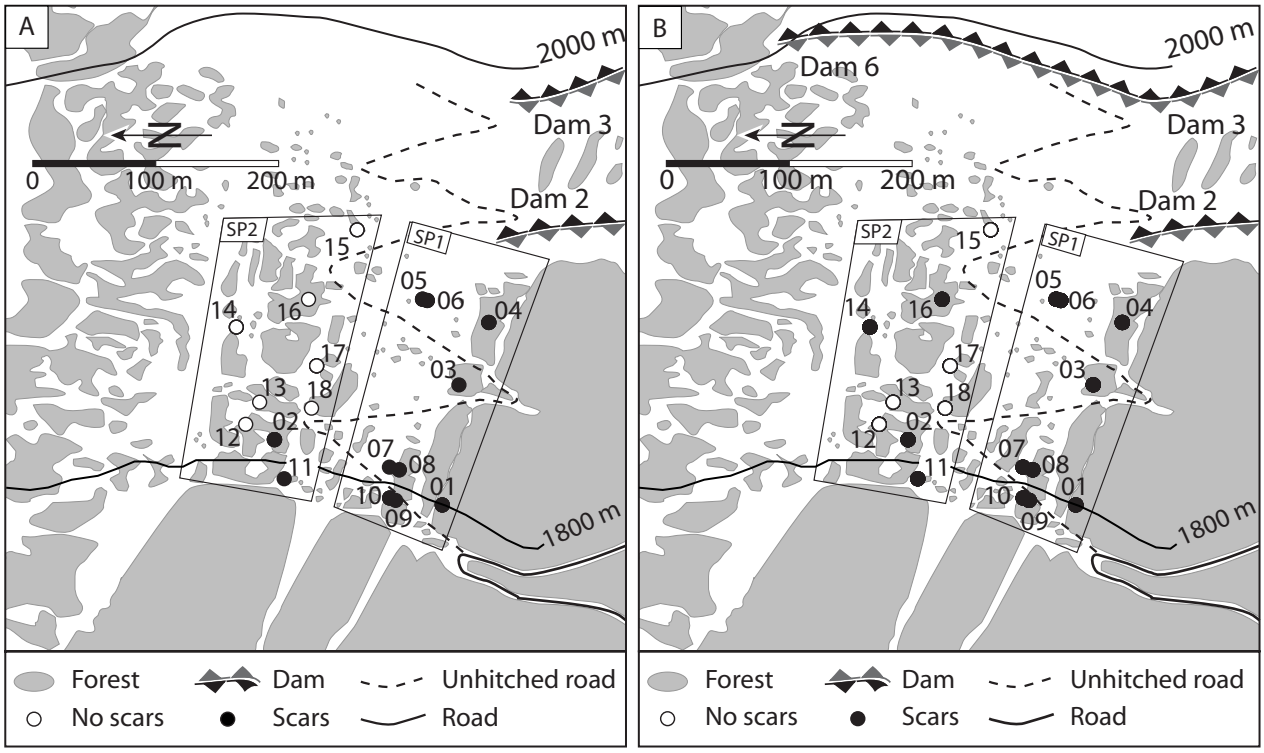

Fig. B1.7 *Spatial distribution of rockfall activity (a) during the construction of the deflection dams (Dams 2 to 5) and (b) the first protection dam (Dam 6).*

Figure B1.8 that scars rarely occur in earlywood (E = 5%). Similarly, injuries are uncommon in latewood, where only 8 scars (L = 7%) can be discerned. A considerable number of scars was linked with abundant rockfall activity in the dormant season.

The spatial distribution of trees injured within the dormant season keenly varies between the individual years: Between 1977 and 1990, scars occurring during dormancy exclusively belong to trees located in SP2. Not a single injury can be discerned in SP1. Starting in 1991, scars repeatedly occurred at SP1, indicating an activation of rockfall originating from Rockfall Source Area 2. In 1993, scars were exclusively restricted to SP1, while SP2 apparently remained unaffected. During the dormant season of 1995, naturally driven rockfall caused injuries to trees in both study plots, but predominantly to those in SP2. In total, 38 injuries attributed to the dormant season are recorded in SP1 between 1991 and 2001. Simultaneously, naturally driven rockfall activity in SP2 accounted for 35 scars, 22 of which occurred during the increased rockfall activity in 1995 and 1996. During the only above-average activity outside the dormant season in EL 1985, rockfall affected trees in SP1 (trees 8, 9 and 10).

1.5 Discussion

In the study we have reported here, the use of stem discs procured a reasonable chart of rockfall activity and the seasonal timing of rockfall events on the *Täschgufer* slope. Similar to investigations on past fire regimes (Brown & Swetnam 1994, Ortloff *et al.* 1995), we introduced a microscopic approach to rockfall research which allowed determination of the seasonal timing of rockfall events by analyzing the position of the scars within the tree-rings.

Results on the rockfall frequency show that years with many scars in the selected trees consistently coincide with findings of geological mandatory opinions reporting on the observed rockfall activity on the slope (e.g., Lauber 1995). Over the last 25 years, naturally driven rockfall activity caused 115 scars in all 18 trees investigated.

Microscopic analyses indicate that rockfall scars were predominantly caused by rockfall events during the dormant season (88%), which locally lasts from mid October through end of May (see Table B1.1). Direct observations on the slope confirm these results, indicating that abundant rockfall tends to be highest in

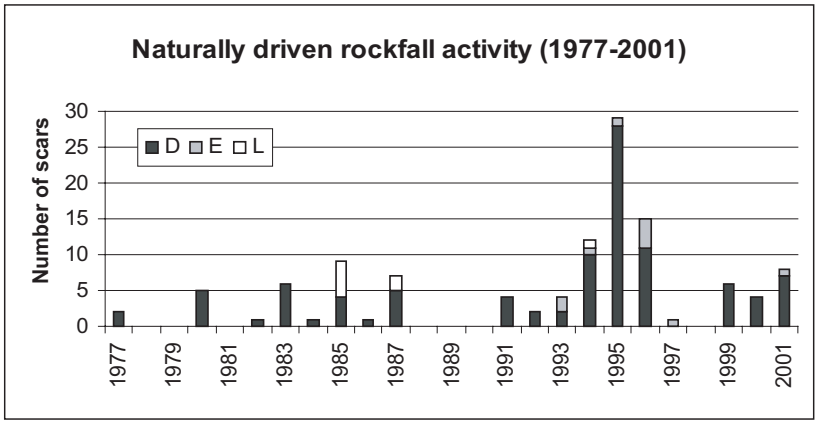

Fig. B1.8 *Reconstructed minimum frequency of naturally driven rockfall on the Täschgufer slope (1977-2001; D = dormancy, E = earlywood, L = latewood). Rockfall triggered by anthropogenic activity on the slope is disregarded.*

April and May. The size of rockfall components (up to 2m^3), the sporadic occurrence of larger events as well as the seasonal timing indicate that rockfall triggering at *Täschgufer* most likely depends on seasonal rather than on diurnal freeze-thaw cycles. At the beginning of snowmelt in mid March, meltwater easily penetrates the heavily jointed and fissured bedrock in the Rockfall Source Areas. The water would then fill the rock joints, which are still at a subfreezing temperature, as described by Matsuoka (2001) and Matsuoka *et al.* (2003). As a consequence, meltwater would refreeze causing permanent opening of the joints. In April and May, direct insolation gradually rises (Hufty & Theriault 1983), favoring the thawing of ice and activating rockfall on the west-facing slope.

Comparisons of meteorological data (Smi 2003) further indicate that periods with increased rockfall activity do not depend on short-term meteorological events. In agreement with the findings of Matsuoka & Sakai (1999), rockfall at *Täschgufer* seems to be neither influenced by thunderstorms in summer nor abundant rainfall in autumn. Even so, there seems to be no (direct) correlation between the only important rockfall event outside dormancy in latewood 1985 and the October 6, 1985 event mentioned in Section B1.2. As the reactions in the injured trees were initiated within the first layers of latewood cells, we suppose that the reconstructed rockfall event occurred between mid July and August 1985 and not in late fall.

Spatial distribution of injuries further show that naturally driven rockfall activity strongly varied over the last 25 years. Between 1977 and 1990, selected trees in study plot 1 (SP1) remained unaffected by rockfall activity linked with thawing processes in spring. Therefore it seems that spring events triggered at Rockfall Source Area 1 only occurred after 1990. In contrast, results indicate that thawing processes in spring regularly triggered rocks from Rockfall Source Area 2.

Dam construction works on the slope in 1989 and again in 1996 and 1997 left 65 rockfall scars in the 18 selected trees. Within these periods, rockfall activity almost caused 22 hits yr^{-1}. Astonishingly, scars are missing during the first year of construction works in 1988, when Dam 1 and the unhitched road for construction traffic were built. While the absence of injuries during the realization of Dam 1 may be explained by the position of the construction site, it may not be accountable for the absence of scars during the construction of the unhitched road, repeatedly crisscrossing study plot 1 (SP1).

This study has taken a step in the direction of investigating the seasonal timing of rockfall activity using a microscopic approach of tree-rings. Due to the small number of trees we used for testing this new approach, the reconstructed event frequency can only give a rough review of rockfall activity over the last 25 years: Firstly, data only reflects punctual rockfall activity in 18 trees. Distances between the selected trees are generally large, allowing rocks to pass without causing damage. Secondly, the minimum height of selected trees proves to be critical for trees 7 and 8, which only trespassed mean impact heights by 1987. Thirdly, broken-off primary crowns and the formation of vertical sprouts growing from former branches ("candelabra form" trees) may furthermore influence the height of trees and therefore reduce the probability of a tree being hit. Tree 15 has, for instance, been decapitated at least four times by rockfall activity since 1977.

As for the intra-annual distribution of scars, microscopic analysis furnishes concise data on the seasonal timing of rockfall occurrence within the vegetation period, i.e. from early June through mid October. In contrast, reactions to injuries caused during dormancy (i.e. mid October to end of May) only occur at the beginning of the succeeding vegetation period and can hence not be analyzed in more detail. Combining

permanent observations of rockfall rates in the field, measurement of rock temperatures and the circulation of water with tree-ring analysis would further help to understand rockfall activity and releasing processes during the dormant season. Finally, future research will need to integrate a larger number of tree samples to draw even more conclusive results on past rockfall activity.

1.6 Conclusion

The approach outlined in this study proves to be a useful tool for analyzing differences in intra-annual rockfall activity on forested slopes. In the case of data available on the different growth phases within the vegetation period of the selected tree species at the study site, results on the seasonal timing of rockfall activity can even be given with almost monthly resolution. In this sense, this method allows one to compare periods with apparently increased rockfall activity reconstructed from dendrochronological analysis with meteorological data. However, for rockfalls occurring within the dormant season, tree-ring analysis may not furnish detailed information on the timing and growth reactions because the formation of callous tissue or resin ducts is only initiated within the first layer produced in the succeeding vegetation period. Therefore, dendrochronological analysis needs to be completed with direct observations on the site.

Acknowledgements: The authors would like to acknowledge Colette Pugin for sample preparation, Michelle Bollschweiler for ring-width measurements and Sabine Stoffel for cutting microsections. Thanks are also given to Gion-Reto Hassler and Dominique Schneuwly, who helped in the dangerous fieldwork. Felix Keller (Academia Engiadina) is kindly acknowledged for helpful data on the local permafrost and Wilfried Haeberli (University of Zurich) for fruitful discussion on permafrost processes triggering rockfall on the slope. Further thanks are due to Andreas Rigling (WSL) for information on tree phenology. Fran King is warmly acknowledged for improving the English of this paper. Last but not least, we acknowledge the local community of Täsch, Reinhold Bumann (civil engineer) and Leo Jörger (local forester) for helpful advice and collaboration.

*****

2. Spatio-temporal fluctuations in rockfall activity (1600-2002)

Markus Stoffel [1], Dominique Schneuwly [1], Michelle Bollschweiler [1], Igor Lièvre [1], Reynald Delaloye [1], Maung Moe Myint [2] and Michel Monbaron [1]

"Analyzing rockfall activity (1600–2002) in a protection forest – a case study using dendrogeomorphology"

[1] *Groupe de Recherches en Géomorphologie (GReG), Department of Geosciences, Geography, University of Fribourg*
[2] *Remote Sensing and GIS Unit, Department of Geosciences, Geography, University of Fribourg*

published in Geomorphology 2005, Vol. 68, No. 3–4, 224–241
revised: 19 November 2004, accepted: 20 November 2004

Abstract

For the first time, dendrogeomorphology has been used to investigate spatial and temporal variations of rockfall activity in a protection forest. We report results of 564 cores from 135 severely injured *Larix decidua* Mill. trees on the west-facing Täschgufer slope, Swiss Alps. While trees sampled reached an age of 297 years on average, the oldest one attained breast height in AD 1318. For reasons of sample depth, the analysis was limited to the period 1600-2002. In total, we reconstructed 741 growth disturbances (GD) during the last four centuries. Impacts were most commonly found in trees located in the southern part of the slope, where GD recurred more than once per decade. In contrast, trees in the northern part were less frequently disturbed by rockfall and define recurrence intervals of more than 150 years.

Throughout the last four centuries, rockfall has caused GD to the trees sampled on the Täschgufer slope, most frequently in the form of low magnitude–high frequency events. In addition, we identified one high magnitude–low frequency event in 1720, which displaced the forest fringe of the northern sector a considerable distance downslope and eliminated an entire forest stand. To analyze past rockfall activity, we introduce a "rate" defined as the number of impacts per meter width of all tree surfaces sampled per decade. Results clearly demonstrate that this rockfall "rate" continually decreased in both sectors after the large 1720 rockfall event. Significantly low rockfall "rates" can be observed during the 1850s, 1960s and 1970s in the northern and during the 1820s in the southern sector. In contrast, high rockfall "rates" were identified during the 1870s and 1990s in the northern, and during the 1770s in the southern sector.

Reconstructed data further show that the forest recolonizing the southern sector after the 1720 event gradually improved its protective function, reducing "rates" by a factor of 13 between the 1740s and the 1990s. In the recent past, "rates" oscillated around 0.7 GD 1 meter width^{-1} (10 years)$^{-1}$. In the well-established forest of the northern sector, the efficacy of the protective forest was temporarily reduced by the rockfalls in 1720, resulting in increased rockfall "rates". Since then, the protective function of the forest stand has increased again, resulting in a rate of 0.4 GD 1 m width^{-1} (10 years)$^{-1}$ during the late 20th century.

Keywords: dendrogeomorphology; rockfall; growth disturbances; frequency; magnitude; protection forest; Swiss Alps

2.1 Introduction

Rockfall represents the most intensely studied geomorphic process of the cliff zone in mountainous areas (Luckman & Fiske 1995). Nevertheless, little information exists on how rockfall frequencies and magnitudes vary over time. So far, studies have mainly been based on short-term observations of contemporary rockfall activity in the field (e.g., Luckman 1976, Douglas 1980, Gardner 1980, 1983), rendering it difficult to estimate long-term accretion rates. Long-term estimates of rockfall accumulation rates have, in contrast, been derived from accumulated talus volumes (e.g., Rapp 1960a). But such rates may, as Luckman & Fiske (1995) pertinently object, neither be representative of the present-day rockfall activities nor of those that prevailed in the past. Hétu & Gray (2000) managed to avoid this problem by combining present-day processes and stratigraphic data to study the dynamics of scree slopes throughout the postglacial period. On slopes composed of siliceous lithologies, lichenometry has repeatedly been used to evaluate the mean age or activity of talus surfaces (André 1986, 1997) or to estimate 50-yr and long-term rates of rockfall accretion (Luckman & Fiske 1995). Finally, McCarroll *et al.* (1998) combined a lichen-based analysis of spatial and temporal patterns of past rockfall activity with a modeling approach. Simultaneously, investigations of forest – rockfall interactions have tended to evolve towards the analysis of mountain forests as a means of protection against rockfall (e.g., Bebi *et al.* 2001, Berger *et al.* 2002). Hétu & Gray (2000) indicated that forest cover would provide effective protection in the case of low magnitude–high frequency rockfall events, but could not prevent the devastating effects of high magnitude events.

However, quantitative information on the effect of forest stands on the downslope movement of rockfall boulders remains insufficient. The previously mentioned studies on rockfall activity or the distribution of scree give a reasonable overview of long-term fluctuations, but they lack more detailed data on decadal or even yearly variations in rockfall activity on a slope. In contrast to their use in other mass movement processes (e.g., Shroder 1980, Wiles *et al.* 1996, Fantucci & Sorriso-Valvo 1999, Solomina 2002, Stoffel *et al.* 2005a), tree-ring analyses have been used only rarely in rockfall research, where the focus in these few cases has been on sedimentation rates, the dynamics of forest fringes on scree slopes (Lafortune *et al.* 1997) or the seasonal timing of past rockfall activity (Stoffel *et al.* 2005b).

It is therefore the purpose of the present paper to use tree-ring analysis in order to: (1) analyze the magnitude and frequency; (2) determine spatial variations; (3) derive decadal and yearly variations in rockfall activity on a forested slope. In it, we use a rockfall "rate" to reconstruct and evaluate fluctuations in rockfall activity. Results were obtained from two neighboring sectors differing in both their age structure and recurrence intervals. In total, 564 increment cores of 135 European larch trees (*Larix decidua* Mill.) were analyzed, documenting decadal and yearly variations in rockfall activity on a forested slope at *Täschgufer* (Valais, Swiss Alps) over more than 400 years.

2.2 Study area

The area investigated was the west-facing *Täschgufer* slope. As can be seen from Figure B2.1, the *Täschgufer* slope descends from the *Leiterspitzen* summit (3214 m a.s.l.) in the *Siviez-Mischabel* nappe, southern Swiss Alps. Rockfall frequently occurs on the slope, originating from the heavily disintegrated gneissic rockwalls below the *Leiter-spitzen* summit. Layers of this weak bedrock generally strike SSW and dip WNW with angles of 40-80° (Lauber 1995), thus containing joints dipping out of the slope. The main rockfall source areas on the slope are located between 2300 and 2600 m a.s.l. (Rockfall Source Area 1) and above 2700 m a.s.l. (Rockfall Source Area 2), where

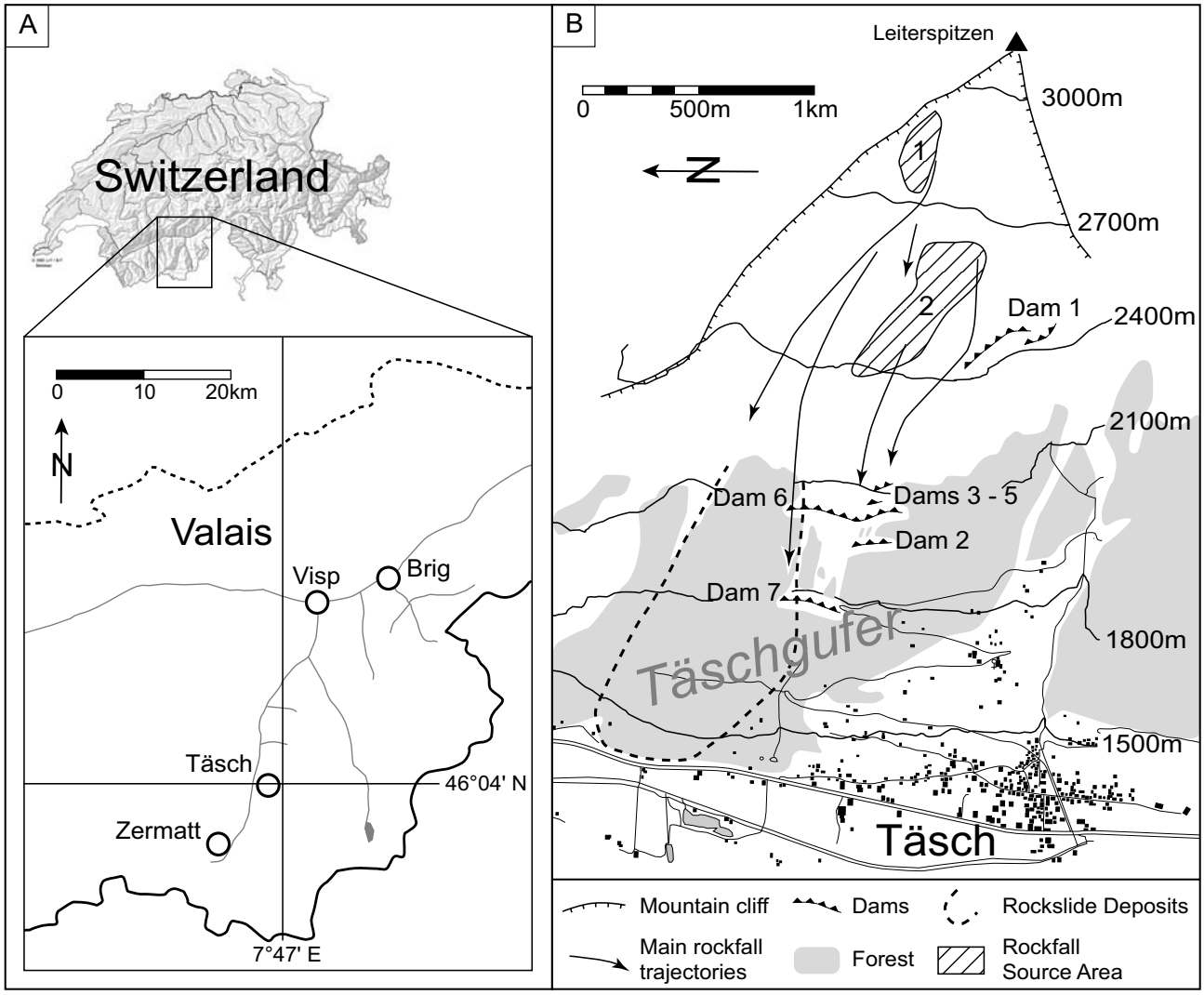

Fig. B2.1 *Location of the study site. (a) The Täschgufer slope is located in the southern Swiss Alps, north-east of the village of Täsch. (b) The detailed sketch illustrates the rockfall slope with the main rockfall source areas and trajectories, the rockslide deposits and the dams built after 1988 (Dams 1-7).*

bedrock is highly fractured with many joints. As suggested by a locally calibrated permafrost distribution model (Gruber & Hoelzle 2001), Rockfall Source Area 1 would be located on the borderline between seasonal frost and permafrost environments. The presence of contemporary permafrost is confirmed on the southern edge of the slope between 2400 and 2500 m a.s.l., where ground ice was encountered during construction work (Haeberli 1992; see Fig. B2.1). On the upper slope, mean slope gradients locally rise up to 48° and gradually decrease to 20° near the valley floor. The volume of single rockfall fragments normally does not exceed 2 m^3. Besides frequent rockfall activity, one rockslide is noted in chronicles (Zurbriggen 1952). Its age was estimated with lichenometry to be at least 600 years BP (Joris 1995). The spatial extent of the rockslide deposits can be seen in Figure B2.1b. Furthermore, small debris flows may occur at *Täschgufer*. Single events generally amount to a few cubic meters and move downslope in well-defined channels. In contrast, snow avalanches have never been witnessed on the slope.

The forest at *Täschgufer* predominantly consists of *Larix decidua* Mill. trees, accompanied by single *Picea abies* (L.) Karst. and *Pinus cembra* ssp. *sibirica* trees. Although the regional timberline is located at approximately 2300 m a.s.l. in the immediate neighborhood, continuous forest cover reaches only 1780 m a.s.l. in the most heavily affected areas of the active rockfall slope. As shown in Figure B2.1b, surfaces are sparsely wooded in this part of the slope and large areas remain free of vegetation.

In the recent past, rockfall regularly caused damage to roads and hiking trails. For example, on October

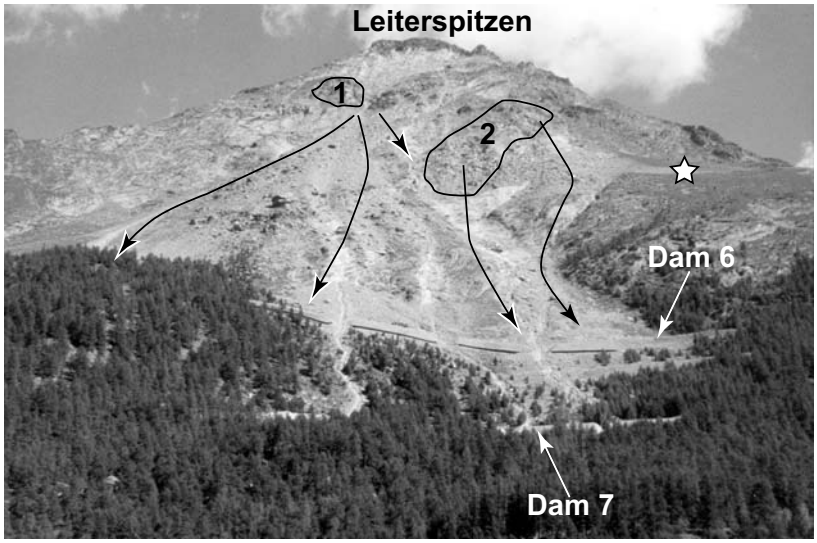

Fig. B2.2 *View of the upper Täschgufer slope and the Leiterspitzen summit (3214 m a.s.l.): Note the main Rockfall Source Areas (1, 2), the main rockfall trajectories (arrows) and the zone where ground ice has been encountered (star) during construction works. (Photo courtesy by Dominique Schneuwly; used with permission)*

6, 1985, single blocks reached the valley floor, damaging agricultural buildings in the village of Täsch (Valais). According to Lauber (1995), rockfall activity at *Täschgufer* apparently increased in the 1980s and again after 1993. These observations have recently been confirmed with dendrochronological analysis (Stoffel *et al.* 2005b), which further indicated that almost 90% of the intra-annual rockfall activity at *Täschgufer* occurs in April and May. As a response to the increased rockfall activity, five deflection dams were erected in 1988 (Dam 1) and 1989 (Dams 2-5; see Fig. B2.1b). In the late 1990s, two large protection dams completed the construction works on the slope (Dams 6-7, see Fig. B2.2).

2.3 Material and methods

2.3.1 Sampling strategy

As shown in Figure B2.3, dendrogeomorphological investigations were conducted in the protection forest [4] north of *Täsch* (1440 to 1760 m a.s.l.). Within the study area covering approximately 39 ha, virtually all trees (*Larix decidua* Mill.) show visible damage related to rockfall activity (i.e. broken crowns or branches, scars, tilted stems). We sampled severely affected trees with obvious signs of growth disturbances (GD) from both the rockslide deposits (northern sector) and the southern sector of the slope. The separation of the two

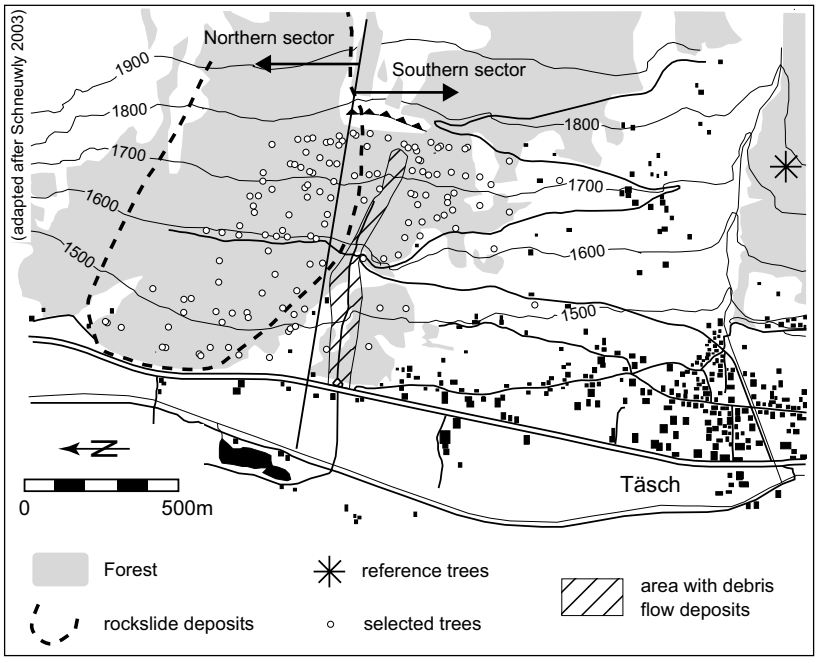

Fig. B2.3 *Distribution of the 135 Larix decidua Mill. trees sampled on the Täschgufer slope (1440 to 1780 m a.s.l.). The area influenced by both debris flow and rockfall activity (hatched surface) has been excluded.*

parts of the slope (Figure B2.3) is based on the different origins of rockfall material. As indicated in Figure B2.3, trees located in the northern sector are normally subject to rockfall fragments from the Rockfall Source Area 1, while the samples growing in the southern sector are predominantly influenced by boulders originating at Rockfall Source Area 2. We therefore analyze the two parts of the slope separately and refer to them as "northern sector" and "southern sector". In addition, we excluded a well-defined area in the southern sector, which is influenced by both rockfall and debris flow activity (Fig. B2.3).

In this investigation, at least 4 cores were extracted per tree using increment borers. Figure B2.4 illustrates that one core was taken upslope (core c), one downslope (core d) and two cores perpendicular to the slope (cores a, b). In the case of visible scars, further increment cores were extracted from the wound and the overgrowing callous tissue. In addition to the disturbed trees sampled at *Täschgufer*, we sampled undisturbed reference trees from a forest stand located south of the rockfall slope, indicated in Figure B2.1. For every reference tree, two cores per tree were extracted perpendicular to the slope (cores a, b). In total, 154 *Larix decidua* Mill. trees were sampled (598 cores) in the fall of 2002: 135 trees (564 cores) from the rockfall slope and 17 trees (34 cores) from the undisturbed reference site south of the rockfall slope. Increment cores of the reference trees were extracted at breast height (~130 cm), whereas those from the disturbed trees were – whenever possible – taken at the height of the visible damage.

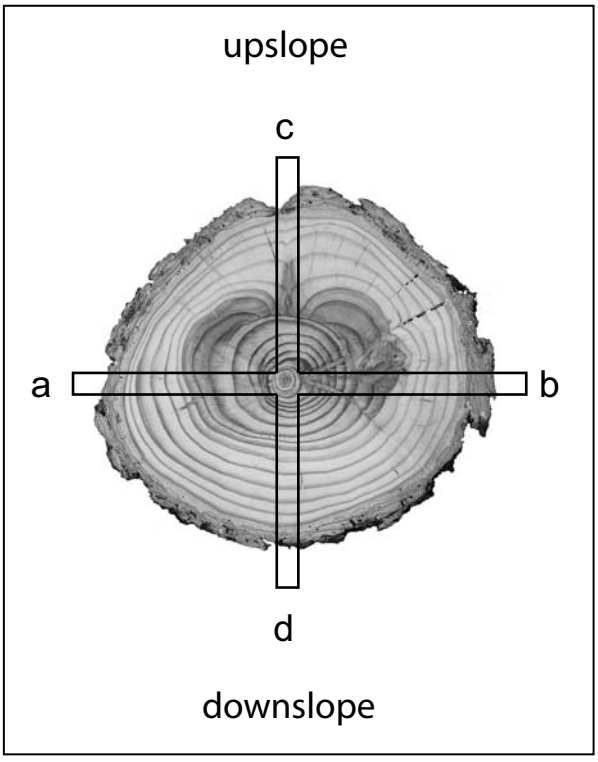

Fig. B2.4 *Core sampling procedure for individual trees.*

Data recorded for each tree sampled included (1) determination of its 3D-position on the slope with a compass and an altimeter (x- and y-values, elevation a.s.l.); (2) sketches and position of visible defects in the tree morphology such as scars, broken crowns or branches, candelabra trees and tilted stems; (3) the position of the sampled cores (i.e. a, b, c, and d); (4) diameter at breast height (DBH) derived from circumference measurements; (5) data on neighboring trees, micro-topography and/or rockfall deposits.

2.3.2 Tree-ring analysis and rockfall

Samples were analyzed and data processed following the standard procedures described in Bräker (2002). Single steps of sample analysis included surface preparation, skeleton plots as well as ring-width measurements using digital LINTAB positioning tables connected to a Leica stereomicroscope and TSAP 3.0 (Time Series Analysis and Presentation) software (Rinntech 2003). Growth curves of the disturbed samples were then crossdated with the reference chronology (1596-2002) constructed from 17 undisturbed *Larix decidua* Mill. trees. This procedure allowed differentiation of climatically driven fluctuations in tree growth within the study area from GD caused by rockfall activity (Cook & Kairiukstis 1990). Growth curves were then used to determine the initiation of abrupt growth reductions or recovery (Schweingruber 1996). In the case of tilted stems, both the appearance of the cells (i.e. structure and color of the reaction wood cells) and the growth curve data were analyzed (e.g., Shroder 1980, Braam *et al.* 1987, Fantucci & Sorriso-Valvo 1999). Further focus was placed on the visual analysis of callous tissue overgrowing rockfall scars and traumatic rows of resin ducts (Larson 1994, Schweingruber 2001). As resin ducts may result from causes other than rockfall (e.g., climate, wind, insects, fraying or browsing by ungulates), thresholds were needed to determine "resin duct events" caused by

[4] Protection forest: forest stand which directly protects people, buildings and infrastructure against the impacts of mass wasting events such as landslides, rockfall or snow avalanches (see Brang 2001).

rockfall activity. Criteria were defined using 270 stem discs sampled on the same slope (Stoffel *et al.* 2005b) that showed both tree damage (scars, decapitation) and resin ducts. As a result, resin ducts were only considered the product of rockfall activity if they formed (a) traumatic, (b) extremely compact and (c) continuous rows. Both the presence of resin ducts on multiple radii in a single year and the occurrence of multiple consecutive years with traumatic rows of resin ducts were used as further indicators but not a compulsory criterion. In contrast, neither dispersed resin ducts within a single tree ring nor the presence of traumatic rows of resin ducts occurring in the years following an event represent "resin duct events". Characteristic examples of disturbed stem discs and respective growth curves are illustrated in Figure B2.5. Reconstructed GD of individual trees were then compiled in a database (Schneuwly 2003). For every individual tree, we determined recurrence intervals by dividing its age at breast height by the number of dated GD.

Judging the frequency or magnitude of single event years or decadal fluctuations in the number of GD proved to pose a considerable problem: So far, dendrogeomorphology has mainly involved the analysis of impacts by geomorphic processes that have a relatively large volume or surface area, such as debris flows, snow avalanches or floods. In contrast, rockfall consists of single falling, bouncing or rolling stones, which may only disturb trees along their trajectories and within a range defined by the size of the clast. Further, only the effects of a single boulder are recorded, whereas the fall itself may be composite. Finally, important differences emerged as to the age of the individual trees, their DBH and their decadal DBH increment which rendered absolute comparisons of past rockfall activity difficult.

We therefore use a rockfall "rate" [5] expressed as number of rockfalls (GD) per meter width of all tree surfaces sampled per decade instead of analyzing abso-

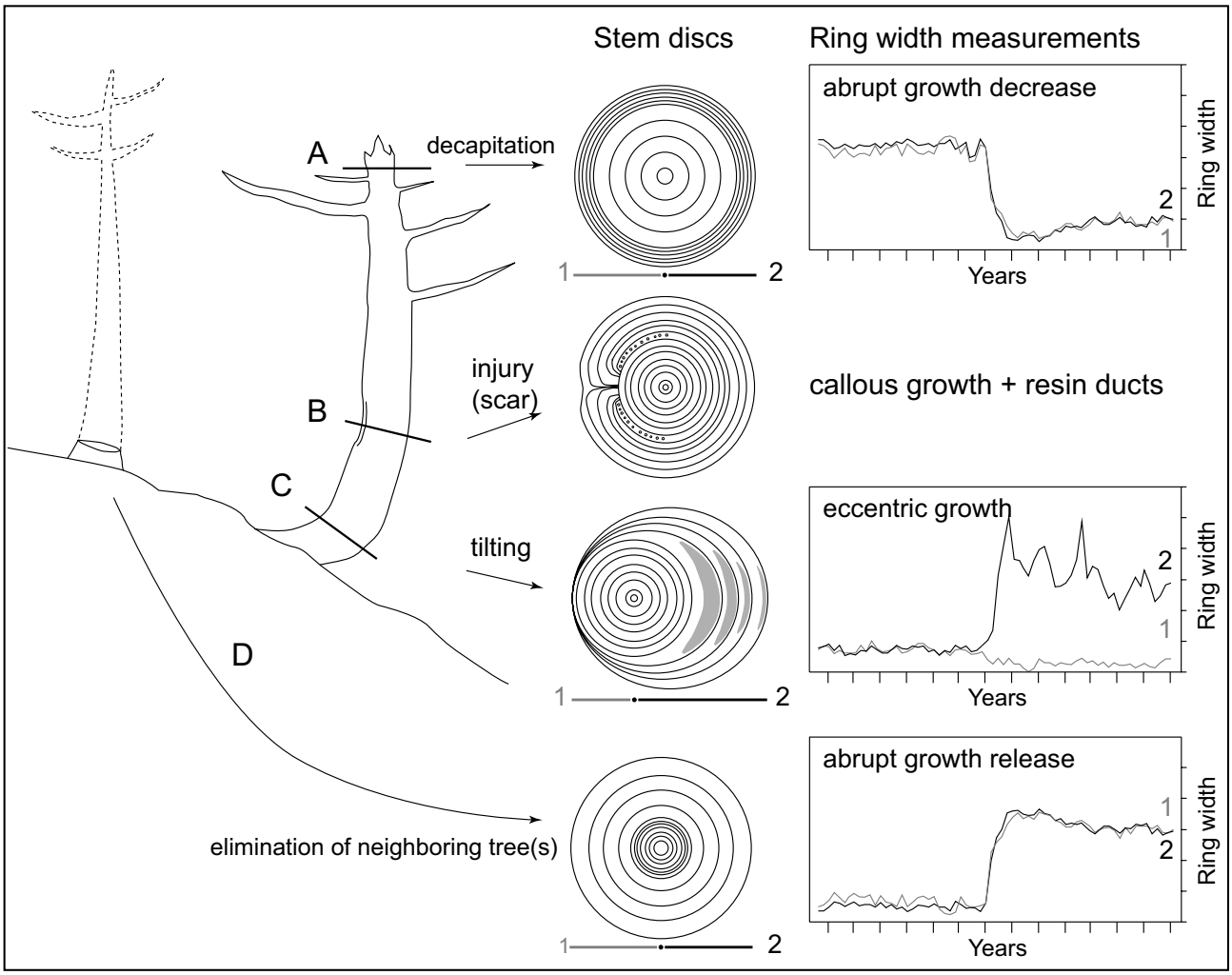

Fig. B2.5 *Evidence used to infer rockfall events.*

lute values. The "rate" is based on the idea that thick stems expose a larger target (DBH) to falling rocks than thin ones and so large trunks are more likely to be subject to GD. We then determined the yearly DBH increment of every individual tree by dividing its DBH by the number of rings between pith and sample year (2002) at breast height. In a further step, values were multiplied by the number of years a tree had existed at the beginning of a particular decade. The DBH values of all trees existing at the beginning of a particular decade were then summarized to comprise what we refer to as exposed diameter (ED; in m). To obtain the rockfall "rate", the decadal sum of GD was finally divided by the ED, indicating the number of GD recorded per meter ED and per decade. Within this study, increment rates in trees were considered to remain constant, disregarding juvenile growth or ageing trends.

In addition to the decadal rockfall "rates", the trees sampled in the two sectors were classed according to their age at breast height (oldest to youngest) and split into two samples each. In both cases, Sample 1 was formed with the uneven samples (i.e. oldest, 3rd oldest, 5th oldest, …), while Sample 2 contained the even ones (i.e. 2nd oldest, 4th oldest, 6th oldest, …). We then calculated rockfall "rates" for these samples as well. In a further step, the rockfall "rates" of the entire populations as well as those of Samples 1 and 2 were converted from real into logarithmic values, a power regression trend line calculated and residuals from the regression model determined.

Due to the difficulties of dendrogeomorphological analysis in rockfall research and in order to analyze variations in decadal rockfall "rates", we arbitrarily chose a range of ±1.15 standard errors on the regression fit, assuming a normal distribution of the residuals from the regression model, as a criterion for identifying exceptional rockfall "rates". Indeed, decadal rockfall "rates" located within these ±1.15 standard errors (called $Var_{75\%}$) were considered to be noise and therefore insignificant. In contrast, the 25% of rockfall "rates" lying beyond these limits were subject to analysis in greater detail.

Finally, we used yearly rockfall "rates" (real values) to analyze short-term fluctuations in rockfall activity for the period 1950-2002. This use of yearly resolved data on GD also allowed estimation of the influence of anthropogenic rockfall triggering during the periods of dam construction work in 1988/89 (Dams 1–5; see Figs. B2.1, B2.2) and 1996-1998 (Dams 6 and 7) as well as the distribution of GD thereafter.

2.3.3 Spatial visualization of single-tree data

Data on single trees included their position, their age at breast height, and the number as well as the years of GD. Tree coordinates were transformed into geo-objects and information from the database linked as attributes to the single trees, allowing spatial visualization of the data in a Geographical Information System (GIS). Data were investigated with the ArcGIS Geostatistical Analyst software (ESRI 2003a) in order to examine spatial relationships between all sample points. Following the procedure described in Johnston *et al.* (2001), skewed data were first transformed to make them normal. Trend analyses were then used to identify directional influences (global trends), and data detrended using second-order polynomials. In a next step, spatial autocorrelations were analyzed using spherical semivariogram models and covariance clouds. As a result, the numbers of lags and bin sizes have been adapted. Finally, cross-validation of measured with predicted points allowed determination of mean prediction errors of the interpolations. After the exploration of the data, the Ordinary Kriging model (Johnston *et al.* 2001) was chosen for the visualization of continuous surfaces. Interpolations were performed including data from five neighboring trees. In angular sections, at least two trees were taken into consideration. Results were edited using ArcView 8.3 software (ESRI 2003b). Within this study, interpolations were performed to visualize the age structure of the forest stand and the spatial distribution of recurrence intervals.

2.4 Results

2.4.1 Age structure of the forest stand

Data on the pith age at breast height indicate that the 135 sampled *Larix decidua* Mill. trees are, on average, 297 years old [6]. Over the centuries, sampled trees gradually (re-) colonized the slope to build up the current forest at *Täschgufer*. However, we observe that 25% of the sampled trees – mostly those located in the southern sector – reached breast height between 1725 and 1759.

[5] The term 'rockfall "rate"' used in this paper is only a proxy for the true rate. We therefore keep the quotation marks whenever using this term.

[6] All of the numbers given below refer to age at breast height and do not indicate germination or reception dates.

Figure B2.6 illustrates the spatial distribution of the age structure at *Täschgufer*, indicating that old trees are largely concentrated on the northern part of the study area. In this sector, 78 trees were considered. The boundaries of age classes broadly correspond with the outer limits of the rockslide deposits mentioned in Chapter B2.2.

The 57 trees sampled in the southern sector are, on the other hand, considerably younger and generally started to (re-)colonize the slope in the early 18th century. The youngest trees are concentrated alongside the rockfall couloirs underneath Dam 7 and at the southeastern edge of the study area. Even so, younger trees are repeatedly located close to the forest fringes on the valley floor, where anthropogenic activity markedly influenced tree growth and succession rates (i.e. farming activities, extraction of fire- and construction wood).

Table B2.1 *Pith age at breast height of the trees sampled for analysis (in years)*

Pith age at breast height	Northern sector	Southern sector
Mean	362	212
Standard deviation	141.4	75.6
Maximum	684	406
Minimum	61	45

The major differences in the age structure between the two sectors also appear in Table B2.1. While the trees sampled in this study averaged 362 years in the northern sector, they have an average age of only 212 years in the southern sector. Similarly, the oldest sample in the northern sector attained breast height in AD 1318 and the youngest tree here reached breast height in 1941. In contrast, the oldest tree from the southern sector dates to 1596 and the youngest to 1957.

2.4.2 Visible defects and growth reactions to rockfall impacts

Investigations permitted identification of 236 visible defects on the 135 *Larix decidua* Mill. stems chosen for analysis. As illustrated in Table B2.2, candelabra trees (= broken crown) largely predominated among the visible defects. This growth feature occurs

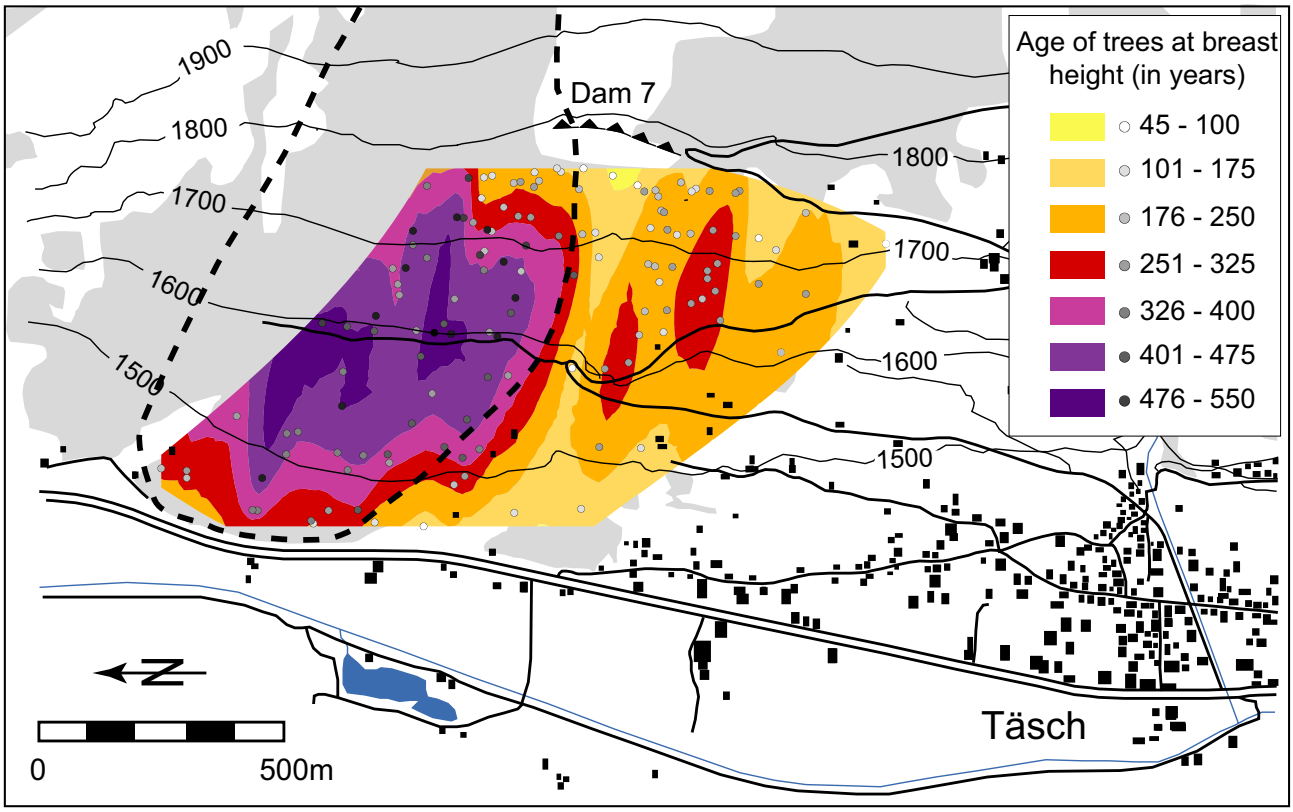

Fig. B2.6 *Mean age of Larix decidua Mill. trees sampled on the Täschgufer slope. The patterns have been generalized based on interpolations. Ages are for tree at breast height.*

after the decapitation of the crown or part of the stem and could be identified in 151 cases (64%). Based on observations in the field, we believe that candelabra trees at *Täschgufer* were largely due to the propagation of impact energies from the lowermost part of the trunk to the apex of the stem, resulting in crown breakage between 2 and 13 m above the ground. In contrast, the decapitation of tree crowns was only rarely caused by high bounces of rockfall fragments. Recent or (partly) overgrown injuries (scars) were observed in 58 cases (25%). Finally, 27 trees (11%) were obviously tilted by rockfall impacts.

The analysis of the 564 cores allowed identification of 786 GD attributed to rockfall activity on the slope. In some cases, impacts caused GD in more than one core of the same tree, reducing the number of different rockfall events to 761. Table B2.2 shows the predominant occurrence of traumatic rows of resin ducts. This feature was used in 675 cases (86%) to determine GD. Abrupt growth suppression occurred in 50 samples (6.5%), whereas abrupt growth release and reaction wood could only be found in 24 cores each (3%). Finally, callous tissue in cores proved to be rather scarce, occurring in only 13 cases (1.5%).

Characteristic increment curves of cores showing compression wood, growth suppression and missing rings after scarring are illustrated in Figure B2.7: Tree A displays an abrupt growth reduction in 1908. As the indexed reference chronology – marked as REF in Figure B2.7 – does not show this sudden change in yearly increment, the growth suppression in Tree A was not driven by climatic variations but by stem breakage due to rockfall. The increment curves of Tree B illustrate that this tree was tilted in 1982 and started to produce reaction wood on the downhill side (core d) thereafter, while tree-ring formation remained unaffected on the uphill side (core c). In this case, eccentric growth lasted until the core was extracted in 2002. Finally, Tree C was apparently scarred in 1970: While the callous tissue had not yet recovered the injury on the uphill side (core c), it overgrew the wound at core b-c by 1981.

2.4.3 Spatial distribution of growth disturbances

In the investigated forest stand at *Täschgufer*, reconstructed rockfall activity varied greatly across the slope. The spatial distribution of interpolated recurrence intervals are given in Figure B2.8, and show that GD abundantly occurred in the trees located above 1700 m a.s.l., where surfaces gradually become more sparsely forested. Similarly, GD have repeatedly been reconstructed in trees growing in the rockfall couloirs of the southern sector below the recently built Dam 7. Here, trees were regularly disturbed by rockfall fragments and recurrence intervals were locally <10 years. In a few century-old trees growing close to the northern sector, dendrogeomorphological analysis indicates that tree growth has been disturbed almost twice a decade since the mid 19th century. In contrast, low numbers of GD can be found in trees growing in the northern sector. In this part of the slope, recurrence intervals proved to be particularly high. Here, intervals between two GD regularly exceeded 150 years and individual century-old trees even showed no GD at all. Not surprisingly, the spatial pattern of recurrence intervals largely coincides with the distribution of the age structure seen in Figure B2.6 and oldest trees are commonly found in areas with relatively low numbers of GD. In contrast, youngest trees are largely concentrated in areas where rockfall repeatedly caused GD, leading to increased mortality and subsequently

Table B2.2 *Different types of damage observed in the field (left) and growth reactions reconstructed from increment cores (right) at Täschgufer (adapted after* Schneuwly 2003*)*

Visible defects		**Growth reactions**	
Broken crown	151 (64 %)	Growth release	24 (3 %)
Tilted stem	27 (11 %)	Growth suppression	50 (6.5 %)
Injuries (scars)	58 (25 %)	Reaction wood	24 (3 %)
		Callous tissue	13 (1.5 %)
		Traumatic resin ducts	675 (86 %)
Total	236 (100 %)	Total	786 (100 %)

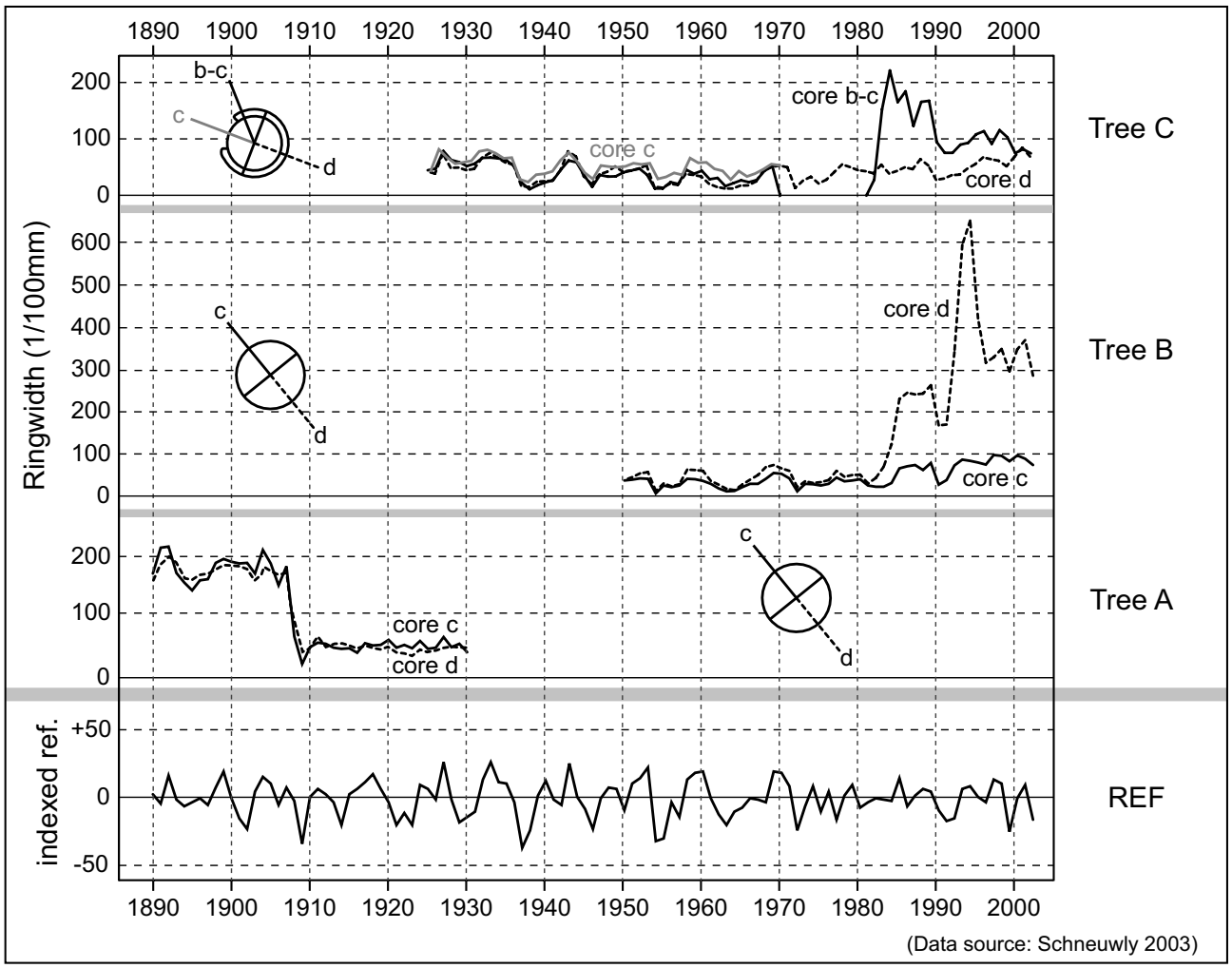

Fig. B2.7 *Examples of growth disturbances produced by rockfall events. Tree A shows an abrupt growth reduction as a result of stem breakage in 1908. Tree B was tilted in 1982 and initiated reaction wood on the downhill side (core d) thereafter. Tree C was scarred in 1970: While the scar is not yet overgrown at core c, callous tissue overgrew the wound at core b-c by 1981. Part of the reference ring width chronology (REF) is also shown.*

to higher recruitment rates by opening up sites for germination.

2.4.4 Rockfall magnitudes and frequencies

Throughout the last four centuries, rockfall fragments have continuously caused GD to the trees sampled for analysis. There seems to have been no period since AD 1600 without rockfall, and activity most commonly consisted of low magnitude–high frequency events. In addition, tree-ring and age structure analyses also allowed identification of one high magnitude–low frequency event, which (almost) completely destroyed the forest stand in the southern sector of the slope in 1720. In the northern sector, trees sampled were disturbed considerably during the rockfalls but largely survived. Figure B2.9 shows that according to the reconstructed data, 13 trees were obviously injured by abundant rockfall. Simultaneously, 11 trees reacted to the event with an abrupt growth release starting in 1721. These trees presumably benefited from the sudden elimination of neighboring trees, which improved their own growth conditions (e.g., light, nutrients, humidity). Within the northern sector, GD mainly occurred in trees located in the upper part of the slope (above 1590 m a.s.l.). Here, 16 of the existing 33 trees (48%) showed GD in 1720. In contrast, trees sampled in the lower part of the slope mostly remained unaffected by the 1720 event and scars were only present in 3 of the 21 existing trees (14%). Even so, abrupt growth releases following the event are missing here. Figure B2.9 also shows that, as an indirect consequence of the high magnitude event in 1720, trees abundantly (re-) colonized the slope. Between 1725 and 1759, 25%

of all sampled trees reached breast height (i.e. 34 trees). Most of the successor trees were located in the southern sector of the slope.

2.4.5 Decadal variations in rockfall activity

2.4.5.1 Northern sector (1600-1999)

Investigations of rockfall activity in the northern sector start in the year 1600, when 29 of the trees sampled were taller than breast height. We hence disregarded 12 rockfall events occurring between 1394 and 1599, since the sample depth appeared to be too low for reliable analysis and the individual trees were unevenly distributed within the sector. The number of GD was reduced to 400 events derived from 78 trees. Among all trees sampled in the sector, the DBH averaged 47.97 cm in 2002. As indicated in Table B2.3, the largest and smallest trees were 76.4 and 17.51 cm DBH in 2002. As a result, the decadal DBH increments varied between 0.6 and 6.29 cm, with an average increment of 1.56 cm $(10 \text{ years})^{-1}$ tree^{-1}. While the exposed diameter (ED) of the trees sampled within the northern sector only totaled 3.9 m at the beginning of the investigated period in 1600, it gradually rose to 37.8 m by 1990. Table B2.3 further illustrates that the decadal rockfall "rates" averaged 0.65 GD 1 m ED^{-1} $(10 \text{ years})^{-1}$.

The reconstructed rockfall "rates" of the entire population as well as the "rates" from Samples 1 and 2 are illustrated in Figure B2.10a. For the period before the important rockfalls in 1720, rockfall "rates" indicate considerable fluctuations in reconstructed numbers of GD. As a result of the high magnitude rockfalls in 1720 and the considerable damage caused to the forest fringe, the highest decadal rockfall "rate" in the last four centuries was noted in the 1720s, causing 1 GD per 0.65 m ED (i.e. a "rate" of 1.53). Since, data indicate that rockfall activity continually decreased after the 1720 event (see Figure B2.10a), interrupted by decades with significantly low (1850s, 1960s, 1970s) and significantly high rockfall "rates" (1870s, 1990s).

During the 19th century, rockfall "rates" indicate rather low values during the 1850s (0.24) and, to a minor extent, the 1810s (0.36). Thereafter, rockfall caused higher "rates" during the late 19th and the early 20th century (i.e. 1870s, 1890s, 1920s, 1940s). Within

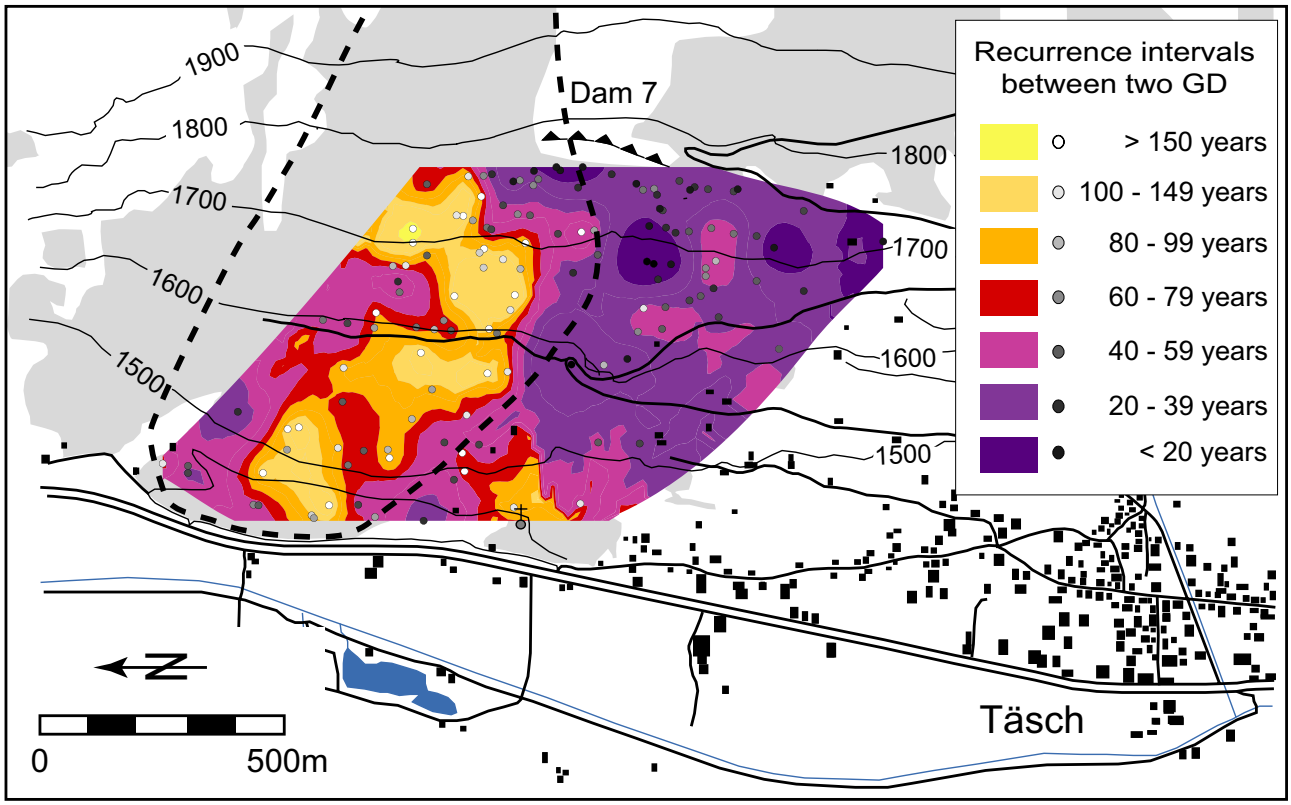

Fig. B2.8 *Recurrence intervals of GD for the forest stand investigated. Intervals designate the number of years passing between two reconstructed growth disturbances on a single tree.*

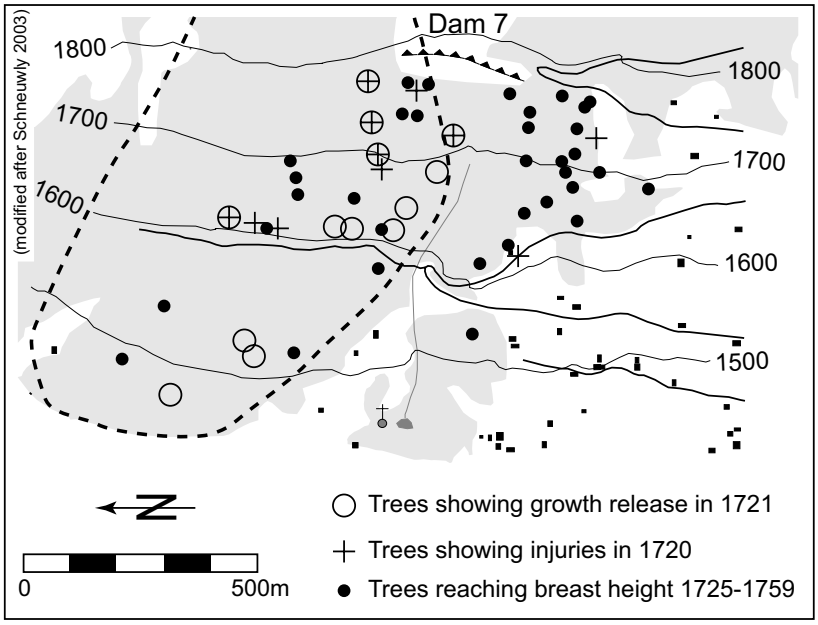

Fig. B2.9 *Damage resulting from the 1720 rockfall. Thirteen trees have been injured (cross) and 11 trees show an abrupt growth release starting in 1721 (white circle). The (re-)colonization of the rockfall slope (black circle) in the succeeding decades (1725-1759) most probably represents a reaction to the 1720 rockfall event.*

the second half of the 20th century, rockfall "rates" indicate a period with low activity lasting from the 1950s until the 1970s. For the 1970s, a decadal value of 0.2 was identified, meaning that only one growth disturbance (GD) occurred every 5 m of exposed diameter (ED). This period of low activity was followed by an increase in the rockfall "rate" during the 1980s (0.54) and, even more, the 1990s (0.57). The importance of this increase as well as the influence of dam construction works on the decadal ratios of the 1980s and 1990s will be analyzed below in Chapter B2.4.6.

2.4.5.2 Southern sector (1740-1999)

Due to the different age structure and the large number of trees sampled that had grown after the high magnitude rockfalls in 1720 in the southern sector, the analysis of rockfall "rates" only starts in the 1740s, when 20 of the trees sampled were greater than breast height. We disregarded 8 reconstructed GD occurring between 1657 and 1734, since the sample depth appeared to be too low for reliable analysis. In total, 341 GD were dated in the 57 trees sampled. Among the trees sampled, the DBH averaged 48.3 cm in 2002. As illustrated in Table B2.4, the largest tree had 79.5 cm and the smallest only 25.4 cm DBH in 2002. As a result, the decadal DBH increment greatly varied between 0.78 and 8.59 cm, with an average DBH increment of 2.70 cm (10 years)$^{-1}$ tree^{-1}. At the beginning of the investigation in 1740, the ED of all trees sampled totaled 0.9 m and gradually rose to 27.7 m by 1990.

Results on decadal rockfall "rates" in the southern sector averaged 2.36 GD 1 m ED^{-1} (10 years)$^{-1}$, which represents a value almost four times higher than that of the northern sector. Reconstructed rockfall "rates" of the entire population as well as the "rates" of Samples 1 and 2 are shown in Figure B2.10b. During the early decades

Table B2.3 *Size statistics of the trees sampled in the northern sector; DBH: diameter at breast height as measured in 2002 (in cm), 10-yr DBH: 10-year increment of the DBH (in cm), and rockfall "rates" (GD 1 m ED^{-1} (10 years)$^{-1}$).*

Northern sector	DBH	10-yr DBH	rockfall "rates"
Mean	47.97	1.56	0.65
Standard deviation	12.62	0.97	0.34
Maximum	76.4	6.29	1.53
Minimum	17.51	0.61	0.2

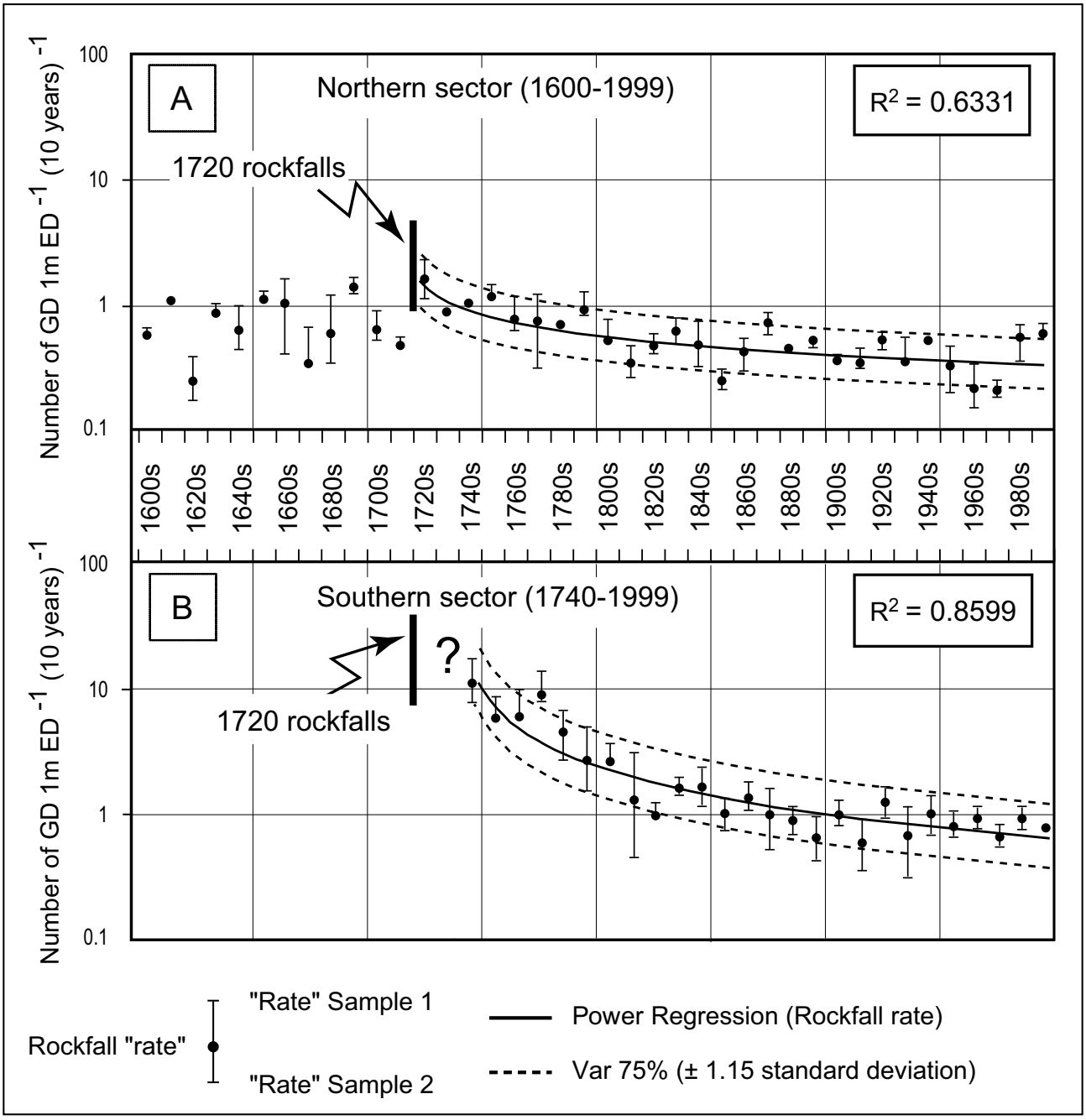

Fig. B2.10 *Reconstructed rockfall activity. Rockfall activity is measured by the rockfall «rate» (for explanation see text). (a) In the northern sector, analyses cover the last four centuries (1600-1999), indicating that the large 1720 rockfalls temporarily reduced the protection afforded by the forest. (b) After the elimination of the forest in the southern sector by the 1720 event, the recolonizing trees permanently improved their protective function, reducing the number of rockfall impacts on the trees sampled by almost 13 times since the 1740s.*

following the high magnitude rockfalls of 1720, the successor trees sampled for analysis were repeatedly subject to GD. As a consequence, the highest rockfall "rate" was reconstructed for the 1740s, when almost 11 disturbances were identified per 1 m ED (i.e. a "rate" of 10.99). Similarly to the northern sector, reconstructed rockfall "rates" continually decreased in the southern sector after the high magnitude rockfalls of 1720.

Unlike the results from the northern sector with six decadal values located beyond the $Var_{75\%}$ boundaries, only two rockfall "rates" lie beyond the $Var_{75\%}$ limits here, namely those of the 1770s and the 1820s (Fig. B2.10b). We note that, after a slight decrease in the 1750s and 1760s, the "rate" indicates a considerable increase in rockfall activity in the 1770s. For this period, the rockfall "rate" gives a value of 8.86 GD 1

m ED^{-1} (10 years)$^{-1}$, approaching that for the 1740s. This period of increased rockfall activity lasted until the 1780s or even 1790s. In contrast to the high magnitude rockfalls of 1720s, reconstructed data indicate that the considerable number of GD identified for the last three decades of the 18th century were not caused by one high magnitude event, but rather by a series of years with high rockfall activity (i.e. 1772, 1774, 1779, 1783, 1792).

Even though the number of GD also increased in the northern sector (see Fig. B2.10a), significant effects remained mostly restricted to the "rates" of the southern sector. Between the 1870s and the 1940s, comparably low numbers of GD were found in the trees sampled, resulting in a considerable decrease in rockfall "rates". During this period, the lowest rockfall "rate" of the last 260 years was derived, totaling 0.63 during the 1910s. In contrast to the northern sector, the rockfall "rate" started to increase again in the 1940s, oscillating around the calculated power regression trend line ever since. However, the changes in the rockfall "rates" seem to be less marked here. Again, the influence of the dam construction works on the decadal ratios of the 1980s and 1990s will be analyzed further down in Chapter B2.4.6.

2.4.6 Yearly fluctuations in rockfall activity (1950–2002)

In complement to the decadal rockfall "rates", yearly fluctuations were analyzed for the period 1950-2002. In total, we identified 172 GD, 105 in the southern (61%) and 67 in the northern sector (39%). On average, more than 3 GD year^{-1} could be identified in the 135 trees sampled. As illustrated in Figure B2.11a, the number of reconstructed GD remained on a comparably low level in the northern sector during the first three decades of investigation, when years without GD occur almost as frequently as years with GD. After 1980, rockfall repeatedly caused more GD to the trees sampled. Reconstructed data neatly reflect the period of increased rockfall activity in the 1980s and the early 1990s, as described for the Täschgufer slope by Lauber (1995). Between 1950 and 2002, yearly rockfall "rates" averaged 0.037 GD 1 m ED^{-1} year^{-1}, indicating that approximately 1 GD was recorded for every 27 m of ED.

In the southern sector, decadal rockfall "rates" slightly increased in the 1940s and thereafter. Yearly resolved "rates" indicate that during the first three decades, (short) periods with increased numbers of GD (e.g., 1959-1964) were followed by several years with (almost) no GD (Fig. B2.11b). Similar to the northern sector, considerably increased rockfall "rates" can be discerned in 1980 and 1992. In contrast, the high rockfall "rate" reconstructed for 1986 (0.28) was probably restricted to the southern sector. On average, yearly "rates" totaled 0.085 GD 1 m ED^{-1} year^{-1}, indicating that more than 1 GD has been recorded per 12 m of ED.

In contrast to the results from trees located in the heavily disturbed forest stand above 1780 m a.s.l. (Stoffel *et al.* 2005b), the construction of Dams 1 to 5 (1988/89; see Fig. B2.11b) only slightly influenced the rockfall "rates" of the present study. In the northern sector, the two GD recorded in 1989 caused an increase in the decadal "rate" from 0.46 to 0.52. Similarly, the only GD recorded in the southern sector in 1989 influenced the "rate", resulting in a value of 0.96 instead of 0.92. In contrast, reconstructed rockfall "rates" prove to be influenced by the construction works (e.g., excavation, blastings) of the two protection dams in the late 1990s. As can be seen from Figure B2.12, rockfall triggered during the construction of Dam 6 in 1996 (~ 2000 m a.s.l.) caused six GD. Growth reactions were even more frequent during the construction of Dam 7 in 1998 (1780 m a.s.l.). As a result of anthropogenic intervention on the slope, six GD were caused in the northern and nine GD in the southern sector. For this reason, the rockfall "rates" of the 1990s given in Chapter B2.4.5 were clearly influenced by anthropogenic intervention on the slope, making it difficult to estimate the undisturbed rockfall frequency over this period.

Table B2.4 *Size statistics of the trees sampled in the southern sector; DBH: diameter at breast height as measured in 2002 (in cm), 10-yr DBH: 10-year increment of the DBH (in cm), and rockfall "rates" (GD 1 m ED^{-1} (10 years)$^{-1}$).*

Southern sector	DBH	10-yr DBH	rockfall "rates"
Mean	48.39	2.70	2.36
Standard deviation	13.89	1.58	2.70
Maximum	79.58	8.59	10.99
Minimum	25.47	0.78	0.63

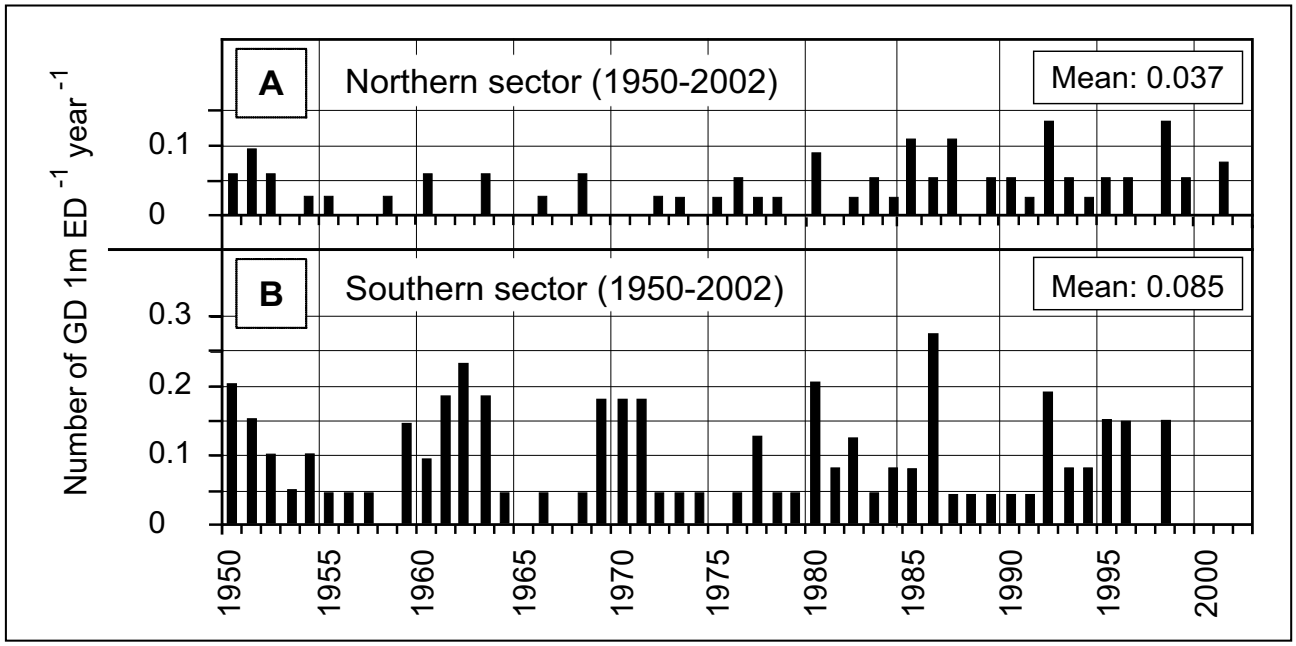

Fig. B2.11 *Annual estimates of rockfall 1950-2002. Note the important variability in reconstructed growth disturbances and different activity in the sectors.*

As a further consequence, anthropogenic intervention on the slope hindered rockfall fragments to cause GD to the trees sampled after 1998. While no GD have been recorded since 1999 in the southern sector (Fig. B2.12), GD could still be identified in the northern sector. As illustrated in Figure B2.12, rockfall fragments apparently passed north of the recently built dams in 1999 and 2001, causing GD to five trees in the northern sector. In the sparsely wooded areas between Dam 6 and 7, reconstructed data clearly indicate that abundant rockfall still occurs on the slope (Stoffel *et al.* 2005b). We therefore have to believe that the recently built dams efficiently stopped rockfall in the recent past and so further influenced the rockfall "rates" of the 1990s.

2.5 Discussion

In the study we report here, cores extracted from 135 living *Larix decidua* Mill. trees allowed reconstruction of yearly and decadal rockfall activities on the *Täschgufer* slope. Similar to analysis used in debris flow, snow avalanche or flooding research (e.g., Schweingruber 1996), we investigated growth disturbances (GD) in increment cores to analyze past rock-fall activity. In the trees sampled, rows of traumatic resin ducts proved to be by far the most common reaction to rockfall impacts. Reaction wood, growth suppression or growth release could be identified less frequently.

We identified 741 GD covering the period 1600-2002. Impacts could be found more commonly in trees located in the southern sector of the slope, where GD rockfall recurred locally more than once per decade. According to the results, we believe that rockfall activity at *Täschgufer* mainly consisted of low magnitude–high frequency events, considered to be typical for rockfall in alpine areas (e.g., Matsuoka & Sakai 1999, Jomelli & Francou 2000). The only high magnitude–low frequency event occurred in 1720, causing considerable damage to the forest in the northern sector. As a result, the forest fringe was displaced downslope. The forest stand in the southern sector was almost completely destroyed by the devastating rockfalls in 1720. Data also show that the high rockfall frequency both inhibited recolonization and caused considerable damage in the juvenile trees of the southern sector thereafter. As a result, considerable differences emerge in the reconstructed numbers of GD between the northern and the southern sector.

In contrast to the analysis of geomorphic processes involving larger volumes, such as debris flows, snow avalanches or flooding, results from dendrogeomorphological investigations of rockfalls cannot immediately be used to illustrate yearly or decadal fluctuations in rockfall activity. As rockfall consists of single falling, bouncing or rolling stones, a single event may only disturb trees along its trajectory. Furthermore, trees at *Täschgufer* were of uneven age and displayed

abundant differences in their DBH as well as the decadal DBH increment. As a result, the number of reconstructed GD steadily increased with time, reaching maximum values for the recent past. Even so, a ratio dividing the decadal number of GD by the number of trees (Tr) existing at the beginning of a particular decade cannot concisely represent the importance of decadal rockfall activity. As illustrated in Table B2.5, GD–Tr ratios regularly increased in periods following major modifications in the sample depth (e.g., 1690s and after 1720 in the northern and after the 1770s in the southern sector), leading to an overestimation of past rockfall activity. Even so, it appears that the GD–Tr ratio may not correctly represent the rockfall activity during the late 20th century, when the lack of succeeding trees and an almost constant sample depth again influence the ratios.

The rockfall "rate", considering the exposed diameter (ED = DBH of all sampled trees within a sector at the beginning of a particular decade), proved, instead, to be a more reliable indicator of past rockfall activity, as it takes account of the diameter exposed to rockfall fragments as well as the gradual changes of the ED with time. As a further result, the rockfall "rates" nicely illustrate the protective function of the two selected forest stands: After the devastating rockfalls of 1720, the recolonizing trees could not efficiently stop rockfall fragments in the southern sector, resulting in considerably high decadal ratios in the early decades of the analysis (e.g., 10.99 GD 1 m ED $^{-1}$ (10 years)$^{-1}$ in the 1740s). Compared to the 1740s, almost 13 times fewer GD are dated per 1 m of ED today. In the forest stand of the northern sector, rockfall "rates" persisted on a relatively low level throughout the last four centuries. Nonetheless, the high magnitude event of 1720 also emerged from the GD–ED data, resulting in the highest decadal rockfall "rate" (1.53 GD 1 m ED^{-1} (10 years)$^{-1}$) recorded since AD 1600. As a further consequence, the efficacy of the protective forest was temporarily reduced, resulting in higher "rates" until the late 18th century. Since then, the protective function has further increased, resulting in a rockfall "rate" based on the linear regression trend of approximately 0.4.

This study represents the first attempt to analyze yearly and decadal fluctuations in rockfall activity on a forested slope. It has furthermore analyzed the age structure of the forest stands. Nevertheless, some issues remain to be resolved. In this study, we tried to select severely injured trees. However, comparisons between visible defects with reconstructed events indicate that scars and "candelabra form" trees may only

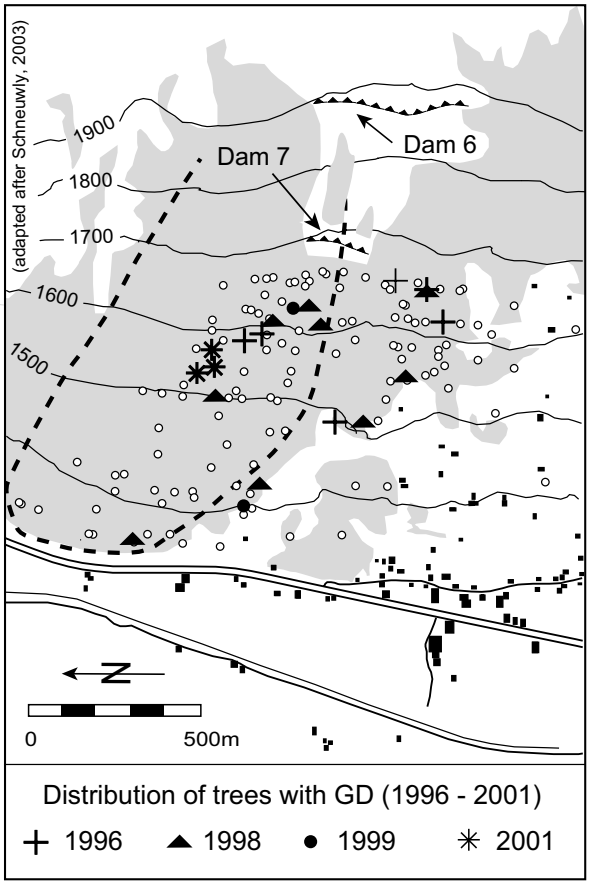

Fig. B2.12 *Rockfall events during and after dam construction, 1996-2002. Growth disturbances have been recorded during construction works at Dam 6 in 1996 (cross), Dam 7 in 1998 (triangle) and in the succeeding years (circle = 1999; star = 2001). No growth disturbances were recorded in the years 1997, 2000 and 2002.*

reflect 28% of the GD (i.e. resin ducts, callous tissue, growth suppression) dated on the cores. We therefore stress the key role played by the sampling strategy by pleading for more random strategies when choosing trees in heavily disturbed rockfall forests. Even so, as the results presented above are from two sectors of one single slope, replicate studies are needed from a variety of similar sites to place our reconstructions as well as the general applicability of the rockfall "rate" in a wider context.

2.6 Conclusion

The approach outlined in this study proved to be a useful tool for analyzing fluctuations in inter-annual and inter-decadal rockfall activity on a forested slope. In contrast to former studies, this analysis was no longer limited by the restricted temporal sample

available for the assessment of long-term variations in rockfall activity or by the temporal resolution of the approach (e.g., lichenometry). Although the techniques used in this investigation need further refinement and minor modifications in the sampling strategy, the results presented above clearly show that dendrogeomorphic investigations have the potential to produce results on yearly fluctuations and decadal ratios of rock-

Table B2.5 *Growth disturbance data by decades for the two sites; GD = growth disturbances; ED = exposed diameter, i.e. DBH of all trees sampled at a particular decade (in m); Tr = decadal number of existing trees, rockfall "rates"= number of GD per 1 m ED and decade; GD–Tr ratio = number of GD per tree (Tr) and decade. Bold numbers indicate maximum, bold italic numbers minimum values.*

Decade	GD		ED (m)		Tr		rockfall "rates"		GD–Tr ratio	
	N	**S**	**N**	**S**	**N**	**S**	**N**	**S**	**N**	**S**
1600s	2	-	3.9	-	29	-	0.51	-	0.07	-
1610s	4	-	4.2	-	29	-	0.95	-	0.14	-
1620s	*1*	-	4.6	-	30	-	0.22	-	*0.03*	-
1630s	4	-	5	-	35	-	0.79	-	0.11	-
1640s	3	-	5.5	-	38	-	0.55	-	0.08	-
1650s	6	-	5.9	-	39	-	1.01	-	0.15	-
1660s	6	-	6.4	-	40	-	0.94	-	0.15	-
1670s	2	-	6.9	-	43	-	0.29	-	0.05	-
1680s	4	-	7.5	-	45	-	0.53	-	0.09	-
1690s	10	-	8.1	-	48	-	1.24	-	0.21	-
1700s	5	-	8.6	-	49	-	0.58	-	0.1	-
1710s	4	-	9.2	-	49	-	0.43	-	0.08	-
1720s	15	-	9.8	-	50	-	1.53	-	0.3	-
1730s	10	-	10.5	-	51	-	0.95	-	0.2	-
1740s	13	10	11.3	0.9	58	19	1.15	10.99	0.22	0.53
1750s	13	8	12.1	1.4	62	22	1.07	5.93	0.21	0.36
1760s	10	11	13	1.8	66	25	0.77	6.01	0.15	0.44
1770s	11	21	13.9	2.4	68	28	0.79	8.86	0.16	0.75
1780s	11	13	14.8	2.9	69	30	0.74	4.42	0.16	0.43
1790s	14	10	15.7	3.6	69	33	0.89	2.75	0.2	0.3
1800s	9	12	16.6	4.4	70	35	0.54	2.75	0.13	0.34
1810s	6	7	17.6	5.1	70	37	0.33	1.36	0.09	0.19
1820s	8	*6*	18.5	5.9	71	38	0.43	1.02	0.11	*0.16*
1830s	12	11	19.5	6.7	71	40	0.62	1.64	0.17	0.28
1840s	10	13	20.5	7.6	71	43	0.49	1.7	0.14	0.3
1850s	5	9	21.5	8.7	74	46	0.23	1.04	0.07	0.2
1860s	9	14	22.6	9.7	74	48	0.4	1.44	0.12	0.29
1870s	16	11	23.7	10.9	75	49	0.68	1.01	0.21	0.22
1880s	11	11	24.8	12.1	76	51	0.44	0.91	0.14	0.22
1890s	13	9	25.9	13.3	76	52	0.5	0.68	0.17	0.17
1900s	9	15	27	14.6	76	53	0.33	1.03	0.12	0.28
1910s	9	10	28.1	15.9	76	54	0.32	*0.63*	0.12	0.18
1920s	14	22	29.3	17.3	77	55	0.48	1.28	0.18	0.4
1930s	10	13	30.5	18.6	77	55	0.33	0.7	0.13	0.24
1940s	15	21	31.7	20	77	55	0.47	1.05	0.19	0.38
1950s	10	18	32.9	21.5	78	57	0.3	0.84	0.13	0.32
1960s	7	22	34.1	23.1	78	57	0.21	0.95	0.09	0.39
1970s	7	17	35.4	24.6	78	57	*0.2*	0.69	0.09	0.3
1980s	19	25	36.6	26.2	78	57	0.52	0.96	0.24	0.44
1990s	21	23	37.8	27.7	78	57	0.56	0.83	0.27	0.4

fall activity over several centuries. Moreover, we have been able to determine spatial variations in rockfall activity, considerable differences in recurrence intervals, and the changes in the efficacy of the protective function of the two forest stands at *Täschgufer*.

Acknowledgements: The authors gratefully acknowledge Sascha Negro for assistance in the field. Simone Perret is warmly acknowledged for providing helpful comments and Heather Murray for improving the English of this paper. The authors also want to thank the local community president Kilian Imboden and the local forester Leo Jörger for coring permission and support. Finally, the authors gratefully acknowledge the suggestions made by the reviewers Nel Caine and Brian H. Luckman.

*****

CHAPTER C

HEIGHT DISTRIBUTION AND THE PERSISTENCE OF ROCKFALL SCARS ON STEM SURFACES

This third part focuses on the vertical distribution of impact scars on stem surfaces of three adult trees felled in the *Altdorfer Bannwald*. Moreover, the visibility of past impacts is addressed and the importance of 'blurred evidence' (i.e. completely overgrown scars) is investigated. The paper presented here has been published in *"Schweizerische Zeitschrift für Forstwesen"*. It provides a first impression on how rockfall may behave on forested slopes and to what degree trees may 'blur' evidence of past events. Simultaneously, the paper raises a large number of questions that will partly be dealt with and answered in Chapter D.

1. Vertical distribution and visibility of scars

Markus Stoffel [1]

"Assessing the vertical distribution and visibility of scars in trees"

[1] *Groupe de Recherches en Géomorphologie (GReG), Department of Geosciences, Geography, University of Fribourg*

published in Schweizerische Zeitschrift für Forstwesen 2005, Vol. 156, No. 6, 195–199
revised: 22 April 2005, accepted: 25 April 2005

Summary

Rockfall generally consists of individual rocks and boulders moving downslope in a falling, bouncing or rolling motion. As a result, impacts on trees may occur almost anywhere between ground level and several meters above. The present paper therefore focuses on the vertical distribution and the visibility of scars on stem surfaces. Three adult trees from the Bannwald of Altdorf were sawn into 307 cross-sections in order to determine impact heights and to assess the number of hidden scars no longer visible from outside. Results indicate that scars can be observed at heights of up to nine meters or more. Depending on the tree species selected, 'blurred evidence' accounted for 16 to 49%. We can suppose that bark properties might influence the blurring of scars.

Zusammenfassung

Untersuchung der vertikalen Verteilung und der Sichtbarkeit von Steinschlagverletzungen an und in Bäumen. Unter Steinschlag versteht man gemeinhin die fallende, springende oder rollende Abwärtsbewegung von Einzelsteinen und -blöcken. Tritt Steinschlag in bewaldeten Hängen auf, so können Baumtreffer aufgrund der unterschiedlichen Bewegungsmechanismen sowohl in Bodennähe wie auch in mehreren Metern Höhe festgestellt werden. Der vorliegende Aufsatz zielt deshalb auf die vertikale Verteilung der Schäden sowie die Sichtbarkeit von Verletzungen auf Stammoberflächen ab. Untersuchungen an 307 Stammscheiben von drei adulten Bäumen aus dem Bannwald von Altdorf zeigen, dass Steinschlagschäden bis in Höhen von mehr als neun Metern auftreten können. Daneben fällt auch auf, dass ein Teil der Schäden von aussen nicht mehr sichtbar ist. Je nach Baumart variert der Anteil der 'versteckten' Schäden zwischen 16 und 49%. Es wird davon ausgegangen, dass unterschiedliche Borkeneigenschaften die Überwallung unterschiedlich stark beeinflussen.

Résumé

Analyse de la répartition verticale et de la visibilité des cicatrices causées sur les arbres par des chutes de pierres. Les chutes de pierres se manifestent sous forme de chute libre, saut ou roulement de pierres ou blocs individuels. En forêt, ces différents phénomènes peuvent causer des impacts sur les arbres, tant à proximité du sol qu'à plusieurs

mètres en dessus. La présente publication a pour but d'analyser la répartition verticale des cicatrices sur le tronc des arbres ainsi que leur visibilité. Pour ce faire, 307 disques provenant de trois arbres adultes du Bannwald d'Altdorf ont été prélevés afin de démontrer que les cicatrices causées par les chutes de pierres peuvent se trouver à des hauteurs allant jusqu'à 9 mètres. En outre, l'étude montre que certaines blessures ne sont plus visibles sur l'écorce même de l'arbre. Selon l'espèce choisie, ce nombre de cicatrices 'cachées' varie entre 16 et 49%, raison pour laquelle on part du principe que les différentes propriétés des écorces (épaisseur, écaillement) influencent le processus de cicatrisation de manière variée.

1.1 Introduction

Rockfall represents a removal of individual and superficial rock fragments from cliff faces (Selby 1993) and generally involves volumes < 5 m^3 (Berger *et al.* 2002). As a consequence, single rockfall fragments may only cause damage to those trees standing in the trajectory of rocks (Ø < 50 cm) and boulders (Ø > 50 cm). In addition, rockfall also differs from other processes, such as debris flows, flooding or wet snow avalanches, owing to the presence of different modes of motion and rotation occurring at once, namely falling, bouncing and rolling. As a result, and in opposition to the "flow" processes mentioned above, rockfall fragments hitting trees may cause impacts at considerably varying vertical positions on the stem surface.

Quantitative information on the vertical distribution of rockfall impacts on trees remains rather scarce. Gsteiger (1993) assessed the vertical distribution of scars on seven adult trees at *Brienzergrat* (*Bernese Prealps*, Switzerland), but he limited his analysis to only a few stem discs (cross-sections) and the two meters above the ground. Perret *et al.* (2004b), by contrast, analyzed the stem surface of 157 trees at *Diemtigtal* (*Bernese Prealps*, Switzerland) and documented more than 1700 visible scars. The study did not, however, take into account that older or relatively small injuries might no longer be visible on the stem surface, thus ignoring a certain number of past impacts.

Last but not least, Rickli *et al.* (2004) gave an overview on maximum bounce heights for different size classes of rockfall fragments. Results were given for slopes with a gradient of 35° and based on a rather small amount of field data. In addition, Rickli *et al.* (2004) considered neither the influence of neighboring trees nor changes in the slope gradient. As a consequence, the above-cited studies on impact heights of rocks and boulders on trees may give a reasonable first impression on the vertical distribution of scars on stems, but lack detail and do not include hidden (i.e. invisible) scars.

This study therefore aims to analyze the vertical distribution of past rockfall impacts (scars) and estimate the number of visible scars on the surface of the stem using a large number of cross-sections (i.e. stem discs) from adult trees. In order to achieve these goals, three adult trees (*Abies alba* Mill., *Fagus sylvatica* L., *Picea abies* (L.) Karsten) were analyzed from the basal area of the stem to the crown with a total of 307 cross-sections. Results illustrate the large array of impact heights occurring in trees from the protection forest above *Altdorf* (*Bannwald of Altdorf,* Canton Uri, Swiss Prealps), and they also give us a good idea of how much evidence of past rockfall events remains visible on the stem surface.

1.2 Study site

The *Bannwald of Altdorf* is located NNE of the village of *Altdorf* (Uri, Switzerland), extends from 440 to 1600 m a.s.l., and covers more than 300 hectares (Annen & Redmann 1993). Mean slope gradients in the forest average 70 to 80 % and stands mainly consist of *Fagus sylvatica* on the lower parts of the slope (< 1200 m a.s.l.), while *Picea abies* predominates in the subalpine forest, which is locally shifted to elevations above 1600 m a.s.l. by the presence of frequent foehn winds. In addition, the local dry soils covering bedrock and exposed cliffs favor colonization with *Pinus sylvestris* L.

Bedrock on the slope is part of the *Schächental Flysch* unit, forming a compilation of sandstone and clay layers (Labhart 1998). Rockfall is frequently triggered from these heavily fissured formations. Individual rockfall fragments are generally quite small, but boulders of up to 10 m^3 (> 30 tons) have been observed as well. On 16 August 1973, rockfalls even triggered 8000 m^3 from the 100 m high cliff at *'Rot Flue'* (Niederberger 2002). Evidence of other large rockfalls can be identified in the field and in local chronicles, indicating that major activity took place in 1268 and 1886. The latter event would have caused severe

Table C1.1 *Age, height, number of cross-sections prepared and number of scars reconstructed for the three trees selected from the Altdorfer Bannwald (Swiss Prealps).*

Tree	Tree Age	Tree height	Cross-sections	Scars
Abies alba	129 yrs	20 m	105	33
Fagus sylvatica	112 yrs	16 m	114	103
Picea abies	97 yrs	15 m	88	53
TOTAL	–	–	307	189

damage to the church and adjacent buildings in the valley floor (Annen & Redmann 1993).

Today, rockfall is most frequently triggered from the rock cliff at *'Rot Flue'*, but other source areas exist on the slope as well. Niederberger (2002) indicates that rockfall activity would be favored locally by frequent freeze–thaw cycles or periods with intense precipitation. Signs of rockfall activity are also preserved in the stems of the trees colonizing the *Bannwald of Altdorf*. According to field data gathered during the 'Sanasilva' program, 36% of the trees growing on the slope would show visible signs of past rockfall impacts (Jahn 1988). In addition, debris flows repeatedly occurred in the *Kapuzinertal*, where they caused loss of human life as well as the destruction of buildings in e.g., 1910 (Niederberger 2002).

As a result of rockfall and debris-flow activity, the *Bannwald of Altdorf* was first declared "protected" (*gebannt*) in 1387 AD. Over the centuries, private needs and economic pressure have however led to considerable overuse of the forest, thus hindering permanent forest cover and continuous regeneration, which are preconditions to maintain the protective effect of the stand. In the 19th century, the miserable state of the protection forest made actions necessary and, between 1878 and 1885, some 100'000 trees were planted in the *Bannwald*.

Similarly, the construction of protection dams was initiated around 1890. These dams are still in use today, together with protection nets installed along forest roads in the last decades. Today, the forest service of the *Korporations-Bürgergemeinde Altdorf* extracts approximately 1000 m^3 of wood and invests ca. CHF 220'000 every year to guarantee desirable forest structures and sufficient long-term protection of the village of *Altdorf*. In late 2002, a guided walk was opened in the *Bannwald of Altdorf* between *Altdorf* and *Eggberge* (*"schutz.wald.mensch", Lernpfad Altdorf*; Niederberger 2002), illustrating inter alia some of the aspects described in this section.

1.3 Methods

In order to assess the vertical distribution of impacts and to estimate the number of scars still visible on the stem surface, three adult trees with a large number of discernible scars on the stem surface were felled at different locations within the protection forest of *Altdorf*. In order to respect the influence of microtopography as well as changes in the slope gradient on bounce heights, two of the trees were sampled in areas with a slope gradient of 45° (*Picea abies, Fagus sylvatica*) and one from a slope gradient of 35° (*Abies alba*). The upslope position of the trees was noted on the stem surface before meter-long pieces were cut between the basal area and the apex of the tree to facilitate transport. Branches were disregarded, unless they showed obvious signs of rockfall impacts.

In the lab, detailed sketches were established for every single piece of the stem and the vertical position of scars noted. In a further step, the meter-long stem pieces were cut into a large number of cross-sections taken every 10 to 15 cm. For every tree, cross-sections were consecutively numbered, before they were polished and analyzed under the binocular eyepiece. Analysis of the cross-sections mainly focused on the identification of hidden or 'internal', overgrown scars and, which were therefore no longer visible on the stem surface (Kaennel & Schweingruber 1995). Subsequently, the age of every single rockfall injury was determined.

1.4 Results

1.4.1 Tree data and rockfall scars

A total number of 307 cross-sections were prepared from the three trees. In detail, 105 cross-sections were taken from a 20 m *Abies alba* stem and even 114 cross-sections prepared from a 16 m tall *Fagus sylvatica* tree. Finally, 88 stem discs were sawn from the 15 m tall *Picea abies*. Data, including the approximate

age of the trees, is given in Table C1.1. As the age was assessed at the lowest level of the cross-section, ages given do not, however, represent germination dates.

First and foremost, results indicate that the three selected trees suffered considerable damage from rockfall activity. For instance, the cross-sections analyzed from the 129-year old *Abies alba* stem show signs of the occurrence of 33 rockfall impacts between 1916 and 1996. In the *Fagus sylvatica* tree, 103 scars are identified on the different cross-sections. As several of the rockfall impacts occurred in the same years or might even have been caused by one and the same event, we reduced the number of years with reconstructed rockfall impacts for this tree to 25 between 1898 and 1994. The histogram presented in Figure C1.1 gives an idea on the temporal distribution of rockfall impacts reconstructed in the *Fagus sylvatica* tree. In addition, it also illustrates one of the lowest cross-sections of the tree with at least a dozen overgrown scars. Finally, the analysis of the *Picea abies* cross-sections enabled us to identify 53 different rockfall impacts, representing more than one event recorded every two years.

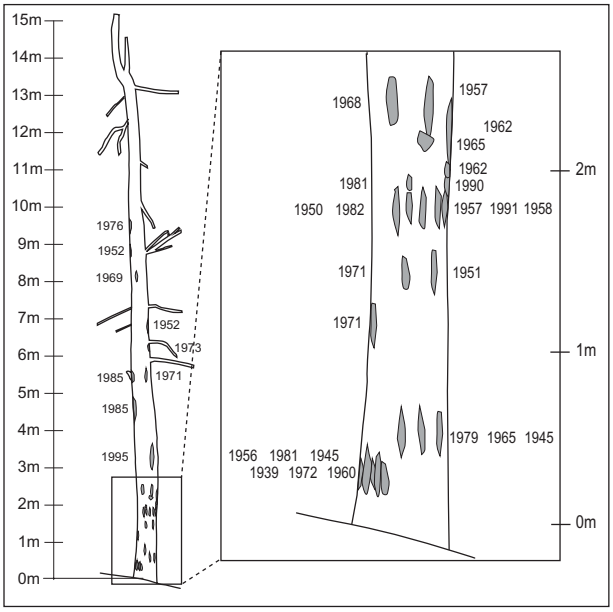

Fig. C1.2 *Vertical and horizontal distribution of 33 rockfall injuries reconstructed on an adult fir tree (Abies alba) from the Altdorfer Bannwald (Swiss Prealps). While most scars were recorded within the first 2 m above ground, the highest injury was found at a height of 930 cm.*

1.4.2 Vertical distribution of scars on stems

Analysis of the vertical distribution of rockfall scars on the stem surface indicate that rockfall can cause damage almost anywhere between ground level and several meters above. As Table C1.2 illustrates, mean impact heights vary only slightly between the three trees, ranging from 233 cm (*Abies alba*) through 238 cm (*Picea abies*) to 244 cm (*Fagus sylvatica*). In a similar way, minimum impact heights are also comparable with 10, 13 and 17 cm. Scars at this height are most probably the result of rolling rocks impinging on the stem surface. We were unable to identify impact damage lower down on the stem, probably owing to the size of rockfall fragments occurring on the slope. In contrast to the relatively uniform data obtained for the mean and minimum impact heights, maximum impact heights vary considerably. In particular, the extremely high impacts observed in the *Abies alba* stem outstrip expectations by a long way (930 cm). The vertical

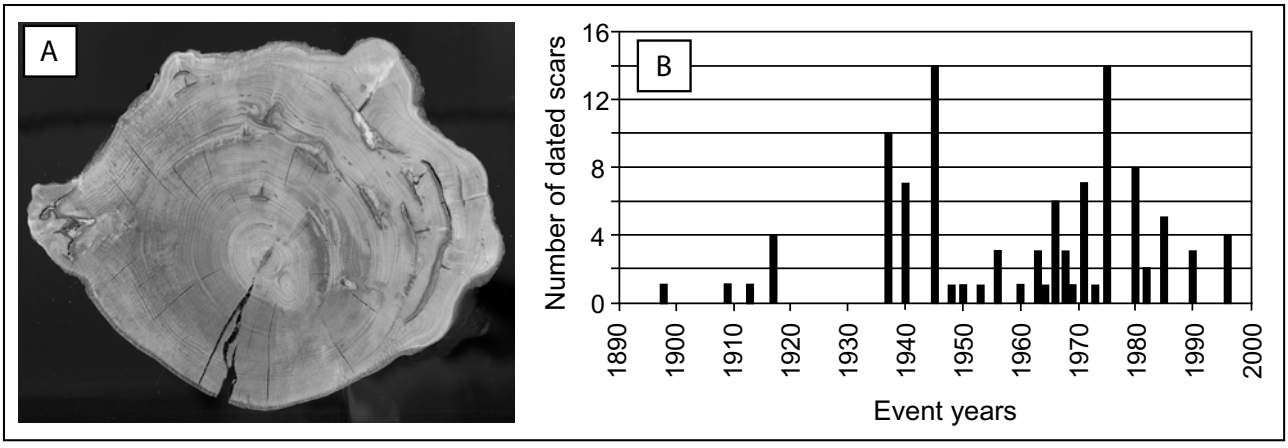

Fig. C1.1 *Rockfall activity based on 114 stem discs of a heavily disturbed beech (Fagus sylvatica) from the Altdorf Bannwald (Swiss Prealps): (A) Cross-section taken at the base of the stem showing 13 scars; (B) Histogram with all event years reconstructed on the stem discs of this beech tree.*

Table C1.2 *Vertical distribution of rockfall scars on trees illustrated with mean, minimum and maximum heights (in cm)*

Tree	Mean	Min.	Max.
Abies alba	233	17	930
Fagus sylvatica	244	13	628
Picea abies	238	10	596

distribution of impact scars, as well as event years are exemplarily illustrated for the *Abies alba* tree in Figure C1.2. The uppermost impact scars observed in the *Fagus sylvatica* and the *Picea abies* stems are, in contrast, located (more than) three meters below and totaled 628 and 596 cm, respectively.

In addition to the minimum, maximum and mean impact heights, the vertical distribution of scars was investigated in greater detail, as shown in Figure C1.3. Results obtained for the *Abies alba* tree indicate that more than every second scar is located within the first two meters above ground level (58%). Figure C1.3 also shows that more than a quarter of the rockfall wounds identified on the *Abies alba* stem are found within 400 cm, while 10% of all rockfall wounds are identified between 630 and 930 cm above ground. Finally, the diagram indicates that, in contrast to the other two trees, scars are most frequently found between 100 and 199 cm and not within the first meter above ground.

Data obtained from the *Fagus sylvatica* cross-sections indicates that 50% of all impacts are found below 206 cm, while 75% of the scars occur in the first four meters of the stem (392 cm). Figure C1.3 makes clear that this relatively high value is influenced by a large number of rockfall scars identified between 300 and 399 cm above ground. Data further indicate that 90% of all injuries take place below 513 cm and that impacts do not occur over 628 cm.

Analysis of rockfall impacts on the *Picea abies* stem shows a similar distribution to that of the *Fagus sylvatica* tree. Every second scar can be identified within the first 183 cm and 75% of all impacts are located below 381 cm. In a similar way, the 90% level only slightly differs (< 499 cm) from the values obtained for the *Fagus sylvatica* tree (< 513 cm) and, as before, the highest scars identified are found at similar heights. There are, however, differences in the number of scars occurring between 100 and 299 cm, where impacts appear to be more frequent in the *Picea abies* than in the *Fagus sylvatica* tree. Further details on the vertical distribution of the scars can also be found in Figure C1.3.

1.4.3 Visible and hidden scars

From the 189 scars identified in the three trees analyzed from the *Bannwald of Altdorf*, almost 70 % of the wounds would have been identifiable from the outside. By contrast, three out of ten scars would have been missed without cutting the cross-sections.

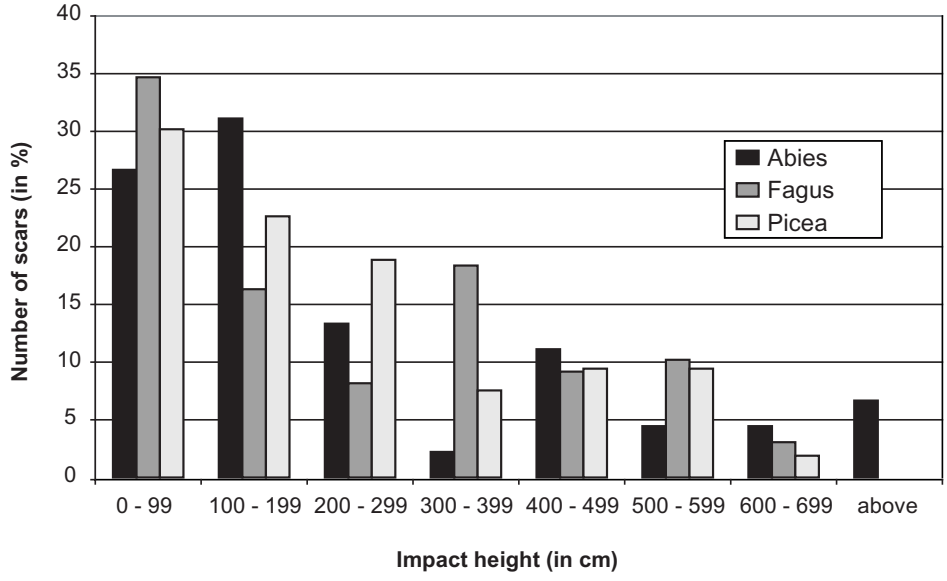

Fig. C1.3 *Vertical distribution of impacts reconstructed in the Abies alba, Fagus sylvatica and Picea abies trees.*

Table C1.3 *Visibility of scars given with the percentage of visible and completely overgrown signs of past rockfall activity.*

Tree	Visible	Overgrown
Abies alba	84%	16%
Fagus sylvatica	75%	25%
Picea abies	51%	49%

Large differences were ascertained between the different trees, as illustrated in Table C1.3. While an astonishing 84% of the rockfall scars can still be seen on the stem surface of the 129-year old *Abies alba* tree, only 51% of the rockfall wounds remain visible on the 97-year old *Picea abies* stem. Data from the 112-year old *Fagus sylvatica* tree indicate that three quarters of all scars would have been identified solely by visual analysis.

1.5 Discussion and conclusion

In the study reported here, we analyzed the vertical distribution of scars of 307 cross-sections prepared from the stems of three trees from the *Bannwald of Altdorf* and assessed the level of visibility of the scars. Results clearly show that scars could occur from almost ground level to several meters above. In addition, data also indicate that some evidence of past events becomes blurred with time and that only between 51 and 84% of scars remain visible on the stem surface.

While the present study provided some further knowledge on the vertical distribution and the visibility of scars on stem surfaces, it also gives rise to numerous questions and research topics for further studies. As only three trees were analyzed, we found considerable differences in the values for the maximum impact heights. Nonetheless, results obtained from the *Abies alba* tree – selected on a surface with a slope gradient of 35° – suggest that Rickli *et al.* (2004) underestimate maximum bounce heights of rocks (Ø < 50 cm) and boulders (Ø > 50 cm) on forested slopes with a gradient of 35°, probably even by several meters! By contrast, data gathered from *Fagus sylvatica* and *Picea abies* trees cannot be compared with the results of Rickli *et al.* (2004), as these trees were selected on terrains with steeper slope gradients (45°).

Results further suggest that, on average, "only" 54% of the scars can be found within the first two meters above ground, whereas 11% of the scars are located at least five meters above the ground. Why do we have such high bounces in the present case? Are they the result of the comparably steep slopes and the size of the rockfall fragments present at the *Bannwald* of *Altdorf*? And do comparable impact heights occur on other sites as well? If so, how do we need to take these impact heights into account when dimensioning rockfall barriers or restraining nets?

As for the visibility of scars on the stem surface, results more or less coincide with data obtained at *Brienzergrat* (Bernese Prealps, Switzerland), where Gsteiger (1989, 1993) assessed hidden scars in seven *Fagus sylvatica* and *Picea abies* trees. In contrast, data considerably disagree with results obtained in a century-old *Larix decidua* Mill. stand near *Täsch* (Valais, Switzerland), where only 8 to 10% of the scars remained visible on the stem surface (Schneuwly 2003, Stoffel *et al.* 2005b, c).

As a consequence, the considerable differences occurring in the number of scars remaining visible on the stem surface should be addressed in greater detail. At first view, bark properties seem to influence the visibility of scars: Data suggests that the sporadic removal of bark pieces ('peeling') occurring in some of the conifer species, such as, e.g., *Picea abies* or *Larix decidua* apparently helps to blur much more evidence from past events than does the smooth and thin bark of, e.g., *Fagus sylvatica*. Is there a relation between bark properties and visibility of past impacts? Does the predominant size of rockfall fragments influence the size of scars and, as a consequence, the time they remain visible on the stem surface? Is it rather the vitality and yearly increment that drive the overgrowing process of scars and the blurring of past impacts? Or is it perhaps a combination of several of these factors?

In addition, current dendrogeomorphological methods in rockfall research should be critically examined. What percentage of rockfall events are we able to reconstruct at sampling height, faced with the proof that impacts can occur almost anywhere between ground level and several meters above? Might studies using increment cores furnish reliable results and how much data on the total number of scars could they provide? There is, indeed, considerable necessity for further research. In particular, replicate studies are needed from a variety of sites in order to assess maximum impact heights occurring on forested rockfall slopes, and to identify the importance of hidden scars.

Acknowledgements I am grateful to the local forester Göran Gfeller (*Forstbetrieb, Korporations-Bürgergemeinde Altdorf*) for supporting this research and for felling the needed trees. I also address my thanks to Felix Imfanger for cutting the stems into handy pieces and to the anonymous helicopter pilot for flying one of the trees out of the protection forest, as well as to Werner Gerber and Jan Esper for getting the stem pieces to WSL. I am indebted to Beat Annen and Hans Grossmann (*Amt für Forst und Jagd, Kanton Uri*), who furnished valuable information on plant sociology and site characteristics. A previous version of this paper has been read and corrected by Simone Perret. Last but not least, I am grateful to Igor Lièvre for preparing some of the samples and for helping with data analysis, as well as to the two anonymous reviewers for their helpful comments.

*****

CHAPTER D

SOME LIMITATIONS OF TREE-RING ANALYSIS IN ROCKFALL RESEARCH

Based on results gathered on the vertical distribution and the visibility of rockfall scars on stem surfaces (Chapter C), the height distribution of scars as well as the problem of overgrown evidence of past impacts have been addressed in greater detail and with data from the principle tree ring–rockfall studies realized within Switzerland. In a further step, the number of scars reconstructed on one single cross-section or several increment cores taken at a specific position have been compared with the total number of scars occurring in the entire tree. The paper reproduced in Chapter D has been submitted for publication to *"Dendrochronologia"*.

1. Limitations of tree-ring analysis in rockfall research

Markus Stoffel [1] and Simone Perret [2]

"Reconstructing past rockfall activity with tree rings: some methodological considerations"

[1] *Groupe de Recherches en Géomorphologie (GReG), Department of Geosciences, Geography, University of Fribourg*

[2] *Applied Geomorphology and Natural Risks, Department of Geography, University of Berne*

submitted for publication to „Dendrochronologia" on 4 February 2005

Summary

This paper considers methodological difficulties arising when trees and tree-ring sequences are used to reconstruct rockfall activity. In contrast to other hazardous processes such as debris flows, floods or snow avalanches, scars caused by rockfall activity are more randomly distributed on trees and may occur at considerably varying heights. Thus both the choice of trees for analysis and the determination of sampling heights need special care. It is the goal of this paper to identify impact heights occurring on trees originating from nine different datasets in the Swiss Alps and Prealps. Secondly, the problem of overgrown wounds is dealt with and the number of scars remaining visible on the stem quantified. In a final step, the number of scars reconstructed on entire trees is compared with the events identified on only one cross-section or a series of increment cores taken at the height with a maximum number of wounds visible on the stem.

Results indicate that the dimension of rockfall fragments and the slope gradient primarily determine impact heights. The number of overgrown scars would, in contrast, much depend on the bark properties of the species, yearly increment rates, the age of the tree and the size of rockfall fragments, resulting in a mass of 'blurred evidence' ranging from 15 to 90%. Analysis of single cross-sections at a given 'test height' indicates that, at best, 13 to 35% of the scars occurring on the entire tree can be detected. Data further suggest that the number of events reconstructed at this 'test height' can be considerably improved as soon as other growth disturbances such as reaction wood, abrupt growth reductions or, if present, traumatic rows of resin ducts are considered as well.

Keywords: Dendrogeomorphology, rockfall, impact height, overgrown scars, missed events, cross-section, increment cores

1.1 Introduction

Dendrogeomorphology is capable of furnishing high-resolution data on frequencies, volumes or seasonal timing of past hydrological or geomorphological events, covering considerably long periods (Bräuning 1995). Consequently, tree-ring sequences have been extensively investigated to study past snow avalanche (Butler *et al.* 1992, Patten & Knight 1994, Rayback 1998), debris flow (Strunk 1995, 1997, Baumann & Kaiser 1999, Stoffel *et al.* 2005a) or flooding activity (Hupp 1988, Bayard & Schweingruber 1991, LePage & Bégin 1996).

Due to the massive volumes that are normally involved in these processes, single events generally affect a large number of trees along their flow paths. As a result, injuries can repeatedly be identified within an area and are – with the exception of wind-blast impacts caused by powder-snow avalanches – restricted to the lowermost parts of the trunk and to a range defined by the flow height of the process in question. A typical distribution of impacts related to such 'flow' processes is exemplified with debris flow deposits in Figure D1.1a.

Rockfall, in contrast, consists of a removal of individual and superficial rockfall fragments from cliff faces (Selby 1993). The motion of single rocks (Ø < 50 cm) or boulders (Ø > 50 cm) is either falling, bouncing or rolling, and masses involved generally remain < 5 m^3 (Berger *et al.* 2002). Rocks and boulders may therefore only disturb a limited number of trees along their trajectories (Stoffel *et al.* 2005c), as shown in Figure D1.1b. The diagram also indicates that, in addition, impact heights on trees may vary considerably. As a result and even though it represents one of the most common geomorphic processes in mountainous regions (Whalley 1984, Luckman & Fiske 1995, Erismann & Abele 2001), rockfall has, so far, only occasionally been assessed with dendrogeomorphological methods (Stoffel 2005a).

It is therefore the purpose of this paper to address difficulties arising when trees and tree-ring sequences are used to reconstruct past rockfall activity. On the basis of results from recent investigations conducted in the Swiss Alps and Prealps, we first analyze differences occurring in rockfall impact heights on trees before illustrating the radial distribution of scars on

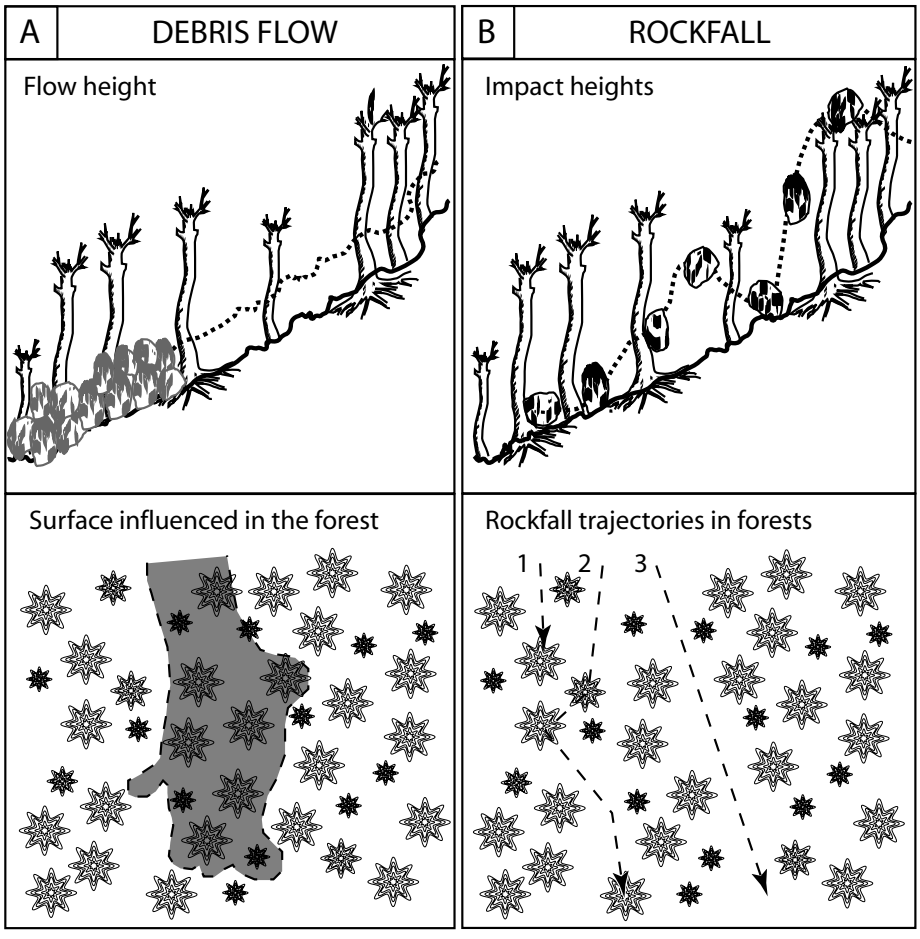

Fig. D1.1 *(a) Flow height and vertical distribution of injuries occurring with debris flow events: Scars can be identified on a comparably large number of trees along the flow path and are restricted to the lowermost part of the trunk, i.e. the (maximum) flow height of the process. (b) As rockfall represents the motion of individual rocks and boulders, scars are, in contrast, only found along the rockfall trajectory and at heights ranging from almost ground level to several meters.*

the stem. We then focus on the problem of overgrown scars and try to quantify the number of wounds remaining visible on the stem surface. In a third step, the number of rockfall scars reconstructed on entire trees is compared with the number of events identified on single cross-sections or increment cores sampled at the height where a maximum of scars is visible on the stem surface. Lastly, we would like to emphasize that this paper primarily aims to provide thought-provoking insights into both progress and problems existing in tree ring–rockfall research, rather than to deliver conclusive and exhaustive guidelines for future studies.

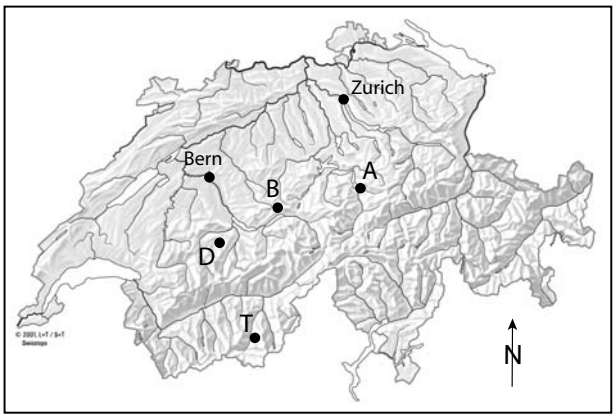

Fig. D1.2 *Location of the different study sites in Switzerland: A = Altdorf (Uri Prealps), B = Brienzergrat (Bernese Prealps), D = Diemtigtal (Bernese Prealps), T = Täschgufer (Valais Alps).*

1.2 Material and methods

Data analyzed in this paper have been compiled from existing dendrogeomorphological studies conducted on rockfall slopes in pre-alpine (*Altdorf I, II, III; Brienzergrat; Diemtigtal I, II, III*) and alpine environments (*Täschgufer I, II*) in Switzerland. The geographical provenance of the different datasets is indicated in Figure D1.2 and the data sources given in Table D1.1.

It can also be seen from Table D1.1 that the nine datasets used for investigations are not homogenous. Some of them contain numerous samples gathered from single trees, while others have been constructed with a large number of trees. Similarly, data were obtained from either cross-sections (*CS*) or increment cores (*IC*). Tree ages of the different datasets vary widely as well, ranging from an average of 37 to 297 years, and datasets contain both mature and juvenile as well as dominant and suppressed trees. In total, the database contains 356 trees, yielding data on 3273 rockfall events.

As for the species, conifers predominate (69%) with European larch (*Larix decidua* Mill.), Norway spruce (*Picea abies (*L.) Karst.) and Silver fir (*Abies alba* Mill.). Broadleaved trees are less readily available and account for 31% of the samples with Common beech (*Fagus sylvatica* L.), Common white beam (*Sorbus aria* (L.) Crantz), Mountain ash (*Sorbus aucuparia* L.) and Sycamore maple (*Acer pseudoplatanus* L.).

Table D1.1 *Datasets used for the analysis of rockfall activity. Rockfall events have been assessed by different authors through the analysis of cross-sections (CS), increment cores (IC) or – in the case of Diemtigtal I – the inventory of scars visible on the stem surface.*

Datasets	species [1]	trees (number)	age (mean)	CS (number)	IC (number)	events	Data sources
Altdorf I	Fa	1	112 yrs	114	–	103	Stoffel (2005b)
Altdorf II	Ab	1	129 yrs	105	–	33	dito
Altdorf III	Pi	1	97 yrs	88	–	53	dito
Brienzergrat	Pi Fa	7	141 yrs	25	–	56	Gsteiger (1989, 1993)
Diemtigtal I	Pi	33	180 yrs	33	–	315	Perret *et al.* (2005a)
Diemtigtal II	Pi	3	121 yrs	100	–	68	dito
Diemtigtal III	Pi So Ac	157	–	–	–	1704	Perret *et al.* (2004a)
Täschgufer I	La	135	297 yrs	–	564	761	Stoffel *et al.* (2005b)
Täschgufer II	La	18	37 yrs	270	–	180	Stoffel *et al.* (2005c)
TOTAL	–	356	–	735	564	3273	–

[1] abbreviations of tree species used in this study include: Ac = *Acer pseudoplatanus* L., Ab = *Abies alba* Mill., Fa = *Fagus sylvatica* L., La = *Larix decidua* Mill., Pi = *Picea abies* (L.) Karst., So = *Sorbus aria* (L.) Crantz and *Sorbus aucuparia* L.

Further details on the datasets, such as the age (*age BH*) or the diameter at breast height (*DBH*), averaged yearly increment rates (*inc. yr* $^{-1}$), or rockfall-specific data (e.g., predominant size of rockfall fragments or slope gradients) can be found in the original literature (cf. Table D1.1) and will only be introduced if needed for interpretation of results. Similarly and in order to facilitate understanding, this article will not follow the common structure of a research paper, but rather circumscribes, analyzes and discusses one 'problematic' aspect of tree ring–rockfall research after another. Finally, and as the data used in this analysis have been gathered by different authors within studies following different goals, only a certain number of datasets can be used for each of the different aspects investigated.

1.3 Results

1.3.1 Height distribution of scars on stems

The success of dendrogeomorphological research largely depends on the height and radial position at which samples are taken on the stem. In contrast to 'flow' processes (e.g., debris flow, flood, wet snow avalanche), rockfall may cause scars almost anywhere between ground level and several meters above. Consequently, tree-ring reconstructions run the risk of remaining rather incomplete by only reconstructing those injuries located at or directly next to the height at which cross-sections or increment cores are taken for analysis. Careful investigation of locally occurring impact heights must, however, imperatively precede sampling in order to determine 'optimal' positions for the extraction of cross-sections or increment cores. At present, quantitative data on the vertical distribution of rockfall impacts on stem surfaces do not readily exist. It is true that Rickli *et al.* (2004) presented results on maximum jump heights of rockfall fragments on slopes with a gradient of 35°, but their results are based on a limited number of field data and do not consider the influence of neighboring trees or changes in the slope gradient. Similarly, the height distribution reported by Gsteiger (1993) at *Brienzergrat* (cf. Table D1.1) was realized with a small number of samples taken from only seven individual trees.

Here, we present the impact heights observed on 305 trees from seven different datasets. Data are shown in Table D1.2 and classified with decreasing slope gradients. In addition, indications on the mean diameter of rocks and boulders occurring on the slopes are given with *S* for small (Ø ~ 20 cm), *M* for medium (Ø ~ 40 cm) and *L* for large (Ø ~ 80 cm) rockfall fragments.

Within this study, we investigate the role of varying slope gradients and rock sizes, as these two aspects, according to Rickli *et al.* (2004), represent the most important factors determining velocities and (kinetic) energies of rockfall fragments and, thus, the bounce respectively impact heights on trees. However, other factors have to be taken into account as well, such as the composition of the forest stand (density, DBH distribution), the presence of low vegetation (e.g., shrubs) or the nature of the ground surface (i.e. roughness, dampening effects). These factors will be used for interpretation of the results given in Table D1.2 where necessary.

Results first of all indicate considerable impact heights for *Altdorf I* and *III*. High bounces have probably been favored by the steepness of the terrain (45°) and the size of the rockfall fragments (M; Ø ~ 40

Table D1.2 *Height distribution of rockfall scars: Datasets are classed with decreasing slope gradients and contain data obtained from inventories of scars on the stem surface (Diemtigtal III; Täschgufer I) and tree-ring analyses (others). In addition, mean diameters of rockfall fragments (rock size) are indicated.*

Datasets	slope	rock size [1]	**50%** (in cm)	**75%** (in cm)	**90%** (in cm)	**Impact heights** < 20 cm	max.	mean
Altdorf I	45°	M	< 206	< 392	< 513	7%	628 cm	244 cm
Altdorf III	45°	M	< 183	< 381	< 499	3%	596 cm	238 cm
Brienzergrat	40°	S	> 40	–	< 150	< 33%	340 cm	–
Diemtigtal II	40°	S	< 49	< 91	< 165	22%	331 cm	73 cm
Diemtigtal III [2]	40°	S	< 69	< 121	< 199	14%	365 cm	85 cm
Altdorf II	35°	M	< 162	< 216	< 632	6%	930 cm	233 cm
Täschgufer I [2]	25°	L	< 150	< 210	< 360	2%	400 cm	174 cm

[1] rock size = mean diameter of rockfall fragments: S (small, Ø ~ 20 cm), M (medium, Ø ~ 40 cm) and L (large, Ø ~ 80 cm).
[2] Data based on inventory of scars visible on the stem surface.

cm). Rockfall-induced scars are, on average, located at ~240 cm above ground, with 75% of the scars below ~385 cm and 90% of the wounds below ~500 cm. Maximum impact heights are identified at ~610 cm and injuries located within the first 20 cm above ground remain – probably due to the size of rockfall fragments – rather scarce (3%, respectively 7%).

For *Altdorf II*, similar rockfall fragments (M; Ø ~ 40 cm) generally cause lower impact heights on a flatter slope (35°). As a consequence, 75% of all scars lay more than 150 cm below those of *Altdorf I* and *III*. However, single rocks at *Altdorf II* apparently perform extremely high bounces and may, thus, cause considerable impact heights. As a result, the uppermost impact can be found at 930 cm, exceeding the values observed for *Altdorf I* and *III* by (more than) three meters. In a similar way, high bounces influence the mean impact height and the height containing 90% of all scars as well. The exceptionally high bounces of a limited number of medium-sized rockfall fragments at *Altdorf II* can only be explained by the position of the selected tree within the slope, located next to a clear-cut surface. As no other trees can decelerate rockfall fragments here, rocks may gain momentum and energy and, thus, perform high bounces.

Compared to the impact heights caused by medium-sized rockfall fragments, the small rocks (S; Ø ~ 20 cm) scarring trees on the 40° steep slopes at *Brienzergrat*, *Diemtigtal II* and *Diemtigtal III* perform comparably modest bounces. Mean impact heights of scars on the stem oscillate at ~80 cm and 90% of the injuries are found (considerably) lower than 2 m above ground. For all three datasets, maximum impact heights only show slight variations, with the uppermost wounds identified between 331 and 365 cm above ground. In contrast, the percentage of scars located at < 20 cm seems to be slightly higher in the relatively dense forest at *Brienzergrat* (2500 trees ha $^{-1}$) than at *Diemtigtal II* and *III* (520 trees ha $^{-1}$).

Due to the large-sized rockfall fragments (L; Ø ~ 80 cm) and the loose forest cover at *Täschgufer I* (150 trees ha $^{-1}$), boulders can perform fairly high bounces on this slope with a gradient of only 25°. As a further result of the size of rockfall fragments, scars located at < 20 cm remain exceptional (2%). At *Täschgufer I*, the uppermost wound is located at 400 cm, while, on average, scars occur at 174 cm.

Overall, data seem to confirm the results of Rickli *et al.* (2004), assuming that slope gradients and the size of rockfall fragments are the most important driving factors of bounce and, thus, influence heights of rock and boulder wounds on stems. However, and as shown in the preceding paragraphs, the composition of the forest stand – and especially its density – has to be taken into account as well. The results obtained from 7 datasets also show that Rickli *et al.* (2004) clearly underestimate maximum bounce heights of both rocks (Ø < 50 cm) and boulders (Ø > 50 cm) in forest stands, probably even by several meters!

1.3.2 Radial distribution of scars on stems

In addition to the height distribution of rockfall impacts, the radial distribution of scars must be assessed before sampling. This step is especially crucial for studies using increment cores, as scars may – depending on the size or the intensity of the shock induced through the impinging rockfall fragment – only be visible on a small portion of the tree ring. Consequently and as will be shown in what follows, some of the growth reactions in trees may be missed when increment cores are used for analysis.

In order to assess the radial distribution of rockfall-induced scars on the stem surface, results from five datasets are illustrated in Figure D1.3: For *Diemtigtal III*, the horizontal distribution of rockfall impacts has been studied with 1704 wounds visible on the stem of adult and juvenile samples. For *Altdorf* (*I*, *II* and *III*), cross-sections were used to investigate the horizontal distribution of scars on three adult trees, whereas stem discs from juvenile trees yielded data on 180 scars for *Täschgufer II*. The radial distribution of the scars is grouped in segments of 10°. With respect to the fall line, 0° represents the upslope and 180° the downslope position of the stem, while 90° and 270° indicate the two segments of the stem surface located perpendicular to the slope.

At first, results clearly indicate that rockfall fragments do not exclusively cause wounds on those parts of the stem located in the direct fall line. In all datasets, only between 7 and 9% of the scars are located within the 10° portion of the stem surface facing the fall line (355 to 5°). As a multitude of factors influences the travel direction of rockfall fragments, such as the form of the rockfall fragment itself, the unevenness of the ground surface or deviations induced by impacts further up the slope, wounds occur almost anywhere on the upslope facing portion of the stem surface: For *Diemtigtal III*, almost two thirds of the rockfall-induced scars (63%) are located within a 90° segment around the fall line (i.e. 315 to 45°).

Similar results are obtained from the juvenile trees at *Täschgufer II* (61%), whereas in the three mature

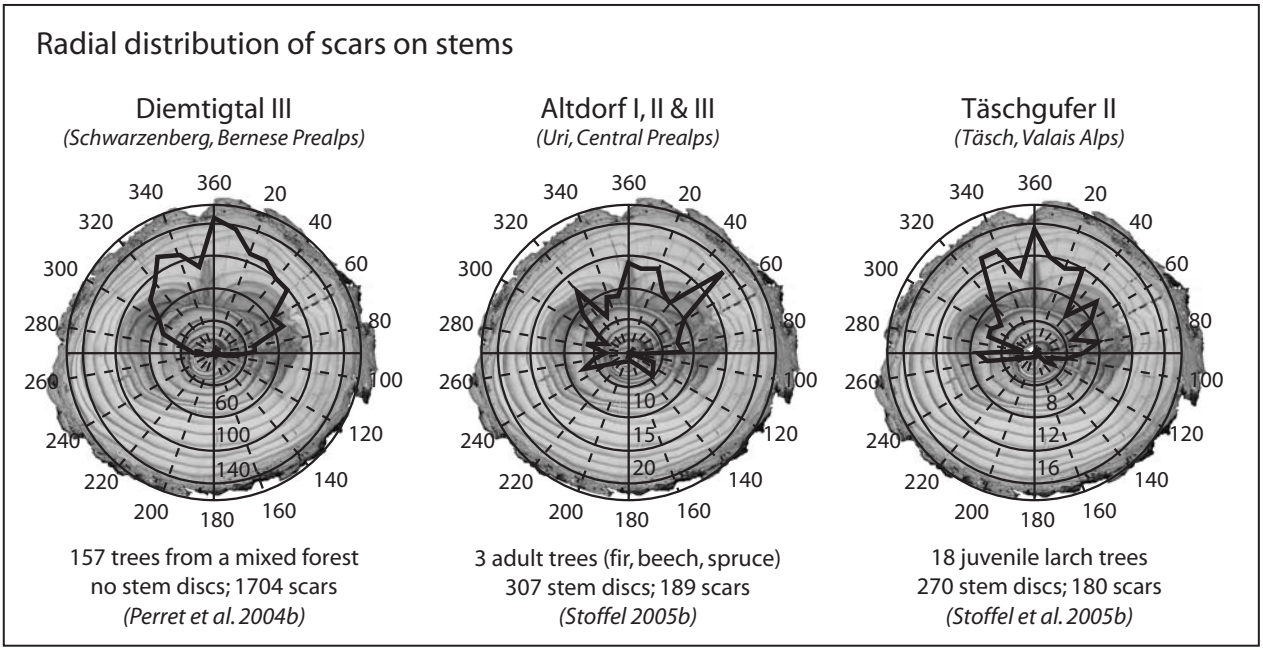

Fig. D1.3 *Radial distribution of scars for Diemtigtal III, Altdorf (I-III) and Täschgufer II: In the field, 360° represents the upslope position of the tree, which more or less corresponds with the fall line of rockfall. In contrast, 180° stands for the downslope position.*

trees at *Altdorf (I, II*, and *III)*, only some 48% of the wounds are found in this segment. Results also show that at least 90 % of the wounds identified on the selected trees are located on the upslope facing half of the stem surface (i.e. 270 to 90 °). Scars located elsewhere on the stem surface are, in contrast, scarce and probably represent secondary effects of rockfall impacts such as tension cracks or injuries caused through the propagation of sinusoidal shockwaves in the stem (i.e. hula-hoop effects; Dorren & Berger 2005).

1.3.3 Visible injuries vs. overgrown scars

A further problem of identifying impacts of past rockfall activity resides in the fact that trees possess the potential of overgrowing injured tissue and, thus, blur evidence of former rockfall events. In rapidly growing trees, small wounds may completely heal over within only a few years (Schweingruber 1996). Similarly, data from *Brienzergrat* indicate that the percentage of overgrown injuries greatly depend on the initial size of the scar (Gsteiger 1989). Among scars affecting less than 5% of the stem's circumference, four out of five were overgrown at *Brienzergrat*, whereas when scars covered more than 15% of the stem's circumference, trees were in no single case able to completely overgrow them. Gsteiger (1989) thus concluded that the larger the rockfall fragment, the larger the wounds and, consequently, the easier it would be to identify scars on trees. Not only the size of the scar, but also the length of time passing between impact and analysis plays an important role: Lafortune *et al.* (1997) realized that from injuries visible on the stem surface of 101 selected trees, only five events could be dated for the period 1571–1910, whereas the yearly number of dated scars in the 20th century rose constantly from 0.53 (1910–1949) to 3.2 after 1975. They believe that scars older than 80 years would have been completely overgrown and no longer externally visible. As a consequence, one might greatly overestimate recent rockfall activity by choosing visibly injured trees and, at the same time, unintentionally neglecting samples with overgrown scars. Thus, scars visible on the stem cannot necessarily be used to investigate past frequencies (Schweingruber 1996) unless there is quantitative data available on the number of overgrown scars.

We therefore investigated more than 1500 rockfall-induced wounds reconstructed on 1274 cross-sections and increment cores and tried to quantify the number of injuries remaining visible on the stem surface of 192 trees. Besides indications of the number of visible scars, Table D1.3 contains information on tree age (*age BH*) and diameter at breast height (*DBH*), averaged yearly increment rates (*inc. yr* $^{-1}$) and diameter of predominating rockfall fragments (*rock size*). Datasets obtained from the same species are presented together and classified according to their age (i.e. oldest to

Table D1.3 *Comparison of scars visible on the stem surface with events reconstructed on cross-sections and increment cores: Data from the same species are grouped, starting with the oldest sample. Between the species, bark thickness has been used as a criterion, starting with thick-barked Larix decidua trees. Further aspects taken into account include the mean diameter of rockfall fragments (rock size), tree age (age BH) and diameter (DBH) at breast height, averaged yearly increment rates (inc yr $^{-1}$) and the number of reconstructed events (events).*

Datasets	species	rock size	age BH (mean)	DBH	inc. yr $^{-1}$	events	**visible scars**
Täschgufer I	Larix	L	297 yrs	49 cm	0.16 cm	761	**8–10%**
Täschgufer II	Larix	L	24 yrs	7 cm	0.29 cm	180	**47%**
Diemtigtal I	Picea	S	180 yrs *	34 cm*	0.19 cm	315	**32%**
Diemtigtal II	Picea	S	121 yrs	7 cm	0.06 cm	68	**74%**
Altdorf III	Picea	M	97 yrs	59 cm	0.61 cm	53	**51%**
Altdorf II	Abies	M	129 yrs	31 cm	0.25 cm	33	**84%**
Altdorf I	Fagus	M	112 yrs	21 cm	0.18 cm	103	**75%**

* DBH measurements at Diemtigtal II were not taken at breast height, but at ~ 30 cm

youngest). Between the different species, bark thickness has been used as a criterion; the list starts with thick-barked *Larix decidua*.

First of all, Table D1.3 indicates that major differences exist in the number of visible scars depending on the species, age and increment rates of trees. In this sense, the percentage of scars remaining visible on the stem surface proves to be very low in the 297-yr old *Larix decidua* trees at *Täschgufer I*, where only 10 % of all reconstructed events can be identified on the stem surface. Similarly and even though little time passed between impact and investigation in the relatively young *Larix decidua* trees at *Täschgufer II*, more than half of the scars could no longer be identified from outside.

These results are even more astonishing as scars at *Täschgufer* tend to be – as a result of the large rockfall fragments (L; Ø ~ 80 cm) – much larger than those in the other datasets. We therefore believe that the thick bark of *Larix decidua* would efficiently blur evidence of past events, as it grows abundantly and sporadically scales off its outermost layers (‘peeling’).

In a similar way, *Picea abies* trees also scale off small rounded pieces of the bark, which is, however, thinner than that of *Larix decidua*. Consequently, the blurring effect appears to be less efficient: for *Diemtigtal I*, two thirds of the scars caused by small rockfall fragments (S; Ø ~ 20 cm) can no longer be seen on the stem of the 180-yr old trees. In contrast, three fourths of the scars remained visible on the thin stems (7 cm DBH) of dataset *Diemtigtal II*. Here, small yearly increment rates (0.06 cm) were apparently not sufficient to completely heal over scars caused by small rockfall fragments (S; Ø ~ 20 cm). For *Altdorf III*, the *Picea abies* tree chosen for analysis grew considerably well (0.61 cm yr $^{-1}$). Due to the larger wounds induced through larger rockfall fragments (M; Ø ~ 40 cm) as well as the inferior age of the tree, scars remaining visible are, apparently, as frequent as invisible ones.

Medium-sized rockfall fragments also predominate at *Altdorf II*, where they caused 33 scars on a 129-yr old *Abies alba* tree. Even though this tree was not suppressed and shows reasonable yearly increment rates (0.25 cm), more than eight out of ten wounds remain visible from outside. In a similar way, the 112-yr old *Fagus sylvatica* tree selected at *Altdorf I* still shows 75% of its scars on the stem surface. As a result of the smooth and relatively thin bark as well as the lack of bark renewal (‘peeling’), the stem surface of these two species would appear to blur evidence much less and, thus, better represent past rockfall impacts than the species mentioned above.

1.3.4 Scars at ‘test height’ vs. injuries to the entire tree

Most of the time, dendrogeomorphological studies use increment cores to investigate past events. In addition, trees are only exceptionally analyzed from base to top. As a consequence, cross-sections and increment cores taken at a specific height are supposed to primarily furnish data on those scars located directly at

Table D1.4 *Scars identified on single samples taken at the 'test height' with a maximum number of injuries visible on the stem surface: (a) Number of scars identified on one cross-section at 'test height' and comparison with the number of scars reconstructed on the entire tree (% $_{tot}$); (b) Number of scars identified on 4 increment cores (0°, 90°, 180°, 270°) at 'test height' and comparison with the number of scars reconstructed on the entire tree (% $_{tot}$); (c) Like (b), but with only two increment cores taken at 0° and 180° (upslope; downslope).*

Datasets	DBH	age BH	inc yr $^{-1}$	test height	**Scars** identified on		
					(a) 1 CS	(b) 4 IC	(c) 2 IC
Altdorf I	21 cm	114 yrs	0.18 cm	47 cm	13 (13%)	5 (5%)	2 (2%)
Altdorf II	31 cm	126 yrs	0.25 cm	40 cm	10 (30%)	4 (12%)	1 (3%)
Diemtigtal II $^{+}$	7 cm	121 yrs	0.06 cm	46 cm	3.0 (13%)	2.3 (10%)	1.0 (4%)
Täschgufer II *	7 cm	24 yrs	0.29 cm	44 cm	3.0 (35%)	2.0 (25%)	1.5 (19%)

$^{+}$ Mean values of 3 *Picea abies* (L.) Karst. trees
* Mean values of 18 *Larix decidua* Mill. trees

or next to the sampling position, while injuries occurring elsewhere on the stem might unintentionally be neglected. In the past, data gathered with such investigations have repeatedly been presented as 'minimum frequencies', but no one has really been able to specify what percentage of the total number of scars per tree such 'minimum frequencies' would represent.

We therefore investigated four datasets containing 23 different trees, as illustrated in Table D1.4. In order to get an idea of the number of scars reconstructed at a specific height, we only analyze one cross-section per tree instead of addressing the entire dataset consisting of 589 samples. Furthermore and in order to realistically 'reproduce' the sampling of one single cross-section per tree (Table D1.4a), we determined the 'test height' at the position with the maximum number of wounds visible on the stem surface. The number of scars identified in these 'test height' samples was then compared with the number of scars reconstructed in their entire trees.

Similarly and in order to 'simulate' the extraction of increment cores from the same 23 'test height' samples, we investigated 6 mm wide strips on each cross-section: two increment cores were 'taken' in the fall line (0°, 180°), two perpendicular to the slope (90°, 270°; Tab. D1.4b, D1.4c). As can be seen from Table D1.4a, results first of all indicate that reconstructions focusing on one single cross-section per tree may, at best, reflect one third of the total number of scars occurring in the entire tree. The small number of datasets only barely allows conclusive explanations for the considerable differences arising in the number of scars seen on the single cross-sections of the 23 different trees. We can therefore only suppose that the number of reconstructed rockfall events would primarily be determined by the size of rockfall fragments and, as a consequence, the dimension of the wound caused to the tree: At *Täschgufer II*, large rockfall fragments (Ø ~ 80 cm) cause scars of up to 2.5 m in length (Schneuwly 2003), thus increasing the chance that wounds are also present at sampling height. In contrast, the small rockfall fragments occurring at *Diemtigtal II* (Ø ~ 20 cm) provoke much smaller injuries (11 cm), which are more easily missed on single cross-sections.

As soon as increment cores are investigated instead of cross-sections, the percentage of events reconstructed at the 'test height' drops further. Table D1.4b indicates that in trees with relatively large stems (DBH > 10 cm), sampling four increment cores (*IC*) does not even allow identification of half of the scars identified on one single cross-section. If only two cores are taken in the fall line (Table D1.4c), the number of scars identified would be even lower, totaling only a few percent of the real number of scars. On very thin stems (DBH < 10 cm), the loss of information appears to be less drastic, but analysis performed with four increment cores (see Table D1.4b) would still miss some of the scars identified on the cross-section at 'test height'. Again, Table D1.4c indicates that results become worse as soon as only two increment cores are extracted. Best results are obtained from the *Täschgufer II* samples, where the large rockfall fragments (Ø ~ 80 cm) apparently tend to leave larger and, thus, more easily identifiable scars.

1.3.5 Growth disturbances at 'test height' vs. injuries to the entire tree

In a next step, we used an approach similar to the one illustrated in the preceding section as well as the

same 'test height' samples. But in addition to the analysis of scars, we also focused on other rockfall-related growth disturbances including reaction wood or – as a consequence of apex loss – abrupt growth reductions. In the case of the *Picea abies* and *Larix decidua* samples from *Diemtigtal II* and *Täschgufer II*, the presence of traumatic rows of resin ducts has been assessed as well.

Results based on single cross-sections are presented in Table D1.5a, indicating that, with the exception of *Fagus sylvatica* (*Altdorf I*), the analysis of several rockfall-related growth disturbances may help to (considerably) improve the number of reconstructed rockfall events. Best results are obtained with the *Picea abies* and *Larix decidua* samples from *Diemtigtal II* and *Täschgufer II*, where traumatic rows of resin ducts are repeatedly found at 'test height', even though the impact as well as the injury are located elsewhere on the stem.

As a result and compared to the analysis of scars only (Table D1.4a), the number of reconstructed events could almost be doubled at *Diemtigtal II*, thus allowing identification of almost one fourth (24%) of the impacts reconstructed for the entire tree. The 'test height' samples at *Täschgufer II* even permitted reconstruction of 52% of the impacts occurring to the entire tree.

In the *Abies alba* tree at *Altdorf II*, reconstructions based on single cross-sections appear to be less complete, as only a limited number of abrupt growth reductions and reaction wood were available. In the *Fagus sylvatica* sample (*Altdorf I*), the non-existence of resin ducts would, most probably, also represent one of the principal reasons why the analysis of different growth disturbances only yielded a limited number of additional data on wounds located elsewhere on the stem.

The loss of information appears to be less important as soon as several rockfall-related growth disturbances are investigated on increment cores sampled at 'test height'. In the *Larix decidua* and *Picea abies* trees assessed in Table D1.5b, increment cores taken in the fall line (0°, 180°) as well as perpendicular to the slope (90°, 270°) allowed identification of almost 25 to 50 % of the impacts reconstructed on the entire tree. In the increment cores of the *Fagus sylvatica* tree (*Altdorf I*), analysis of scars, tension wood and growth reductions allowed identification of almost twice as many impacts compared to the investigation of scars only.

By extracting only two cores in the fall line of rockfall (0°, 180°; see Table D1.5c), the number of reconstructed events is again reduced. Nonetheless, the abundant presence of traumatic rows of resin ducts still allows identification of many impacts for *Diemtigtal II* and *Täschgufer II*. The loss of information is greater in the *Fagus sylvatica* tree (*Altdorf I*), where not even half as many events can be seen on only two increment cores. Data further suggest that rockfall-related growth disturbances would be more readily present on both cross-sections and increment cores if the impacts were caused by large- (Ø ~ 80 cm; *Täschgufer II*) or medium-sized (Ø ~ 40 cm; *Altdorf II*) rockfall fragments. As a consequence of the considerable impact forces and the large scars, chances are that signs of past rockfall activity would be present at sampling height in these trees, even though the impact itself might have occurred elsewhere on the stem. Both in contrast to and in agreement with the results of Perret *et al.* (2005a), the small rockfall fragments (Ø ~ 20 cm) occurring at *Diemtigtal II* would only cause growth disturbances in those areas of the stem located around the impact and, thus, signs would not necessarily be present on cross-sections or increment cores taken at sampling height.

Table D1.5 *All rockfall induced growth disturbances identified on single samples taken at 'test height' (i.e. scars, reaction wood, abrupt growth reduction, traumatic rows of resin ducts). For explanations see Table D1.4 and text.*

Datasets	DBH	age BH	inc yr $^{-1}$	test height	**Growth disturbances** identified on		
					(a) 1 CS	(b) 4 IC	(c) 2 IC
Altdorf I	21 cm	114 yrs	0.18 cm	47 cm	13 (13%)	9 (9%)	4 (4%)
Altdorf II	31 cm	126 yrs	0.25 cm	40 cm	12 (36%)	10 (30%)	7 (21%)
Diemtigtal II $^{+}$	7 cm	121 yrs	0.06 cm	46 cm	5.3 (24%)	5.3 (24%)	4.7 (21%)
Täschgufer II *	7 cm	24 yrs	0.29 cm	44 cm	4.0 (52%)	3.7 (49%)	3.5 (45%)

$^{+}$ Mean values of 3 *Picea abies* (L.) Karst. trees

* Mean values of 18 *Larix decidua* Mill. trees

1.4 Overall discussion and conclusions

The objective of the present paper was to address difficulties arising when trees and tree-ring sequences are used to reconstruct past rockfall activity. Aspects investigated included the analysis of impact heights and the radial distribution of scars on stem surfaces. In addition, we tried to quantify the number of overgrown scars ('blurred evidence') and the loss of data occurring when samples are only taken at one specific height. Even though results obtained within this paper pretend to be neither conclusive nor exhaustive, they furnish valuable data on different aspects of rockfall–tree interactions on forested slopes.

In this sense, the analysis of impact heights of rockfall fragments on the stem surface has for the first time allowed comparison of mean and maximum impact heights occurring in forests with different slope gradients and varying size classes of rockfall fragments. Results clearly show that impact heights generally increase on steeper slopes and that the size of rockfall fragments would considerably influence (kinetic) energy and, thus, impact heights. The present study also focused on the number of scars remaining visible on the stems of selected trees. Results indicate that the visibility of scars would depend on the tree species and, consequently, the properties as well as the thickness of the bark. Evidence of old scars was most efficiently blurred in *Larix decidua* trees, which sporadically scale off the outermost layers of their thick and crevassed bark. In trees with thinner and comparably smooth barks, such as *Abies alba* or *Fagus sylvatica,* evidence of rockfall impacts remained, in contrast, largely visible on the stem. As a consequence, studies which exclusively inventory scars visible on the stem surface (Jahn 1988, Gsteiger 1993, Baumgartner 2002, Perret *et al.* 2004b) imperatively need to consider data on the predominating size of rockfall fragments or yearly increment rates of trees as well, as these factors chiefly influence the number of visible scars.

Results also suggest that trees should be selected more randomly in future tree ring–rockfall studies. Otherwise, recent rockfall activity, large injuries or disturbances in slowly growing trees might be vastly overestimated. Conversely, older rockfall activity, small scars or wounds in fast growing trees will run the risk of being underestimated. The distribution of visible scars should therefore be used as an indicator for the height at which to take samples, but not as a primary criterion for selecting trees. Last but not least, sampling a large number of trees may further help to reduce the risk of incomplete or unbalanced reconstructions. Wherever possible, cross-sections should be analyzed instead of increment cores and growth disturbances other than scars, such as traumatic rows of resin ducts, reaction wood or abrupt growth reductions, scrutinized as well.

As for the methodological aspects addressed within this paper, research should further investigate the process of wound healing and the blurring of scars: How long does it take a tree to completely overgrow scars? What factors drive this process and to what degree could they influence the healing and blurring of scars on different sites with different species or growth conditions?

Particular attention should also be addressed to the influence of bark properties on the occurrence of scars in trees, as this aspect remains largely unexplored in tree ring–rockfall research. Analyses of impacts caused by forest fires clearly indicate that trees are more susceptible to cambium damage and scarring as long as their trunk circumference remains < 40 cm (Hengst & Dawson 1993, Pinard *et al.* 1997, van Mantgem & Schwartz 2003, Wilson & Witkowski 2003, Schoonenberg *et al.* 2003). Would young and slowly growing trees, thus, be more vulnerable, with scarring influenced by both the age and the growth rate, as suggested by Guyette & Stambaugh (2004)? Even so, future investigations should try to differentiate impact intensities and study their effect on scar formation or growth disturbances, as Hohl *et al.* (2002) emphasize that, in the case of hail, only extreme events would be able to leave injuries on branches of Mountain pine (*Pinus mugo* var. *uncinata*). To what extent might bark properties prevent the occurrence of cambial damage in trees and, consequently, hinder researchers from studying past rockfall events? Further, is there a threshold bark thickness at which a tree may prevent cambial damage caused by a specific size of rockfall fragment, as suggested for trees suffering from fires (Pinard *et al.* 1997)?

Overall, the present study has furnished valuable data on methodological problems occurring when trees and tree rings are assessed to study past rockfall activity. However, future studies will need to further investigate methodological aspects of dendrogeomorphology in order to corroborate or, eventually, replace currently used approaches. Special attention should be given to theoretical studies focusing on the questions and research needs addressed above, while replicate investigations should gather further data on the aspects dealt with in the present paper.

Acknowledgements The authors want to express their gratitude to Marc Baumgartner, Peter Gsteiger and Dominique Schneuwly, whose raw data collected on different study sites allowed investigation of different aspects of tree ring–rockfall research in this paper. The authors also acknowledge Profs. Michel Monbaron and Hans Kienholz for both financial and moral support. Finally, we are grateful to Michelle Bollschweiler for helpful comments on an earlier version of this paper and Heather Murray for improving the English.

*****

CHAPTER E

OVERALL CONCLUSIONS

In the overall conclusions, a brief summary of each paper is given along with some concluding remarks on the results obtained as well as suggestions for future studies.

1. Overall Conclusions

1.1 Summary of main results and overall conclusions

In conclusion, new insights about the possibilities and limitations of tree ring–rockfall research have been gained in this thesis. A detailed discussion of the results concerning the seasonal timing, frequency and magnitude of rockfall activity, the height distribution and visibility of scars on stem surfaces as well as the strengths, weaknesses or methodological uncertainties of tree ring–rockfall analyses have been presented in the concluding sections of each of the four papers forming the centerpiece of this thesis. As a result, I will limit this summary to the main results and overall conclusions in the following paragraphs:

European larch primarily reacts to rockfall impacts with the formation of traumatic rows of resin ducts or callous tissue. If the disturbance takes place within the growth period of the tree, reactions will immediately occur. A detailed study of the position of callous tissue or traumatic rows of resin ducts within a single tree ring may therefore be used to determine the intra-annual timing of rockfall with almost monthly resolution. In contrast, impacts caused during the dormancy of trees will only leave "signs" within the first row of cells in the new tree ring. Here, tree-ring analysis needs to be complemented with field data. At *Täschgufer*, 88% of the scars observed in 270 cross-sections of 18 juvenile *Larix decidua* trees occurred during dormancy. While direct observations indicate a climax in rockfall activity during April and May, we should consider that rockfall might be quite frequent in early winter (October through early December) as well.

Short- and long-term changes in the frequency and magnitude of rockfall activity since 1600 AD were – for the first time – assessed with a large number of increment cores selected from heavily disturbed *Larix decidua* trees growing at *Täschgufer*. In contrast to former studies, this investigation on variations in rockfall activity was neither limited by a restricted temporal sample nor by the temporal resolution of the approach. Furthermore, the use of a 'rockfall rate' allowed reliable reconstructions of yearly fluctuations and decadal ratios of rockfall activity over several centuries as well as the identification of one high magnitude–low frequency event in 1720 AD. Moreover, the large number of samples chosen for analysis permitted illustration of spatial variations in rockfall activity and allowed identification of a steady improvement of the protective effect since the forest stand was partly destroyed by the large rockfalls in 1720 AD.

The vertical distribution and the visibility of scars on the stem surface have been investigated with 307 cross-sections of three adult trees (*Abies alba*, *Fagus sylvatica*, *Picea abies*) from the *Altdorfer Bannwald*. Results on the vertical distribution of impact scars on the stem surface suggest that rockfall fragments may cause damage to trees between ground level and more than nine meters above. Data further shows that less than 7 % of injuries are located within the first 20 cm, whereas every second scar would, on average, be located within the first two meters. The investigation of visible versus hidden (i.e. internal) scars indicates that 51 to 84% of the injuries caused to these century-old trees are still visible on the stem surface today.

Based on the results obtained at *Altdorfer Bannwald*, the height distribution and visibility of scars have been addressed in greater detail with datasets from other rockfall slopes located within Switzerland (i.e. *Brienzergrat, Diemtigtal, Täschgufer*). Furthermore, the focus was put on the number of scars recons-

tructed on entire trees and compared them with events identified on only one cross-section or a series of increment cores taken at the height with a maximum number of wounds visible on the stem surface. Results indicate that the size of rockfall fragments and slope gradients primarily determine impact heights.

The importance of 'hidden' scars would, in contrast, not only depend on the bark properties of the tree species (e.g., thickness, sporadic scaling), but also be influenced by yearly increment rates as well as the age and diameter of the tree. As a consequence, the quantity of 'blurred evidence' may range from 15 to 90%. Analysis of single cross-sections sampled indicates that, at best, 13 to 35% of the scars occurring on the entire tree can be detected at a given 'test height'. Data further suggests that the number of events reconstructed at this 'test height' can be considerably improved as soon as other growth disturbances such as reaction wood, abrupt growth reductions or, if present, traumatic rows of resin ducts are considered as well. Finally, the 'loss' of information appears to be least important when analyses are realized on slopes with large rockfall fragments (e.g., *Täschgufer*).

Since its development within this PhD thesis, the 'rockfall rate' has been successfully tested in a tree-ring analysis focusing on century-long fluctuations in rockfall activity on the foot of a rock cliff in the *Diemtigtal* (Perret *et al*. 2005b, Chapter F, Appendix 2). Similarly, Perret *et al.* (2005b) determined the intra-seasonal timing of rockfall activity with the approach introduced in Chapter B1. It therefore seems that the approaches developed within this PhD study can be applied on sites with different slope characteristics, varying geology, much smaller rockfall fragments and denser stand structures as well. Replicate investigations are nonetheless needed, as there is a potential for a number of improvements and further research.

1.2 Outlook and further research needs

The important and unsolved issues mentioned in the following paragraphs merit special consideration in further studies focusing on rockfall with tree as well as tree-ring analysis:

1.2.1 Traumatic rows of resin ducts: where do they occur?

Studies focusing on conifer species such as e.g., *Larix decidua* Mill. or *Picea abies* (L.) Karst. should, for instance, investigate the occurrence and vertical distribution of traumatic rows of resin ducts in tree-ring sequences. As illustrated in Figure E1.1, there is still a considerable lack of knowledge on how far from the location of scars, evidence of rockfall would be discernable through the presence of traumatic rows of resin ducts. While we believe to know that the large boulders at *Täschgufer* would more easily cause traumatic rows of resin ducts over large distances in the tree-ring in question, we do not know if there are energy or rock mass thresholds driving the formation of resin ducts on sites with comparably small rockfall

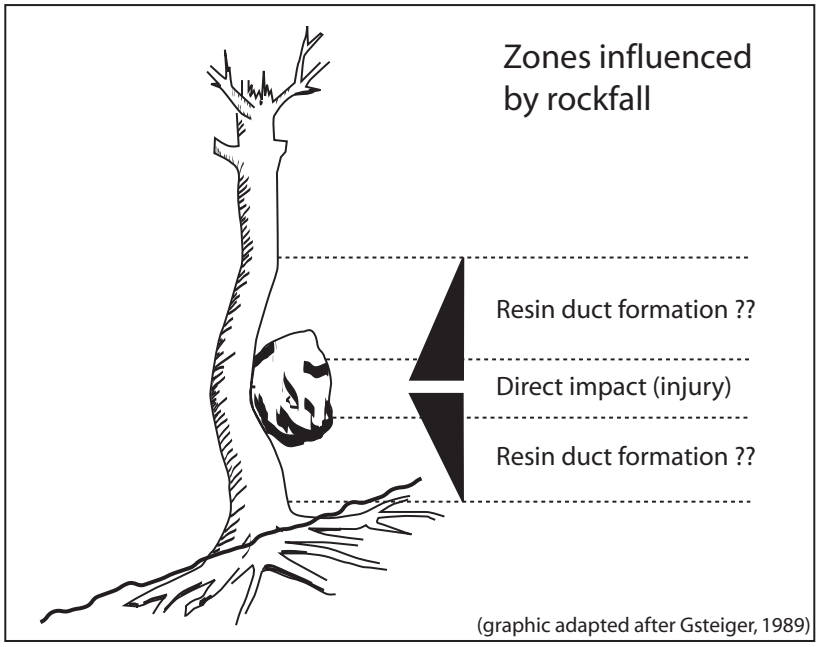

Fig. E1.1 *We can identify the scar caused to the stem of e.g., Larix decidua or Picea abies trees, but where and at what distance from the injury do we expect to find traumatic rows of resin ducts as well?*

fragments. Systematic analysis of the vertical extent of traumatic rows of resin ducts from the center of impact should therefore be studied with large numbers of cross-sections.

1.2.2 Vertical distribution of scars on trees: Did we greatly underestimate bounce heights previously?

In addition, attention should be addressed to the vertical distribution of scars on the stem surface, as current data on maximum bounce heights of rocks and boulders on forested slopes (Rickli *et al.* 2004) appear to largely underestimate the potential of bouncing rockfall fragments. Results obtained from an *Abies alba* Mill. felled on a 35° steep slope within the *Altdorfer Bannwald* show that 60% of all scars registered in this tree occur at heights ranging from 114 to 930 cm and, thus, largely above the maximum bounce height of 110 cm as indicated by Rickli *et al.* (2004) for rock fragments with diameters < 50 cm. As there is still limited knowledge available on the behavior of rocks in forests, the coupling of tree-ring data with evidence found in the field (impact craters, jump distances) as well as process-specific parameters (bounce height–jump distance ratios, velocities, energies) could help to understand the rockfall process and the efficacy of protection forests in greater detail.

1.2.3 Does seismic activity in Valais trigger rockfall(s) at Täschgufer?

The evolution of landscape strongly depends on current and past uplifts, the associated seismic activity (Burbank & Anderson 2001, Schlunegger & Hinderer 2001, 2003) as well as the erodability of the bedrock on slopes (e.g., Kühni & Pfiffner 2001). In the *Nikolaital*, differential uplift movements in the order of 0.015 mm km^{-1} $year^{-1}$ as well as seismic activity repeatedly result in the triggering of mass movements along recent or ancient faults. According to Jaboyedoff *et al.* (2003a, b), the 1991 *Randa* rockslide or the 2002 *Medji* (*St. Niklaus*) rockfalls would have been caused by the uplift rates along two regional fault lines, while the 1855 rockfalls at *Durlochhorn* and the *Stägjitschuggen* rock faces near *Grächen* and *St. Niklaus* were clearly caused by seismic activity (e.g., Eisbacher & Clague 1984, Joris 1995).

As the environs of *Täschgufer* have been subject to repeated earthquake events with MSK intensities between VII and IX during the last centuries (1755, 1855, 1874, 1880, 1924, 1946, 1960; Mayer-Rosa *et al.* 1997, Stoffel 1999), and as the bedrock of paragneissic origin is heavily disintegrated, the influence of seismic activity on the triggering of rockfall fragments appears to be likely. The currently available tree-ring sequences from *Täschgufer* do not show signs of enhanced rockfall frequency related to seismic activity. As rockfall fragments at *Täschgufer* are regularly stopped on the talus slope and before penetrating into the protection forest, the currently available reconstructions cannot be used to reconstruct past earthquake activity. In contrast, it would be worthwhile to select increment cores from all trees located along the upper forest fringe, where chances are that rocks and boulders did hit trees during seismic activity.

1.2.4 Are there correlations between rockfall and climate at Täschgufer?

Future studies should also try to assess the impact of possible modifications in the existing permafrost (e.g., Schiermeier 2003, Lewkowicz & Harris 2005), the influence of so-called 'warm winter spells' (Beniston 2005) or 'excessively' hot summers (Keller 2003, Gruber *et al.* 2004) on the rockfall activity at *Täschgufer*. At first sight, rockfall appears to occur more frequently in times with dry and warm weather conditions than during cold and humid periods. In this sense, a comparison of reconstructed rockfall 'rates' with archival data on climatic variations in Switzerland (Pfister 1999) indicates that enhanced rockfall activity coincides very well with the dry and warm periods observed in the 1650s, 1660-1669, 1718-1724, 1943-1952 or during the 1990s. In contrast, climatic data may not explain the considerable increase in rockfall activity observed in the 1770s. Similarly, the presence of cold and humid summers with repeated snowfall within the Alps appears to be again represented in comparably low rockfall rates between 1851 and 1854, during the 1880s or around 1915.

Based on rockfall data presented as the number of events reconstructed in the trees available during a specific decade (i.e. GD-Tr ratios, cf. Chapter B2.5), Schneuwly (2003) suggests that phases of glacier retreat reconstructed at nearby *Gornergletscher* (*Zermatt*; Holzhauser 1995) would generally coincide with increased rockfall activity observed at *Täschgufer*, while during periods of glacier advance, rockfall ratios would be less pronounced.

Figure E1.2 gives an idea of the GD-Tr ratios from the trees sampled on the *Täschgufer* slope and the glacier phases at *Gornergletscher* for the last 400 years. A final comparison shall be made here between the decadal rockfall 'rates' presented in Chapter B2 and Northern hemisphere April–September temperatures reconstructed from tree-ring sequences (Briffa *et al.* 2001a, b). Results are represented in Figure E1.3 for

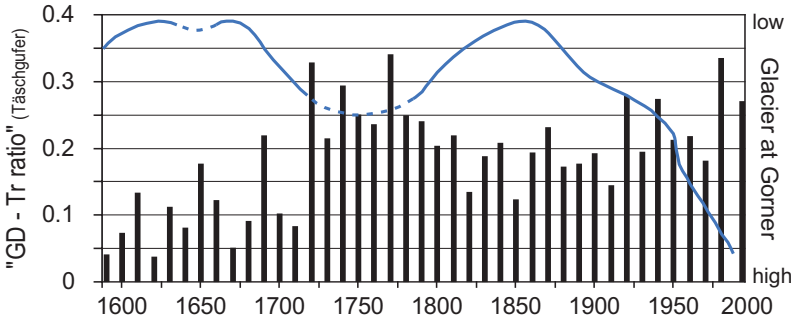

Fig. E1.2 *Is there a negative correlation between the reconstructed rockfall activity at Täschgufer and glacier fluctuations observed at Gornergletscher (Zermatt;* Holzhauser 1995*)?*

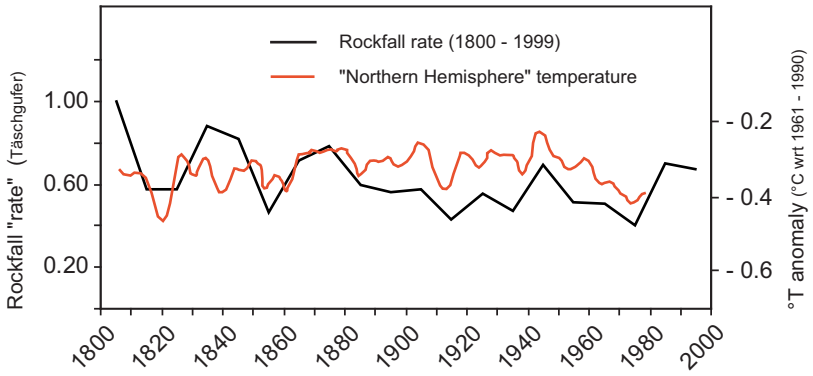

Fig. E1.3 *Or are we even able to identify a positive correlation between decadal rockfall 'rates' and Northern hemisphere temperatures (April–September) reconstructed with extensive data from a tree-ring density network (*Briffa *et al.* 2001a, b*)?*

the period 1800-1999 AD. Again, increased rockfall activity seems to be linked with warmer temperatures while comparably small rockfall 'rates' occur in times with colder temperatures. Even though the previous illustrations indicate a link between climatic factors and rockfall activity, the presence of significant correlations between climate and rockfall has yet to be proved with data from nearby meteorological stations (i) being representative for the study site and (ii) covering sufficiently long periods of the past (e.g., *Grand St. Bernard*).

*****

CHAPTER F

APPENDICES

Chapter F first of all includes three papers (co-)written by the author of this Philosopher's Degree thesis. Even though these papers do not form the core of this thesis, their topics as well as the results obtained are considered to be worth reproducing within this publication. The first paper gives a literature review of tree-ring analysis dealing with rockfall (Stoffel 2005a), the second one focuses on spatio-temporal variations of 20th century rockfall activity on a forested slope in the *Diemtigtal* (Perret *et al.* 2005b; *Bernese Prealps*, Switzerland) and the third one assesses the accuracy of the 3D process-based rockfall model Rockyfor and determines the protective effect of forest stands on several sites within Switzerland (Stoffel *et al.* 2005d). In addition, the study site *Täschgufer* is illustrated in Chapter F4 with a series of photographs, before a detailed description is given in Chapter F5 on how increment cores and cross-section have been sampled, tree-ring data processed and micro-cuts prepared within this thesis.

Appendix 1

Markus Stoffel [1]

"A review of studies dealing with tree rings and rockfall activity: The role of dendrogeomorphology in natural hazard research"

[1] *Groupe de Recherches en Géomorphologie (GReG), Department of Geosciences, Geography, University of Fribourg*

accepted for publication in "Natural Hazards"
revised: 20 July 2005, accepted: 9 September 2005

Abstract. Over the last few years, rockfall research has increasingly focused on hazard assessment and risk analysis. Input data on past rockfall activity were gathered from historical archives and lichenometric studies or were obtained through frequency–volume statistics. However, historical records are generally scarce, and lichenometry may only yield data with relatively low resolutions. On forested slopes, in contrast, tree-ring analyses may help, generally providing annual data on past rockfall activity over long periods. It is the purpose of the present literature review to survey the current state of investigations dealing with tree-ring sequences and rockfall activity, with emphasis on the extent to which dendrogeomorphology may contribute to rockfall research. Firstly, a brief introduction describes how dendrogeomorphological methods can contribute to natural hazard research. Secondly, an account is provided of the output of dendrogeomorphological studies investigating frequencies, volumes or spatial distributions of past rockfall activity. The current and potential strengths of dendrogeomorphology are then presented before, finally, the weaknesses of tree rings as natural archives of past rockfall activity are discussed and promising directions for further studies outlined.

Keywords rockfall, tree rings, dendrogeomorphology, frequency, volume, spatial patterns, seasonality.

1.1 Introduction

In mountainous regions, rockfalls repeatedly impinge on inhabited areas or transportation corridors (Kienholz *et al.* 1988, Hungr *et al.* 1999, Budetta 2004), where they occasionally destroy buildings (Evans & Hungr 1993) or even cause fatalities (Bunce *et al.* 1997, Guzzetti 2000, Baillifard *et al.* 2003). As a result, rockfalls have become one of the most intensively studied geomorphic processes of the cliff zone. Initially, studies mainly relied on direct observations in the field (Luckman 1976, Douglas 1980, Gardner 1983) or lichenometric analysis (Bull *et al.* 1994, Luckman & Fiske 1995, André 1997, McCarroll *et al.* 2001) to derive frequencies, volumes or spatial aspects of past rockfall activity.

Fig. F1.1 *Trees are able to provide efficient protection from rockfall by slowing down or stopping falling, bouncing or rolling rocks and boulders. In the present case, a rock has even been lodged in a stem in the Ticino Alps, Switzerland. (Photo courtesy by Fritz H. Schweingruber, used with permission)*

More recently, research has gradually evolved in the direction of hazard assessment and risk analysis (e.g., Hungr & Beckie 1998, Guzzetti *et al*. 2004). Data on past rockfall activity is commonly gathered from historical archives (e.g., Hantz *et al.* 2003, Barnikel 2004, Guzzetti & Tonelli 2004) and further investigated with frequency–volume statistics (Dussauge-Peisser *et al.* 2002, Dussauge *et al.* 2003) or frequency densities (Malamud *et al.* 2004).

However, Guzzetti *et al.* (1999) pertinently emphasize that historical records are only rarely available and difficult to obtain for single events or event-prone areas. Lichenometry also has its limitations, as the method (i) tends to be hindered by a paucity of widely accepted measurement and analytical procedures (Bull & Brandon 1998) and (ii) may only yield relatively low resolution data. Finally, observation-based rockfall studies consider present rates of activity and rarely extend for more than a few years, thus making it difficult to scale-up results either spatially or temporally (McCarroll *et al.* 1998). As a consequence, information on frequencies *(how often)*, volumes (*how large*), spatial distributions (*where*) or the seasonality (*when*) of past rockfall activity remains scarce and, for the most part, fragmentary.

Tree rings, in contrast, have the potential to yield yearly resolved data on frequencies, volumes, spatial distributions and/or the seasonal timing of past events (DeGraff & Agard 1984, Guzzetti *et al.* 1999). Consequently, tree rings have been widely used, over the last decades, in the analysis of landslides (e.g., Lateltin *et al.* 1997, Fantucci & Sorriso-Valvo 1999, Stefanini 2004), debris flows (e.g., Strunk 1995, Baumann & Kaiser 1999, Stoffel *et al.* 2005a), flooding (e.g., Hupp 1988, LePage & Bégin 1996, St. George & Nielson 2003), snow avalanches (e.g., Patten & Knight 1994, Rayback 1998, Hebertson & Jenkins 2003), earthquakes (e.g., Jacoby *et al.* 1988, Jacoby 1997, Lin & Lin 1998) and volcanic eruptions (e.g., Kaiser & Kaiser-Bernhard 1987, Baillie 1994, Biondi *et al*. 2003).

In contrast, tree rings have only rarely been taken into account when investigating rockfall on forested slopes, even though Schweingruber (1996: 272) persuasively argued that "geomorphological processes in mountain forests are very common and only dendrochronology is able to provide information about the frequency and extent of the past events". It is therefore the aim of this literature survey to give an overview of the results of studies dealing with tree rings and rockfall, with a description of, firstly, the different methods and approaches used in the field of dendrogeomorphology. Secondly, to illustrate the potential of dendrogeomorphology, examples are given of how frequencies, volumes, the spatial distribution or the seasonality of rockfall have been studied using dendrogeomorphological techniques. Finally, the strengths and weaknesses of tree rings as natural archives of past rockfall activity are discussed and promising directions for further studies outlined.

1.2 Dendrogeomorphological applications and methods

Over the past few decades, tree-ring research has gradually evolved from the dating of wood (dendrochronology, dendroarcheology) to the much broader

field of dendroecology, including all areas of science involved in drawing environmental information from tree-ring sequences (Schweingruber 1996). In this sense, 'dendrogeomorphology' represents one of the many subfields of dendroecology and has been widely used to study and date past geomorphic processes. The approach, developed by Alestalo (1971) and refined by Shroder (1978), takes advantage of the fact that trees form yearly increment rings that can precisely date external disturbances (see Fig. F1.1).

Growth cycles in trees are driven by the seasonality of climate. In the temperate climate of the Northern Hemisphere, the 'vegetation period', and thus also cell growth, lasts from around May to September and can be divided into two distinct periods (Camarero *et al.* 1998, Rigling *et al.* 2002): At the beginning of the growth cycle, large thin-walled earlywood cells and (depending on the species) vessels are formed. Later on, reproductive cambium cells start producing smaller and denser latewood cells. Thereafter, cell growth ceases and 'dormancy' sets in (October to April). The subdivision of a tree ring into 'dormancy', earlywood and latewood is illustrated in Section F1.3.4.

As trees react immediately to any type of disturbance, the position of abnormal growth features affecting a tree ring, such as scars, callus tissue, traumatic rows of resin ducts or reaction wood, can be used as dating indicators for the intra-seasonal timing of events with almost monthly resolutions (Brown & Swetnam 1994, Ortloff *et al.* 1995).

Figure F1.2 summarizes different reactions of trees to geomorphic events and shows how growth responses may appear in tree-ring sequences. A tree's

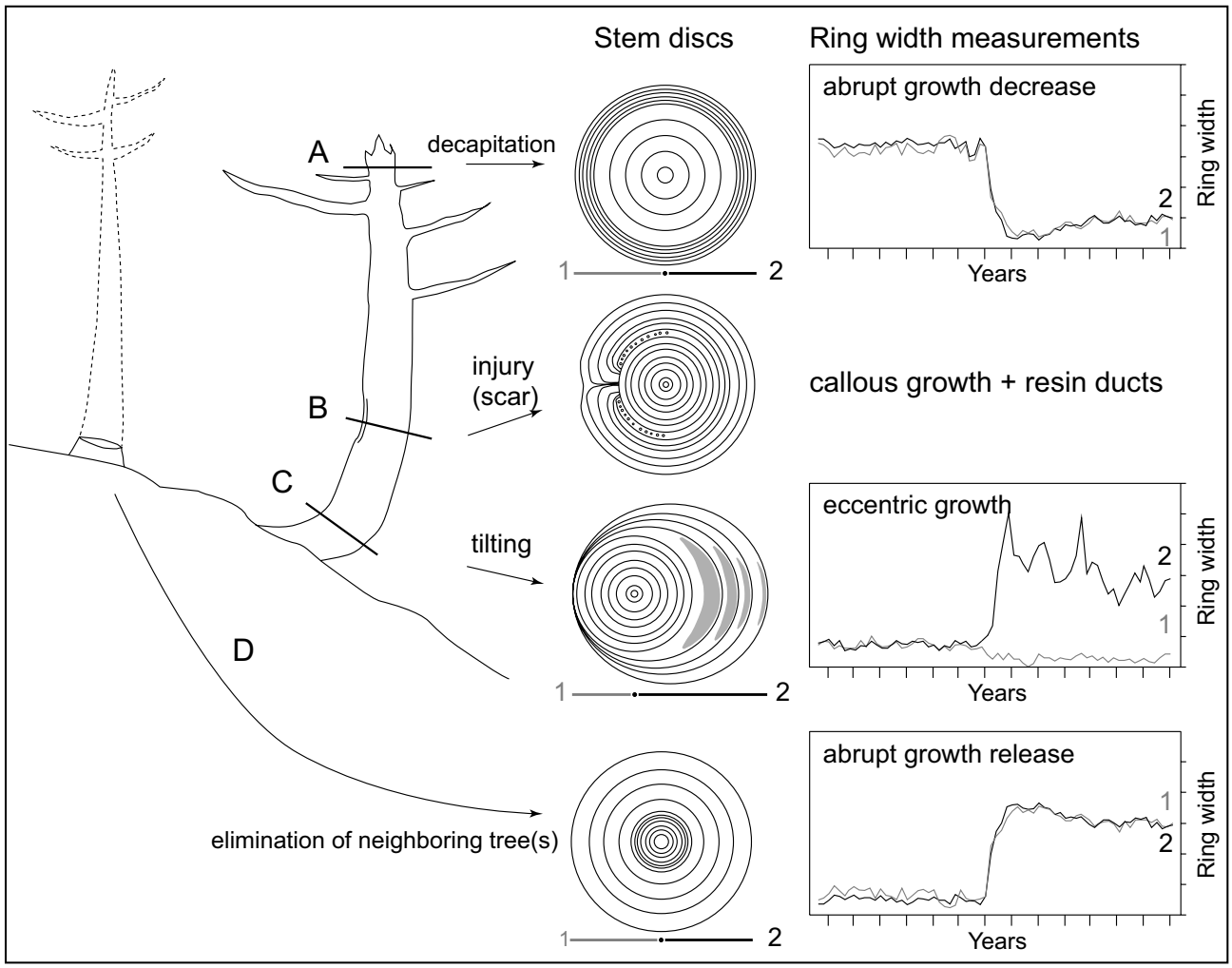

Fig. F1.2 *Evidence used to infer rockfall events from tree-ring sequences: Visual analysis of the samples (left) and the measurement of tree-ring widths (right) allows identification of sudden growth releases, growth suppressions, reaction wood, callus tissue or traumatic rows of resin ducts.*

reaction to the impacts caused by snow avalanche, landslide, debris flow or rockfall can lead to (A) cell formation concentrating in areas vital for survival after decapitation and the loss of main branches; (B) scars that become overgrown after injury and (C) a gradual straightening of the stems through the formation of reaction wood after tilting due to instability or unilateral pressure. Sudden reductions in tree-ring growth may also occur as a reaction to the exposure of roots through erosional processes or the partial burying of the stem and subsequent reduction in nutrient supply (Strunk 1997).

In addition, the elimination of trees through geomorphic events can result in (D) growth releases in undamaged neighboring trees as they take advantage of improved environmental conditions (e.g., more light, nutrients and water). Finally, after cambial damage certain conifer species may form traumatic rows of resin ducts. Further details on the principles of dendrogeomorphology or tree reactions to external processes can be found in Shroder (1980), Shroder & Butler (1987), Bräuning (1995) or Wiles *et al.* (1996).

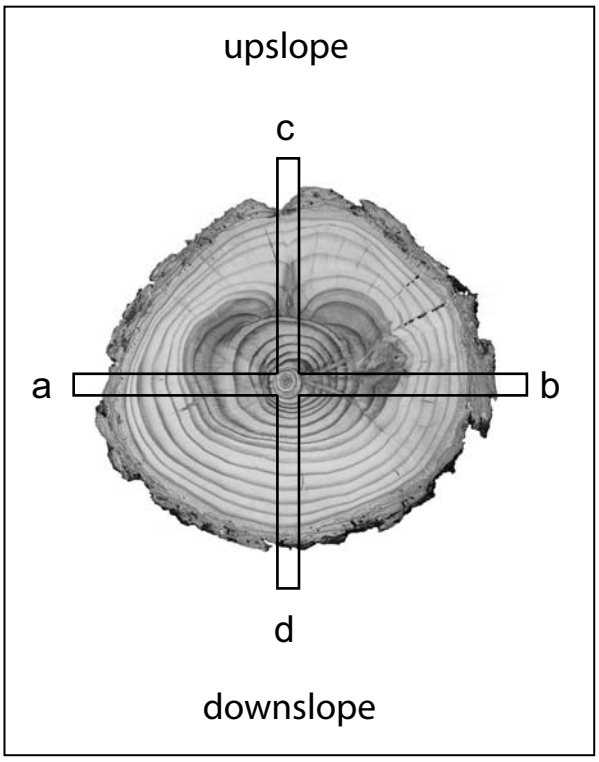

Fig. F1.3 *Cross-section of a scarred European larch (Larix decidua) with indication of the sampling positions a, b, c and d for increment cores.*

Dendrogeomorphological analyses comprise both investigations in the field and work in the laboratory: In the field, detailed geomorphic investigations and process analyses must precede tree sampling. Only when the geomorphic process and its area of influence has been determined, should cores either be extracted from trees with increment borers or, ideally, stem discs (cross-sections) sawn.

As illustrated in Figure F1.3, increment cores are normally taken in the fall line of the process in question, i.e. one core upslope (core c) and one core downslope (core d). In addition, and because rockfall may also injure trees laterally, further samples should be taken perpendicular to the slope (cores a, b) as well as cores extracted from the visible wound and any overgrowing calluses.

Samples are then prepared in the laboratory (Phipps 1985, Krusic *et al.* 1987) and analyzed visually, with obvious growth anomalies such as abrupt growth changes, the onset of reaction wood, resin ducts or scars noted on skeleton plots (Schweingruber *et al.* 1990). This graphic method assists in cross-dating samples by helping in the identification and location of missing or false rings through comparison of one tree-ring sequence with another or reference sequences (Wiles *et al.* 1996). In a further step, ring-widths are measured using digital measuring tables. Thereafter, data are processed following the procedures described by Bräker (2002).

As growth reactions can be caused by other than geomorphic factors, increment curves of disturbed trees then need to be cross-dated with a reference chronology. This chronology, built with undisturbed samples from a nearby forest stand, reflects growth conditions driven exclusively by environmental factors such as altitude, slope exposure, temperature, precipitation or occasional insect outbreaks (Fritts 1976, Graybill 1982, Cook & Kairiukstis 1990, Schweingruber 1996). A comparison of the reference chronology with the tree-ring sequences of disturbed trees enables (i) identification of locally predominant growth patterns from disturbances induced by geomorphic processes and (ii) accurate dating of disturbances within a year or less.

Results from the different trees sampled within the study area can then be compared and, sample depth permitting, frequencies or volumes for the geomorphic process in question can be derived. In addition, spatial information on the dispersion or reach of single events can be analyzed and represented with interpolations (Stoffel *et al.* 2005c).

1.3 Case studies focusing on tree rings and past rockfall activity

1.3.1 The beginnings

Surprisingly, and despite the potential of dendrogeomorphological methods, rockfall activity has only rarely been studied through the analysis of tree-ring sequences. The work of Moore & Mathews (1978) seems to represent the first (published) attempt to use dendrogeomorphological methods to date the impacts of rocks on trees. This study resulted in the reconstruction of the historical *'Rubble Creek'* rockfall avalanche in southwestern *British Columbia* (Canada). Later, work by Butler *et al.* (1986) dated two recent 'rockfall avalanches' in *Glacier National Park* (*Montana*, USA). Hétu (1990), Lafortune *et al.* (1997) and Hétu & Gray (2000) analyzed stem discs from the *Gaspé Peninsula* (Canada) to determine annual sedimentation rates and recent displacements of forest edges on active scree slopes.

Even though the material causing the scars was in all cases of rockfall origin, the process responsible for the damage to the trees was not rockfall. In the studies presented by Moore & Mathews (1978) and Butler *et al.* (1986), the process was described as a downslope displacement of rock particles in a "rapid flow-like movement", while different debris transfer processes (e.g., frost-coated clast flows, niveo-aeolian sedimentation, debris flows, snow avalanches) were identified responsible for the remobilization of small rockfall clasts (Ø 2,36 cm) on the slopes of the *Gaspé Peninsula*.

The first dendrogeomorphological analysis purely focusing on rockfall activity was performed on different slopes at *Brienzergrat* (*Bernese Oberland*, Switzerland), where Gsteiger (1989) analyzed three beech (*Fagus sylvatica*) and four Norway spruce trees (*Picea abies*). The trees were felled for analysis and 25 stem discs prepared. In total, 56 rockfall scars were identified, 37 in the beech and 19 in the spruce samples. Even though the century-old trees were felled for analysis, only the lowermost sections of the trunks were analyzed; scars occurring higher on stems were disregarded.

1.3.2 Later works

1.3.2.1 Studies using stem discs

A later study using stem discs to determine past rockfall activity was performed at the foot of a slope near *Bourg St. Pierre* (*Valais*, Switzerland), where a "rockfall chronology" (1890–1987) was constructed from 30 cross-sections taken from the base of previously felled Norway spruce trees (Schweingruber 1996). A total of 66 scars were identified and periods with either abundant (1953–1960) or infrequent rockfall activity (1941–1949) were determined. The study also indicated that the construction of a road across the slope prevented rockfall from reaching the lowermost part of the slope after 1970. Schweingruber (1996) finally concluded that "rockfall frequency", here, is most likely to be correlated with the frequency of precipitation.

Systematic felling campaigns (bark-beetle eradication) in a forest located at the base of a high limestone cliff in *Diemtigtal* (*Bernese Oberland*, Switzerland) allowed investigation of rockfall activity on 33 cross-sections from Norway spruce trees (Perret *et al.* 2005b). Discs were sawn from the remaining tree stumps at about 30 cm above ground and used to study past rockfall activity (1880–2000). In total, analyses allowed identification of 75 scars and 175 traumatic rows of resin ducts. Results from decadal rockfall activity neatly show that rockfall frequencies remained at a relatively low level throughout the first half of the 20th century. Starting in the 1960s, frequencies gradually increased, resulting in a relatively high value during the 1990s (Perret *et al.* 2005b).

In the protection forest of *Altdorf* (Uri, Switzerland), Stoffel (2005b) felled three century-old trees and, in contrast to the studies mentioned above, for the first time trees were studied from base to top by taking a large number of cross-sections: Analysis of the 88 cross-sections of a 97 year-old Norway spruce tree showed 53 different scars located between 10 and 596 cm above ground. In addition, 105 stem discs were cut and prepared from a 129-year old fir tree (*Abies alba*): as can be seen from Figure F1.4, this tree suffered from rockfall impacts 33 times between 1916 and 1995 and scars were found at heights ranging from 17 to 930 cm above ground. Finally, a 112-year old beech tree was cut into 114 cross-sections. Analysis of the beech discs allowed identification of 103 different scars representing 25 single event years between 1898 and 1994. Figure F1.5 illustrates one of the lowermost stem discs of this tree with several overgrown scars and includes a histogram showing all reconstructed event years.

In a heavily disturbed protection forest at *Täschgufer* (Valais, Switzerland), Stoffel *et al.* (2005b) felled 18 juvenile European larch trees (*Larix decidua*). In total, 270 stem discs were prepared, with discs taken from the basal area of the trunk up to the crown. Analysis

of these discs allowed dating of 180 rockfall impacts for the period 1977–2002. Although rockfall activity caused almost continuous damage to the sampled trees, activity was found to have increased between 1994 and 1996.

All the studies mentioned above furnished valuable evidence of past rockfall activity for the slopes in question. However, they suffer from the limited number of available trees or cross-sections (since trees cannot normally be felled in protection forests and stumps of felled trees are not always readily available). With the exception of possibly Perret *et al.* (2005b), the term 'frequency' should, thus, be read with caution in these studies.

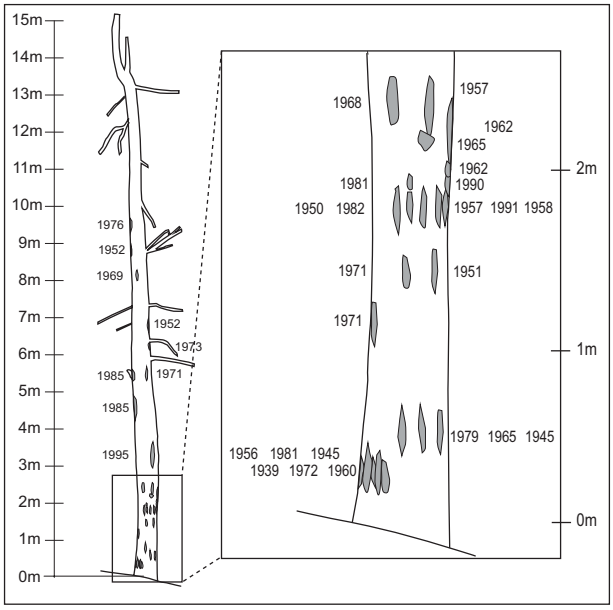

Fig. F1.4 *Vertical and horizontal distribution of 33 rockfall injuries reconstructed on an adult fir tree (Abies alba) from the Altdorfer Bannwald (Swiss Alps). While most scars can be found within the first 2 m above ground, the highest injury was found at a height of 930 cm.*

1.3.2.2 Studies using increment cores

In areas where it is impossible to fell trees, the extraction of increment cores represents a valuable and non-destructive alternative. Moreover, this method normally allows the sampling of a larger number of trees.

Until now, only the protection forest at *Täschgufer* (Valais, Switzerland) has been extensively studied using increment cores. In this location, a total of 135 severely damaged European larch trees were chosen for analysis (Schneuwly 2003, Stoffel *et al.* 2005c). At least 4 cores were extracted per tree using increment borers (see Fig. F1.3) and further cores were extracted from wounds or overgrown scars, resulting in a depth of 564 samples. In contrast to most studies using stem discs, Stoffel *et al.* (2005c) studied all types of growth disturbances, illustrated in Figure F1.2, to date past rockfall activity, mainly focusing on the occurrence of traumatic rows of resin ducts.

In total, 741 growth disturbances were dated between 1600 and 2002. Results indicate that rockfall most commonly occurred in the form of high frequency events of limited volume. However, they also show one large event in 1720, which would have considerably displaced the local forest fringe downslope and eliminated a part of the forest stand in the southern sector of the study area. Rockfall frequencies are represented by means of a rockfall 'rate', which Stoffel *et al.* (2005c) define as the number of recons-

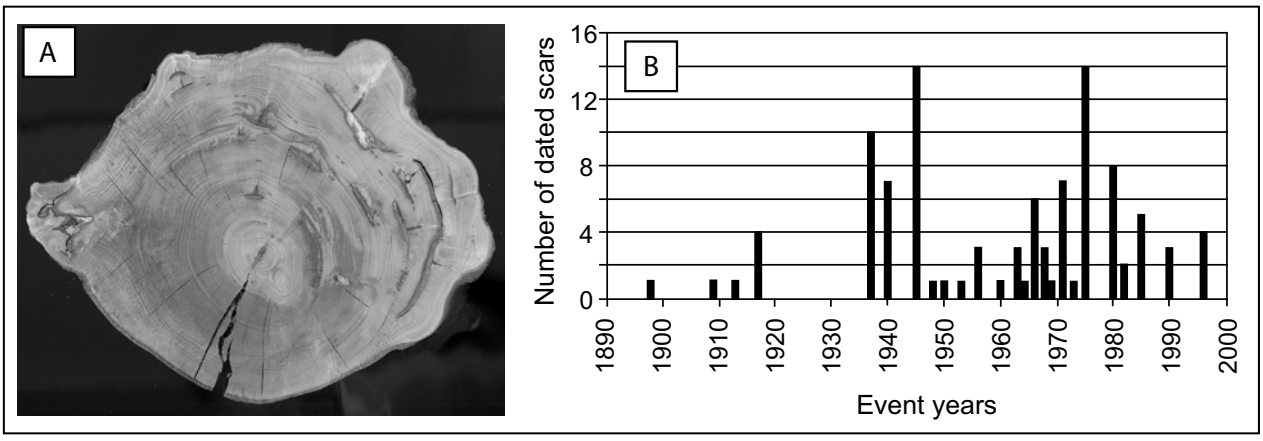

Fig. F1.5 *Rockfall activity based on 114 stem discs of a heavily disturbed beech (Fagus sylvatica) from the Altdorf Bannwald (Swiss Alps): (a) Cross-section taken at the base of the stem showing 13 scars; (b) Histogram with all event years reconstructed on the stem discs of this beech tree.*

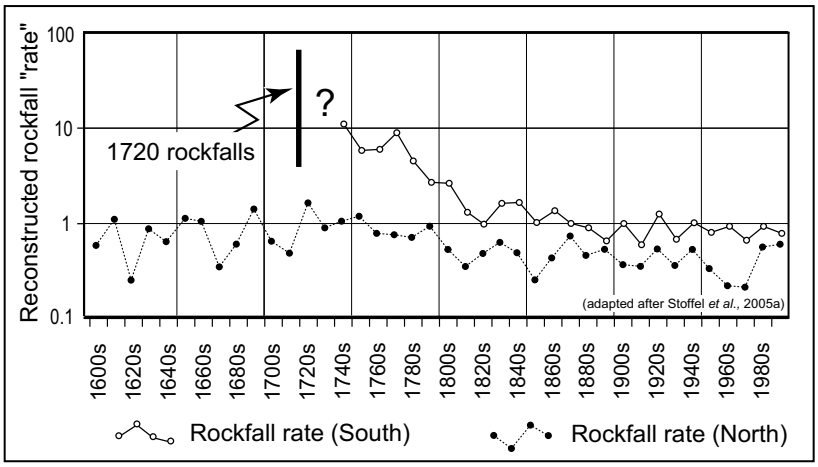

Fig. F1.6 *Reconstructed rockfall activity at Täschgufer (Swiss Alps) covering the period: Rockfall activity is represented by the rockfall 'rate' (for explanation see text), indicating that the large 1720 rockfalls temporarily reduced the protection afforded by the forest.*

tructed rockfall events per meter tree diameter exposed to rockfall (per decade). The results of this analysis are illustrated in Figure F1.6, showing rockfall periods of high or low frequencies in both the northern and southern sector of the Täschgufer slope. In addition, Figure F1.6 also illustrates the extent to which the large rockfall of 1720 led to increased activity in the southern sector throughout the 18th century.

1.3.2.3 Combined stem disc and core analyses

On a slope in the *Val Calanca* (Grisons, Switzerland), Hopfmüller (1997) sampled 52 stem discs from previously felled and 66 increment cores from 33 living Norway spruce trees. While 42 injuries were found in the cross-sections, the increment cores enabled identification of 52 further scars. However, only two thirds of the scars could be precisely dated, as the wood of 22 samples proved to be rotten. The injury age in the decaying samples was less precisely dated with an error margin ranging from ±1 to ±10 years. Results indicated increased rockfall activity during the 1940s as well as between 1955 and 1965. In addition to small high frequency rockfall events, two large rockfalls (*Felsstürze*) were identified, causing 12 scars in the winter of 1938/39 and 30 more wounds in the subsequent winter (1939/40).

1.3.3 Studies on the spatial distribution of rockfall activity

The spatial distribution of rockfall activity can reveal the maximal range, the lateral dispersion and the distribution of recurrence intervals on a slope. Gsteiger (1993) was the first to attempt to illustrate spatial variations in rockfall activity by analyzing the number and distribution of scars visible on stem surfaces to derive rockfall activity maps (*Aktivitätskartierung*). Quantitative analysis of rockfall activity using dendrogeomorphological methods only began to be applied in 1996. Schweingruber (1996) represented the distribution of injured and non-injured trees on a slope near *Bourg St. Pierre* (Valais Alps, Switzerland) with different dots. In a similar way, Hopfmüller (1997) illustrated the spatial distribution of scars associated with two considerable rockfalls (*Felsstürze*) in the late 1930s. He also provided an indication of the fall tracks, the range and lateral spread of rockfall boulders. More recently, Stoffel *et al.* (2005b) used tree rings to differentiate rockfall activity originating from two different source areas at *Täschgufer* (Valais Alps, Switzerland). In addition, scars induced by natural rockfall activity were clearly separated from rockfall impacts triggered during dam construction works (i.e., excavation works, blasting).

The large amount of rockfall data reconstructed from increment cores at *Täschgufer* (Stoffel *et al.* 2005c) made it possible to divide spatial information on past rockfall activity into different time periods. In Figure F1.7, four 25-year periods were chosen from the last century (1901–2000) to illustrate spatio-temporal variations in rockfall activity on the Täschgufer slope. Again, trees were differentiated into scarred and unaffected trees and results illustrated with either black or white dots.

While all of the preceding studies illustrated the presence or absence of rockfall impacts on trees, no information was given on the frequency or the number of reconstructed scars. Very few studies analyzed recurrence intervals of rockfall impacts on trees together with their distribution across slopes in order to illustrate both spatial and temporal variations in rockfall activity. Stoffel *et al.* (2005c) used interpolations to represent the position of scarred trees and the time elapsed between single events. As can be seen from Figure F1.8, they found considerable spatial differen-

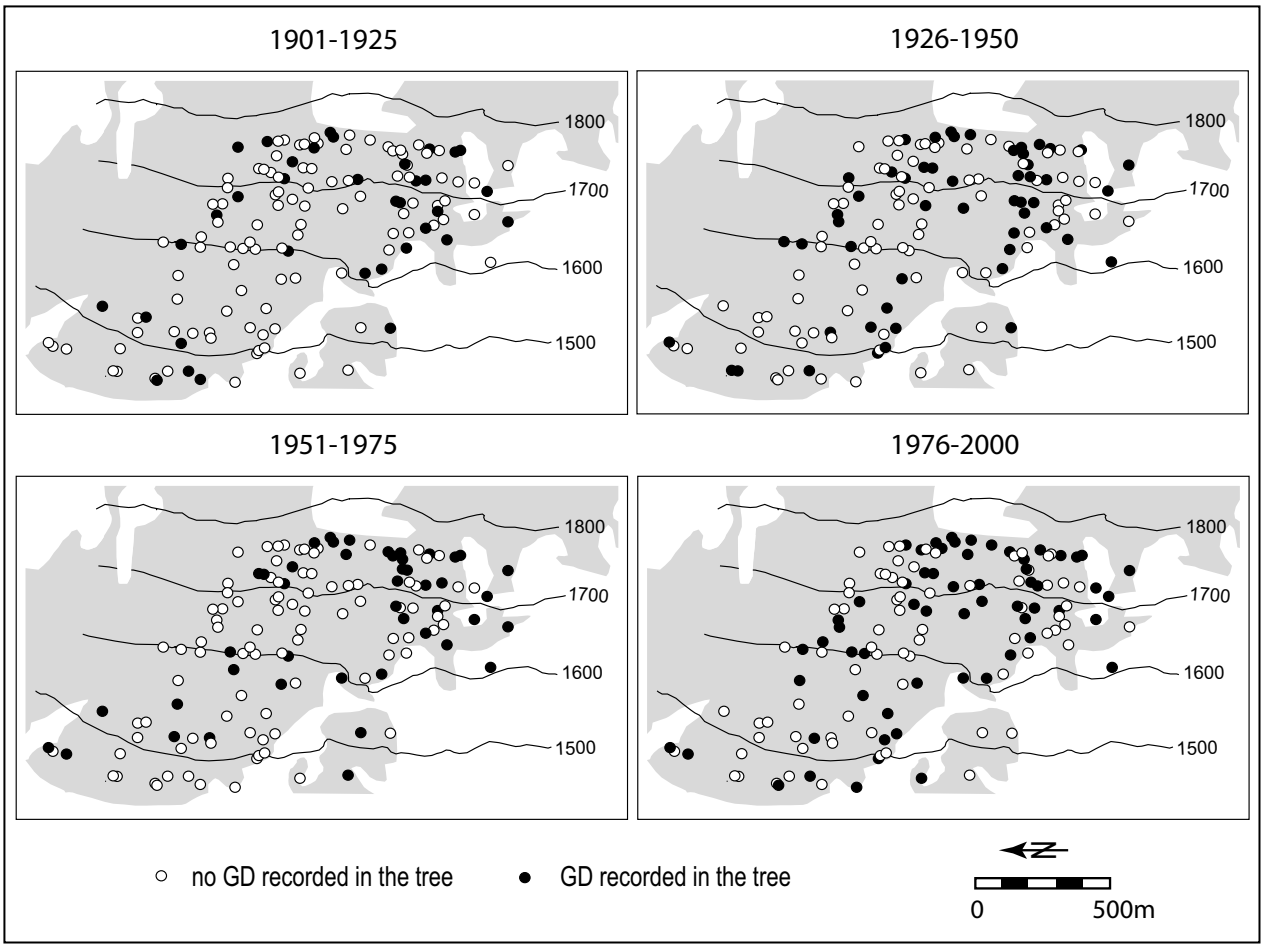

Fig. F1.7 *Spatio-temporal variations in rockfall activity derived from different growth disturbances (= GD; e.g., scars, traumatic rows of resin ducts, abrupt growth reductions, reaction wood) at Täschgufer (Swiss Alps). Data are resolved in 25-yr segments for the last century (1901-2000).*

ces in recurrence intervals across the slope, ranging from < 10 years in some areas to > 150 years in others. In general, rockfall seems to have caused more damage upslope, while the lower parts of the protection forest suffered less from the disturbances caused through falling, bouncing or rolling rocks and boulders.

1.3.4 Studies on the seasonal timing of rockfall activity

The seasonal timing of rockfall activity can be assessed by analyzing the position of scars or traumatic rows of resin ducts within individual tree rings, as illustrated in Figure F1.9A. Stoffel *et al.* (2005b) applied this approach while investigating scars and traumatic rows of resin ducts in juvenile European larch trees collected at *Täschgufer*. Figure F1.9B shows relative distributions of 'dormancy', earlywood and latewood events at *Täschgufer* between 1977 and 2001, showing that 88% of the rockfall injuries were caused before the 'vegetation period' (i.e., during 'dormancy'). Direct observations on the slope confirmed these findings, indicating that rockfall was most abundant in April and May, when the active layer of locally existing permafrost starts to thaw along with the ice formed in bedrock joints. In contrast, injuries occurring during the 'vegetation period' were scarce and less frequent during the period of earlywood (5%) than latewood formation (7%).

Following the procedures described above, Perret *et al.* (2005b) analyzed the seasonal timing of events in growth rings of Norway spruce trees on a rockfall slope in the Swiss Prealps (*Diemtigtal*, *Bernese Oberland*). Here, seasonal frost prevails and there is no permafrost. As can be seen from Figure F1.9C, scars and resin ducts most commonly occurred before the onset of the 'vegetation period' (74%) between 1950 and 2002. However, scars caused during 'dormancy' are less predominant at Diemtigtal than at Täschgufer and rockfall events during the 'vegetation period' are more frequent; with 15% of all scars found in earlywood and 11% in latewood cell layers.

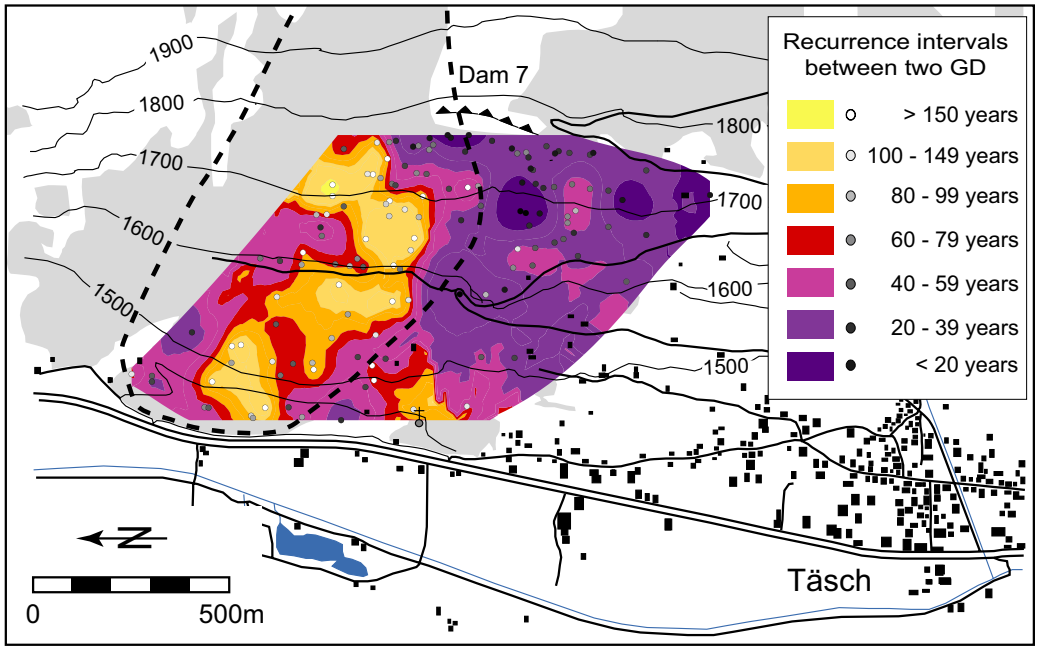

Fig. F1.8 *Interpolated recurrence intervals of rockfall at Täschgufer (Swiss Alps) covering the last four centuries. Intervals designate the number of years passing between two reconstructed growth disturbances (GD) on a single tree.*

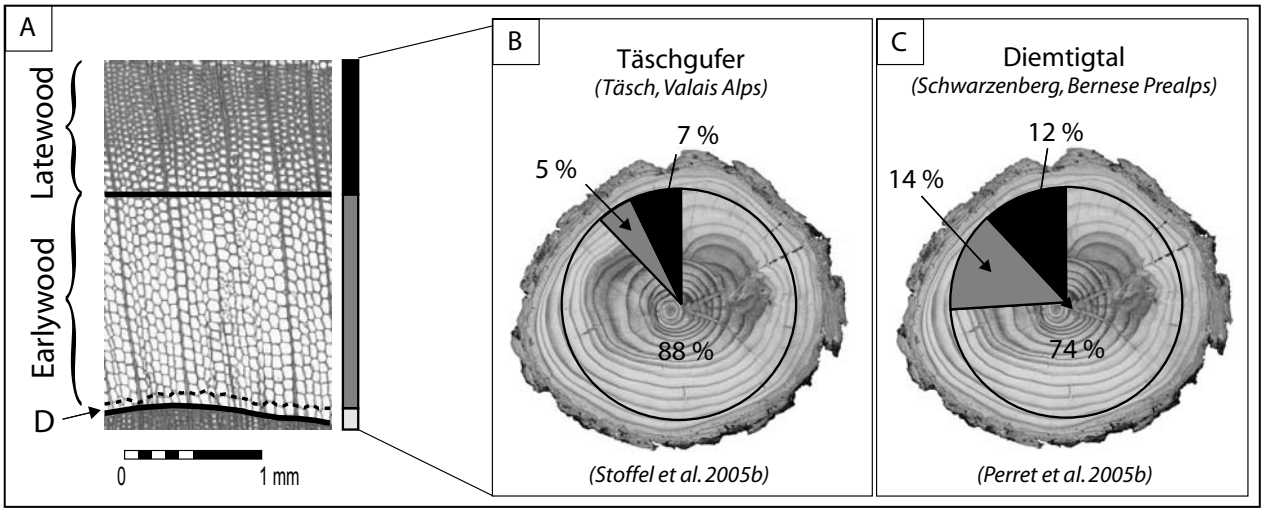

Fig. F1.9 *(a) During the period of cell growth, trees first form thin-walled earlywood cells (E) before they start to produce thick-walled latewood (L) cells. At the end of the vegetation period, cell formation ceases and dormancy (D) sets in. The seasonal timing of rockfall activity was assessed on two different slopes in Switzerland, namely on the (b) Täschgufer (Swiss Alps) and the (c) Diemtigtal (Swiss Prealps) slopes. While permafrost exists locally at Täschgufer, seasonal frost occurs during the winter months at Diemtigtal.*

1.4 Discussion and conclusions

1.4.1 Strengths and weaknesses

One of the primary strengths of dendrogeomorphology is that it can be used to supply data on rockfall activity on forested slopes where historical records are either incomplete or lacking. In such situations it can provide researchers with data on the frequencies, volumes, spatial distributions and seasonality of past rockfalls. Results from dendrogeomorphological rockfall research may be used to improve the quality of data in studies dealing with hazard or risk assessment in a number of ways:

- The seasonal timing of rockfall activity can be estimated to help in the better management of risks on hiking trails allowing them to be closed during periods of enhanced rockfall activity.

- Seasonal differentiation of events may also be integrated with analysis focusing on other features such as transportation corridors or inhabited areas.

- Engineers can be provided with information on where and how often rockfalls recurred in the past and, thus, improve the quality of the data upon which countermeasures such as rockfall dams, barriers or restraining nets are based.

- The influence of rockfall protection dams on the range and distribution of rockfall events can be determined (Stoffel *et al.* 2005c).

- Tree-ring data can be used for controlling results from rockfall modeling, as recently demonstrated on different slopes in Switzerland by Stoffel *et al.* (2005d).

- Forest managers can use dendrogeomorphological studies to define their future priorities (e.g., Kienholz & Mani 1994, Berger & Rey 2004). As Motta & Haudemand (2000) pertinently argue, appropriate management and accurate evaluation of the ecosystem integrity of protection forests not only relies on information dealing with past silvicultural treatments, but also has to consider past evidence of disturbances such as rockfall.

Although this review clearly shows that dendrogeomorphology has an enormous potential for showing yearly fluctuations, decadal ratios or spatial distribution in rockfall activity over several centuries, there are a number of weaknesses. Techniques and methods need further refinement, and sampling strategies such as the determination of sampling heights or the choice of trees have to be carefully established, as they strongly influence the quality and quantity of results (Stoffel & Perret 2005). Similarly, because trees may overgrow wounds and, thus, blur evidence of past events on the stem surface, cross-sections and increment cores should be selected randomly within the forest stand. Otherwise, there is a danger of overestimating recent and underestimating older rockfall events.

1.4.2 Future directions

In the future, tree-ring analysis will need to incorporate further promising research directions, such as the analysis of rockfalls triggered during seismic activity. The role of earthquakes on rockfall activity has so far only been investigated through lichenometric (Bull & Brandon 1998) or radiocarbon methods (Becker & Davenport 2003), but not with dendrogeomorphology. There is thus a great need to incorporate this promising aspect into tree ring and rockfall research as well. While snow avalanches, debris flows or flooding have been analyzed extensively using tree-ring sequences, studies of past rockfall activity are comparatively scarce. The great potential of dendrogeomorphology for rockfall research has been largely ignored. Thus, we should need Solomina's (2002) plea for comparative studies conducted in different regions aimed at identifying or possibly even quantifying the influence of past and current climate variations on rockfall activity.

Acknowledgements
Michel Monbaron is acknowledged for both financially and morally supporting this research. While Simone Perret and Michelle Bollschweiler made helpful comments on an earlier version of the paper, Heather Murray improved the English. Finally, I gratefully acknowledge the suggestions made by Vanessa Winchester and an anonymous reviewer.

*****

APPENDIX 2

Simone Perret [1], Markus Stoffel [2] and Hans Kienholz [1]

"Spatial and temporal rockfall activity in a forest stand in the Swiss Prealps – a dendrogeomorphological case study"

[2] *Applied Geomorphology and Natural Risks, Department of Geography, University of Berne*
[1] *Groupe de Recherches en Géomorphologie (GReG), Department of Geosciences, Geography, University of Fribourg*

accepted for publication in "Geomorphology"
revised: 5 August 2005, accepted: 5 August 2005

Abstract

Rockfall is a major threat to settlements and transportation routes in large parts of the Alps. While protective forest stands in many locations undoubtedly reduce rockfall risk, little is known about the exact frequency and spatial distribution of rockfall activity in a given place, or about how these parameters can be assessed. Therefore the objective of the present study was to reconstruct rockfall events with dendrogeomorphological methods, and to analyse the spatial and temporal rockfall activity in a subalpine forest stand lying in the transit zone of frequently passing, rather small rockfall fragments (mean diameter 10 to 20 cm). In all, 33 stem discs from previously felled *Picea abies* trees found at the foot of *Schwarzenberg* in *Diemtigtal* (Swiss Prealps) were sampled, and a total number of 301 rockfall events were dated to between 1724 and 2002 AD.

Results showed that the spatial distribution of rockfall changed slightly with time, and that rockfall activity increased considerably over the last century. In contrast, rockfall magnitude presumably remained on a comparable level. The seasonal occurrence of rockfall showed a clear peak during the dormant season of trees, most probably in early spring. Furthermore, on a 10-year moving average basis, Rockfall Rates were positively correlated with mean annual as well as summer and winter temperatures, which means that higher temperatures result in increased rockfall activity. On the other hand no correlation with annual or seasonal precipitation totals or the annual number of frost days was revealed. Overall, this study provides an appropriate method for the detailed assessment of spatial and temporal variations in rockfall activity in a given place.

Keywords: Rockfall; Protective Forest; Dendrogeomorphology; Scars; Natural Hazards; Swiss Prealps

2.1 Introduction

In large parts of the Alps and other mountainous regions rockfall is a major threat to settlements and transportation routes (Varnes 1978, Hutchinson 1988, Flageollet & Weber 1996, Hungr *et al.* 1999, Erismann & Abele 2001, Budetta 2004). As a consequence, measures have to be taken for public protection. In some cases technical measures may help to reduce rockfall risk. However, in many places protective forest stands turn out to provide the most sustainable form of protection, and even at a lower price than technical measures. For this reason the protective function of mountain forest stands has recently gained particular interest (Bebi *et al.* 2001, Berger *et al.* 2002, Dorren *et al.* 2004a). Although the general protective effect of mountain forests against rockfall is not questioned nowadays (Brang *et al.* 2001, Berger & Rey 2004), much is still unknown about the assessment of rockfall frequency and distribution in a given place, as well as about the ideal properties of a protective forest stand (Stoffel *et al.* 2005d). Therefore, a better understanding of major processes in mountain forests is needed (Kienholz 1995, Kräuchi *et al.* 2000, Naylor *et al.* 2002).

So far several studies have assessed the interaction between rockfall and forest on a local scale, but not on the scale of individual trees (Jahn 1988, Zinggeler *et al.* 1991, Mani & Kläy 1992, Frehner *et al.* 2005, Dorren *et al.* 2004b, Perret *et al.* 2004b). Furthermore, research has mainly focused on short-term observations of contemporary rockfall activity in the field (Luckman 1976, Douglas 1980, Gardner 1983, Matsuoka & Sakai 1999). On the other hand, dendrogeomorphological studies have primarily concentrated on the analysis of mass movements such as landslides (e.g. Braam *et al.* 1987, Lateltin *et al.* 1997, Fantucci & Sorriso-Valvo 1999, Oswald 2003, Stefanini 2004), while rockfall processes have only rarely been investigated using tree-ring analysis (Stoffel 2005a). Nonetheless, as recently shown by Stoffel *et al.* (2005c) for a protective forest in the southern Swiss Alps, dendrogeomorphological methods have the potential to yield data on past rockfall activity on a very detailed spatial scale, as well as over a considerably long time period. However, similar studies for other parts of the Swiss Alps are so far lacking.

The objective of the present study therefore was (i) to reconstruct rockfall events with dendrogeomorphological methods, (ii) to analyse the spatial distribution of rockfall as well as (iii) to assess the temporal rockfall activity in a subalpine forest stand in the Swiss Prealps. The investigated stand is situated at the foot of a high cliff in the transit zone of frequently passing, rather small rockfall fragments (mean diameter 10 to 20 cm). Spatial analyses were performed by interpolating the number of rockfall injuries per tree, whereas temporal analyses comprised the calculation of rockfall rates, trends in rockfall activity and their correlations with mean annual or seasonal temperatures, precipitation totals as well as number of frost days.

2.2 Material and methods

2.2.1 Study site and sampling

The study presented was performed at the site of *Schwarzenberg*, which is located in *Diemtigtal* (*Bernese Oberland*, 7°33'E, 46°36'N, 1250 m a.s.l.) in the Swiss Prealps. *Schwarzenberg* is an approximately 400 m high Triassic limestone cliff, at the foot of which a deep, south-east exposed talus slope with a slope angle of about 40° is found (see Fig. F2.1). This talus slope with a relatively homogenous, stony surface is forested with a *Picea abies* (L.) Karst stand (*Polygalo chamaebuxi Piceetum*) that also contains *Sorbus aria* (L.) Crantz, *Sorbus aucuparia* L. and *Acer pseudoplatanus* L. According to Ott *et al.* (1997) this forest type is usually met in montane to subalpine environments in the northern limestone Alps on dry, alkaline, steep and south facing sites.

The study site, covering an area of 0.3 ha, is located in the uppermost part of the talus slope, in the transit zone of frequent rockfall fragments, which only have a mean diameter of about 10 to 20 cm. Investigations on the site started in 2001 with a detailed field inventory and analysis of rockfall injuries visible on stem surfaces (Perret *et al.* 2005a). Within this study, analysis of 157 trees allowed identification of 1704 rockfall injuries.

Due to a severe bark beetle outbreak succeeding the storm Lothar (Wsl & Buwal 2001), a major deforestation was undertaken at the foot of *Schwarzenberg* in autumn 2002. As a result, 33 of the previously studied *Picea abies* trees in the lower part of the investigated area (see Fig. F2.1) were felled during the deforestation campaign. From each of the 33 *Picea abies* tree stumps, which remained in the field, one stem disc (cross-section) was sampled at a mean height of 30 cm above ground (upslope side of the trunk), independently of the presence or absence of scars visible on the stem surface. Diameters of the single stem discs ranged from 9 to 55 cm, with a mean diameter of 34 cm. Thereafter, the 33 samples were sanded in the

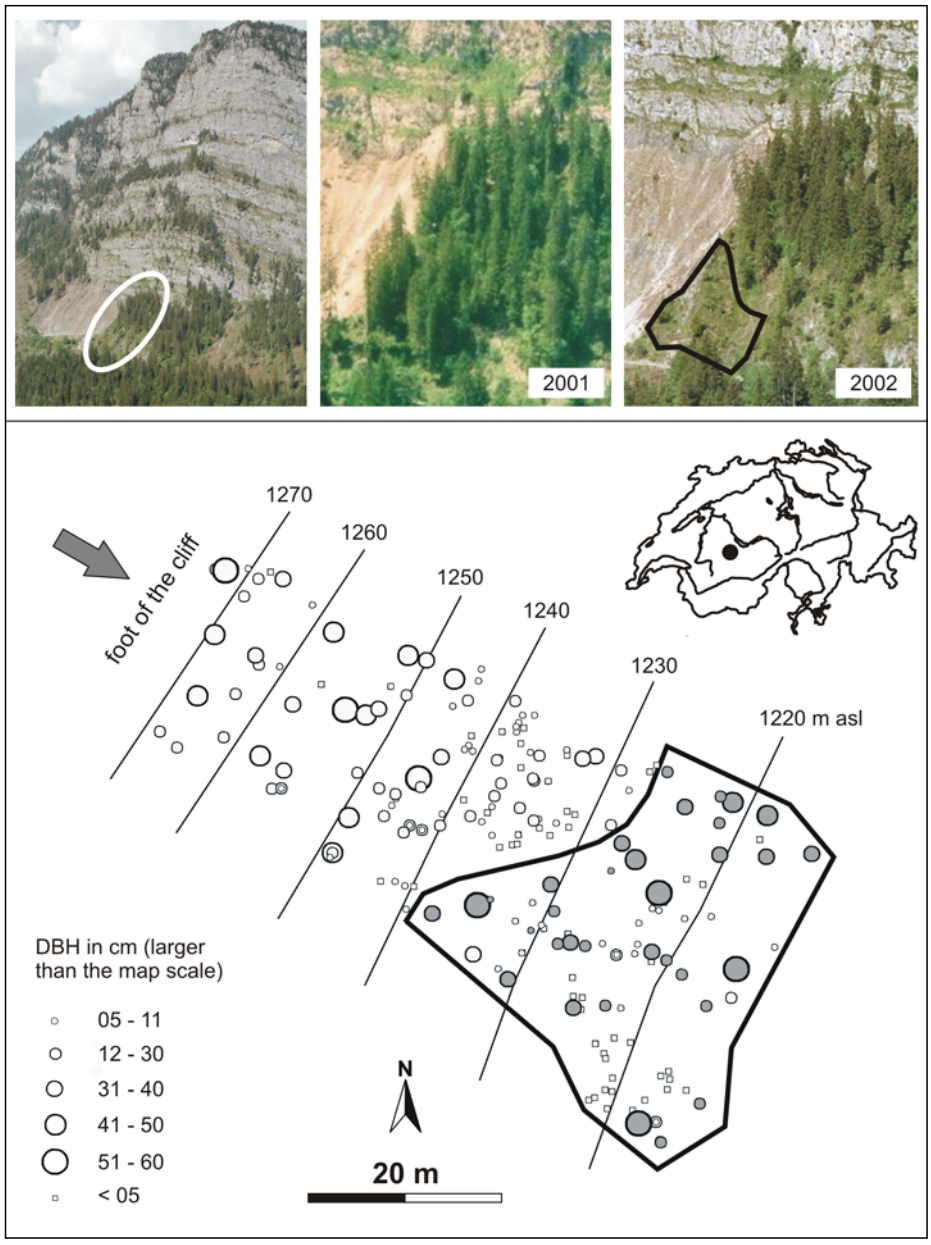

Fig F2.1 *Study site at Schwarzenberg in Diemtigtal (Bernese Oberland, Swiss Prealps, 7°33'E, 46°36'N) before (2001) and after (2002) deforestation. The map shows the location of the study site in Switzerland (right corner) and the tree distribution in the investigated stand. Stem discs from the Picea abies trees marked in grey (within the black perimeter) were samples for dendrogeomorphological analysis. The grey arrow indicates the main fall direction of rocks.*

laboratory so as to allow the dendrogeomorphological analyses described below.

2.2.2 Recording past rockfall events

Depending on their size, velocity and energy, falling, rolling or bouncing rock fragments can injure trees by breaking, tilting or scarring stems. As a reaction to a rock impact, *Picea abies* trees may produce reaction wood, traumatic rows of resin ducts or callous tissue. Because these signs remain visible in tree-ring sequences (Bräuning 1995, Schweingruber 1996, 2001), they can be analysed and dated with dendrogeomorphological methods, so as to reconstruct rockfall frequency in a given area.

Consequently, sampled stem discs were processed in a first step as proposed by Bräker (2002) and Wiles *et al.* (1996). Ring widths were measured, growth curves crossdated in order to correct the age of the samples where applicable, and tree rings were then dated. Ring width measurements were performed with a digital LINTAB positioning table connected to a Leica stereomicroscope and to TSAP 3.0 software (Time Series Analysis and Presentation by Rinntech 2005). In a second step, samples were visually inspected to identify evidence of past rockfall events, allowing reconstruction of spatial and temporal rockfall patterns in the investigation area. Reconstructions included the recording of scars visible on the stem disc, as well as traumatic rows of resin ducts belon-

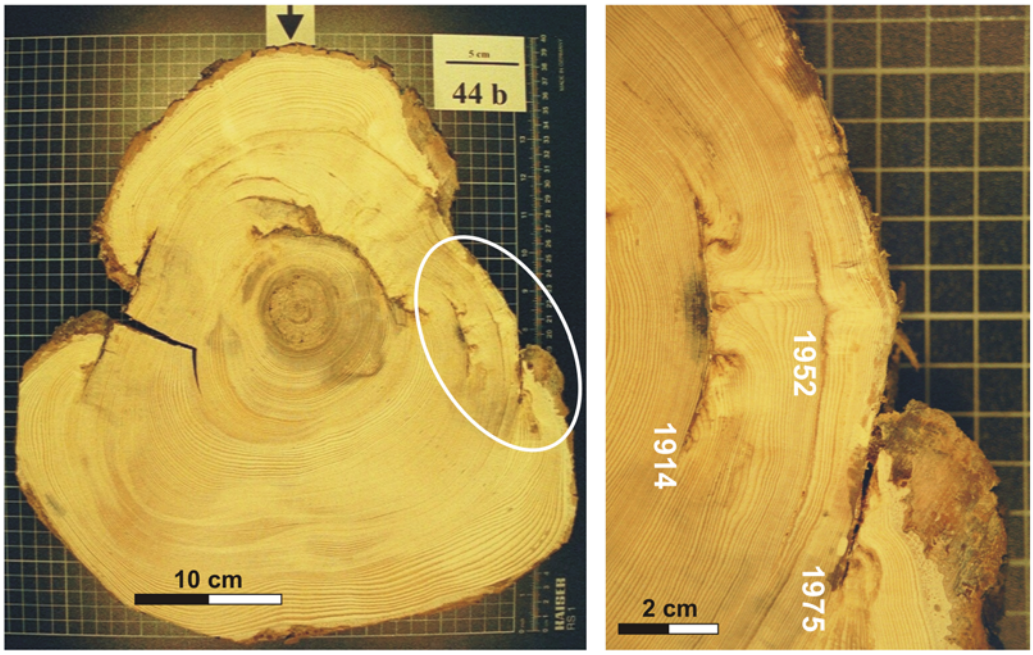

Fig. F2.2. *Example of a Picea abies stem disc sampled at Schwarzenberg with several rockfall injuries (5 scars and 10 traumatic rows of resin ducts). Sampling height 18 cm, disc diameter 37 cm, pith 1762 AD, death 2002 AD, age 240 years. The black arrow indicates the upslope side of the trunk. The second picture shows a detail from the disc with three scars.*

ging to injuries located elsewhere in the stem. Figure F2.2 shows an example of a sampled stem disc with several rockfall injuries. All scars and traumatic rows of resin ducts were dated with yearly precision. For the scars the seasonal timing of the rockfall event was also determined, following the procedure described by Stoffel *et al.* (2005b). Furthermore, descriptive parameters such as injury width, presence of injured wood and stage of healing were registered for the scars.

2.2.3 Spatial and temporal data analysis

As soon as rockfall events were reconstructed, data were analysed with respect to their spatial and temporal distribution between 1881 and 2000 AD. In order to illustrate spatial patterns of rockfall activity, the number of injuries per tree was interpolated within *ArcView GIS 3.2* (Esri 2005a). Tree coordinates were available from a previous study (Perret *et al.* 2005a) and could be linked with the number of reconstructed injuries per tree. By performing linear interpolations with 10 neighbouring trees and using a grid size of 1 m^2, the spatial distribution of injuries was visualised. Prior to the deforestation on the study site, a similar interpolation was performed based on field inventory data, showing the number of injuries per square meter visible on the stem surface of all living trees (Perret *et al.* 2005a). Therefore it was possible to compare data obtained from tree-ring analysis with data from the field inventory. Varying spatial patterns of rockfall activity over time were furthermore shown by dividing data from tree-ring analysis (1881 to 2000 AD) into four time sequences of 30 years each.

For further exploration of temporal rockfall activity, the annual Rockfall Rate was calculated following Stoffel *et al.* (2005c). This Rockfall Rate represents the number of rockfall injuries per meter tree diameter exposed to rockfall. To determine whether annual Rockfall Rates significantly changed over the last century, they were also tested with the Mann-Kendall trend test (two-tailed Z test, significance level 0.01).

This trend test was also applied in the analysis of temperatures, precipitation and frost days from nearby climate stations. From mean monthly temperatures

Table F2.1. *Age of trees at sampling height (about 30 cm above ground level)*

	Pith age (years)	Pith age (AD)
Mean	180	
Minimum	118	1884
Maximum	278	1724

Table F2.2. *Number of reconstructed rockfall events*

Number of…	**1724-2002 AD**	**1881-2000 AD**
Scars	87	75
Mean per stem disc	2 - 3	
Minimum / Maximum per stem disc	0 / 9	
Discs without scars	4	
Traumatic rows of resin ducts	214	175
Mean per stem disc	6 / 7	
Minimum / Maximum per stem disc	1 / 20	
Discs without traumatic rows of resin ducts	0	
Dated rockfall events	301	250

for the period 1901 to 2000 AD at *Château d'Oex* (46°29'N / 07°09'E, 985 m a.s.l.; MeteoSwiss 2005), which was the closest climate station with a sufficiently long series of temperature measurements, mean annual as well as summer (April to September) and winter (October to March) temperatures were calculated. Moreover, for the same period monthly precipitation totals from *Boltigen*, *Erlenbach i.S.* and *Frutigen* (=BEF; MeteoSwiss 2005) were used to derive annual as well as summer and winter precipitation totals.

Within this study, BEF represents the averaged precipitation totals recorded at the meteorological stations of *Boltigen* (46°37'N / 07°23'E, 855 m a.s.l.), *Erlenbach i.S.* (46°40'N / 07°33'E, 683 m a.s.l.) and *Frutigen* (46°35'N / 07°39'E, 815 m a.s.l.), which lie in a triangle around *Schwarzenberg* (see Fig. F2.6). Finally, the annual number of frost days was calculated from daily minimum and maximum temperatures from *Adelboden* (46°30'N / 07°33'E, 1320 m a.s.l.), which were only available since 1967. *Adelboden* was chosen because it has the closest climate station lying at an altitude similar to the one of *Schwarzenberg* (essential for frost days).

In a second step, as proposed by Oswald (2003) in his analysis of variations in nearby landslide activity, the 10-year moving average for the annual Rockfall Rate as well as for mean annual and seasonal temperatures, precipitation totals and number of frost days was calculated. Thereafter, correlations (Pearson correlation coefficient) between the averaged Rockfall Rate and averaged temperatures and precipitations respectively were calculated and tested with a two-tailed t-test at a significance level of 0.01.

2.3 Results

2.3.1 Characteristics of trees and their rockfall injuries

As given in Table F2.1, the 33 *Picea abies* trees had a mean age of 180 years at sampling height (about 30 cm above ground level). The youngest tree reached this height in 1884 AD, i.e. 118 years before sampling, and the oldest one in 1724 AD, i.e. 278 years prior to sampling. Thus, starting in 1884 AD, all trees sampled were available for analysis over more than one century. Crossdating of the samples showed that only four trees died shortly before sampling in 2002 AD. The oldest evidence of past rockfall activity was recorded in 1767 through the presence of a traumatic row of resin ducts, whereas the oldest scar was dated to 1850. Table F2.2 provides the total and mean number of scars and traumatic rows of resin ducts. Overall, 301 rockfall events were reconstructed, and many more traumatic rows of resin ducts (214) than scars (87) were identified. In 1994 nine injuries were registered, which is the highest number of events found in one single year, followed by eight injuries in 1970, 1975 and 1988.

The mean size (width on the stem disc) of scars amounted to 3.8 cm (minimum 0.2 cm, maximum 14 cm). In 26% of all scars, rock impacts had not only injured bark und the underlying cambium, but previously formed wood as well. Interestingly, most scars (87%) identified on the cross-sections were already totally overgrown at the time of sampling. While some of these overgrown scars were still visible on the stem surface, 63% of all scars were no longer visible from

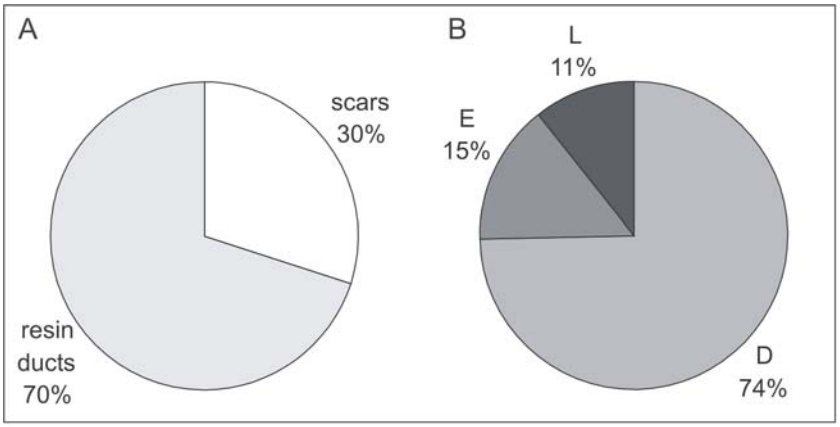

Fig. F2.3. *(A) Percentage of scars and traumatic rows of resin ducts registered in the 33 stem discs between 1881 and 2000; (B) Seasonal distribution of scars (D = Dormancy, E = Earlywood, L = Latewood).*

outside. Thus, all these hidden scars would have been missed if only injuries visible on the stem surface had been assessed. Further data on injury healing and visibility of scars are presented in Stoffel & Perret (2005).

For reasons of sample depth, only those rockfall events occurring between 1881 and 2000 AD were used for spatial and temporal analysis. Consequently, as indicated in Table F2.2, the number of scars (75) and traumatic rows of resin ducts (175) was reduced. The proportion of scars (30%) and traumatic rows of resin ducts (70%) for this time period is given in Figure F2.3A. Figure F2.3B, furthermore, shows the seasonal distribution of the scars registered between 1881 and 2000 AD. Obviously, most scars (74%) were caused during the dormant season (D) of trees, approximately lasting from October to May. In contrast, 15% of scars emerged during earlywood growth (E) and only 11% during latewood growth (L).

2.3.2 Spatial rockfall distribution for different time periods

Figure F2.4A gives the results of the spatial interpolation of rockfall injuries registered on the stem discs (i.e. data from tree-ring analysis) on the one hand, and the injuries recorded on the stem surfaces (i.e. data from field inventory) on the other. Trees included in analysis are marked in grey. Overall, results suggest that with the field inventory a slightly larger number of injuries was registered than with tree-ring analysis. Moreover, the spatial pattern of data gained from tree-ring analysis appears to be quite different from – in fact, just the opposite of – field inventory data. In tree-ring data most injuries were located on trees in the northern part of the investigated perimeter, whereas field inventory data showed the largest number of injuries in the southern part.

In Figure F2.4B a time series ranging from 1881 to 2000 AD, showing the spatial distribution of rockfall injuries as reconstructed with tree-ring analysis, is provided. Every map represents 30 years of rockfall activity and gives the interpolated number of injuries per square meter. The first map covers the time period from 1881 to 1910, when only very few injuries (about 0–1 injury per square meter) occurred in the whole area. The second map shows the distribution of injuries caused between 1911 and 1940. In this period, slightly more injuries were identified, i.e. predominantly 1–2 injuries per square meter. Similarly to the first time sequence, injuries are rather evenly distributed. In the third time sequence ranging from 1941 to 1970, a distinct increase in the number of injuries can be observed: the predominating number of injuries rose to 2–4, again quite evenly distributed over the area. The last map covers the time period from 1971 to 2000 and shows a clear increase in the number of injuries up to a maximum of 6–8 injuries per square meter. This time, however, the spatial distribution of injuries is no longer homogeneous, with most injuries occurring in the northern part of the investigated perimeter. As a consequence, rockfall activity over the last 30 years appears to have played a major role in the pattern gained from tree-ring analysis (1881 – 2000 AD) as shown in Figure F2.4A. Overall, the time series presented also suggests a distinct increase in rockfall activity over the last century.

2.3.3 Temporal rockfall activity and its correlation with climate parameters

The apparent increase in rockfall activity was further explored by calculating annual Rockfall Rates between 1881 and 2000, represented by the histogram in Figure F2.5. As can be seen, the Rockfall Rate (number of rockfall injuries per meter exposed tree diameter) steadily increased over the 20th century. Simultaneously, the number of years without any rock-

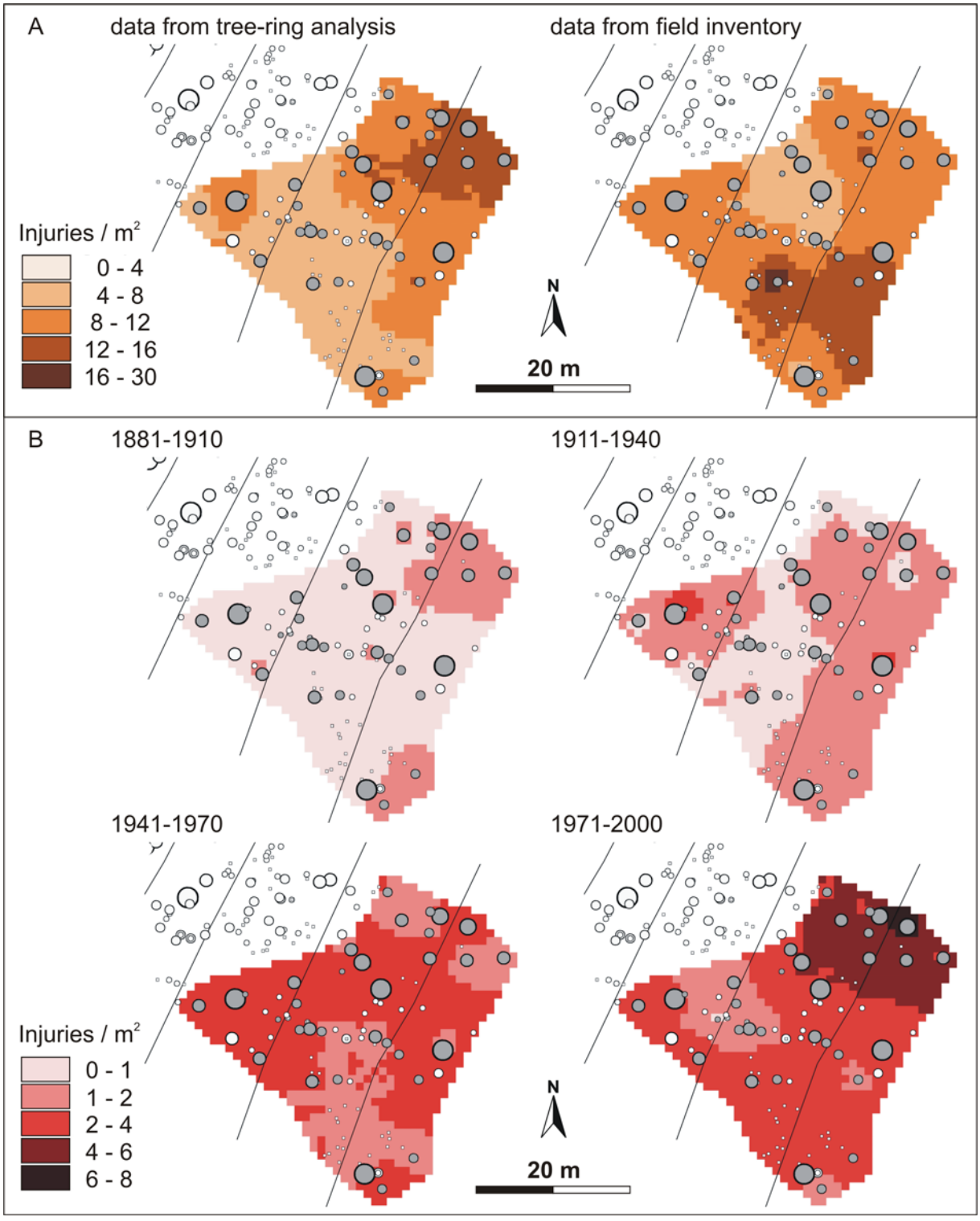

Fig. F2.4. *Reconstructed spatial rockfall distribution in the investigated perimeter (cf Fig. F2.1). Maps show the interpolated (linear, with 10 neighbouring trees) number of injuries per square meter. (A) data from tree-ring analysis versus data from field inventory; (B) four time sequences covering 30 years each.*

fall event became less frequent. Apart from 1986, at least one rockfall event was registered for every year since 1952. The highest Rockfall Rate was calculated for 1970.

To further underline the increase of rockfall events, the 10-year moving average of the annual Rockfall Rate, showing a clear positive trend, is provided in Figure F2.5 (line chart). In order to verify this trend,

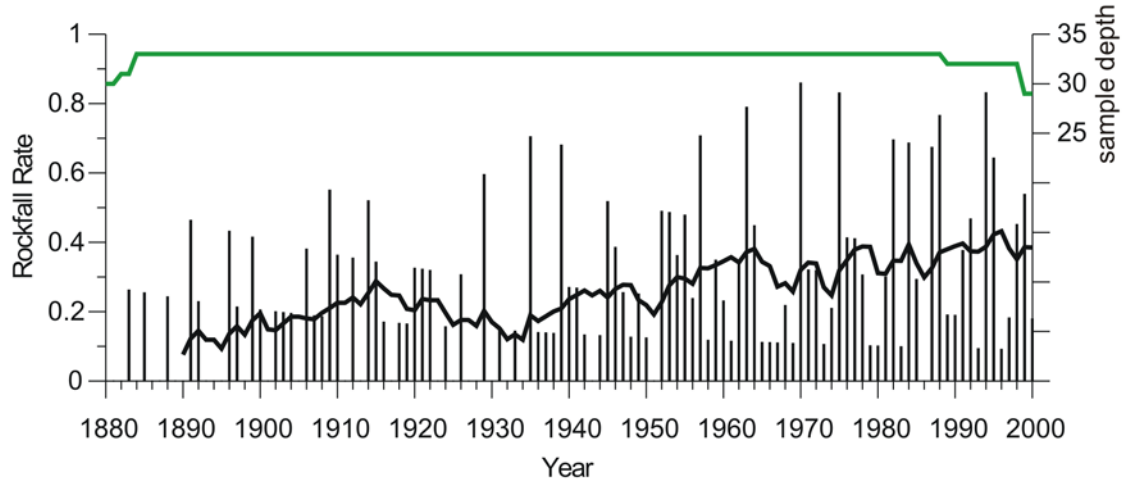

Fig. F2.5. *Annual Rockfall Rate (number of injuries per 1 m exposed tree diameter) and its 10-year moving average, as well as sample depth.*

the annual Rockfall Rate was tested with the Mann-Kendall trend test, and in fact, as can be seen in Table F2.3, it shows a statistically highly significant, positive trend (p=0.005). Table F2.3 further illustrates the fact that mean annual as well as summer and winter temperatures at *Château d'Oex* show a highly significant, positive trend between 1910 and 2000 as well. In contrast, precipitation totals for BEF (= mean of *Boltigen*, *Erlenbach*, *Frutigen*; for details see section F2.2.3), as well as the number of frost days per year for *Adelboden* (1967 to 2000) apparently have no significant trends at all.

As shown in Figure F2.6, based on 10-year moving averages, the evolution of the Rockfall Rate was compared with that of mean temperatures, precipitation totals and number of frost days per year. The calculated correlation coefficients between the 10-year moving averages of the Rockfall Rate and the climate parameters mentioned are provided in Table F2.4. Data clearly revealed that mean annual as well as summer and winter temperatures are positively correlated with the Rockfall Rate at a high level of statistical significance (p=0.000 for all correlations). Thus high temperatures are connected with a high Rockfall Rate, whereas low temperatures result in decreased rockfall

Table F2.3. *Mann-Kendall trend test (two-tailed Z test, significance level 0.01) for (1) Rockfall Rate at Schwarzenberg, (2) temperature at Château d'Oex and (3) precipitation at BEF between 1901 and 2000 AD (BEF = mean of Boltigen, Erlenbach, Frutigen; for details on locations see methods and Figure 6), as well as for (4) number of frost days at Adelboden between 1967 and 2000 AD.*

Mann-Kendall trend test for…		Z=	p=	Trend
(1)	Annual Rockfall Rate, Schwarzenberg	2.807	0.005	Significant, positive
(2)	Mean annual temperature, Château d'Oex	6.966	0	Significant, positive
	Mean summer temperature (April-Sept)	5.527	0	Significant, positive
	Mean winter temperature (Oct-March)	5.436	0	Significant, positive
(3)	Total annual precipitation, BEF	0.748	0.455	Not significant
	Total summer precipitation (April-Sept)	0.372	0.71	Not significant
	Total winter precipitation (Oct-March)	0.732	0.464	Not significant
(4)	Total annual number of frost days, Adelboden	0.222	0.824	Not significant

Table F2.4. *Correlation between Rockfall Rate at Schwarzenberg and (1) temperature at Château d'Oex, as well as (2) precipitation at BEF between 1910 and 2000 AD (BEF = mean of Boltigen, Erlenbach, Frutigen; for details on locations see methods and Figure 6), and (3) number of frost days at Adelboden between 1976 and 2000. r is the Pearson correlation coefficient, tested with a two-tailed t-test at a significance level of 0.01.*

	Correlation between 10-year moving average (av) Rockfall Rate and…	r=	p=	Trend
(1)	10-year moving av temperature, Château d'Oex	0.650	0.000	Significant, positive
	10-year moving av summer temperature (April-Sept)	0.558	0.000	Significant, positive
	10-year moving av winter temperature (Oct-March)	0.655	0.000	Significant, positive
(2)	10-year moving av precipitation, BEF	0.176	0.095	Not significant
	10-year moving av summer precipitation (April-Sept)	0.235	0.025	Not significant
	10-year moving av winter precipitation (Oct-March)	-0.005	0.965	Not significant
(3)	10-year moving av number of frost days, Adelboden	0.048	0.818	Not significant

activity. On the other hand, neither precipitation nor frost days showed a significant correlation with the Rockfall Rate.

2.4 Discussion

The objective of the study presented was to reconstruct rockfall events with dendrogeomorphological methods and to analyse the spatial and temporal rockfall activity in a subalpine forest stand, exposed to frequent but small rockfall events (mean rock diameter 10 to 20 cm). Therefore 33 stem discs from *Picea abies* trees were sampled at the foot of *Schwarzenberg* in *Diemtigtal* (Swiss Prealps), and a total number of 301 rockfall events were dated starting from 1724 AD. For reasons of sample depth, spatial and temporal analyses were limited to the period 1881 to 2000 AD, reducing the number of dated rockfall events to 250. About one third of past rockfall events were dated with scars visible at sampling height and two thirds through the presence of traumatic rows of resin ducts belonging to scars located elsewhere on the stem.

The seasonal occurrence of rockfall activity on the slope shows a clear peak during the dormant season of trees. Due to field observations, it is assumed that most rockfall occurs in early spring, just before the growing season starts locally with the formation of earlywood cells in the *Picea abies* trees. These results from *Schwarzenberg* are in agreement with results published by Stoffel *et al.* (2005b) for a study site in the southern Swiss Alps, which yielded a clear peak of rockfall activity in dormancy as well. However, due to the lower altitude of the study site at *Schwarzenberg* as well as the absence of permafrost, the peak during dormancy is less pronounced here. On the basis of reconstructed rockfall events and field observations, we believe that a maximum in rockfall activity from the 400 m high rock cliff at *Schwarzenberg*, similarly to the site investigated by Matsuoka & Sakai (1999) in the *Japanese Alps*, occurs right after the meltout of the rock cliff in early spring.

The comparison of spatial rockfall distribution derived from tree-ring analysis with that from field inventory data yielded quite different patterns. While dendrogeomorphological data indicated enhanced rockfall activity in the northern part of the investigated area, field inventory data showed more activity in the southern part. For the southern sector, this discrepancy is slightly reduced when, for field inventory data, only those injuries located within the first 60 cm above ground are taken into account. This restriction gives preference to those injuries identified close to the mean sampling height of stem discs at about 30 cm. Nonetheless, considerable differences between data from tree-ring analysis and data from field inventory still persist in the northern part of the investigated area. We believe that these differences most probably resulted from the presence of several hidden injuries, which were no longer visible on stem surfaces but could be reconstructed on cross-sections. As 63% of all scars identified on stem discs could no longer be seen on the stem surface, this scenario appears to be quite realistic. Furthermore, as previously proposed by Perret *et al.* (2005a), it is possible that some of the injuries registered in the field might have been caused by more than one rock impact, but were classified as only one scar. In the case of overgrown wounds, it

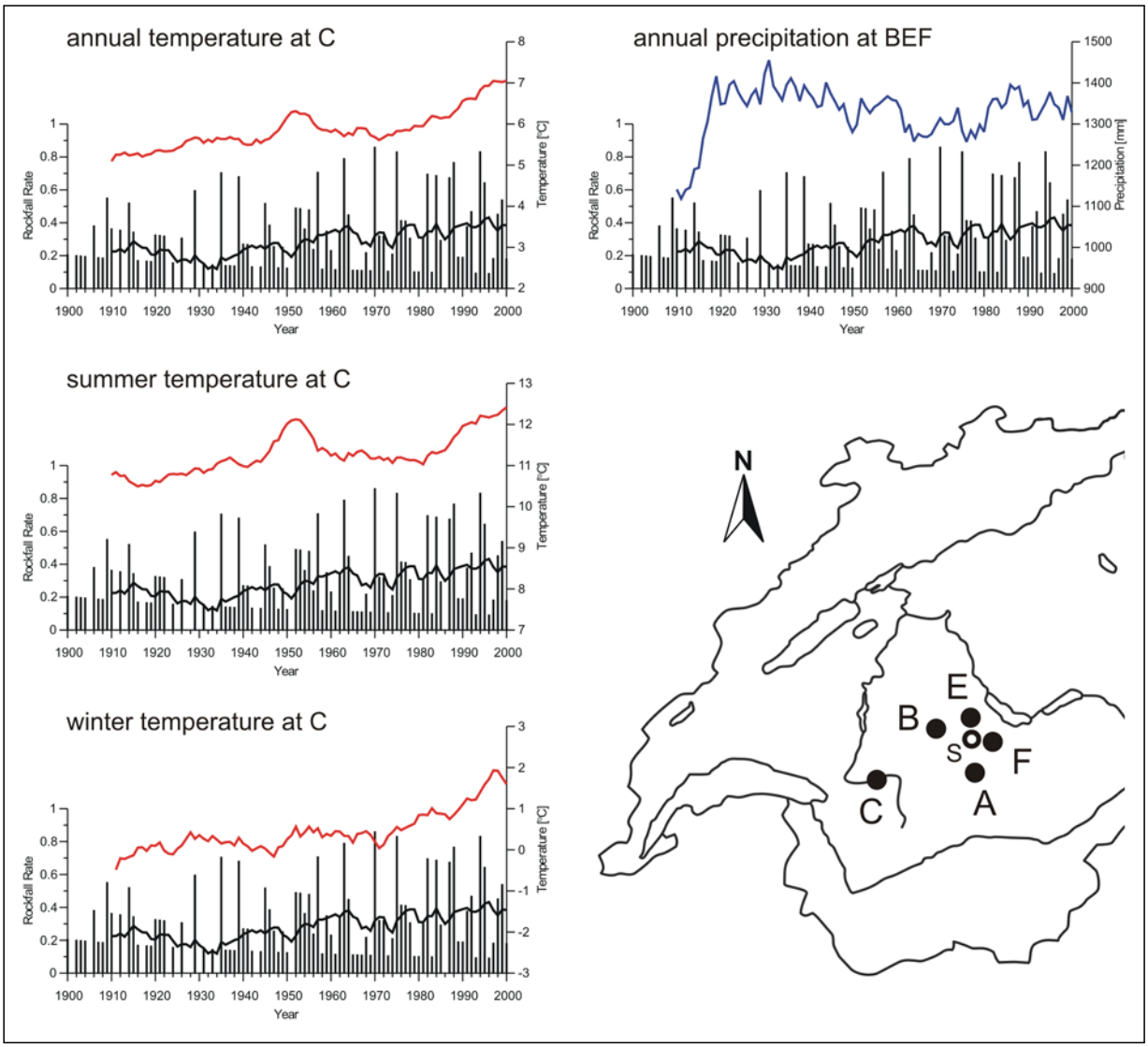

Fig. F2.6. *Correlation between the 10-year moving averages of the Rockfall Rate at Schwarzenberg (=S in the map of Switzerland) and the annual as well as summer and winter temperatures of Château d'Oex (C), and the annual precipitation of BEF from 1900 to 2000 (B=Boltigen, E=Erlenbach i.S., F=Frutigen; A=Adelboden), used for frost day calculation; for details see section 2.2.3 and Fig. F2.1).*

is especially difficult to distinguish between different scars at the same location.

Furthermore, analysis of spatial rockfall patterns for different time periods indicated a clear increase in rockfall activity over the last century and revealed that the reconstructed peak in rockfall activity for the northern part of the investigated area was predominantly caused between 1971 and 2000 AD. Nonetheless, several of these rather recent scars could obviously no longer be identified on the stem surface. Therefore we suppose that the relatively small rockfall fragments occurring during the usual low magnitude but high frequency events would tend to cause quite small scars, which would completely heal over within only a few years. These results lead us to believe that field inventory data focusing on scars visible on the stem surface of trees (e.g. Jahn 1988, Dorren *et al.* 2004a, Perret *et al.* 2005a) probably give a reasonable idea of current rockfall activity or signs of unusually large events in the past. At the same time, however, such field inventories run the risk of neglecting long-term variations in spatial rockfall activity.

Similarly to results obtained from spatial analysis, data from temporal analysis clearly showed a positive trend in the calculated Rockfall Rate, indicating that rockfall activity significantly increased over the 20th century. Data further showed a steady increase in the number of rockfall events per year since the 1950s,

whereas years without rockfall events simultaneously decreased. Thus, at the end of the 20th century a rather high rockfall frequency with usually several events per year can be observed. In contrast, on the basis of the size of the investigated rockfall injuries and fresh rockfall fragments deposited on the slope, we must assume that the magnitude of rockfall has remained unchanged at a rather low level.

Results furthermore showed that at the same time as rockfall frequency increased, the mean annual as well as summer and winter temperatures in the investigated area rose as well. Explanations for the positive trend in temperatures are for example given in OcCC (2003) and will not be further discussed here. The highly significant positive correlation, based on 10-year moving averages, which emerged between the annual Rockfall Rate and mean annual as well as summer and winter temperatures clearly indicates that rockfall from the *Schwarzenberg* rock cliff tends to be triggered by higher temperatures. Consequently, in line with findings of Matsuoka & Sakai (1999), temperature presumably plays a predominant role at *Schwarzenberg*. In this sense, increased winter temperatures might for example favour the occurrence of frequent freeze-thaw cycles in the rock cliff, and thus facilitate weathering and the production of rockfall fragments (Raetzo-Brülhart 1997), although the comparison of Rockfall Rate and number of frost days on a 10-year moving average basis did not reveal a correlation.

Neither did, analysis detect any significant correlation between the Rockfall Rate and precipitation totals. In contrast to common assumptions, higher precipitation totals apparently did not result in more rockfall events at *Schwarzenberg*. However, it is clear that single thunderstorms, which might well trigger rockfall (Raetzo-Brülhart 1997), are poorly represented by precipitation totals. On the other hand, results obtained at Schwarzenberg are in agreement with data gathered by Matsuoka & Sakai (1999), who could not identify correlations between rockfall activity and precipitation either.

Besides climatic parameters there are many other – especially short-term – influencing factors that might drive or inhibit rockfall activity on a local scale. As a consequence, despite the reasonably good correlation between temperature and Rockfall Rate based on 10-year moving averages, it still remains quite difficult to identify clear connections between the reconstructed rockfall activity at *Schwarzenberg* and the extraordinarily warm seasons observed in Switzerland for single years (Pfister 1999). On a yearly basis, both the method chosen for analysis (i.e. dendrogeomorphology) as well as the large number of interacting factors that influence rockfall triggering on a local scale would still preclude analysis of rockfall – climate interactions in greater detail.

Like Stoffel *et al.* (2005c), we finally believe that the calculated Rockfall Rate is a valuable indicator for assessing past rockfall activity, as it takes account of the tree diameter exposed to rockfall fragments as well as its gradual change with time. However, as rockfall usually consists of single falling, bouncing or rolling rock fragments, a single event may only affect trees along its trajectory. In addition, some rocks do not hit any tree at all, whereas others might impact several trees on their way down the slope. Furthermore, we have to assume that in the stem discs sampled at about 30 cm above ground, injuries located very high on the stem, as well as rather small scars were not detected through the analysis of traumatic rows of resin ducts. The question of how far away from the location of an impact traumatic rows of resin ducts can be detected therefore remains. Nevertheless, despite all these influencing factors, the Rockfall Rate may provide a realistic approximation of how rockfall activity in a given place varied over time.

2.5 Conclusion

The results of this study clearly showed that in the investigated forest stand at the foot of a rock cliff in the Swiss Prealps, the spatial rockfall distribution changed slightly over the last decades and that rockfall activity increased considerably over the last century, whereas rockfall magnitude presumably remained on a comparably low level. The seasonal timing of rockfall activity indicated a clear peak during the dormant season of trees, most probably in early spring. Furthermore, based on 10-year moving averages, a highly significant positive correlation between mean temperatures and the Rockfall Rate at *Schwarzenberg* was identified, meaning that higher temperatures result in increased rockfall activity. On the other hand, no correlation with precipitation totals and the number of frost days was revealed.

Overall, this study provided an appropriate method for the assessment of spatial and temporal variations in rockfall activity in a given place. Results also showed that dendrogeomorphological analyses clearly have the potential to produce detailed and sound results on annual or decadal fluctuations of rockfall activity over a long time period, as well as on varying spatial rockfall patterns. Altogether, this study has taken a step in

the direction of a better understanding of rockfall processes on forested slopes. However, conclusions concerning the protective effect of an ideal forest stand remain, so far, rather limited. Further case studies as well as experimental tests on other sites are needed, so as to improve and refine methods used within this study as well as the overall understanding of rockfall – forest interactions.

Acknowledgement The authors would like to thank the Swiss Federal Office for Education and Science for funding the European scientific project *ROCK-FOR – Rockfall and Forest Interrelation* (QLK5-CT-2000-01302). MeteoSwiss is gratefully acknowledged for providing the climate data. Special thanks go to Franz Baumgartner for his professional help with the sampling of stem discs, as well as to Marc Baumgartner, Michelle Bollschweiler and Bernhard Wehren for their great support in the field, lab and office.

*****

Appendix 3

Markus Stoffel [1], André Wehrli [2], Roderick Kühne [3], Luuk K. A. Dorren [4], Simone Perret [3] and Hans Kienholz [3]

"Quantifying the protective effect of mountain forests using a 3D simulation model"

[1] *Groupe de Recherches en Géomorphologie (GReG), Department of Geosciences, Geography, University of Fribourg (Switzerland)*
[2] *Silvicultural Strategies, Swiss Federal Research Institute WSL, Birmensdorf (Switzerland)*
[3] *Applied Geomorphology and Natural Risks, Department of Geography, University of Berne (Switzerland)*
[4] *Cemagref Grenoble, Saint Martin d'Hères Cedex (France)*

accepted for publication in „Forest Ecology and Management"
revision still pending

Abstract

Managing forests that protect transportation corridors and settlements against rockfall is a complex task and demands the consideration of forest stand as well as rockfall characteristics. As empirical data on the effect of different stand structures on rockfall hazard remain unavailable, simulation models could be used to quantify the protective effect of different stand structures. We therefore used one of the few rockfall models explicitly taking trees into account and compared the results obtained with the 3D simulation model Rockyfor with empirical data on tree impacts at three mountain forests in Switzerland. We subsequently quantified the protective effect of these stands by assessing differences in the simulation scenarios "current forest cover" and "non-forested slope". Even though we used model input data with different resolutions at the study sites, Rockyfor accurately predicted the spatial distribution of trajectory frequencies at all sites (*Root Mean-squared Error*: 3.1%). In contrast, Rockyfor underestimated mean impact heights observed on trees at the two sites where high- and medium-resolution input data were available and overestimated them at the site where input data with the lowest resolution data were used. By comparing the results of the simulation scenarios "current forest cover" and "non-forested slope", we quantified the protective effect of the stands at all three sites. The number of rockfall fragments reaching the bottom parts of the study sites would, on average, almost triple if the "current forest cover" were absent.

We therefore conclude that Rockyfor is able to predict the spatial distribution of rockfall trajectories on forested slopes accurately, based on input data with a resolution of at least 5m × 5m. With the increasing availability of high-resolution data, it provides a useful tool for assessing the protective effect of mountain forests against rockfall.

Keywords: Protection forest, Natural hazards, Rockyfor, Dendrogeomorphology, Rockfall, simulation model, Swiss Alps

3.1 Introduction

Many mountain forests effectively protect people and their assets against natural hazards such as rockfall, snow avalanches, landslides, debris flows, soil erosion and floods (Brang *et al.* 2001). As a consequence, numerous settlements and transportation corridors in alpine regions directly depend on the protective effect offered by these forests and would – at least temporarily – become uninhabitable or inaccessible if this protection were to disappear or become inadequate (Bloetzer & Stoffel 1998, Agliardi & Crosta 2003).

In the Swiss Alps, rockfall and snow avalanches comprise the most common hazards, with evidence of rockfall observed in 31% and moving snow recorded in 37% of all mountain forests (Mahrer *et al.* 1988). While the large volumes and high energies occurring with snow avalanches often limit the protective effect of stands (Bartelt & Stöckli 2001), the small masses that are generally involved in single rockfall events (< 5 m^3; Berger *et al.* 2002) allow mountain forests to absorb falling rocks (Leibundgut 1986, Lafortune *et al.* 1997, Hétu & Gray 2000). On forested slopes, both living and dead trees can stop falling rocks (Cattiau *et al.* 1995), whereas stems lying on the ground or root plates may act as barriers to (rolling) rocks moving downslope (Mössmer *et al.* 1994, Schönenberger *et al.* subm.). Taking advantage of these effects on falling rocks, forest managers repeatedly tried to optimize the protective effect of their forests by applying target values for stand parameters such as tree density, spatial tree distribution, species composition and tree conditions (Chauvin *et al.* 1994, Wasser & Frehner 1996, Frehner *et al.* 2005). While these target values undoubtedly provided a valuable tool for forest managers, they currently remain unsatisfactory, since values are predominantly based on expert knowledge rather than on empirical data. Empirical data are very sparse, which is why the protective effect of a stand on a given site with a given damage potential could, up to now, only be assessed with considerable uncertainty. Given this lack of extensive empirical data on rockfall in mountain forests, dynamic modeling could provide a valuable tool for investigating the protective effect of different stand structures against rockfall and for improving target values for forest management.

To be useful, a model should accurately predict different patterns of rockfall processes such as the spatial envelope of rockfall trajectories, impact heights of rockfall fragments, and runout zones. Furthermore, it should be applicable under various site and stand conditions and should consider the interaction of falling rocks with trees – as investigated by Jahn (1988), Zinggeler *et al.* (1991), Gsteiger (1993), Krummenacher & Keusen (1996), Berger & Lievois (1999) or Dorren *et al.* (2005) – in sufficient detail.

The recently developed 3D rockfall model Rockyfor has accurately predicted different rockfall patterns for several forested and non-forested sites in mountainous terrain. The model operates with high-resolution input data (2.5 m × 2.5 m) so as to obtain sound results at the forest stand level. Such data hardly exist for many areas of the Alps, however. The model has also been shown to predict maximal runout zones with reasonable accuracy, even if based on low-resolution input data, i.e. 25 m × 25 m (Dorren & Heuvelink 2004). In contrast, the minimum resolution of input data required to obtain realistic simulation results for other important rockfall features characterizing the protective effect of a stand (e.g. envelope of rockfall trajectories, mean impact height, mean velocity of rocks) is not yet known. Furthermore, even if Rockyfor has produced good data at several sites in France and in Austria, it remains unknown whether it will reliably produce comprehensive results for other sites.

It was therefore the purpose of the present study (i) to test the accuracy of Rockyfor in simulating rockfall processes in different mountain forest stands with varying slope and stand characteristics, and (ii) to assess the protective effect of these stands. To achieve these objectives, we performed rockfall simulations

with Rockyfor using input data with different resolutions from three study sites in the Swiss Alps. The simulated rockfall patterns were then compared with empirical data obtained from these study sites. Finally, we used Rockyfor to quantify the protective effect of the investigated forest stands by comparing the results of simulation scenarios with and without a forest cover.

3.2 Methods

3.2.1 The Rockyfor model

Rockyfor is a process-based rockfall simulation model that was originally developed with data obtained from field investigations in the Austrian Alps (Dorren *et al.* 2004b). The model has since been improved and validated with data from 218 real-size rockfall experiments on forested and non-forested slopes in the French Alps (Le Hir *et al.* 2004, Dorren *et al.* 2005).

Rockyfor uses raster maps as input files and simulates trajectories of falling, bouncing and rolling rocks (Ø < 0.5 m; Buwal *et al.* 1997) and boulders (Ø > 0.5 m) within single raster cells. Moreover, it explicitly simulates the impact of rocks and boulders against trees. The model consists of three main modules. The first module calculates the rockfall trajectory, based on the topography of a site, which is represented by a Digital Elevation Model (DEM). At every step in the simulation, the fall direction of a rock can be towards one of the downslope cells from the cell where the rock is located during that simulation step. Hence, the model produces diverging rockfall trajectories.

The second main module calculates the energy loss due to impacts against single trees. As a result, the exact position of a falling rock and its current energy are modeled. If an impact against a tree takes place, the rock dissipates energy as a function of the relative position between rock and tree center and the stem diameter of the corresponding tree as follows:

$$\Delta E = -0.046 + \frac{0.98 + 0.046}{1 + 10^{(0.58 - ((Pi\text{-}CTA)/0.5*DBH))*-8.007}} \quad (1)$$

where D*E* = percentage of maximum amount of energy that can be dissipated by the tree [%]; *Pi–CTA* = horizontal distance between the position of the impact and the vertical central axis of the tree as seen from the impact direction [m]; *DBH* = stem diameter at breast height [m]. Thereby, the maximum amount of energy that can be dissipated by a tree (*max. E. diss.*) is a function of its DBH [m] as follows:

$$max.\ E.\ diss. = 38.7 \times DBH^{2.31} \quad (2)$$

These functions were derived from real-size rockfall experiments in a mountain forest in the French Alps (Dorren & Berger 2005). Equation 2 represents the maximum energy that can be dissipated by *Abies alba* Mill., which with respect to its resistance to impacting rocks is considered to be an average species (Dorren & Berger 2005)

The third main module calculates the velocity of the falling rock after a rebound on the slope surface (for details see Dorren *et al*. 2004b). Here, the decrease of velocity after a rebound is mainly dependent on the tangential coefficient of restitution (r_t), which is determined by the composition and size of the material covering the surface as well as the radius of the falling rock itself (Kirkby & Statham 1975). The coefficient is calculated as a function of the radius of the rockfall fragment and the mean radius of the material on the ground as follows:

$$rt = \frac{1}{1 + (D_{mean} / D_{rock})} \quad (3)$$

where D_{mean} = the mean diameter of the material on the slope surface [m]; D_{rock} = the diameter of the falling rockfall fragment [m]. The calculated r_t is randomly varied with 10% in order to take account of the enormous variation in the size of material covering rockfall slopes. Furthermore, its value is limited to the range [0.1, 0.99] as to avoid unrealistic energy loss.

3.2.2 Study sites

Rockyfor was applied to three mountain forest sites in different areas of Switzerland. Figure F3.1 gives an overview of the sites, while a summary of relevant site characteristics is presented in Table F3.1.

The first site is a forest stand in the Diemtigtal (site *DT*) in the Swiss Prealps. The site lies at the foot of an approximately 400 m high limestone cliff (Fig. F3.1) on a southeast exposed talus slope with a mean slope gradient of 40°. The stand is dominated by *Picea abies* (L.) Karst. (77%), but other species such as *Sorbus aria* (L.) Crantz, *Sorbus aucuparia* L. or *Acer pseudoplatanus* L. occur as well (23%). The study site covers 0.3 ha, located between 1210 and 1280 m a.s.l. in the uppermost part of the talus slope. This area is in the transit zone of frequent, but mainly small falling rocks. Below the study site, hiking trails and forest roads, which could be endangered by rockfall, traverse the slope.

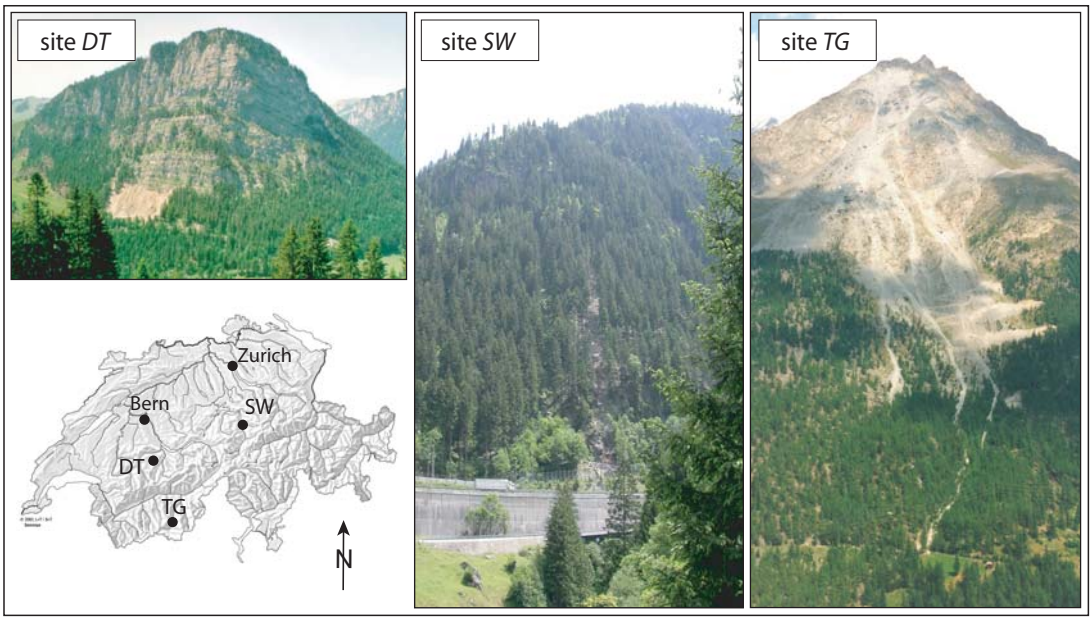

Fig. F3.1 *Localization of the study sites Diemtigtal (site DT), Stotzigwald (site SW) and Täschgufer (site TG) within Switzerland.*

The second site is the Stotzigwald (site *SW*), a stand in the central Swiss Alps covering a steep slope with a mean slope gradient of 45° and some interspersed cliffs (Fig. F3.1). This forest protects one of the most heavily used traffic routes connecting Germany and Italy. The elevation of the forest ranges from 650 to 1650 m a.s.l., but rockfall activity is mainly restricted to a zone of approximately 7.5 ha in the lower part of the forest, i.e. up to approximately 1000 m a.s.l. The stand within this zone mainly consists of *Picea abies* (83%) and *Abies alba* (13%). The slope is covered with rocks, boulders and morainic material. Bedrock consists of heavily weathered granite and gneiss (Thali 1997). As a result, rockfall frequently occurs and rockfall fragments regularly reach the highway (Kläger 2003).

The third site is Täschgufer (site *TG*), which is located in the southern *Sw*iss Alps (Fig. F3.1). Here, rockfall is frequently triggered from the heavily disintegrated paragneissic rockwalls below the Leiterspitzen summit (3214 m a.s.l.). In the upper part of the site, which covers 26 ha, mean slope gradients reach 48° and gradually decrease to 20° near the valley floor (1430 m a.s.l.). In the central area affected by rockfall, continuous forest cover reaches 1780 m a.s.l., whereas the upper part of the slope remains mostly free of vegetation. The stand predominantly consists of *Larix*

Table F3.1. *Characteristics of the three study sites.*

Study site (area)	Altitudinal range [m a.s.l.]	Mean slope	*Stand characteristics (main tree species, tree density, mean DBH)*	*Predominating size of rocks (mean diameter)*
Diemtigtal (DT) 0.3 ha	1210 – 1280	40°	*Picea abies* 520 trees ha $^{-1}$ 21 cm	*0.2 m*
Stotzigwald (SW) 7.5 ha	650 – 1000	45°	*Picea abies*, *Abies alba* 561 trees ha $^{-1}$ 38 cm	*0.7 m*
Täschgufer (TG) 26 ha	1430 – 3214	20° – 48°	*Larix decidua* 150 trees ha $^{-1}$ 30 cm	*0.9 m*

decidua Mill. (95%), accompanied by single *Picea abies* and *Pinus cembra* ssp. sibirica. In the recent past, rockfall regularly reached the valley floor, causing damage to roads, hiking trails and agricultural buildings (Wicht & Joris 1985, Lauber 1995).

3.2.3 Model input data

For all sites, extensive data on stand structure, geomorphological characteristics and rockfall patterns were available from earlier field studies. In addition, dendrogeomorphological data on century-long fluctuations in rockfall activity exist for *site TG*. A summary of all input data used for the simulation with Rockyfor is presented in Table F3.2.

In addition to the pre-existing data, complementary data on different site characteristics were gathered in the field (Kühne 2005): Firstly, potential rockfall source areas were mapped, integrated into a Geographical Information System (GIS) and converted to raster maps. Secondly, terrain and vegetation parameters were mapped and polygons with homogeneous terrain characteristics described. From this data, a raster map was created for the normal coefficient of restitution (r_n; cf. Dorren & Seijmonsbergen 2003) and for the mean diameter of the material covering the slope surface. The latter was required to calculate the tangential coefficient of restitution (r_t).

In a third step, complementary data on stand structure and empirical rockfall patterns were gathered on validation plots of approximately 225 m^2 (15 m × 15 m) at sites *SW* and *TG* so as to provide (i) data on the tree diameter distribution and (ii) validation data for the simulation experiments. On these validation plots, DBH was therefore measured for all individual trees with a DBH < 8 cm. Rock impacts were assessed on the stem surface of trees, and the mean and maximum impact heights measured on every single tree. In order to derive forest stand maps as needed by Rockyfor, field data were coupled with a tree distribution map obtained from photogrammetric analyses, where every individual tree crown was mapped on orthophotos (scale 1 : 9000). For site *DT*, no complementary data on stand and rockfall patterns were gathered, since exhaustive data for every single tree on the site were available.

Finally, high resolution Digital Elevation Models (DEM) with a support of 1m × 1m (site *DT*) and 5m × 5m (sites *SW* and *TG*) were produced. For site *DT*, the DEM was directly derived from highly resolved laser scan data (resolution: 0.5 m; Swisstopo, 2004) using the Spatial Analyst module in ESRI® ArcGIS™ (Esri 2005b). For site *SW*, the DEM was derived from contour lines (equidistance: 12.5 m) created on the basis of photogrammetric analyses realized with high quality aerial photographs (scale 1:9000). At site *TG*, in contrast, surface points and breakline features were generated from orthophotos (scale 1:9000) with ERDAS® Stereo Analyst™ (Leica 2005) software and coupled with 10 m contour lines so as to derive a topogrid file in ESRI® ArcMap™ (Esri 2005a). Here, contour lines were digitized from a topographic map in a scale of 1:10'000.

3.2.4 Simulation set-up

Since Rockyfor models rockfall on the basis of various stochastic algorithms, at least one hundred simulation runs from each potential rockfall source cell were needed to obtain sufficiently stable results (Dorren & Heuvelink 2004). Furthermore and in order to account for the varying size of falling rocks and boulders at the three sites, we simulated varying numbers of rockfall fragments for each size class (cf. Table F3.4). The selected number of simulations per size class was derived from estimates in the field and represents the diameter size distribution of rockfall fragments at the three sites.

The initial fall height of the rocks for the simulation experiments was set to 30 m at site *DT*, to 5 m at site *SW* and to 3 m at site *TG*. These values depended on the morphology of the rockfall source areas. Simulation runs were first realized on the slopes with the "current forest cover", before trees were removed in the "non-forested" scenario and simulation runs repeated.

3.2.5 Assessment of model accuracy

Simulated and empirical rockfall patterns were compared on the basis of (i) the spatial distribution of rockfall impacts on trees, which is an indicator for the spatial distribution of the rockfall trajectories, and (ii) mean impact heights, which are indicators for bounce heights of rockfall fragments. At site *DT*, the accuracy of the model was assessed at the level of single trees, since detailed data were available (Perret *et al.* 2005b). At sites *SW* and *TG*, however, the analysis was performed on validation plots of 225 m^2 (see section F3.2.3). At site *TG*, simulation results were also compared with data on spatio-temporal variations in rockfall activity derived from dendrogeomorphological analysis of 129 living trees for the last 400 years (Stoffel *et al.* 2005c).

Table F3.2. *Data used for the simulation experiments.*

Feature class	Available data	Sampling method	Source	Derived model input
Stand structure	Species composition	Inventory sampling procedure on stand plots	Perret *et al.* 2004, Wehrli et al. subm., Stoffel et al., 2005b, c	Stand raster map
	Diameter distribution	Inventory sampling procedure on stand plots	Kühne 2005, Perret *et al.* 2004b, Wehrli *et al.* subm., Schneuwly 2003	
	Tree density	Analysis of aerial photographs	Kühne 2005, Perret *et al.* 2004b	
Surface roughness	Granular composition of surface material	estimation in 5 classes (< 0.2 m, 0.2-0.5 m, 0.5-1 m, 1-2 m, > 2 m)	Kühne 2005	r_t -raster map
	Vegetation cover	estimation of proportion of bushes and shrubs	Kühne 2005	
Subsurface damping	Damping properties of subsurface	estimation in 6 classes (bedrock, scree/talus, stony soil, dry forest soil, fine humid soil)	Kühne 2005	r_n -raster map
DEM	Laser scan data (site DT)	Interpolation to raster using Spatial Analyst (Esri 2005)	DTM-AV © 2004 Swisstopo (DV033531)	DEM
	Aerial photographs (sites *SW & TG)*	Deriving contour lines from aerial photographs and interpolation to raster using Spatial Analyst (Esri 2005); surface points and breakline features assessed with ERDAS Stereo Analyst (Leica 2005)	DEM © 2004 WSL, P. Thee (site *SW*) DEM © 2005 GIUB, R. Kühne (site TG)	
Rock properties	rock size	Estimation of rock size Description of recent accumulation (3 granular classes)	Kühne 2005	rock size
Validation data	number of tree impacts due to rockfall	Count of tree injuries due to rockfall in test plots	Kühne 2005, Perret *et al.* 2004b	Validation raster map
	mean and max. impact heights	Assessment of H_{max} , H_{mean}	Kühne 2005, Perret *et al.* 2004b, Schneuwly 2003, Stoffel *et al.* 2005b, c	

The number of rockfall impacts per tree was directly assessed from the empirical data for site *DT*. For sites *SW* and *TG*, a Tree Impact Coefficient *(TIC*) was calculated as:

$$TIC = \frac{TreeHits_j}{n_{Trees\,j}} \qquad (4)$$

where $TreeHits_j$ = sum of tree impacts per validation plot *j*, and $n_{Trees,\,j}$ = number of trees in validation plot *j*. For standardization purposes, both empirical and simulated data were expressed as proportion relative to the summed values over all trees (*site DT*), and over all validation plots (*sites SW* and *TG*), respectively. The mean impact height was calculated for every single tree (site *DT*) and for every validation plot (sites *SW* and *TG*). At site *TG*, impact heights were also taken from a set of dendrogeomorphological data (Stoffel *et al.* 2005c). However, since evidence of past rockfall impacts appears to be no longer visible in up to 90% of all cases in these century-old *Larix decidua* stems (Stoffel & Perret 2005), only 38 out of 129 trees showed scars recognizable on the stem surface and could, thus, be used for comparison.

In a subsequent step, mean (*ME*) and root mean-squared errors (*RMSE*) between the predicted and the observed number of impacts and mean impact heights were calculated as follows:

$$ME = \frac{1}{n}\sum_{i=1}^{n}(P_i - O_i) \qquad (5)$$

$$RMSE = \sqrt{\frac{1}{n}\sum_{i=1}^{n}(P_i - O_i)^2} \qquad (6)$$

where = number of trees (site *DT*) or validation plots (sites *SW* and *TG*); P_i = predicted (i.e. simulated) and O_i = observed rock impacts at tree *i* (site *DT*) and validation plot *i* (sites *SW* and *TG)*.

Furthermore, the proportional difference between the predicted and the observed number of impacts was calculated for each tree (site *DT*) and each validation plot (sites *SW* and *TG*), and then illustrated for deviations >2.5% and > 5%. Thus, the simulated trajectories of all size classes of rockfall fragments were totaled and compared with the empirical patterns.

3.2.6 Assessment of the protective effect of the different stands

The protective effect of the stands was then assessed at the three sites by quantifying changes in the frequency of simulated rockfall trajectories between the scenarios "current forest cover" and "non-forested slope". Differences were assessed in evaluation zones at the foot of every test slope where high damage potential exists (i.e. roads or buildings). The zones were designed as shapefiles in the GIS and the differences in the number of passing rockfall fragments analyzed per diameter class of rockfall fragments using the Spatial Analyst module in ESRI® ArcGIS™ (Esri 2005b). In addition, the ratio between the two scenarios was calculated for each diameter class of rockfall fragments (*RF*) as:

$$RF\_ratio_i = \frac{PR_{non\text{-}forested\_slope,\ i}}{PR_{forested\_slope,\ i}} \qquad (7)$$

where $PR_{non\text{-}forested\_slope,\ i}$ and $PR_{forested\_slope,\ i}$ = number of rocks per diameter class *i* passing the evaluation zone on the "non-forested" and forested slope. Furthermore, the protective effect of the two scenarios was compared graphically after totaling the simulated trajectories over all diameter classes of rockfall fragments.

3.3 Results

3.3.1 Model accuracy

In general, the simulation experiments yielded very close matches between simulated and empirical spatial distributions of tree impacts on all three sites. However, for mean impact heights, the correspondence between simulated and observed data varied considerably.

At site *DT*, the simulated number of tree hits corresponds very well with the empirical data, as indicated by the *RMSE* of 0.9% (Table F3.3). Figure F3.2a shows that differences predominantly occur in the uppermost sector of the study site, where the model overestimates the number of hits in nine trees by +2.5 and +5%. On the southwestern edge of the study site, the model, in contrast, underestimates the number of impacts in one tree by more than –5%. For the remaining 128 trees (93%), differences between the predicted and the observed number of tree hits remain between ±2.5%. On the other hand, differences can

Table F3.3. *Mean (ME) and Root Mean-Squared Errors (RMSE) between observed number of tree hits and impact heights (h_{mean}) and model results obtained at study sites DT, SW, TG* dataset *1 and TG* dataset 2 *(for explanation see text).*

Site	Number of Trees	Number of Tree Hits or TIC		Mean Impact Height		
		ME [%]	*RMSE* [%]	h_{mean} observed [m]	*ME* [m (%)]	*RMSE* [m (%)]
DT	138	0	0.9	0.8	-0.2 (-26)	0.4 (57)
SW	23	0	3.6	1.1	2.6 (230)	3.5 (310)
TG dataset 1	46	0	4.4	1.1	-0.6 (-59)	1.1 (96)
TG dataset 2	129 / 38	0	3.6	1.7	-1.4 (-85)	1.7 (101)

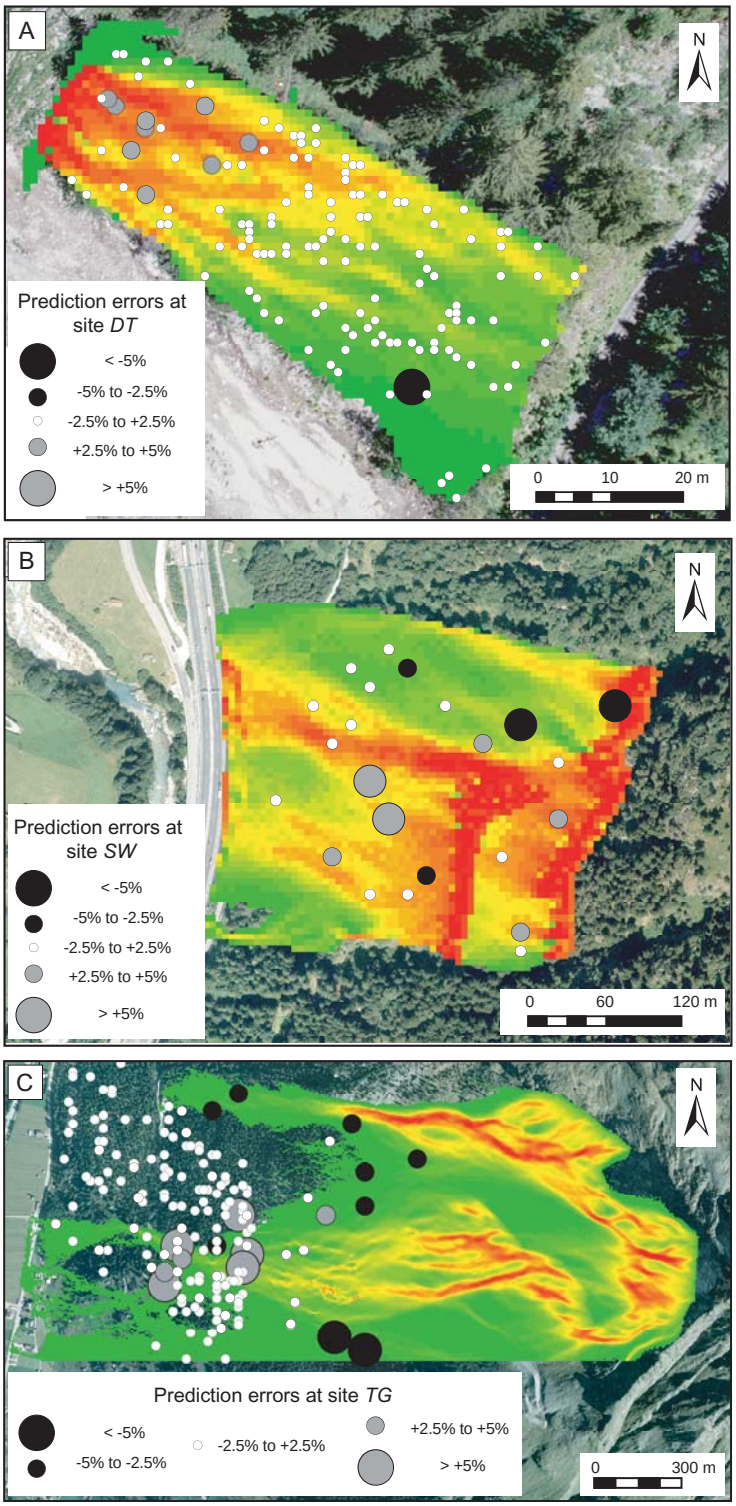

Fig. F3.2. *Differences between simulated and observed number of rock impacts on trees or validation plots at (a) site DT, (b) site SW and (c) site TG. Gray circles indicate an overestimation by the model, whereas black circles show underestimation. White circles represent trees or validation plots with a very similar number of rock impacts for simulations and observations (±2.5%) (Orthophoto sources: site DT: © Baumgartner (2002); site SW: © Kanton Uri; site TG: © swissphoto)*

be seen with impact heights, where Rockyfor underestimates the mean impact height by –0.21 m (*ME*) and 0.46 m (*RMSE*). As can be seen from Table F3.3, deviations from the observed mean impact height (0.85 m), therefore, account for 26% (*ME*) and 57% (*RMSE*). At site *SW*, the predicted *Tree Impact Coefficient (TIC)* pattern corresponds reasonably well with empirical data from the validation plots, resulting in a *RMSE* of 3.6% (Table F3.3). As illustrated in Figure F3.2b, the model more commonly overestimates the number of tree hits, but underestimates occur as well. Differences exceeding ±5% are identified in four validation plots and prediction errors ranging from 2.5 to 5% are present in six plots. In the other 13 validation plots (i.e. 56%), the difference between the predicted and the observed number of tree hits remains within a

range of ±2.5%. As shown in Table F3.3, Rockyfor largely overestimates, in contrast, mean impact heights with a *ME* of +2.6 m and a *RMSE* of 3.5 m. Compared to the mean impact height of 1.1 m observed in the field, this corresponds to an overestimation of 210% (*ME*) and 310% (*RMSE*), respectively.

At *site TG*, simulated rockfall data are compared with data gathered on 46 validation plots in the field (*TG dataset 1*) as well as with results from dendrogeomorphological reconstructions of past rockfall activity (*TG dataset 2*). As indicated in Table F3.3, the model again accurately predicts the empirical *TIC* pattern with a *RMSE* of 4.4% for *TG dataset* 1 and 3.6% for *TG dataset 2*. For *TG dataset 1*, underestimation occurs in eight validation plots with differences between the observed and the predicted number of tree impacts primarily remaining between –2.5 and –5%. For *TG dataset 2*, in contrast, overestimation can be observed in seven out of 129 validation plots, mostly exceeding +5%, whereas underestimation can only be found in one plot. Interestingly, the overestimated validation plots are largely concentrated along the upper fringe of the continuous forest stand and near the rockfall channel, as shown in Figure F3.2c. Results also indicate that in 80% (*TG dataset 1*) and 94% (*TG dataset 2*) of the validation plots, differences between simulated and predicted *TIC* patterns remain within a range of ±2.5%.

In contrast, the correspondence between empirical and simulated impact heights is, once again, rather low: For *TG dataset 1*, the model underestimates the mean impact height observed in the field (1.1 m) with a *ME* of –0.6 m and a *RMSE* of 1.1 m. As can be seen from Table F3.3, this corresponds to a relative underestimation of 85% and 96%, respectively. For TG *dataset* 2, the observed mean impact height (1.7 m) is underestimated with a *ME* of –1.4 m (85%) and a *RMSE* of 1.7 m (101%).

3.3.2 Protective effect

The comparison between the two simulation scenarios "current forest cover" and "non-forested slope" yielded significant differences for all three sites. Table F3.4 first of all shows that the number of rocks and boulders passing the evaluation zones was considerably higher in the "non-forested" scenario.

At site *DT*, the complete removal of the forest stand would result in more rocks passing the evaluation zone at the foot of the study site, as indicated by the high *RF_ratio*s between the two scenarios. As can be seen from Table F3.4, this is particularly true for the smallest rock diameter class (0.1 m) used in the simulation runs, for which the *RF_ratio* increased by a factor of 8.5, as compared to the scenario with the "current forest cover". Figure F3.3a gives a qualitative impression of the differences emerging between the two scenarios, indicating that the increase in the transit of rocks is most obvious in the northeastern and central parts of the study site. In contrast, negative effects appear to be less drastic in the southern half, where

Table F3.4. *Assessment of the protective effect of the investigated stands. The number of rockfall fragments (RF) triggered per diameter class and start cell is given as n. The percentage of rocks and boulders passing the evaluation zones is given for the scenarios "forested slope" and "non-forested slope" and the differences between the two scenarios expressed with a RF_ratio (for explanation see text).*

		diameter of RF [m]	0.1	0.2	0.3	0.4	0.6	0.8	1	1.2	1.4	1.6	1.8	**2**
site DT **start cells 12**		RF triggered	1500	2000	1500	-	-	-	-	-	-	-	-	-
	forested	passing RF [%]	0.7	5.2	13	-	-	-	-	-	-	-	-	-
	non-forested	passing RF [%]	6	18.1	32.4	-	-	-	-	-	-	-	-	-
		RF_ratio	8.5	3.5	2.5	-	-	-	-	-	-	-	-	-
site SW **start cells 331**		RF triggered	-	1200	-	1500	1200	1000	600	500	200	200	100	100
	forested	passing RF [%]	-	1.5	-	3	5.2	5.7	6.7	7.9	8.4	8.8	8.7	8.7
	non-forested	passing RF [%]	-	3.9	-	6.8	8.8	9.5	15.8	9.9	9.9	9.9	9.9	9.9
		RF_ratio	-	2.5	-	2.3	1.7	1.7	2.4	1.3	1.2	1.1	1.1	1.1
site TG **start cells 7692**		RF triggered	-	1200	-	1500	1200	1100	1000	800	700	600	500	400
	forested	passing RF [%]	-	0	-	0	0	0.001	0.002	0.003	0.006	0.011	0.035	0.057
	non-forested	passing RF [%]	-	0	-	0	0	0.004	0.011	0.018	0.026	0.043	0.076	0.107
		RF_ratio	-	0	-	0	0	4.5	6.7	5.5	4.1	4.1	2.2	1.9

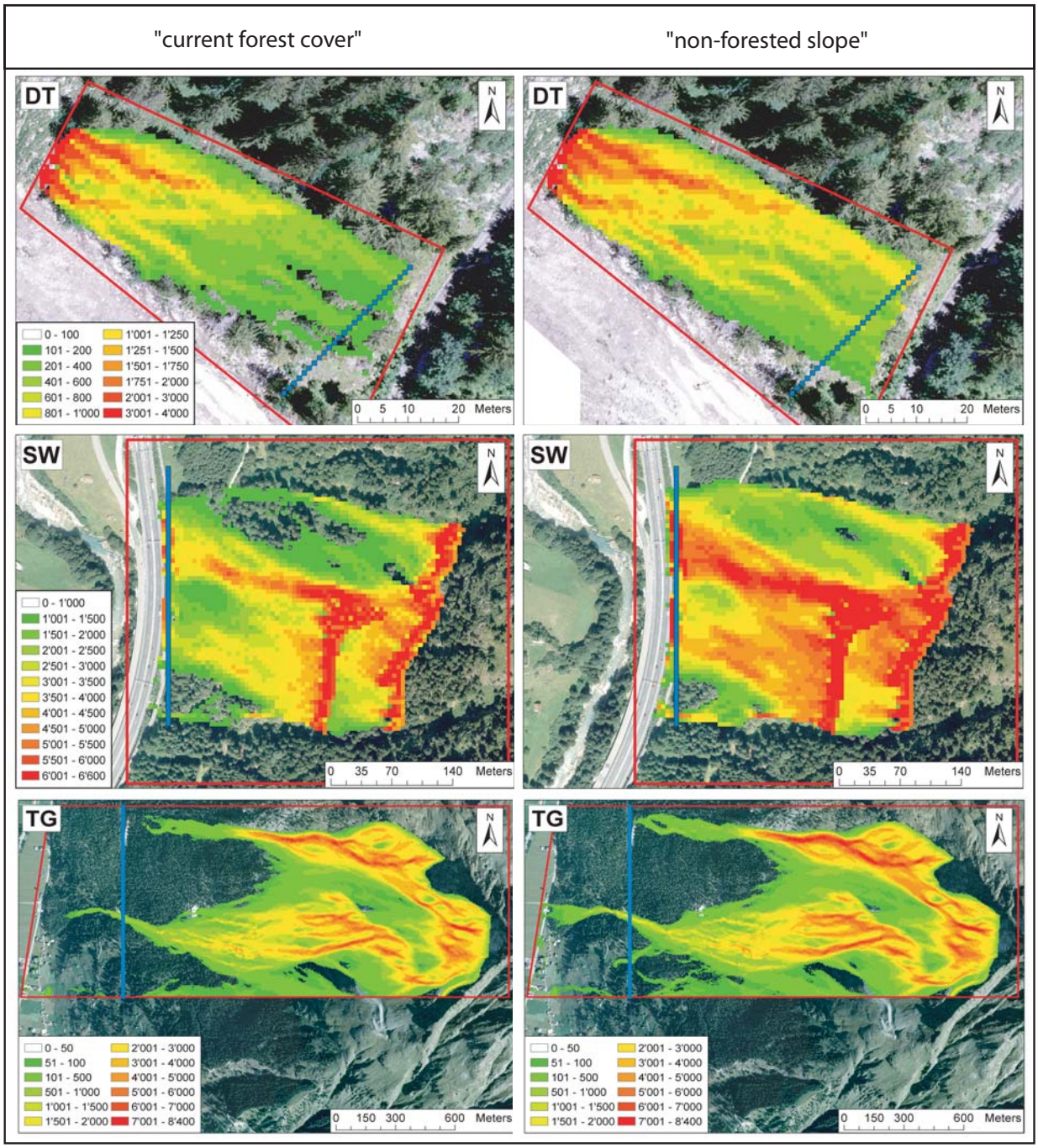

Fig. F3.3. *Comparison of simulated rockfall trajectories for the "current forest cover" (left) and for the "non-forested slope" (right) at (a) site DT, (b) site SW, and (c) site TG. Evaluation zones are indicated with blue lines.*

frequencies only slightly increased in the "non-forested" scenario.

At *site SW*, the number of rockfall fragments passing the evaluation zone is rather high in both scenarios. As shown in Table F3.4, differences between the two scenarios are most obvious for rocks and small boulders of up to 1 m in diameter, where *RF_ratio*s varied between a factor of 1.7 and 2.5. Figure F3.3b illustrates that in the "non-forested" scenario, a considerable increase in the number of rockfall trajectories can be observed below the subvertical cliff in the central part of the study site. Results also indicate that in the scenario with the "current forest cover", rockfall fragments originating from this cliff would be partly stopped through the presence of trees, whereas the absence of trees would allow most rocks and boulders to travel down the slope and reach the adjacent

highway. A similar protective effect of the stand is evident for rockfall fragments originating from the uppermost cliff area.

In contrast to sites *DT* and *SW*, Table F3.4 indicates that the differences in the number of rocks and boulders passing through the evaluation zone at site *TG* are considerably smaller for most diameter classes. Nonetheless, significant differences arise between the two scenarios for boulders with diameters > 0.8 m, as indicated by the high *RF_ratio*s in Table F3.4. The qualitative comparison of the scenarios in Figure F3.3c indicates a minor increase in the number of rocks passing down the slope in the rockfall channel located in the northwestern part of the study site, where the number of deposited rocks and boulders doubles in some locations. In the central part of the study site, rockfall activity increases as well, meaning that boulders would more frequently reach the main road in the valley floor (Fig. F3.3c).

3.4 Discussion

3.4.1 Model accuracy

In the study we report here, the 3D rockfall simulation model Rockyfor was tested and its capability to accurately predict rockfall patterns assessed at three forested sites in the Swiss Alps. Overall, the comparison of observed with simulated rockfall patterns yielded a high correspondence for the spatial distribution of tree impacts and a low correspondence for the mean impact heights.

The closest match between empirical and simulated distributions of tree impacts was obtained at site *DT*, where a highly resolved DEM (1 m × 1 m) allowed very accurate modeling of rockfall trajectories. At sites *SW* and *TG*, the simulation based on a 5 m × 5 m DEM derived from contour lines with an equidistance of 12.5 m (site *SW*) and 10 m (site *TG*) still yielded close matches between the empirical and predicted distribution of tree impacts with *RMSE* < 4.4%. As stochastic elements are involved in rockfall processes, a complete agreement of empirical and simulated trajectories is unlikely, which is why we believe that for an accurate prediction of the spatial envelope of rockfall trajectories, a DEM with a resolution of 5 m × 5 m – as used at sites *SW* and *TG* – is largely sufficient.

In contrast to the spatial distribution of rockfall trajectories, the prediction of mean impact heights was less accurate. Even at site *DT*, predicted mean impact heights were considerably lower than the values observed in the field. This low correspondence is particularly surprising, since Rockyfor produced close matches between empirical and simulated mean impact heights for a site in the French Alps, based on a DEM with a resolution of 2.5 m × 2.5 m (Dorren *et al.* subm.). The underestimation of mean impact heights further increased at site *TG*, where the model produced a negative bias for both *TG dataset* 1 and *TG dataset* 2. In contrast, Rockyfor largely overestimated mean impact heights at site *SW*.

The reasons for the poor correspondence between the predicted and the observed mean impact heights may be manifold. Since Rockyfor was calibrated on the basis of more than 200 real-size experiments (Dorren *et al.* 2005) and different rockfall patterns, including mean impact heights accurately predicted before, we believe the main reasons for the rather low agreement between empirical and simulated mean impact heights to be model-independent rather than model-intrinsic.

A first factor that might have affected the accuracy of the simulation results is the DEM, i.e. its spatial resolution. This is particularly true for sites *SW* and *TG*, where DEMs were derived from contour lines with relatively low resolution. Consequently, microtopographical structures are neglected in the DEM, which in turn can influence the velocity of falling rocks. For instance, huge boulders from ancient rockslide deposits could not be included in the DEM at site *TG*. These boulders may, however, cause rockfall fragments to bounce and therefore produce higher impacts than suggested by the model. At site *SW*, the rather coarse DEM was probably the main reason for the large overestimation of the mean impact height, since on this steep slope with an average inclination of 45°, the frequently occurring, abrupt changes in the slope gradient could probably not be reproduced in the DEM with sufficient accuracy. These observations are in agreement with Agliardi & Crosta (2003), who report a decrease in bounce height in the flatter parts of the slope and an increase in bounce height on steeper slopes as soon as the resolution of support data decreases. When using a 5 m × 5 m DEM, it would, therefore, be preferable if the underlying data had a support of at least five meters as well (e.g., 1–5 m contour lines or LIDAR data), so as to take essential terrain features into account.

A second factor influencing the mean impact height in the model can be identified in the uncertainty related to the delineation of rockfall source areas and initial fall heights. Within the present study, we determined rockfall source areas based on observations and geo-

logical advisory opinions. A large number of rockfall fragments were triggered from these start cells with a given initial fall height, which again was determined based on qualitative field observations. It is, however, clear that these observations can only be seen as an approximation to reality, since precise determination of rockfall source areas and initial fall heights was rendered impossible by complex terrain features such as the 400 m high limestone cliff at site *DT*, or subvertical cliffs at site *SW*. Nonetheless, a more precise assessment of the rockfall source areas and the initial fall heights seem to be decisive for a better prediction of bounce heights of rockfall fragments and, consequently, impact heights on trees.

A third factor affecting modeled impact heights is represented by the validation datasets, which were mainly based on the assessment of impact scars visible on the stem surface of trees. As previously shown by Stoffel (2005b) or Stoffel & Perret (2005), scars as evidence of past rockfall events may become completely blurred after some time and are, as a consequence, no longer visible on the stem surface.

On the other hand, it is also conceivable that large scars caused by high-energy impacts at unusually high positions may persist for a long time on the stem surface and therefore lead to an overestimation of rare impact heights. Furthermore, the accuracy of the validation datasets was also influenced by the tree species and the age of single trees. At site *TG*, for instance, the overestimated plots illustrated in Figure F3.2c largely occur in areas where juvenile trees are recolonizing the slope. In contrast to their older neighbors, these trees only show a comparably low number of scars in the field, as there has not been sufficient time for scarring.

Other factors such as the small number of test plots for site *SW* or minor inaccuracies in the r_t/r_n-maps may have influenced the prediction of mean impact heights as well, but the three factors mentioned above are probably of prime importance. Nevertheless, model results clearly indicate that the 3D process-based model Rockyfor is able to accurately predict the spatial envelope of rockfall trajectories based on input data with a resolution of 5m × 5m.

3.4.2 Protective effect

The second aim of this study was to assess the protective effect of the investigated stands against rockfall through a comparison of simulation scenarios with the "current forest cover" and on a "non-forested slope". This allowed quantification of the protective effect of the forest stands at the three sites, as indicated by the *RF_ratio*s between the scenarios.

The protective effect of the stands is highest for rocks and small boulders (diameter < 1 m) at sites *DT* and *SW* (cf. Table F3.4). Here, the number of rockfall fragments passing through the evaluation zones is between 1.7 and 8.5 times higher in the "non-forested" scenario, indicating an effective protective function of the current stands. At site *TG*, the stand seems, in contrast, to protect objects at risk from (large) boulders ranging from 0.8 to 2 m in diameter rather than from smaller rocks. Even though rockfall fragments passing through the evaluation zone appear to occur much less frequently here, the protective effect of the stand should not be discounted.

We therefore believe that at all three sites, the hazard potential would increase strongly without the current stands: At site *DT*, rocks would more frequently reach the forest road and endanger the nearby hiking trails, whereas at sites *SW* and *TG*, important infrastructure would be endangered (site *SW*: highway, site *TG*: main road, buildings). Given the high damage potential at sites *SW* and *TG*, several countermeasures have been taken in the recent past. At site *SW*, restraining nets have been constructed along the highway, whereas at site *TG*, seven dams have been built on the slope. As evident from our simulation results, these countermeasures are more than justified.

3.5 Conclusions

This study clearly showed that, based on input data with a resolution of at least 5m × 5m, Rockyfor is able to accurately predict the spatial distribution of rockfall trajectories on forested sites with different slope and stand characteristics. In contrast, an accurate prediction of mean impact heights was not possible in the present study. We believe that high-resolution input data including e.g., a laser scan based DEM, a better knowledge of rockfall source areas, and data on initial fall heights would considerably improve the quality of the predicted impact heights. Additionally, dendrogeomorphological analysis should be used more systematically in old-growth stands, so as to detect hidden scars and, consequently, to improve the quality of validation datasets. Due to its ability to accurately predict the spatial envelope of rockfall trajectories, the present version of Rockyfor also provides a valuable tool for the investigation of the protective effect offered by different stand structures and, therefore, for the management of rockfall protection forests.

Acknowledgements We are grateful to the European Commission for the Marie Curie Fellowship (QLK5-CT-2002-51705). Additional funding was provided by the Swiss National Science Foundation (grant 4048-064409) and the Swiss Forest Agency. We kindly acknowledge Marc Baumgartner, Catherine Berger, Monika Fässler, Connie Hett, Dominique Schneuwly and Mathias Zesiger for assistance in the field. Igor Lièvre and Patrick Thee are acknowledged for generating contour lines for sites *TG* and *SW*. We are grateful to Walter Schönenberger for his valuable comments on a former draft and Heather Murray for improving the English of the paper. Finally, we would like to thank Swisstopo for providing the aerial pictures.

*****

Appendix 4:
A «picturesque» trip on the Täschgufer slope

Plate 1: Bedrock

Top

Summit area of the west-facing Leiterspitzen (3214 m a.s.l.) with bedrock striking SSW and dipping WNW with angles of 40–80°, thus containing joints dipping out of the slope. (Photo courtesy by CREALP/Christian Marro, used with permission)

Center

Detail of the bedrock right below the summit area as illustrated above. While relatively large volumes of bedrock are subject to instability, the size of single rockfall fragments is supposed to remain at 1–2 m^3 here. (Photo courtesy by CREALP/Christian Marro, used with permission)

Bottom

Open discontinuities can be identified behind these layers of heavily fissured bedrock with a volume of approximately 10’000 m^3 (Photo courtesy by CREALP/Christian Marro, used with permission)

Plate 2: Discontinuities and fissures

Top and bottom

The paragneissic units at Täschgufer belong to a contact zone between the Siviez-Mischabel and the Monte Rosa nappes and are heavily fissured. Results from structural and geomechanical analysis indicate that the schistosity would only allow the release of superficial rockfall events with volumes remaining limited – in the worst case – to some hundreds of cubic-meters. (Photo courtesy by Theo Lauber, used with permission)

Plate 3: Loose debris and remobilization of rocks and boulders

Top

Besides the release of rocks and boulders from disintegrated bedrock, rockfall fragments may also be (re-)mobilized from the large talus accumulations in the upper parts of the slope. (Photo courtesy by Theo Lauber, used with permission)

Center

Water may influence the triggering of loose debris, as illustrated with this fresh departure zone located at approximately 2650 m a.s.l. in the central part of the slope. (Photo courtesy by Theo Lauber, used with permission)

Bottom

The action of seasonal frost and refreezing meltwater may cause single rocks and boulders of these unstable layers to be released during thawing. (Photo courtesy by Theo Lauber, used with permission)

Plate 4: Talus slope and forest fringe

Top, center and bottom

In the main area of rockfall, trees located near the forest fringe (~ 1780 m a.s.l.) repeatedly suffer from the impact of rockfall fragments. Apparently, the relatively young trees located in this sector were able to recolonize the slope during the last few decades, before they again became more frequently affected by rocks and boulders in the 1980s and 1990s. (Photo courtesy by Theo Lauber, used with permission)

Plate 5: Protection dams

Top

During the construction of Dam 1 located in the southeastern edge of the Täschgufer slope and at approximately 2500 m a.s.l., contemporary permafrost in the form of massive ground ice was encountered. Even though observations as well as the results of rockfall simulation (cf. Chapter F3) indicate that rockfall would repeatedly pass by the location of the dam, rockfall fragments have not been deposited since the construction of the dam in 1989 and the realization of this picture in 1995. (Photo courtesy by Theo Lauber, used with permission)

Center

Dams 2 to 5 as seen from the summit area of the Leiterspitzen. As rockfall caused severe damages to the earth-fill deflection dams built in 1989, authorities decided to enlarge the uppermost dam and to construct a 400 m long, enforced dam (i.e. Dam 6) crossing the entire talus slope present on this picture. (Photo courtesy by Theo Lauber, used with permission)

Bottom

The lowermost dam constructed at Täschgufer has a length of 260 m and its construction was finished in 1998. As debris flows occur on the slope as well, small apertures have been left as to retain the solid charge of debris flow surges, while letting the fluid part of surges pass further down. (Photo courtesy by Theo Lauber, used with permission)

Plate 6: Injuries caused to trees growing at Täschgufer

Top and bottom

Heavily injured trees located in the sparsely wooded stand above the lowermost protection dam (Dam 7) at approximately 1830 m a.s.l., where rockfall frequently occurs. A majority of trees have no crown at all or show “candelabra” growth, while almost all trees exhibit large, open scars. (Photo courtesy by Simone Perret, used with permission)

Plate 7: Cross-sections and micro-cuts

Top

Cross-sections prepared from the 18 juvenile *Larix decidua* trees analyzed in Chapter B1. Some of the scars are already overgrown and "hidden", while others are still visible from outside. The size of scars and the portion of the stem affected by the rockfall impact varied as well: While some impacts left quite small injuries, others deleted the cambium on more than half of the stem surface (e.g., in the cross-section illustrated to the right at the bottom).

Bottom

Micro-cuts prepared from the stem discs used in Chapter B1 illustrating the presence of wounds and overgrowing callous tissue (upper row) as well as traumatic rows of resin ducts in the areas next to the direct impact (lower row)

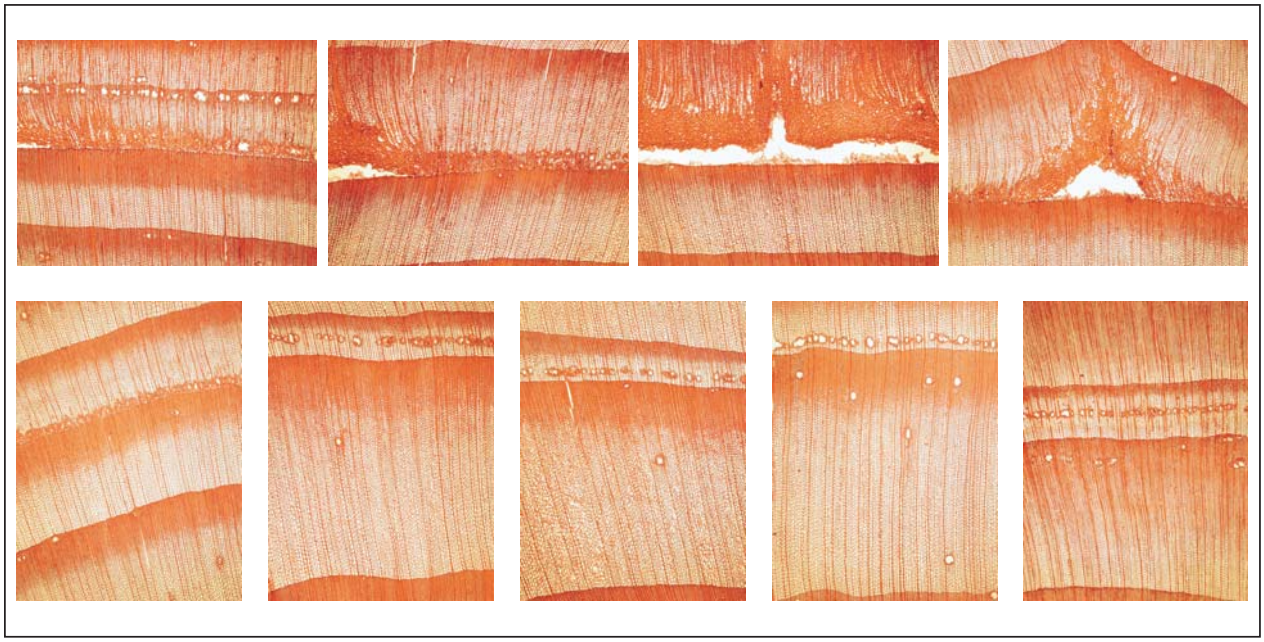

Appendix 5: Methods used to study past rockfall activity

Over the past few decades, tree-ring research gradually evolved from the pure dating of wood (e.g., dendrochronology or dendroarcheology) to the much broader field of dendroecology, including all branches of science involved in drawing some type of environmental information from tree-ring sequences (Schweingruber 1996). Dendrogeomorphology represents one of the many subfields of dendroecology and has repeatedly been used to study geomorphic processes and to date past events. The approach – developed by Alestalo (1971) and refined by Shroder (1978) – takes advantage of the fact that trees form yearly increment rings and that they immediately react to external disturbances.

5.1 Sampling trees and sample preparation

Dendrogeomorphological analyses comprise both investigations in the field and work in the lab: In the field, detailed geomorphic investigations and process analyses must precede the sampling of trees. In the case of rockfall, geomorphic maps indicating deposits may be helpful, but not compulsory. Once other geomorphic processes are identified and the area of "pure" rockfall influence determined, cores are extracted with increment borers or cross-sections sawn from trees. In the case of increment cores, we selected one core in the fall line of rocks and boulders (core c) and one core downslope (core d). In addition and because rockfall may also injure trees laterally, further samples were taken perpendicular to the slope (cores a, b) along with cores extracted from visible wounds and the overgrowing callous (also cf. Figs. A2.2 and B2.4). The extraction of increment cores as well as an example of an untreated *Larix decidua* core is illustrated in Figure F5.1.

Immediately after extraction, increment cores are labeled with (i) an abbreviated species name (e.g., LADE for *Larix decidua*, PCAB for *Picea abies*) as well as with (ii) an eight-digit identification code (e.g., STC0113c; with S = Stoffel, T = Täsch, C = Switzer-

Fig. F5.1 *Core extraction from the overgrowing callous of a heavily disturbed Larix decidua trees was realized with Suunto increment borers (*Forestry Suppliers 2005*) as to obtain increment cores allowing reconstruction of past rockfall activity. (Photo courtesy by Michelle Bollschweiler [a, b] and Dominique Schneuwly [c], used with permission)*

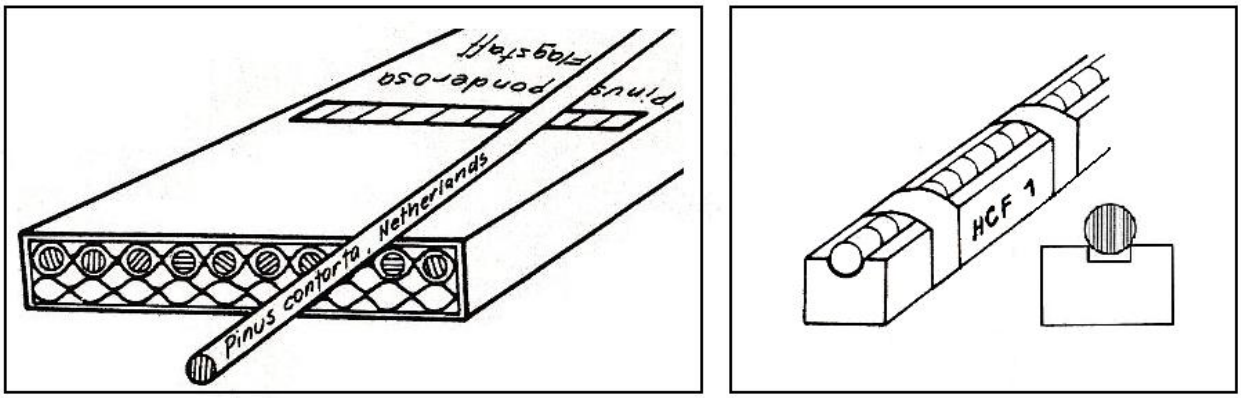

Fig. F5.2 *Increment cores are labeled for transport and stored in a receptacle (left), before they are mounted on woody support. Special care has to be given to the orientation of cores, as analysis is only possible as long as wood-fibers are oriented vertically (adapted after* Schweingruber 1983*).*

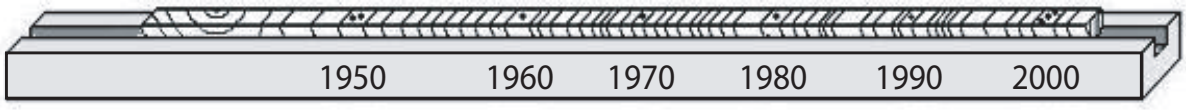

Fig. F5.3 *Counting tree rings and labeling increment cores (*Schneuwly 2003*).*

land, 01 = first transect, 13 = thirteenth tree, and c = upslope core). As shown in Figure F5.2 [7], samples are then stored in a receptacle for transport, before they are glued on woody supports and stabilized for at least one day with adhesive tape. Special care has to be given to the direction of wood-fibers, as analysis of the increment rings is only possible if the wood-fibers of the core are glued vertically on the support (Iseli & Schweingruber 1989).

As soon as the glue is completely dry (but the wood still sufficiently humid), the upper core surface is either sanded (polished) or cut with a cutter in order to allow analysis of individual tree rings or intra-annual features under the binocular. The visibility of individual increment rings or additional growth features can be further improved through the filling of cells with white chalk powder (crayon; Iseli & Schweingruber 1989).

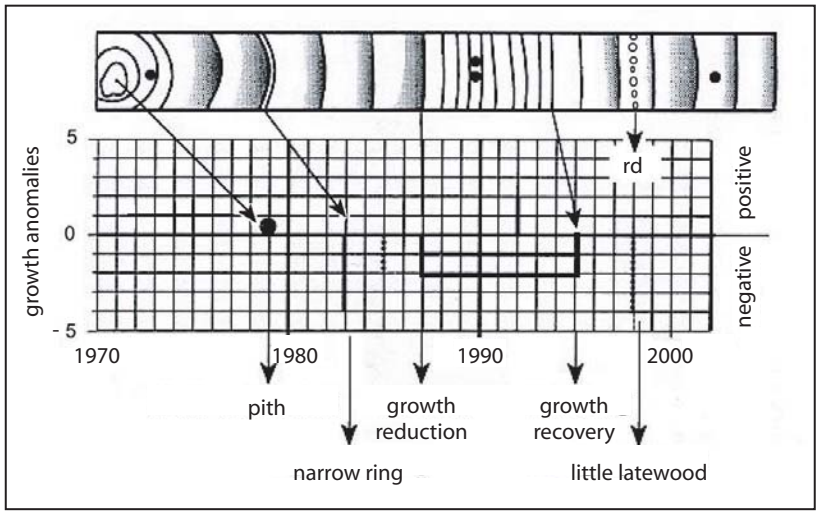

Fig. F5.4 *The realization of 'skeleton plots' consists in a systematic identification of abnormal growth features observed on single increment cores and helps in identifying e.g., missing or false tree rings or rockfall events (adapted after* Schweingruber 1996 *and* Kaennel & Schweingruber 1995*).*

[7] Most graphics used in Appendix F5 have initially been prepared by Dominique Schneuwly (Schneuwly 2003) and are used with permission.

Fig. F5.5 *In certain regions, Larix decidua trees sporadically suffer from larch bud moth outbreaks (Zeiraphera diniana Gn.): Caterpillars systematically 'graze' the young buds (left, center) before they change into a chrysalis as to become moths (right). (Photo courtesy by* Cfl *[*2003*; left, center] and Werner Baltensweiler [right], used with permission)*

5.2 Counting tree rings, skeleton plots and tree-ring measurement

The first analytical procedure consists in a counting of the increment rings, starting with the outermost tree ring (e.g., 2004). Tree rings indicating the beginning of a decade (1990, 1980) are marked with a dot, tree rings indicating the middle of a century (1950, 1850) with two dots and every century change (2000, 1900, 1800) is labeled with three dots. This procedure is illustrated in Figure F5.3, facilitates analysis and also helps with measurement.

In a following step, cores are analyzed visually and remarkable rings (e.g., extremely large or narrow increment rings, much or little latewood, reaction wood, traumatic rows of resin ducts, resin pockets or callous tissue) noted on skeleton plots (Schweingruber *et al.* 1990). As illustrated in Figure F5.4, this procedure allows identification of characteristic years present in a large number of samples (i.e. pointer years) as well as abnormal growth features occurring in single cores.

In addition, this graphical method not only assists in cross-dating samples, but also aims at identifying and locating missing or false rings through comparison of one tree-ring sequence with the next sequential record (Wiles *et al.* 1996). In the case of the *Larix decidua* trees sampled at *Täsch*, larch bud moth outbreaks (*Zeiraphera diniana Gn.*; Fig. F5.5) repeatedly caused abrupt growth reactions in both the reference samples and the trees influenced through rockfall activity. As such insect outbreaks leave characteristic marks in the growth pattern of all *Larix decidua* on the study site (i.e. abrupt growth reduction, narrow latewood), they can considerably help in assessing the completeness of tree-ring sequences, the accuracy of measurement or even facilitate the localization of mistakes (see Chapter F5.4). A compilation of micro-cuts with characteristic larch bud moth years is illustrated in Figure F5.6.

Thereafter, ring-widths are measured using a digital LINTAB positioning table connected to a Leica binocular. The software used (T. S. A. P. = Time Series Analysis and Presentation; Rinntech 2003) allows measurements of individual tree rings with a precision of 1/100 mm and visualization of ring-width graphs on the computer. The same program will also be used to test the quality of growth curves and to add missing tree rings.

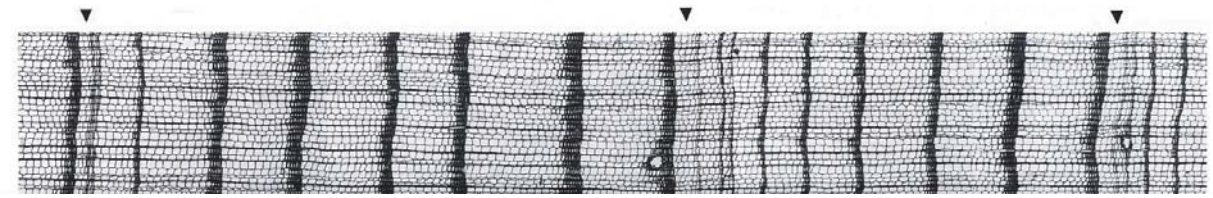

Fig. F5.6 *On the increment core, years with larch bud moth outbreaks are characterized with narrow rings and the quasi-absence of dark-colored latewood cells (adapted after* Schweingruber 2001*).*

5.3 Building a reference chronology with undisturbed trees

As growth reactions can be caused by factors other than geomorphic, samples of undisturbed reference trees have to be selected as well and a reference chronology needs to be built. This chronology is established with data from at least 15 trees growing in an undisturbed forest stand in the immediate neighborhood of the study site. In contrast to the disturbed trees, samples are taken perpendicular to the slope (i.e. cores a, b), as to avoid the presence of e.g., reaction wood. The characteristics of the reference site (e.g., elevation, slope exposure) need to correspond with those existing at the study site chosen for dendrogeomorphological analysis.

All in all, the reference chronology helps to differentiate locally predominant growth conditions driven by environmental factors such as e.g., temperatures, precipitation or occasional insect outbreaks (Cook & Kairiukstis 1990, Schweingruber 1996) from geomorphic disturbances in trees.

After the counting of increment rings on the cores, the realization of skeleton plots and the ring-width measurements, cores belonging to the same reference tree are compared both visually as well as with statistical procedures. Special attention is addressed to the *Gleichläufigkeit (Glk)* and the cross-dating index *(CDI)*, allowing identification of measuring mistakes as well as evaluation of the sample quality (Rinntech 2003). Only samples meeting the quality requirements of the *Glk* and the *CDI* are kept for further analysis. In a following step, one mean curve is derived for each of the remaining reference trees from cores a and b, as shown in Figure F5.7.

Thereafter, mean increment curves of individual reference trees are indexed, before long-term trends

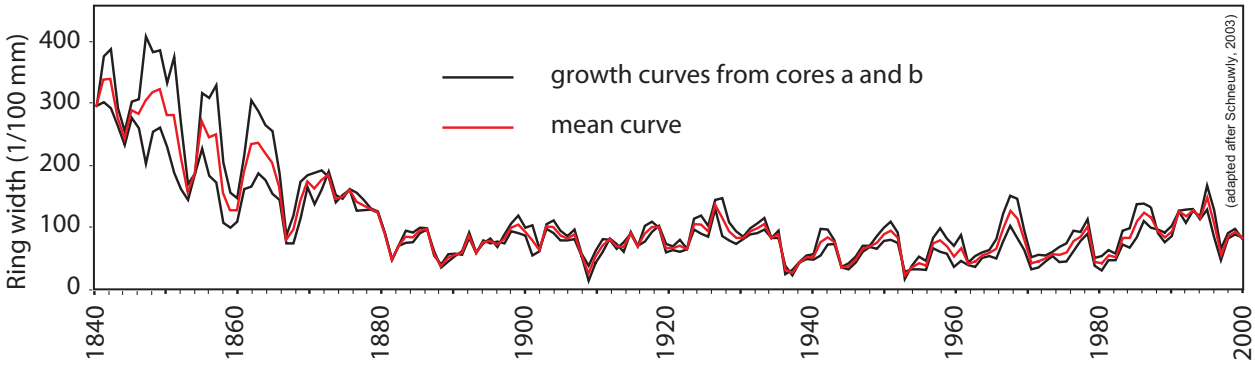

Fig. F5.7 *In a first step, a mean curve is built from the two growth curves (cores a, b) sampled for each reference tree.*

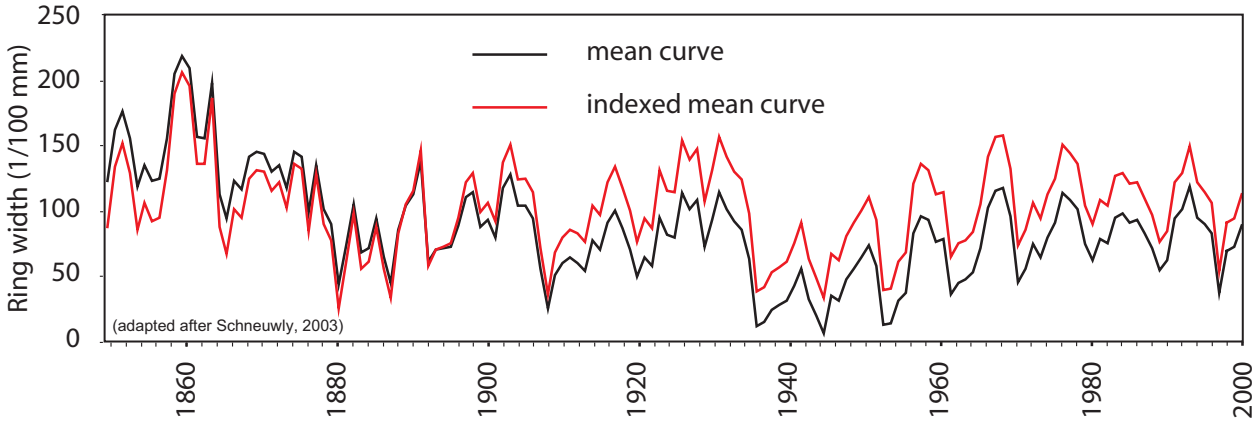

Fig. F5.8 *The mean (growth) curve of individual trees is indexed as to equalize growth of different intensity between the different trees to a comparable level.*

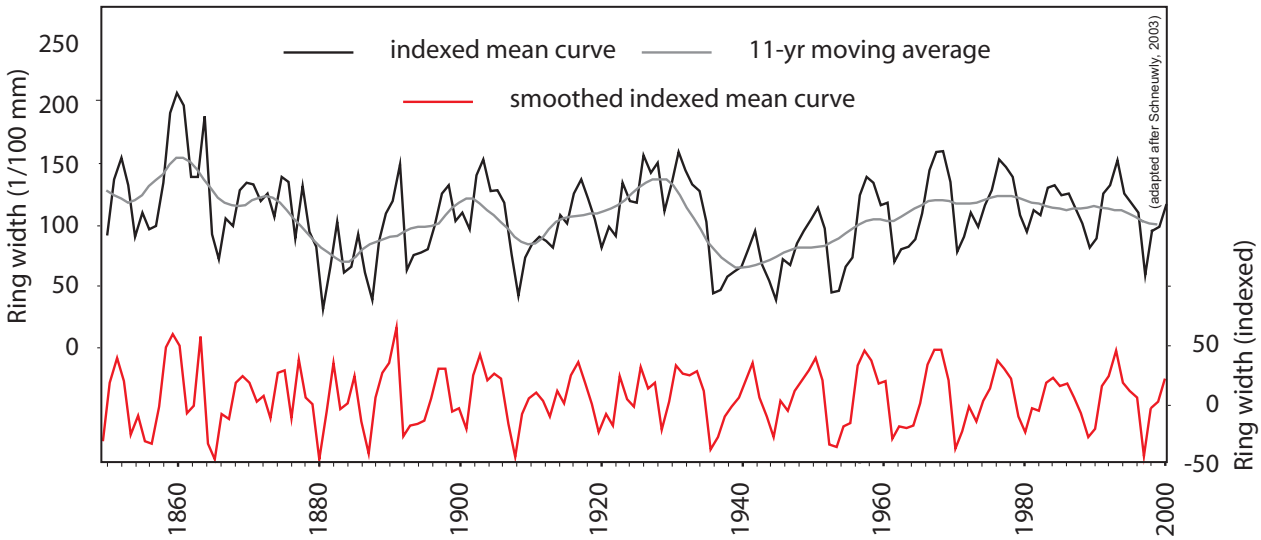

Fig. F5.9 *A 11-yr moving average is then applied as to remove long-term trends (e.g., ageing) from the indexed mean curve, resulting in a smoothed indexed mean curve illustrated in red.*

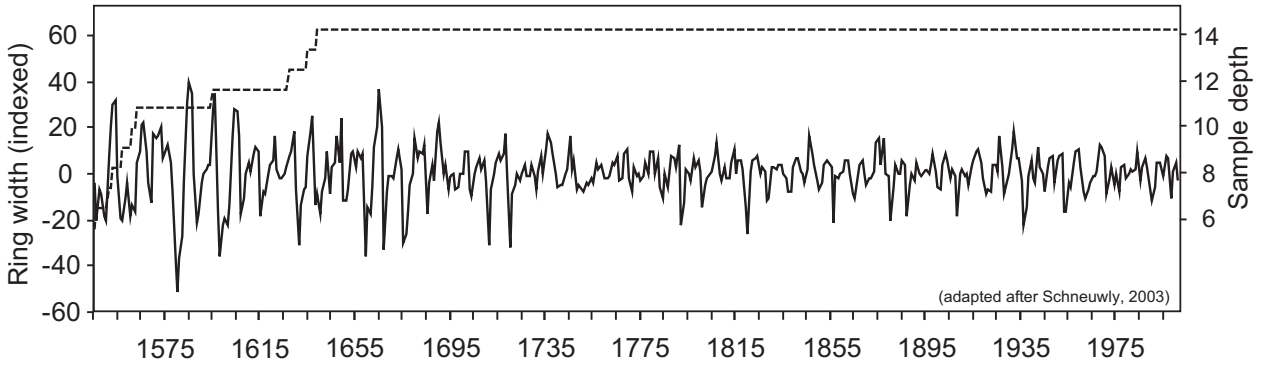

Fig. F5.10 *All the smoothed indexed mean curves are put together and an overall "mean curve" (i.e. reference chronology) derived. As can be seen from the illustration, the reference chronology built for analysis at Täschgufer covers the period 1545 – 2002 AD with a sample depth of at least five trees.*

such as ageing are smoothed with an 11-yr moving average. The two procedures are described in detail by Cook & Kairiukstis (1990) and illustrated in Figures F5.8 and F5.9. They considerably help to eliminate variations from the mean values. Only once all mean curves indexed and smoothed, an overall mean curve (i.e. reference chronology) can be established. An example of such a reference chronology is given in Figure F5.10. As reference trees normally are of non-uniform age, the number of data available for a reference chronology is gradually reduced the further back we go in time. As a consequence, the reference chronology at *Täschgufer* was only considered trustworthy as long as sample depth was larger than 5 trees.

5.4 Assessing past events in increment rings of disturbed trees

The analysis of heavily disturbed trees starts with the counting of tree rings, establishment of skeleton plots and the measurement of tree rings, as described for the realization of reference chronologies in Chapter F5.2. Thereafter and in contrast to the reference samples, tree-ring series are corrected where applicable. This procedure may consist in the elimination of false tree rings (e.g., wrong counting, presence of density fluctuations in the wood) or the insertion of missing rings. As illustrated in Figure F5.11, single cores of a disturbed tree are first compared among

each other and in a second step with the reference chronology. In the present case, one increment ring apparently misses in core a, whereas the other cores of the disturbed tree fit with the reference chronology. As a consequence, the position of the missing ring needs to be identified and a tree ring with a value 1 (i.e. 1/100 mm) added, as illustrated in Figure F5.12. Only once all increment cores of the disturbed trees corrected, rockfall events can be assessed and dated with yearly precision.

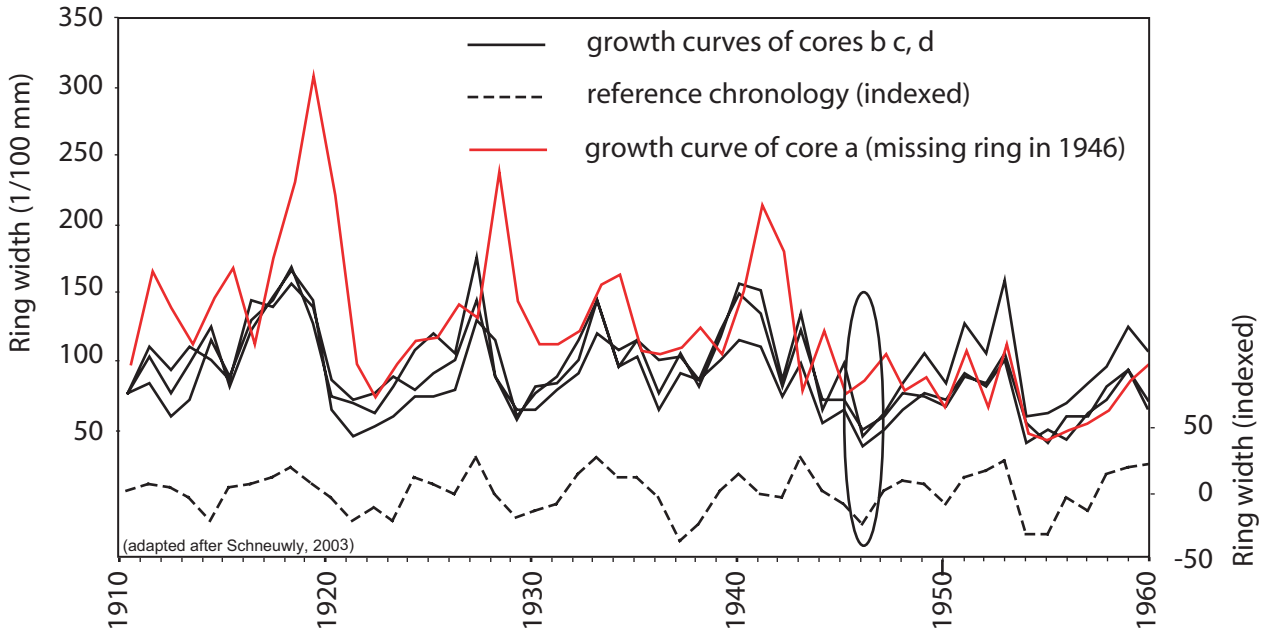

Fig. F5.11 *Comparison of four increment curves from the same disturbed tree with the indexed reference chronology. While general growth patterns neatly fit between cores b, c, d and the reference chronology, one increment ring is apparently missing in core for the year 1946.*

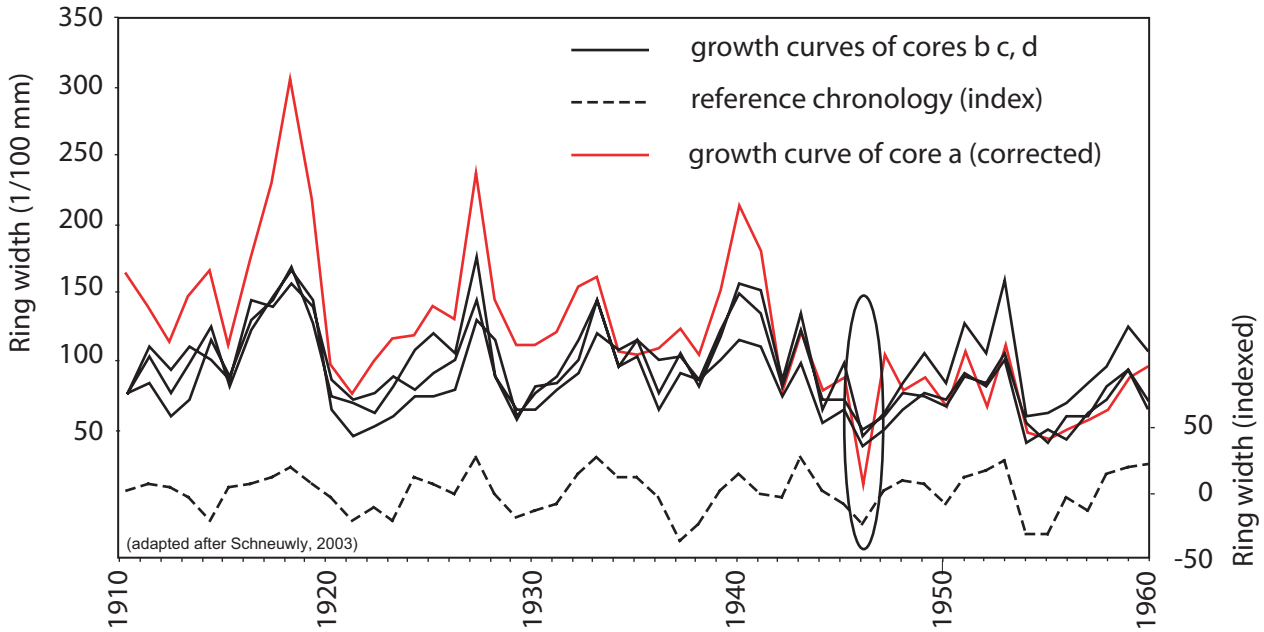

Fig. F5.12 *As soon as the missing ring is inserted with a value of 0.01 mm in core a, increment curves of this sample start to fit with the reference chronology as well.*

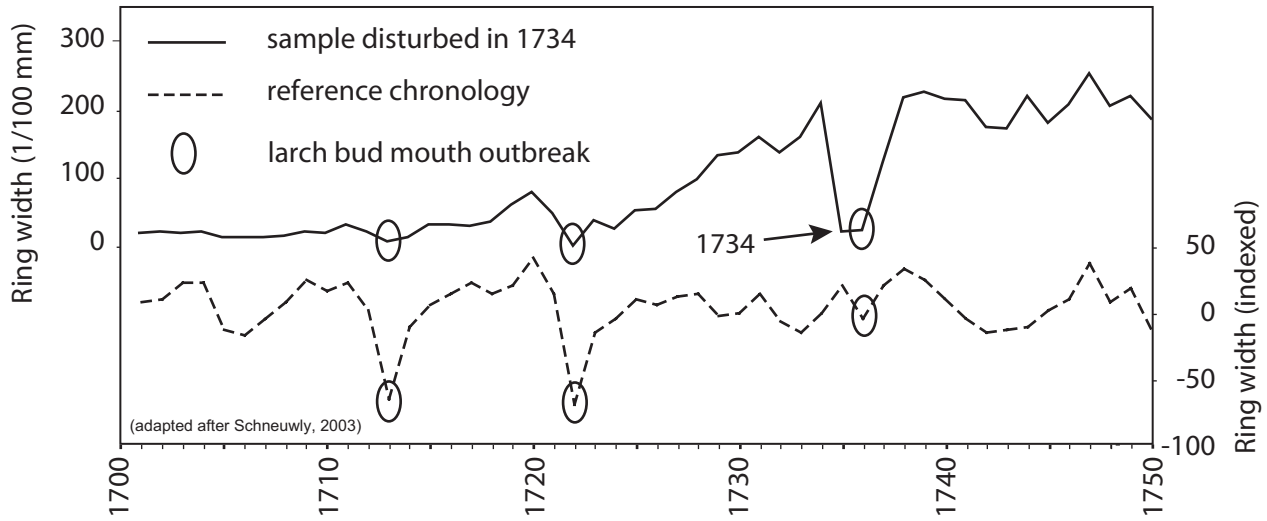

Fig. F5.13 *Abrupt growth reduction observed in the increment curve of a Larix decidua sample in 1734 AD: While growth reductions in 1713 and 1722 have been caused through insect outbreaks and are therefore present in the disturbed sample as well as in the reference chronology, the abrupt change in growth observed in 1734 was caused through rockfall.*

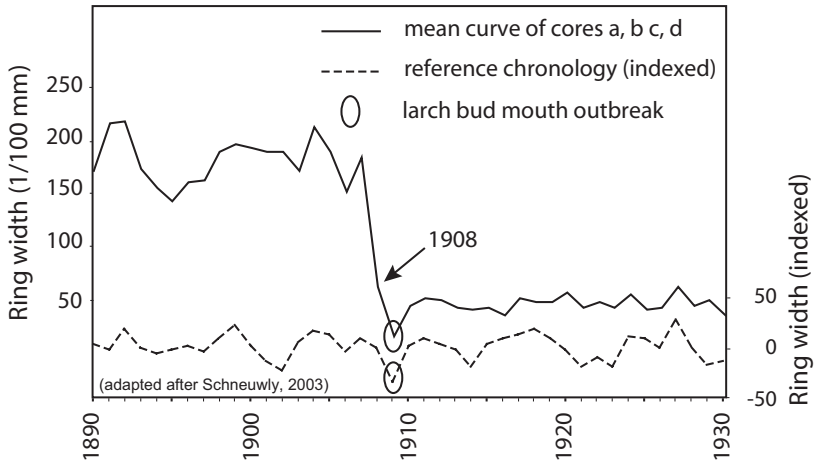

Fig. F5.14 *Abrupt growth reduction observed in samples a, b, c, and d – represented as a mean curve – with respect to the reference chronology. The traumatic event occurred in 1908, whereas the further reduction in 1909 was caused through a larch bud moth outbreak.*

In the trees selected at *Täschgufer*, the comparison of disturbed samples with the reference chronology mainly allowed identification of abrupt growth reduction, growth releases as well as the presence of reaction wood. The presence of abrupt growth reductions is illustrated in Figures F5.13 and F5.14. In the first example, larch bud moth outbreaks caused abrupt growth decreases in 1713 and 1722 in both the reference and the disturbed samples. In contrast, the abrupt growth reduction in 1734 was not provoked by insects, but through the impact of a rockfall fragment.

Similarly, the sample illustrated in Figure F5.14 badly suffered from rockfall activity in 1908, resulting in reduced growth. In addition, an insect outbreak in the following year (1909) further reduced the vitality of this tree, resulting in a long-lasting growth reduction.

The elimination of trees through rockfall activity sometimes results in growth releases in undamaged neighboring trees, as these trees can suddenly take advantage of improved environmental conditions (e.g., light, nutrients, water). Figure F5.15 illustrates the positive growth reactions observed in three *Larix decidua* trees after the high magnitude–low frequency rockfalls identified at *Täschgufer* in 1720. Growth releases are more difficult to date with yearly precision, reason why other signs of rockfall activity – such as scars or traumatic rows of resin ducts in neighboring trees – need to be assessed in order to correlate event data.

Further, the tilting of stems through rockfall impacts and the formation of reaction wood have been assessed to date past events. A characteristic example of reaction wood is illustrated in Figure F5.16. Here, the tree has been tilted downslope in 1922. As a consequence,

it immediately started with the formation of reaction wood in core d (downslope), whereas increment rings did not show any reactions in core c (upslope position).

Most commonly, past rockfall activity has, however, been assessed through the presence of traumatic rows of resin ducts and the presence of callous tissue (cf. Fig. F5.17) visible on the increment cores. As resin ducts may result from causes other than rockfall (e.g., climate, wind, insects, fraying or browsing by ungulates), thresholds were needed to distinguish rockfall-induced "resin duct events" from those of different origin. In the present case, resin ducts were only considered a result of rockfall activity if they formed (i) traumatic, (ii) extremely compact and (iii) continuous rows, as illustrated in Figure F5.18a. Both the presence of resin ducts on multiple radii in a single year and the occurrence of multiple consecutive years with traumatic rows of resin ducts were used as further indicators but not a compulsory criterion. In contrast, neither dispersed resin ducts within a single tree ring (cf. Fig. F5.18b) nor the presence of traumatic rows of resin ducts occurring in the years following an event represent (additional) rockfall-induced "resin duct events".

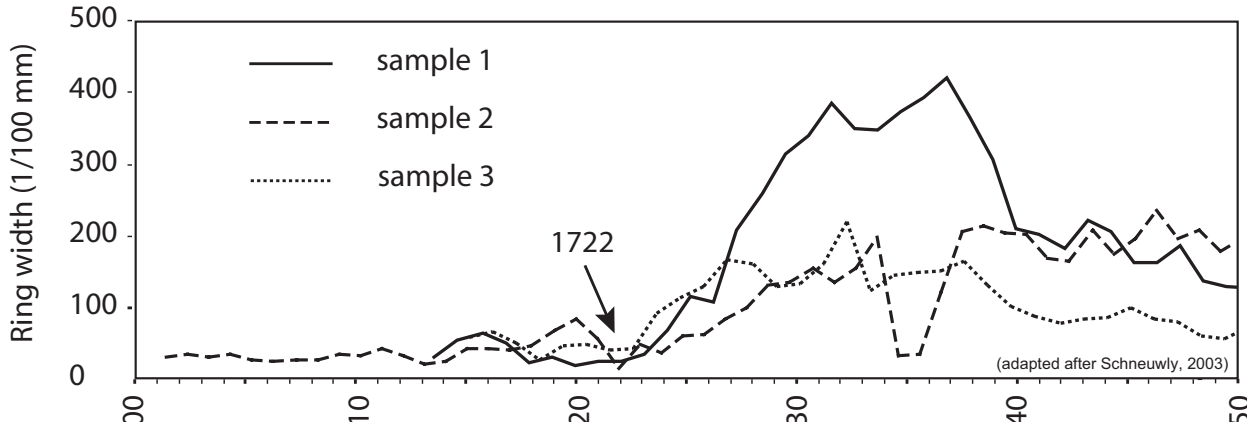

Fig. F5.15 *In the case of an elimination of neighboring trees, survivors sometimes show a release in their growth as a reaction to improved environmental conditions (e.g., light, water, nutrients). As to exactly assess the year of the event, periods with growth releases are normally dated with evidence found in other trees (reaction wood, traumatic rows of resin ducts, scars, etc.).*

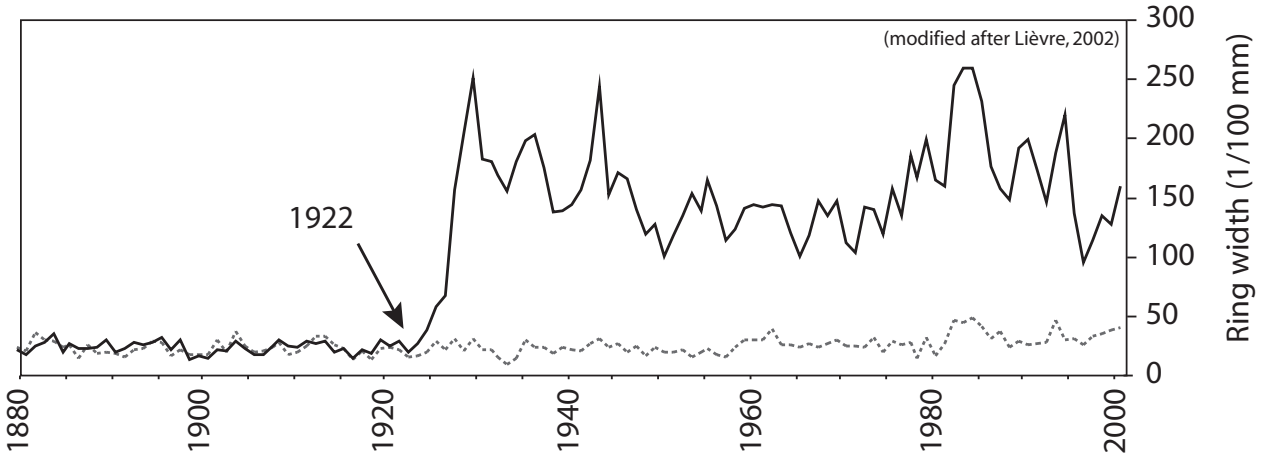

Fig. F5.16 *The tilting of stems causes conifer trees to produce reaction wood in order to redress their stems. As a consequence, abnormally large increment rings can be identified on the downslope side of the trunk, while in the cores facing upslope, tree growth remains unchanged.*

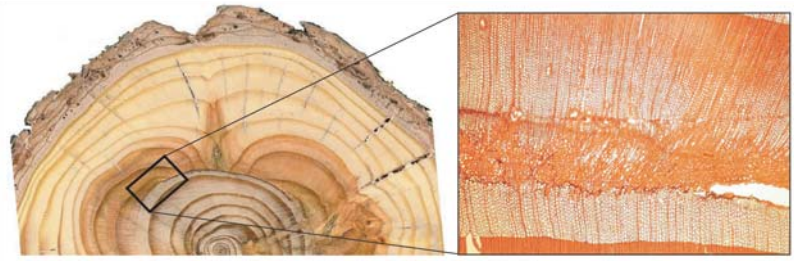

Fig. F5.17 *The formation of callous tissue after scarring is another good indicator of past events. While it rarely helps to date events with increment cores, it facilitates the determination of intra-annual rockfall activity on cross-sections or micro-cuts.*

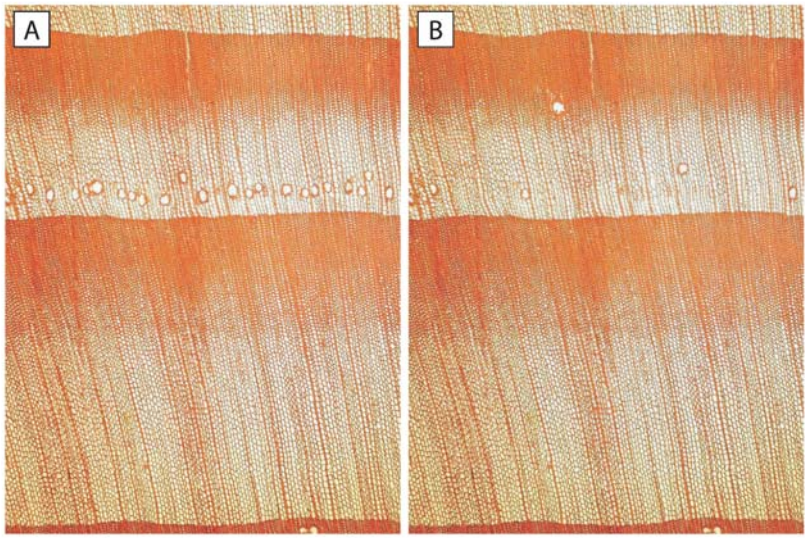

Fig. F5.18 *The presence of resin ducts in Larix decidua or Picea abies may be caused by a large array of environmental factors. As a consequence, resin ducts were only considered to be the result of past rockfall activity if they formed (i) traumatic, (ii) extremely compact and (iii) continuous rows, as illustrated in micro-cut (a). In contrast, the single dispersed resin ducts within a tree ring – illustrated in (b) – have been disregarded.*

5.5 Preparing micro-cuts from cross-sections

In order to assess the exact intra-annual position of traumatic rows of resin ducts and the onset of callous tissue formation, micro-cuts (also called thincuts) have been prepared from previously dated and age-corrected cross-sections in Chapter B1.

Micro-cuts are widely used in natural sciences in order to study microscopic changes, reason why the different techniques and procedures have repeatedly been described before (e.g., Schömmer 1949, Harms 1965, Schweingruber 1978, Clark 1981, Gerlach 1984). I will therefore only provide a short description on how micro-cuts have been prepared within this PhD study. For further details, Schweingruber (2001) and Schoch *et al.* (2004) give a comprehensive description.

The preparation of micro-cuts starts with the separation of small cubes (6-8 mm edges) from the *Larix decidua* cross-sections with a sharp knife or a small ax and a hammer. As to allow preparation of good micro-cuts and appropriate analysis of microscopic growth disturbances such as e.g., traumatic rows of resin ducts, reaction wood or the onset of callous tissue, samples have to be carefully oriented along the radial and tangential direction of cell structures. Thereafter, samples are inscribed with waterproof felt-tipped pen and cooked for about ten minutes as to soften the wood.

The cutting of micro-cuts from the woody blocks is then realized with a Reichert sliding microtome and very sharp wedge-shaped blades. The sharpness of the blade as well as the absence of notches are crucial for the realization of high quality micro-cuts, reason why the blades are regularly grinded with a high-precision Leica SP 9000 grinding-machine. Both a Reichert sliding microtome and a Leica SP 9000 grinding-machine were used at the Swiss Federal Research Institute WSL within this PhD study.

Once the wood softened and the blades sharpened, the small blocks are fixed to the sliding microtome and the cutting angle between the blade and the sectional plane adjusted to approximately 15° as well as the

thickness of the cut put to approximately 15 micrometers. During the cutting process, a thin paintbrush is holding on the sectional plane as to avoid rolling of the micro-cuts. The preparation is then carefully put on a slide and analyzed under the binocular. If the quality of the cut is satisfying, the sample is covered with several drops of glycerin as to avoid the drying up of the sample and to allow short-time storage of the samples.

In a following step, cell contents (stark grains) are removed and samples bleached with NaOCl (javel water). The micro-cut is left for 15 to 30 minutes in this sodium hypochlorite solution. Thereafter, it is put on a copper sieve and extensively rinsed for two to three minutes with de-ionized water. As soon as there is no NaOCl odor left, the micro-cut is stained for several minutes with a 1% watery safranin solution. In a following step, excessive color is removed with de-ionized water and the sample rinsed with 50% alcohol. Rinsing is repeated (i) two to three times with 96% alcohol in order to remove excessive stain and (ii) once more with 100% alcohol, before the micro-cut is transferred into a xylol solution. If the liquid turns murky, rinsing is repeated with 100% alcohol.

In a final step, the micro-cut is again put on a slide, fixed with some droplets of synthetic resin (e.g., Canada balm), and mounted with a coverslip. Slides are then heated in order to remove air bubbles and fixed with magnets on a metal plate and kept for at least 24 hours in a drying-closet (60° C) or for two weeks at room temperature in order to allow hardening of slide preparations. Thereafter, micro-cuts are ready for analysis of e.g., intra-annual positions of traumatic rows of resin ducts or the onset of callous tissue formation. In contrast to the analysis of increment cores or cross-sections alone, micro-cuts allow investigations in much greater detail, as illustrated in Figure F5.19.

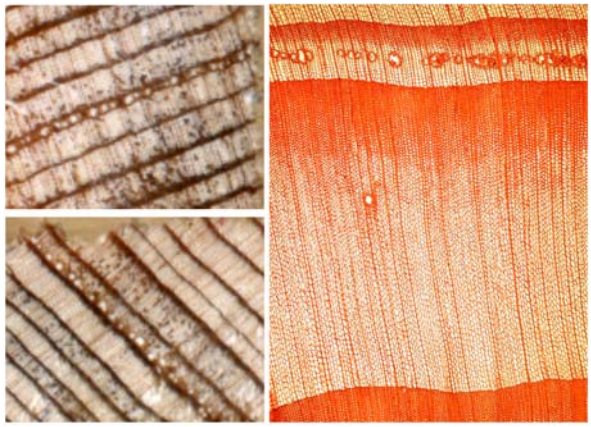

Fig. F5.19 *Traumatic rows of resin ducts as seen on increment cores (left) and micro-cuts (right). While cores are largely sufficient to accurately date event years with resin ducts, the intra-seasonal timing can only be assessed on neatly polished cross-sections or on micro-cuts (right).*

*****

Bibliography

A

Abele, G., 1971. *Bergstürze in den Alpen.* Wissenschaftliche Alpenvereinshefte 25. München.

– , 1994. Large rockslides: their causes and movement on internal sliding planes. *Mountain Research and Development* **14(4)**, 315–320.

Agliardi, F., Crosta, G. B. 2002a. High-resolution 3D numerical modelling of rockfalls. *Geophysical Research Abstracts* **EGS02-A-02514**.

– , 2002b. 3D numerical modelling of rockfalls in the Lecco urban area (Lombardia Region, Italy). In: de Gama C., Ribeiro e Sous, L. (eds.), *Proceedings of the EUROCK 2002, I.S.R.M. International Symposium on Rock Engineering for Mountainous Regions, Madeira*, pp. 79–86.

– , 2003. High resolution three-dimensional numerical modelling of rockfalls. *International Journal of Rock Mechanics and Mining Sciences* **40**, 455–471.

Agliardi, F., Cardinali, M., Crosta, G. B., Guzzetti, F., Detti, R., Reichenbach, P., 2001. A computer program to evaluate rockfall hazard and risk at the regional scale. Examples from the Lombardy Region. *Geophysical Research Abstracts* **3**, 8617.

Alestalo, J., 1971. Dendrochronological interpretation of geomorphic processes. *Fennia* **105**, 1–139.

Allen, R. B., Bellingham, P. J., Wiser, S. K., 1999. Immediate damage by an earthquake to a temperate montane forest. *Ecology* **80**, 708–714.

André, M.-F., 1986. Dating slope deposits and estimating rates of rockfall wall retreat in Northwest Spitsbergen by lichenometry. *Geografiska Annaler* **68**, 65–75.

– , 1997. Holocene rockwall retreat in Svalbard: a triple-rate evolution. *Earth Surface Processes and Landforms* **22**, 423–440.

– , 2003. Do periglacial landscapes evolve under periglacial conditions? *Geomorphology* **52**, 149–164.

Annen, B., Redmann, M., 1993. *Bannwald Altdorf.* Amt für Forst- und Jagdwesen. Gisler Druck, Altdorf.

Antonini, G., Ardizzone, F., Cardinali, M., Galli, M., Guzzetti, F., Reichenbach, P., 2002. Surface deposits and landslide inventory map of the area affected by the 1997 Umbria-Marche earthquake. *Bolletino della Società Geologica Italiana* **121(2)**, 843–853.

Ayala-Carcedo, F. J., Cubillo-Nielson, S., Alvarez, A., Dominguez, M. J., Lain, J., Lain, R., Ortiz, G., 2003. Large scale rockfall reach susceptibility maps in La Cabrera Sierra (Madrid) performed with GIS and dynamic analysis at 1:5,000. *Natural Hazards* **30**, 325–340.

Azzoni, A., Barbera, G. L., Zanizetti, A., 1995. Analysis and prediction of rockfalls using a mathematical model. *International Journal of Rock Mechanics and Mining Science* **32**, 709–724.

B

Bachrach, T., Jakobsen, K., Kinney, J., Nishimura, P., Reyes, A., Laroque, C. P., Smith, D. J., 2004. Dendrogeomorphological assessment of movement at Hilda rock glacier, Banff National Park, Canadian Rocky Mountains. *Geografiska Annaler* **86A**, 1–9.

Badoux, A., Hegg, C., Kienholz, H., Weingartner, R., 2002. Investigations on the influence of storm caused damage on the runoff formation and erosion in small torrent catchments. In: *International Congress Interpraevent 2002 in the Pacific Rim (IPR), Matsumoto, Japan*, pp. 961–971.

Baillie, M. G. L., 1994. Dendrochronology raises questions about the nature of the AD 536 dust-veil event. *Holocene* **4**, 212–217.

Baillifard, F., Jaboyedoff, M., Sartori, M., 2003. Rockfall hazard mapping along a mountainous road in Switzerland using a GIS-based parameter rating approach. *Natural Hazards and Earth System*

Sciences **3**, 431–438.

Barnikel, F., 2004. The value of historical documents for hazard zone mapping. *Natural Hazards and Earth System Sciences* **4**, 599–613.

Bartelt, P., Stöckli, V., 2001. The influence of tree and branch fracture, overturning and debris entrainment on snow avalanche flow. *Annals of Glaciology* **32**, 209–216.

Baumann, F., Kaiser, K.F., 1999. The Multetta debris fan, eastern Swiss Alps: a 500-year debris flow chronology. *Arctic and Alpine Research* **31(2)**, 128–134.

Bayard, M., Schweingruber, F. H., 1991. Ein Baumgrenzstandort: Das Wildwasserbett der Maggia im Tessin, Schweiz. Eine dendroökologische Studie. *Botanica Helvetica* **101**, 9–28.

Bearth, P., 1964. *Geologischer Atlas der Schweiz 1:25'000. Blatt Randa.* Erläuterungen. Schweizerische Geologische Kommission, Bern.

Bebi, P., Kienast, F., Schönenberger, W., 2001. Assessing structures in mountain forests as a basis for investigating the forests' dynamics and protective function. *Forest Ecology and Management* **145**, 3–14.

Becker, A., Davenport, C. A., 2003. Rockfalls triggered by the AD 1356 Basle Earthquake. *Terra Nova* **15**, 258–264.

Beniston, M., 2005. Warm winter spells in the Swiss Alps: Strong heat waves in a cold season? A study focusing on climate observations at the Saentis high mountain site. *Geophysical Research Letters* **32**, L01812.

Berger, F., Lievois, J., 1999. Determination of priority forest work areas and creation of green areas in risk prevention plans – an example of researcher-specialist transfer. In: *Proceedings International Conference on Mountain Natural Hazards, Grenoble, France*, pp. 412–416.

Berger, F, Rey, F., 2004. Mountain protection forests against natural hazards and risks: New French developments by integrating forests in risk zoning. *Natural Hazards* **33**, 395–404.

Berger, F., Quetel, C., Dorren, L. K. A., 2002. Forest: A natural protection mean against rockfall, but with which efficiency? The objectives and methodology of the ROCKFOR project. In: *Proceedings International Congress Interpraevent 2002 in the Pacific Rim, Matsumoto, Japan,* pp. 815–826.

Biondi, F., Estrada, I. G., Ruiz, J. C. G., Torres, A. E., 2003. Tree growth response to the 1913 eruption of Volcán de Fuego de Colima, Mexico. *Quaternary Research* **59**, 293–299.

Bloetzer, W., Stoffel, M., 1998. Klimawandel als Herausforderung für die Raumplanung der Vispertäler. In: Bloetzer, W., Egli, T., Petrascheck, A., Sauter, J., Stoffel, M. (eds.), *Klimaänderungen und Naturgefahren in der Raumplanung – Methodische Ansätze und Fallbeispiele.* Synthesebericht NFP31. vdf Hochschulverlag, Zürich, pp. 127–200.

Bloetzer, W., Egli, T., Petrascheck, A., Sauter, J., Stoffel, M., 1998. *Klimaänderungen und Naturgefahren in der Raumplanung – Methodische Ansätze und Fallbeispiele.* Synthesebericht NFP31. vdf Hochschulverlag, Zürich.

Bollschweiler, M., Stoffel, M., Schneuwly, D., 2005. Entwicklung der Murrinnen im Täschgufer seit 1936. *wasser, energie luft* **97(7–8)**, 218–223.

Bozzolo, D., Pamini, R., 1986. Simulation of rock falls down a valley side. *Acta Mechanica* **63**, 113–130.

Bozzolo, D., Pamini, R., Hutter, K., 1988. Rockfall analysis – a mathematical model and its test with field data. In: *Proceedings of the 5th International Symposium on Landslides, Lausanne*, pp. 555–560.

Braam, R. R., Weiss, E. E. J, Burrough, P. A., 1987. Spatial and temporal analysis of mass movement using dendrochronology. *Catena* **14**, 573–584.

Bräker, O. U., 2002. Measuring and data processing in tree-ring research – a methodological introduction. *Dendrochronologia* **20(1-2)**, 203–216.

Bräuning, A., 1995. Zur Anwendung der Dendrochronologie in den Geowissenschaften. *Die Erde* **126**, 189–204.

Brang, P., 2001. Resistance and elasticity: promising concepts for the management of protection forests in the European Alps. *Forest Ecology and Management* **145**, 107–117.

Brang, P., Schönenberger, W., Ott, E., Gardner, B., 2001. Forests as protection from natural hazards. In: Evans, J. (ed.), *The Forests Handbook Volume 2*. Blackwell Science, Oxford, pp. 53–81.

Brauner, M., Weinmeister, W., Agner, P., Vospernik, S., Hoesle, B., 2005. Forest management decision support for evaluating forest protection effects against rockfall. *Forest Ecology and Management* **207**, 75–85.

Briffa, K. R., Osborn, T. J., Schweingruber, F. H., Harris, I. C., Jones, P. D., Shiyatov, S. G., Vaganov, E. A., 2001a. Low-frequency temperature variations from a northern tree ring density network. *Journal of Geophysical Research* **106 (D3)**, 2929–2941.

Brown, P. M., Swetnam, T. W., 1994. A cross-dated fire history from coast redwood near Redwood National Park, California. *Canadian Journal of Forest Research* **24**, 21–31.

Budetta, P., 2004. Assessment of rockfall risk along

roads. *Natural Hazards and Earth System Sciences* **4**, 71–81.

Budetta, P., Santo, A., 1994. Morphostructural evolution and related kinematics of rockfalls in Campania (southern Italy). *Engineering Geology* **36**, 197–210.

Bull, W. B., Brandon, M. T., 1998. Lichen dating of earthquake-generated regional rockfall events, Southern Alps, New Zealand. *Geological Society of America Bulletin* **110**, 60–84.

Bull, W. B., King, J., Kong, F., Moutoux, F., Phillips, W. M., 1994. Lichen dating of coseismic landslide hazards in alpine mountains. *Geomorphology* **10**, 253–264.

Bunce, C. M., Cruden, D. M., Morgenstern, N. R., 1997. Assessment of the hazard of rock fall on a highway. *Canadian Geotechnical Journal* **34**, 344–356.

Burbank, D. W., Anderson, R. S., 2001. *Tectonics geomorphology.* Blackwell Science, Oxford.

Butler, D. R., Oelfke, J. G., Oelfke, L. A., 1986. Historic rockfall avalanches, northeastern Glacier National Park, Montana, USA. *Mountain Research and Development* **6**, 261–271.

Butler, D. R., Malanson, G. P., Walsh, S. J., 1992. Snow-avalanche paths: conduits from the periglacial-alpine to the subalpine-depositional zone. In: Dixon, J. C., Abrahams, A. D. (eds.), *Periglacial Geomorphology*. John Wiley, Chichester, pp. 185–202.

Buwal, Brp, Bww, 1997. *Naturgefahren. Empfehlungen 1997. Berücksichtigung der Massenbewegungsgefahren bei raumwirksamen Tätigkeiten.* Bundesamt für Umwelt, Wald und Landschaft, Bundesamt für Raumplanung und Bundesamt für Wasserwirtschaft, Bern.

C

Camarero, J. J., Guerrero-Campo, J., Gutiérrez, E., 1998. Tree-ring growth and structure of Pinus uncinata and Pinus sylvestris in the Central Spanish Pyrenees. *Arctic and Alpine Research* **30(1)**, 1–10.

Cancelli, A., Crosta, G., 1993. Hazard and risk assessment in rockfall prone areas. *Proceedings of the Conference on Risk and Reliability in Ground Engineering, London,* 177–190.

Cardinali, M., Reichenbach, P., Guzzetti, F., Ardizzone, F., Antonini, G., Galli, M., Caccione, M., Castellani, M., Salvati, P., 2002. A geomorphological approach to estimate landslide hazard and risk in urban and rural areas in Umbria, central Italy. *Natural Hazards and Earth System Sciences* **2**, 57–72.

Carter, R., LeRoy, S., Nelson, T., Laroque, C. P., Smith, D. J., 1999. Dendroglaciological investigations at Hilda Creek rock glacier, Banff National Park, Canadian Rocky Mountains. *Géographie physique et Quaternaire* **53**, 365–371.

Cattiau, V., Marie, E., Renaud, J. P., 1995. Forêt et protection contre les chutes de rochers. *Ingénieries Cemagref Eau–Agrigulture–Territoire* **3**, 45–54.

Chau, K. T., Wong, R. H. C., Lee, C. F., 1998. Rockfall problems in Hong Kong and some new experimental results for coefficient of restitution. *International Journal of Rock Mechanics and Mining Science & Geomechanical Abstracts* **35**, 662–663.

Chau, K. T., Tang, Y. F., Wong, R. H. C., 2004. GIS based rockfall hazard map for Hong Kong. *International Journal of Rock Mechanics and Mining Science* **35(4)**, 662–663.

Chauvin, C., Renaud, J.P., Rupé, C., 1994. Stabilité et gestion des forêts de protection. *ONF Bulletin Technique* **27**, 37–52.

Chen, H., Chen, R., Huang, T., 1994. An application of an analytical model to a slope subject to rockfall. *Bulletin of the Association of Engineering Geologists* **31(4)**, 447–458.

Church, M., Stock, R. F., Ryder, J. M., 1979. Contemporary sedimentary environments on Baffin Island, N.W.T., Canada: debris slope accumulations. *Arctic and Alpine Research* **11**, 371–402.

Clark, G., 1981. *Staining procedures*. Williams and Wilkins, Baltimore and London.

Cook, E. R., Kairiukstis, L. A., 1990. *Methods of dendrochronology – Applications in the environmental sciences.* Kluwer, London.

Coutard, J. P., Francou, B. 1989. Rock temperature measurements in two alpine environments: implications for frost shattering. *Arctic and Alpine Research* **21**, 399–416.

Crosta, G. B., Agliardi, F., 2003. A methodology for physically based rockfall hazard assessment. *Natural Hazards and Earth System Sciences* **3**, 407–422.

– , 2004. Parametric evaluation of 3D dispersion of rockfall trajectories. *Natural Hazards and Earth System Sciences* **4**, 583–598.

Crosta, G. B., Agliardi, F., Frattini, P., Imposimato, S., 2004. A three dimensional hybrid numerical model for rockfall simulation. *Geophysical Research Abstracts* **6**, 04502.

Cruden, D. M., Varnes, D. J., 1996. Landslide types and processes. In: Turner, A. K., Schuster, R. L. (eds.), *Landslides, investigation and mitigation. Transportation Research Board.* Special Report 247. Washington D.C., pp. 36–75.

D

Davies, M. C. R., Hamza, O., Harris, C., 2001. The effect of rise in mean annual temperatures on the stability of rock slopes containing ice filled discontinuities. *Permafrost and Periglacial Processes* **12**, 137–144.

Day, R. W., 1997. Case studies of rockfall in soft versus hard rock. *Environmental and Engineering Geoscience* **3(1)**, 133–140.

DeGraff, J. V., Agard, S. S., 1984. Defining geologic hazards for natural resources management using tree-ring analysis. *Environmental Geology and Water Sciences* **6(3)**, 147–155.

Descoeudres, F., 1990. L'éboulement des Crétaux: Aspects géotechniques et calcul dynamique des chutes de blocs. *Mitteilungen der Schweizerischen Gesellschaft für Boden- und Felsmechanik* **121**, 19–25.

Descoeudres, F., Zimmermann, T., 1987. Three-dimensional dynamic calculation of rockfalls. In: Herget, G, Vongpaisal, S. (eds.), *Proceedings of the Sixth International Congress on Rock Mechanics, Montreal.* Balkema, Rotterdam, pp. 337–342.

Donzé, F., Magnier, S. A., Montani, S., Descoeudres, F., 1999. Numerical study of rock block impacts on soil-covered sheds by a discrete element method. In: *Cinquième Conférence Nationale en Génie Parasismique AFPS '99, Cachan*.

Dorren, L. K. A., 2002. *Mountain geoecosystems – GIS modeling of rockfall and protection forest structure.* Dissertation. Universiteit van Amsterdam.

– , 2003. A review of rockfall mechanics and modelling approaches. *Progress in Physical Geography* **27(1)**, 69–87.

Dorren, L. K. A., Seijmonsbergen, A. C., 2003. Comparison of three GIS-based models for predicting rockfall runout zones at a regional scale. *Geomorphology* **56**, 49–64.

Dorren L. K. A., Heuvelink, G. B. M., 2004. Effect of support size on the accuracy of a distributed rockfall model. *International Journal of Geographical Information Science* **18(6)**, 595–609.

Dorren, L. K. A., Berger, F., 2005. Energy dissipation and stem breakage of trees at dynamic impacts. *Tree Physiology* **26**, 63–71.

Dorren, L. K. A., Berger, F., Imeson, A. C., Maier, B., Rey, F., 2004a. Integrity, stability and management of protection forests in the European Alps. *Forest Ecology and Management* **195**, 165–176.

Dorren, L. K. A., Maier, B., Putters, U. S., Seijmonsbergen, A. C., 2004b. Combining field and modelling techniques to assess rockfall dynamics on a protection forest hillslope in the European Alps. *Geomorphology* **57**, 151–167.

Dorren, L. K. A., Berger, F., Le Hir, C., Mermin, E., Tardif, P., 2005. Mechanisms, effects and management implications of rockfall in forests. *Forest Ecology and Management* **215(1-3)**, 183–195.

Dorren, L. K. A., Berger, F., subm. Real size experiments and 3D simulation of rockfall on forest slopes. *Natural Hazards and Earth System Sciences*, in review.

Douglas, G. R., 1980. Magnitude frequency study of rockfall in Co. Antrim, Northern Ireland. *Earth Surface Processes and Landforms* **5**, 123–129.

Duc, P., Brändli, U. B., Brassel, P., 2004. Der Schutzwald im zweiten Schweiz. Landesforstinventar (LFI2). In: Eidgenössische Forschungsanstalt WSL (ed.), *Schutzwald und Naturgefahren. Forum für Wissen 2004.* Bruhin AG, Freienbach, pp. 7–13.

Dussauge, C., Grasso, J. R., Helmstetter, A., 2003. Statistical analysis of rockfall volume distribution: Implications for rockfall dynamics. *Journal of Geophysical Research* **108(B6)**, 2286.

Dussauge-Peisser, C., Helmstetter, A., Grasso, J. R., Hantz, D., Desvarreux, P., Jeannin, M., Giraud, A., 2002. Probabilistic approach to rock fall hazard assessment: potential of historical data analysis. *Natural Hazards and Earth System Sciences* **2**, 15–26.

E

Eberhardt, E., Willenberg, H., Loew, S., Maurer, H., 2001. Active rockslides in Switzerland – understanding mechanisms and processes. In: *International Conference on Landslides – Causes, Impacts and Countermeasures, Davos,* pp. 25–34.

Eberhardt, E., Stead, D., Coggan, J. S., 2004. Numerical analysis of initiation and progressive failure in natural rock slopes – the 1991 Randa rockslide. *International Journal of Rock Mechanics and Mining Sciences* **41**, 69–87.

Eberhart-Phillips, D., Haeussler, P. J., Freymueller, J. T., Frankel, A. D., Rubin, C. M., Craw, P., Ratchkovski, N. A., Anderson, G., Carver, G. A., Crone, A. J., Dawson, T. E., Fletcher, H., Hansen, R., Harp, E. L., Harris, R. A., Hill, D. P., Hreinsdottir, S., Jibson, R. W., Jones, L. M., Kayen, R., Keefer, D. K., Larson, C. F., Moran, S. C., Personius, S. F., Plafker, G., Sherrod, B., Sieh, K., Sitar, N., Wallace, W. K., 2003. The 2002 Denali fault earthquake, Alaska: a large magnitude, slip-partitioned event. *Science* **300**, 1113–1118.

Eisbacher, G. H., Clague, J. J., 1984. Destructive mass movements in high mountains: hazard and management. *Geological Survey of Canada Paper* **84-16**, 1–230.

Erismann, H. T., 1986. Flowing, rolling, bouncing, synopsis of basic mechanisms. *Acta mechanica* **64**, 101–110.

Erismann, H. T., Abele, G., 2001. *Dynamics of rockslides and rockfalls*. Springer, Berlin, Heidelberg and New York.

Evans, S. G., 1997. Fatal landslides and landslide risk in Canada. In: *Proceedings of the International Workshop on Landslide Risk Assessment, Honolulu, USA*. Balkema, Rotterdam, pp. 620–636.

Evans, S. G., Hungr, O., 1993. The assessment of rockfall hazards at the base of talus slopes. *Canadian Geotechnical Journal* **30**, 620–636.

F

Fahey, B. D., Lefebure, T. H., 1988. The freeze-thaw weathering regime at a section of the Niagara Escarpment on the Bruce Peninsula, Southern Ontario, Canada. *Earth Surface Processes and Landforms* **13**, 293–304.

Fantucci, R., 2002. Dendroseismological analysis of the Irpina fault (South Italy). In: *Proceedings 6th International Conference on Dendrochronology,* August 2002, Quebec City, , pp. 94–96.

Fantucci, R., Sorriso-Valvo, M., 1999. Dendrogeomorphological analysis of a slope near Lago, Calabria (Italy). *Geomorphology* **30**, 165–174.

Faz, 2003. Wetterfolgen. Matterhorn nach Felssturz gesperrt. *Frankfurter Allgemeine Zeitung* **163** (17.07.2003), 7.

Flageollet, J. C., Weber, D., 1996. Fall. In: Dikau, R., Schrott, L., Brunsden, D., Ibsen, M. (eds.), *Landslide Recognition.* Wiley, West Sussex, pp. 13–28.

Foetzki, A., Jonsson, M., Kalberer, M., Simon, H., Mayer, A. C., Lundström, T., Stöckli, V., Ammann, W. J., 2004. Die mechanische Stabilität von Bäumen: das Projekt Baumstabilität des FB Naturgefahren. In: Eidgenössische Forschungsanstalt WSL (ed.), *Schutzwald und Naturgefahren. Forum für Wissen 2004.* Bruhin AG, Freienbach, pp. 35–42.

Frehner, M., Wasser, B., Schwitter, R., 2005. *Nachhaltigkeit und Erfolgskontrolle im Schutzwald. Wegleitung für Pflegemassnahmen in Wäldern mit Schutzfunktion.* Bundesamt für Umwelt, Wald und Landschaft, Bern.

Fritts, H. C., 1976. *Tree Rings and Climate*. Academic Press, London.

G

Gardner, J., 1970. Rockfall: a geomorphic process in high mountain terrain. *Albertan Geographer* **6**, 15–20.

–, 1980. Frequency, magnitude, and spatial distribution of mountain rockfalls and rockslides in the Highwood Pass Area, Alberta, Canada. In: Coates, R., Vitek, J. D. (eds.), *Thresholds in Geomorphology.* Allen and Unwin, New York, pp. 267–295.

– , 1983. Rockfall Frequency and Distribution. *Zeitschrift für Geomorphologie N.F.* **27(3)**, 311–324.

Gascuel, J. D., Cani-Gascuel, M. P., Desbrun, M., Leroi, E., Mirgon, C., 1998. Simulating landslides for natural disaster prevention. In: Arnaldi, B., Hegron, G. (eds.), *Computer animation and simulation ’98. Proceedings of the Eurographics Workshop, Lisbon*, pp. 1–12.

Gerber, C., Elsener, O., 1998. Niederwaldbetrieb im Steinschlaggebiet. *Wald Holz* **14**, 8–11.

Gerber, W., 1998. *Waldwirkungen und Steinschlag.* Kursunterlagen WSL, Birmensdorf.

– , 2001, *Guideline for the approval of rockfall protection kits.* Swiss Agency for the Environment, Forests and Landscape SAEFL and Swiss Federal Research Institute WSL, Berne.

Gerlach, D., 1984. *Botanische Mikrotechnik*. Thieme Verlag, Stuttgart and New York.

Gertsch, E., Kienholz, H., 2004. Einfluss auf den Feststoffhaushalt. In: Hegg, C., Thormann, J. J., Böll, A., Germann, P., Kienholz, H., Lüscher, P., Weingartner, R. (eds.), *Lothar und Wildbäche. Schlussbericht eines Projektes im Rahmen des Programms „Lothar Evaluations- und Grundlagenprojekte“.* Swiss Federal Research Institute WSL, Birmensdorf, pp. 51–68.

Glawe, U., Zika, P., Zvelebil, J., Moser, M., Rybar, J., 1993. Time prediction of a rock fall in the Carnic Alps. *Quarterly Journal of Engineering Geology* **26**, 185–192.

Götz, A., Zimmermann, M., 1993. The 1991 rock slides in Randa: causes and consequences. *Landslide News* **7**, 22–25.

Goodman, R. E., Kieffer, D. S., 2000. Behaviour of rock in slopes. *Journal of Geotechnical and Geoenvironmental Engineering* **126**, 675–684.

Graybill, D. A., 1982. Chronology development and analysis. In: Hughes, M. K., Kelly, P. M., Pilcher, J. R., LaMarche Jr., V. C. (eds.), *Climate from Tree Rings*. Cambridge University Press, Cambridge, pp. 21–28.

Grebner, D., 1994. Meteorologische Analyse des Unwetters von Brig und Saas Almagell vom 24. September 1993. *wasser, energie, luft* **86(1-2)**, 41–44.

Grove, J. M., 1988. *The Little Ice Age*. Methuen, London.

Gruber, S., Hoelzle, M., 2001. Statistical modelling of mountain permafrost distribution: local calibration and incorporation of remotely sensed data. *Permafrost and Periglacial Processes* **12**, 69–77.

Gruber, S., Hoelzle, M., Haeberli, W., 2004. Permafrost thaw and destabilization of Alpine rock walls in the hot summer of 2003. *Geophysical Research Letters* **31**, L13504.

Gsteiger, P. 1993. Steinschlagschutzwald. Ein Beitrag zur Abgrenzung, Beurteilung und Bewirtschaftung. *Schweizerische Zeitschrift für Forstwesen* **144(2)**, 115–132.

Gude, M., Barsch, D., 2005. Assessment of geomorphic hazards in connection with permafrost occurrence in the Zugspitze area (Bavarian Alps, Germany). Geomorphology **66**, 85–93.

Guyette, R., Stambaugh, M. C., 2004. Post-oak fire scars as a function of diameter, growth, and tree age. *Forest Ecology and Management* **198**, 183–192.

Guzzetti, F., 2000. Landslide fatalities and evaluation of landslide risks in Italy. *Engineering Geology* **58**, 89–107.

Guzzetti, F., Tonelli, G., 2004. Information system on hydrological and geomorphological catastrophes in Italy (SICI): a tool for managing landslide and flood hazards. *Natural Hazards and Earth System Sciences* **4**, 213–232.

Guzzetti, F., Carrarra, A., Cardinali, M., Reichenbach, P., 1999. Landslide hazard evaluation: an aid to a sustainable development. *Geomorphology* **31**, 181–216.

Guzzetti, F., Crosta, G., Detti, R., Agliardi, F., 2002. STONE: a computer program for the three-dimensional simulation of rock-falls. *Computers and Geosciences* **28**, 1079-1093.

Guzzetti, F., Reichenbach, P., Wieczorek, G. F., 2003a. Rockfall hazard and risk assessment in the Yosemite Valley, California, USA. *Natural Hazards and Earth System Sciences* **3**, 491–503.

Guzzetti, F., Reichenbach, P., Cardinali, C., Ardizzone, F., Galli, M., 2003b. Impact of landslides in the Umbria Region, Central Italy. *Natural Hazards and Earth System Sciences* **3**, 491–503.

Guzzetti, F., Reichenbach, P., Ghigi, S., 2004. Rockfall hazard and risk assessment along a transportation corridor in the Nera Valley, Central Italy. *Environmental Management* **34(2)**, 191–208.

H

Haeberli, W., 1992. Construction, environmental problems and natural hazards in periglacial mountain belts. *Permafrost and Periglacial Processes* **3**, 111–124.

– , 1995. Permafrost und Blockgletscher in den Alpen. *Vierteljahresschrift der Naturforschenden Gesellschaft Zürich* **140(3)**, 113–121.

Hall, K., 1997. Rock temperatures and implications for cold region weathering. New Data from Viking Valley, Alexander Island, Antarctica. *Permafrost and Periglacial Processes* **8**, 69–90.

Hanks, T. C., Kanamori, H. 1979. A moment magnitude scale. *Journal of Geophysical Research* **84**, 2348–2350.

Hantz, D., Vebgeon, J. M., Dussauge-Peisser, C., 2003a. Rock fall hazard assessment: from qualitative to quantitative failure probability. In: Picarelli, L. (ed.), *Fast slope movements, prediction and prevention for risk mitigation.* Patrone Editore, Napoli, pp. 263–267.

Hantz, D., Vebgeon, J. M., Dussauge-Peisser, C., 2003b. An historical, geomechanical and probabilistic approach to rock-fall hazard assessment. *Natural Hazards and Earth System Sciences* **3**, 693–701.

Harms, H., 1965. *Handbuch der Farbstoffe für die Mikroskopie.* Staufen-Verlag, Kamp-Lintfort.

Harp, E. L., Wilson, R. C., 1995. Shaking intensity thresholds for rock falls and slides: evidence from the 1987 Whittier Narrows and Superstition Hills earthquake strong motion records. *Bulletin of the Seismological Society of America* **85**, 1739–1757.

Harris, C., Davies, M. C. R., Etzelmüller, B., 2001. The assessment of potential geotechnical hazards associated with mountain permafrost in a warming global climate. *Permafrost and Periglacial Processes* **12**, 145–156.

Hebertson, E. G., Jenkins, M. J., 2003. Historic climate factors associated with major avalanche years on the Wasatch Plateau, Utah. *Cold Regions Science and Technology* **37**, 315–332.

Heim, A., 1932. Bergsturz und Menschenleben. *Vierteljahresschrift der Naturforschenden Gesellschaft in Zürich* **77**, 1–218.

Hengst, G. E., Dawson, J. O., 1994. Bark properties and fire resistance of selected tree species from the central hardwood region of North America. *Canadian Journal of Forest Research* **24(4)**, 688–696.

Hétu, B., 1990. Evolution récente d'un talus d'éboulis en milieu forestier, Gaspésie, Québec. *Géographie physique et Quaternaire* **44**, 199–215.

Hétu, B., Gray, J. T., 2000. Effects of environmental change on scree slope development throughout the postglacial period in the Chic-Choc Mountains in the northern Gaspé Peninsula, Québec. *Geomorphology* **32**, 335–355.

Hohl, R., Schweingruber, F. H., Schiesser, H. H., 2002.

Reconstruction of severe hailstorm occurrence with tree rings: a case study in central Switzerland. *Tree-Ring Research* **58(1/2)**, 11–22.

Holzhauser, H. P., 1995. Gletscherschwankungen innerhalb der letzten 3200 Jahre am Beispiel des Grossen Aletsch- und des Gornergletschers. In: Schweizerische Akademie der Naturwissenschaften (ed.), *Gletscher im ständigen Wandel. 100 Jahre Gletscherkommission – 100'000 Jahre Gletschergeschichte*, vdf Hochschulverlag, Zürich, pp. 101–122.

Hufty, A., Thériault, M., 1983. Atlas d'abaques pour le calcul du rayonnement solaire par beau temps. Laboratoire de Climatologie, Département Géographie, Université Laval, Québec. *Notes de recherche* **18**.

Huggel, C., Kääb, A., Haeberli, W., Teysseire, P., Paul, F., 2002. Remote sensing based assessment of hazards from glacier lake outbursts: a case study in the Swiss Alps. *Canadian Geotechnical Journal* **39**, 316–330.

Huggel, C., Kääb, A., Haeberli, W., 2003. Regional-scale models of debris flows triggered by lake outbursts: the June 25, 2001 debris flow at Täsch (Switzerland) as a test study. In: Rickenmann, D., Chen, C. (eds.), *Debris Flow Hazard Mitigation: Mechanics, Prediction, and Assessment* 1, pp. 243–253.

Hungr, O., Evans, S. G., 1988. Engineering evaluation of fragmental rockfall hazards. In: *Proceedings of the 5th International Symposium on Landslides, Lausanne*, pp. 685–690.

– , 1989. Engineering aspects of rockfall hazards in Canada. *Geological Survey of Canada, Open File* **2061**.

Hungr, O., Beckie, R. D., 1998. Assessment of the hazard from rock fall on a highway. *Canadian Geotechnical Journal* **35**, 409.

Hungr, O., Evans, S. G., Hazzard, J., 1999. Magnitude and frequency of rock falls along the main transportation corridors of south-western British Colombia. *Canadian Geotechnical Journal* **36**, 224–238.

Hungr, O., Evans, S. G., Bovis, M. J., Hutchinson, N. J., 2001. A review of the classification of landslides of the flow type. *Environmental and Engineering Geoscience* **7**, 221–238.

Hupp, C. R., 1988. Plant ecological aspects of flood geomorphology and paleoflood history. In: Baker, V. R., Kochel, C. R., Patton, P. C. (eds.), *Flood geomorphology*. Wiley and Sons, New York, pp. 335–356.

Hurand, A., Berger, F., 2002. Forests and natural risks. Protection against erosion, ground movements and avalanches. *Houille Blanche* **3**, 64–67.

Hutchinson, J. N., 1988. Morphological and geotechnical parameters of landslides in relation to geology and hydrogeology. In: Bonnard, C. (ed.), *Landslides*. Balkema, Rotterdam, pp. 3–35.

I

Iseli, M., Schweingruber, F. H., 1989. Sichtbarmachen von Jahrringen für dendrochronologische Untersuchungen. *Dendrochronologia* **4**, 145–157.

J

Jaboyedoff, M., Ornstein, P., Rouiller, J. D., 2004. Design of a geodetic database and associated tools for monitoring rock-slope movements: the example of the top of Randa rockfall scar. *Natural Hazards and Earth System Sciences* **4**, 187–196.

Jaboyedoff, M., Baillifard, F., Derron, M. H., 2003a. Preliminary note on uplift rates gradient, seismic activity and possible implications for brittle tectonics and rockslide prone areas: The example of western Switzerland. *Bulletin de la Société Vaudoise des Sciences naturelles* **88.3**, 401–420.

– , 2003b. Uplifts, seismic zones and landslides: the example of Switzerland. EGS-EUG-AGU Joint Assembly, Nice 2003. *Geophysical Research Abstracts* **5**, 03556.

Jaboyedoff, M., Baillifard, F., Rouiller, J. D., 2003c. Rock instability hazard assessment based on detailed topographic analysis. *Geophysical Research Abstracts* **5**, 03462.

Jacoby, G. C., 1997. Application of tree ring analysis to paleoseismology. *Reviews of Geophysics* **35(2)**, 109–124.

Jacoby, G. C., Sheppard, P. R., Sieh, K. E., 1988. Irregular recurrence of large earthquakes along the San Andreas Fault. Evidence from trees. *Science* **241**, 196–199.

Jacoby, G. C., Williams, P. L., Buckley, B. M., 1992. Tree ring correlation between prehistoric landslides and abrupt tectonic events in Seattle, Washington. *Science* **258**, 1621–1623.

Jacoby, G. C., Bunker, D. E., Benson, B. E., 1997. Tree-ring evidence for an A.D. 1700 Cascadia earthquake in Washington and northern Oregon. *Geology* **25(11)**, 999–1002.

Jahn, J., 1988. Entwaldung und Steinschlag. In: *Proceedings International Symposium Interpraevent 1988, Graz* **1**, pp. 185–198.

Jibson, R. W., Harp, E. L., Michael, J. A., 1998. A method for producing digital probabilistic seismic landslide hazard maps: an example from the Los Angeles, California, area. *US Geological Survey, O-F Report* **98-113**.

Jibson, R. W., Harp, E. L., Schulz, W., Keefer, D. K., 2004. Landslides triggered by the 2002 Denali Fault, Alaska, Earthquake and the inferred nature of the strong shaking. *Earthquake Spectra* **20(3)**, 669–691.

Johnston, K., Ver Hoef, J. M., Krivoruchko, K., Lucas, N., 2001. *Using ArcGIS Geostatistical Analyst*. ESRI, Redlands.

Jomelli, V., Francou, B., 2000. Comparing the characteristics of rockfall talus and snow avalanche landforms in an Alpine environment using a new methodological approach: Massif des Ecrins, French Alps. *Geomorphology* **35(3)**, 181–192.

Joris, C.-L., 1995. Der Bergsturz, ein Zufallsereignis unter vielen. In: Naturforschende Gesellschaft Oberwallis (ed.), *Der Bergsturz von Randa 1991*. Neue Buchdruckerei Visp AG, Visp, pp. 43–49.

K

Kaennel, M., Schweingruber, F. H., 1995. *Multilingual glossary of dendrochronology.* Swiss Federal Research Institute WSL, Birmensdorf. Paul Haupt, Bern, Stuttgart, Wien.

Kaiser, K. F., Kaiser-Bernhard, C., 1987. The Katmai eruption of 1912 and the Alaska earthquake of 1964 as reflected in the annual rings of Sitka Spruce on Kodiak Island. *Dendrochronologia* **5**, 111–125.

Keefer, D. K., 1984. Rock avalanches caused by earthquake-source characteristics. *Science* **223**, 1288–1290.

– , 1994. The importance of earthquake-induced landslides to long-term slope erosion and slope-failure hazards in seismically active regions. *Geomorphology* **10**, 265–284.

– , 2000. Statistical analysis of an earthquake-induced landslide distribution – the 1989 Loma Prieta, California event. *Engineering Geology* **58**, 231–249.

Keylock, C., Domaas, U., 1999. Evaluation of topographic models of rockfall travel distance for use in hazard applications. *Arctic, Antarctic, and Alpine Research* **31(3)**, 312–320.

Kienholz, H., 1995. Gefahrenbeurteilung und -bewertung – auf dem Weg zu einem Gesamtkonzept. *Schweizerische Zeitschrift für Forstwesen* **146(9)**, 701–725.

– , 1998. *Landschaftsökologie II: Geomorphologie.* Lecture script. Department of Geography, University of Berne.

Kienholz, H., Mani, P., 1994. Assessment of geomorphic hazards and priorities for forest mangement on the Rigi north face, Switzerland. *Mountain Research and Development* **14(4)**, 321–328.

Kienholz, H., Mani, P., Kläy, M., 1988. Rigi Nordlehne. Beurteilung der Naturgefahren und waldbauliche Prioritätenfestlegung. In: *Proceedings International Symposium Interpraevent 1988, Graz,* **1**, pp. 161–174.

King, L., 1996. Dauerfrostboden im Gebiet Zermatt–Gornergrat–Stockhorn: Verbreitung und permafrostbezogene Erschliessungsarbeiten. *Zeitschrift für Geomorphologie NF Supplement-Band* **104**, 73–93.

Kirkby, M. J., Statham, I., 1975. Surface stone movement and scree formation. *Journal of Geology* **83**, 349–362.

Knutti, R., Stocker, T. F., Joos, F., Plattner, G. K., 2002. Constraints on radiative forcing and future climate change from observations and climatic model ensembles. *Nature* **416**, 719–723.

Kobayashi, Y., Harp, E. L., Kagawa, T., 1990. Simulation of rockfalls triggered by earthquakes. *Rock Mechanics and Rock Engineering* **23**, 1–20.

Koo, C. Y., Chern, J. C., 1998. Modification of the DDA method for rigid block problems. *International Journal of Rock Mechanics and Mining Science* **35(6)**, 683–693.

Körner, H. J., 1980. Modelle zur Berechnung der Bergsturz- und Lawinenbewegung. In: *Proceedings International Conference Interpraevent, Klagenfurt, Austria*, pp. 15–55.

Košták, B., Dobrev, N., Zika, P., Ivanov, P., 1998. Joint monitoring on a rock face bearing an historical bas-relief. *Quarterly Journal of Engineering Geology* **31**, 37–45.

Kräuchi, N., Brang, P., Schönenberger, W., 2000. Forests of mountainous regions: gaps in knowledge and research needs. *Forest Ecology and Management* **132**, 73–82.

Krummenacher, B., 1995. Modellierung der Wirkungsräume von Erd- und Felsbewegungen mit Hilfe Geographischer Informationssysteme (GIS). *Schweizerische Zeitschrift für Forstwesen* **146**, 741–761.

Krummenacher, B., Keusen, H. R., 1996. Rockfall simulation and hazard mapping based on digital terrain model (DTM). *European Geologist* **12**, 33–35.

Krusic, P. M., Kenney, M., Hornbeck, J., 1987. Preparing increment cores for ring-width measurements. *Northern Journal of Applied Forestry* **4**, 104–105.

Kühni, A., Pfiffner, O. A., 2001. The relief of the Swiss Alps and adjacent areas and its relation to lithology and structure: topographic analysis from 250-m DEM. *Geomorphology* **41**, 285–307.

L

Labhart, T. P., 1998. *Geologie der Schweiz.* Ott Verlag, Thun.

Ladner, F., Rovina, H., Pointner, E., Dräyer, B., Sambeth, U., 2004. Geological monitoring and instrumentation of the Medji rockfall (St. Niklaus / Switzerland). *Felsbau* **22(3)**, 37–45.

Lafortune, M., Filion, L., Hétu, B., 1997. Dynamique d'un front forestier sur un talus d'éboulis actif en climat tempéré froid (Gaspésie, Québec). *Géographie physique et Quaternaire* **51(1)**, 1–15.

Larson, P. R., 1994. *The vascular cambium. Development and structure.* Springer, Berlin.

Lateltin, O., Beer, C., Raetzo, H., Caron, C., 1997. Landslides in Flysch terranes of Switzerland: Causal factors and climate change. *Eclogae Geologicae Helvetiae* **90(3)**, 401–406.

Le Hir, C., Berger, F., Dorren, L. K. A., Quetel, C., 2004. Forest: A natural means of protection against rockfall, but how to reach sustainable mitigation? In: *Proceedings International Symposium Interpraevent 2004. Riva/Trient, Italy,* **V**, pp. 59–69.

Leibundgut, H., 1986. *Unsere Gebirgswälder.* Paul Haupt Verlag, Bern, Stuttgart.

LePage, H., Bégin, Y., 1996. Tree-ring dating of extreme water level events at Lake Bienville, Subarctic Québec, Canada. *Arctic and Alpine Research* **28(1)**, 77–84.

Lewkowicz, A. G., Harris, C., 2005. Frequency and magnitude of active-layer detachment failures in discontinuous and continuous permafrost, northern Canada. *Permafrost and Periglacial Processes* **16**, 115–130.

Lin, A., Lin, S., 1998. Tree damage and surface displacement: the 1931 M 8.0 Fuyun Earthquake. *Journal of Geology* **106**, 751–757.

Liniger, M., 2000. Computersimulation von Stein- und Blockschlägen. *Felsbau* **18**, 64–68.

Luckman, B. H., 1976. Rockfalls and rockfall inventory data: some observations from Surprise Valley, Jasper National Park. *Earth Surface Processes and Landforms* **1**, 287–298.

Luckman, B. H., Fiske, C. J., 1995. Estimating long-term rockfall accretion rates by lichenometry. In: Slaymaker, O. (ed.), *Steepland Geomorphology*. Wiley, Chichester, pp. 233–255.

M

Mahrer, F., Bachofen, H., Brändli, U.-B., Brassel, P., Kasper, H., Lüscher, P., Riegger, W., Stierlin, H.-R., Strobel, T., Sutter, R., Wenger, C., Winzeler, K., Zingg, A., 1988. *Schweizerisches Landesforstinventar: Ergebnisse der Erstaufnahme 1982-1986.* Eidgenössische Forschungsanstalt für Wald, Schnee und Landschaft, Birmensdorf.

Malamud, B. D., Turcotte, D. M., Guzzetti, F., Reichenbach, P., 2004. Landslide inventories and their statistical Properties. *Earth Surface Processes and Landforms* **29**, 687–711.

Mani, P., Kläy, M., 1992. Naturgefahren an der Rigi-Nordlehne. Die Beurteilung von Naturgefahren als Grundlage für die waldbauliche Massnahmenplanung. *Schweizerische Zeitschrift für Forstwesen* **143**, 131–147.

Marquínez, J., Menéndez Duarte, R., Farias, P., Jiménez Sanchez, M., 2003. Predictive GIS-based model of rockfall activity in mountain cliffs. *Natural Hazards* **30**, 341–360.

Marzorati, S., Luzi, L., De Amicis, M., 2002. Rock falls induced by earthquakes: a statistical approach. *Soil Dynamics and Earthquake Engineering* **22**, 565–577.

Matsuoka, N., 2001. Direct observations of frost wedging in alpine bedrocks. *Earth Surface Processes and Landforms* **26**, 601–614.

Matsuoka, N., Sakai, H., 1999. Rockfall activity from an alpine cliff during thawing periods. *Geomorphology* **28**, 309–328.

Matsuoka, N., Ikeda, A., Hirakawa, K., Watanabe, T., 2003. Contemporary periglacial processes in the Swiss Alps: seasonal, inter-annual and long-term variations. In: Philipps, M., Springman, S. M., Arenson, L. U. (eds.), *Permafrost. Proceedings of the 8th International Conference on Permafrost.* Balkema Publishers, Lisse, Abingdon, Exton and Tokyo, pp. 735–740.

Mayer-Rosa, D., Rüttener, E., Fäh, D., Schindler, C., Beer, C., Wagner, J. J., Frischknecht, C., 1997. *Erdbebengefährdung und Mikrozonierung in der Schweiz. Ein Beitrag zur Erforschung des Erdbebenrisikos in Abhängigkeit vom geologischen Untergrund.* Schlussbericht NFP 31, vdf Hochschulverlag AG, Zürich.

Mazzoccola, D., Sciesa, E., 2000. Implementation and comparison of different methods for rockfall hazard assessment in the Italian Alps. In: *Proceedings 8th International Symposium on Landslides, Cardiff, UK*, pp. 1035–1040.

McCarroll, D., Shakesby, R. A., Matthews, J. S., 1998. Spatial and temporal patterns of Late Holocene rockfall activity on a Norwegian talus slope: lichenometry and simulation-modelling approach. *Arctic and Alpine Research* **30**, 51–60.

– , 2001. Enhanced Rockfall Activity during the Little Ice Age: Further lichenometric evidence from a Norwegian talus. *Permafrost and Periglacial Processes* **12**, 157–164.

Meissl, G., 1998. Modellierung der Reichweite von Felsstürzen. Fallbeispiele zur GIS-gestützten Gefahrenbeurteilung aus dem Bayerischen und Tiroler Alpenraum. PhD Thesis. Universität Innsbruck, Innsbruck. *Innsbrucker Geographische Studien* **28**.

– , 2001. Modelling the runout distances of rockfalls using a geographic information system. *Zeitschrift für Geomorphologie N.F. Supplementband* **125**, 129–137.

Menéndez Duarte, R., Marquínez, J., 2002. The influence of environmental and lithologic factors on rockfall at a regional scale: an evaluation using GIS. *Geomorphology* **43**, 117–136.

Moore, D. P., Mathews, W. H., 1978. The Rubble Creek landslide, southwestern British Columbia. *Canadian Journal of Earth Sciences* **15**, 1039–1052.

Moriwaki, H., 1987. Geomorphological prediction of the travel distance of a debris. In: *Proceedings of the China-Japan Field Workshop on Landslide*. *Xian-Lanzhou, China*, 79–84.

Mössmer, E. M., Ammer, U., Knoke, T., 1994. Technisch-biologische Verfahren zur Schutzwaldsanierung in den oberbayrischen Kalkalpen. *Forstliche Forschungsberichte München* **145**: 135.

Motta, R., Haudemand, J. C., 2000. Protective forests and silvicultural stability – an example of planning in the Aosta Valley. *Mountain Research and Development* **20(2)**, 180–187.

Müller, H. N., 1980. Jahrringwachstum und Klimafaktoren: Beziehungen zwischen Jahrringwachstum von Nadelbaumarten und Klimafaktoren an verschiedenen Standorten im Gebiet des Simplonpasses (Wallis, Schweiz). *Veröffentlichungen der Forstlichen Bundes-Versuchsanstalt Wien* **25**, Agrarverlag, Wien.

N

Naylor, L. A., Viles, H. A., Carter, N. E. A., 2002. Biogeomorphology revisited: looking towards the future. *Geomorphology* **47**, 3–14.

Niederberger, K., 2002. *Schutz Wald Mensch Lernpfade. Altdorf Uri.* Emsig Druck AG, Ibach.

Nilsen, B., 2000. New trends in rock slope stability analysis. *Bulletin of Engineering Geology and the Environment* **58**, 173–178.

O

OcCC (ed.), 2003. *Extremereignisse und Klimaänderung.* Organe consultatif sur les changements climatiques, Bern.

Okura, Y., Kitahara, H., Sammori, T., 2000a. Fluidization in dry landslides. *Engineering Geology* **56(3)**, 347–360.

Okura, Y., Kitahara, H., Sammori, T., Kawanami, A., 2000b. The effects of rockfall volume on runout distance. *Engineering Geology* **58(2)**, 109–124.

Ortloff, W., Goldammer, J. G., Schweingruber, F. H., Swetnam, T. W., 1995. Jahrring-analytische Untersuchungen zur Feuergeschichte eines Bestandes von Pinus ponderosa Dougl. ex Laws. in den Santa Rita Mountains, Arizona, USA. *Forstarchiv* **66**, 206–214.

Oswald, D., 2003. *Analyse de l'activité de glissements de terrain et relation avec les conditions climatiques: Exemples dans les Préalpes fribourgeoises (Suisse).* PhD thesis, Department of Geosciences, Geology, University of Fribourg. *GeoFocus* **8**, 1–147.

Ott, E., Frehner, M., Frey, H. U., Lüscher, P., 1997. *Gebirgsnadelwälder: Ein praxisorientierter Leitfaden für eine standortgerechte Waldbehandlung.* Paul Haupt, Bern, Stuttgart, Wien.

P

Patten, R. S., Knight, D. H., 1994. Snow avalanches and vegetation pattern in cascade canyon, Grand Teton National Park, Wyoming, USA. *Arctic and Alpine Research* **26(1)**, 35–41.

Peila, D., Polizza, S., Sassudelli, S., 1998. Evaluation of behaviour of rockfall retaining nets by full scale tests. *International Journal of Rock Mechanics and Rock Engineering* **31**, 1–24.

Perret, S., Dolf, F., Kienholz, H., 2004a. Rockfall into forests: analysis and simulation of rockfall trajectories – considerations with respect to mountainous forests in Switzerland. *Landslides* **1**, 123–130.

Perret, S., Baumgartner, M., Kienholz, H., 2004b. Steinschlagschäden in Bergwäldern – Eine Methode zur Erhebung und Analyse. In: *Proceedings International Symposium Interpraevent 2004. Riva/ Trient, Italy,* **V**, pp. 87–98.

– , 2005a. Inventory and analysis of tree injuries in a rockfall-damaged forest stand. *European Journal of Forest Research*. in press.

Perret, S., Stoffel, M., Kienholz, H., 2005b. Spatio-temporal rockfall activity in a forest stand in the Swiss Prealps – a dendrogeomorphological case study. *Geomorphology*, in press.

Pfeiffer, T. J., Bowen, T. D., 1989. Computer simulation of rockfalls. *Bulletin of the Association of Engineering Geologists* **XXVI(1)**, 135–146.

Pfister, C., 1999. *Wetternachhersage. 500 Jahre Klimavariationen und Naturkatastrophen.* Paul Haupt Verlag, Bern Stuttgart, Wien.

Phipps, R. L., 1985. Collecting, preparing, crossdating, and measuring tree increment cores. *U.S. Geological*

Survey Water Resources Investigations Report 85–4148.

Pinard, M. A., Pinard, M. A., Huffman, J., 1997. Fire resistance and bark properties of trees in a seasonally dry forest in eastern Bolivia. *Journal of Tropical Ecology* **13(5)**, 727–740.

Porter, S. C., Orombelli, G., 1980. Catastrophic rockfall of September 12, 1717 on the Italian flank of the Mont Blanc Massif. *Zeitschrift für Geomorphologie N. F.* **24**, 200–218.

R

Raetzo-Brülhart, H., 1997. *Massenbewegungen im Gurnigelflysch und Einfluss der Klimaänderung*. PhD thesis 1168. Department of Geosciences, Geology University of Fribourg.

Rapp, A., 1960a. Talus slopes and mountain walls at Tempelfjorden, Spitzbergen. *Norsk Polarinstitutt Skrifter* **119**.

– , 1960b. Recent development of mountain slopes in Kärkevagge and surroundings, Northern Scandinavia. *Geografiska Annaler* **42**, 65–200.

Rayback, S. A., 1998. A dendrogeomorphological analysis of snow avalanches in the Colorado Front Range, USA. *Physical Geography* **19(6)**, 502–515.

Rey, F., Chauvin, C., 2001. Forest restoration in marly southern French Alps. In: *Proceedings International Conference "Forest Research: A Challenge for an Integrated European Approach". Thessaloniki, Greece,* **1**, pp. 365–369.

Rickli, C., Graf, F., Gerber, W., Frei, M., Böll, A., 2004. Der Wald und seine Bedeutung bei Naturgefahren geologischen Ursprungs. In: Eidgenössische Forschungsanstalt WSL (ed.), *Schutzwald und Naturgefahren. Forum für Wissen 2004.* Bruhin AG, Freienbach, pp. 27–34.

Rigling, A., Bräker, O., Schneiter, G., Schweingruber, F., 2002. Intra-annual tree-ring parameters indicating differences in drought stress of Pinus sylvestris forests within the Erico-Pinion in the Valais (Switzerland). *Plant Ecology* **163**, 105–121.

Ritchie, A. M., 1963. Evaluation or rockfall and its control. *Highway Research Record* **17**, 13–28.

Ritter, D. F., Kochel, G. R., Miller, J. R., 2002. *Process geomorphology*. McGraw-Hill, New York (4th edition).

Rouiller, J. D., Jaboyedoff, M., Marro, C., Philipposian, F, Mamin, M., 1998. *Matterrock: une méthodologie d'auscultation des falaises et de detection des éboulements majeur potentials.* Schlussbericht NFP 31. vdf Hochschulverlag AG, Zürich.

S

Sachs, T., 1991. *Pattern, formation in plant tissues*. Cambridge University Press, Cambridge.

Sartori, M., Baillifard, F., Jaboyedoff, M., Rouiller, J. D., 2003. Kinematics of the 1991 Randa rockslides (Valais, Switzerland). *Natural Hazards and Earth System Sciences* **3**, 423–433.

Schär, C., Vidale, P. L., Lüthi, D., Frei, C., Häberli, C., Liniger, M., Appenzeller, C., 2004. The role of increasing temperature variability in European summer heatwaves. *Nature* **427**, 332–336.

Schiermeier, Q., 2003. Alpine thaw breaks ice over permafrost's role. *Nature* **424**, 712.

Schindler, C., Cuénod, Y., Eisenlohr, T., Joris C. L., 1993. Die Ereignisse vom 18. April und 9. Mai 1991 bei Randa (VS) – ein atypischer Bergsturz in Raten. *Eclogae Geologicae Helvetiae* **86(3)**, 643–665.

Schlunegger, F., Hinderer, M., 2001. Crustal uplift in the Alps: why the drainage matters. *Terra Nova* **13**, 425–432.

– , 2003. Pleistocene/Holocene climate change, reestablishment of fluvial drainage network and increase in relief in the Swiss Alps. *Terra Nova* **15**, 88–95.

Schneebeli, M., Laternser, M., Föhn, P., Ammann, W., 1998. *Wechselwirkungen zwischen Klima, Lawinen und technischen Massnahmen.* Schlussbericht NFP31. vdf Hochschulverlag, Zürich.

Schömmer, F., 1949. *Kryptogamen-Praktikum*. Francklinsche Verlagshandlung, Stuttgart.

Schönenberger, W., Noack, A., Thee, P., 2005. Effect of timber removal from windthrow slopes on snow avalanches and rockfall. *Forest Ecology and Management* **213**, 197–208.

Schoonenberg, T., Pinard, M., Woodward, S., 2003. Responses to mechanical wounding and fire in tree species characteristic of seasonally dry tropical forest of Bolivia. *Canadian Journal of Forest Research* **33(2)**, 330–338.

Schweigl, J., Ferretti, C., Nossing, L., 2003. Geotechnical characterization and rockfall simulation of a slope: a practical case study from South Tyrol (Italy). *Engineering Geology* **67(3-4)**, 281–296.

Schweingruber, F. H., 1978. *Mikroskopische Holzanatomie.* Flück, Teufen.

– , 1983. *Der Jahrring: Standort, Methodik, Zeit und Klima in der Dendrochronologie.* Paul Haupt, Bern.

– , 1996. *Tree Rings and Environment. Dendroecology.* Paul Haupt, Bern, Stuttgart, Wien.

– , 2001. *Dendroökologische Holzanatomie*. Paul Haupt, Bern, Stuttgart, Wien.

Schweingruber, F. H., Eckstein, D., Serre-Bachet, F., Bräker, O. U., 1990. Identification, presentation and interpretation of event years and pointer years in dendrochronology. *Dendrochronologia* **8**, 9–39.

Segalini, A., Giani, G. P., 2004. Numerical Model for the analysis of the evolution mechanisms of the Grossgufer rock slide. *Rock Mechanics and Rock Engineering* **37(2)**, 151–168.

Selby, M. J., 1993. *Hillslope materials and processes*. Oxford University Press, Oxford.

Shroder, J. F., 1978. Dendrogeomorphological analysis of mass movement on Table Cliffs Plateau, Utah. *Quaternary Research* **9**, 168–185.

– , 1980. Dendrogeomorphology: review and new techniques of tree-ring dating. *Progress in Physical Geography* **4**, 161–188.

Shroder, J. F., Butler, D. R., 1987. Tree-ring analysis in the earth sciences. In: *Proceedings International Symposium on Ecological Aspects of Tree-Ring Analysis, Tarrytown NY,* pp. 186–212.

Smi (Swiss Meteorological Institute), 2000. *Klimaatlas der Schweiz.* Verlag des Bundesamtes für Landestopographie, Wabern-Bern.

– , 2003. *Annals of the Swiss Meteorological Institute.* Zurich (mean values of 1960-2001 precipitation sums).

Solomina, O., 2002. Dendrogeomorphology: research requirements. *Dendrochronologia* **20(1-2)**, 233–245.

Statham, I., 1976. A scree slope rockfall model. *Earth Surface Processes* **1**, 43–62.

Stefanini, M. C., 2004. Spatio-temporal analysis of a complex landslide in the Northern Apennines (Italy) by means of dendrochronology. *Geomorphology* **63**, 191–202.

St. George, S., Nielsen, E., 2003. Palaeoflood records for the Red River, Manitoba, Canada, derived from anatomical tree-ring signatures. *Holocene* **13(4)**, 547–555.

Stoffel, M., 2002. Analysis of microscopic growth reactions caused by rockfall or snow avalanches. In: *Proceedings 6th International Conference on Dendrochronology,* August 2002, Quebec, 327–329.

– , 2005a. A review of studies dealing with tree rings and rockfall activity: The role of dendrogeomorphology in natural hazard research. *Natural Hazards*, in press.

– , 2005b. Assessing the vertical distribution and visibility of rockfall scars in trees. *Schweizerische Zeitschrift für Forstwesen* **156(6)**, 195–199.

Stoffel, M., Perret, S., 2005. Reconstructing past rockfall activity with tree rings: some methodological considerations. *Dendrochronologia*, in review.

Stoffel, M., Lièvre, I., Conus, D., Grichting, M. A., Gärtner, H., Monbaron, M., 2004. Rekonstruktion der Muraktivität im Ritigraben (VS) und Vergleich mit Chronikdaten benachbarter Gewässer. *Mitteilungen der VAW* **184**, 25–40.

Stoffel, M., Lièvre, I., Conus, D., Grichting, M., Raetzo, H., Gärtner, H., Monbaron, M., 2005a. 400 years of debris flow activity and triggering weather conditions: Ritigraben VS, Switzerland. *Arctic, Antarctic and Alpine Research* **37(3)**, 387–395.

Stoffel, M., Lièvre, I., Monbaron, M., Perret, S., 2005b. Seasonal timing of rockfall activity on a forested slope at Täschgufer (Swiss Alps) – a dendrochronological approach. *Zeitschrift für Geomorphologie* **49(1)**, 89–106.

Stoffel, M., Schneuwly, D., Bollschweiler, M., Lièvre, I., Delaloye, R., Myint, M., Monbaron, M., 2005c. Analyzing rockfall activity (1600-2002) in a protection forest – a case study using dendrogeomorphology. *Geomorphology* **68(3-4)**, 224–241.

Stoffel, M., Wehrli, A., Kühne, R., Dorren, L. K. A., Perret, S., Kienholz, H., 2005d. Quantifying the protective effect of mountain forests against rockfall using a 3D simulation model. *Forest Ecology and Management*, in press.

Stoffel, M., Kühne, R., Krummenacher, B., Keusen, H.R., Pfeifer, R., Zesiger, M., Monbaron, M. in prep. Steinschlagmodellierung im Gebirgswald – Fallbeispiele aus den Schweizer Alpen. *Schweizerische Zeitschrift für Forstwesen*, in prep.

Strunk, H., 1992. Reconstructing debris flow frequency in the southern Alps back to AD 1500 using dendrogeomorphological analysis. *IAHS Publications* **209**, 299–307.

– , 1995. *Dendrochronologische Methoden zur Ermittlung der Murfrequenz und Beispiele ihrer Anwendung.* Roderer Verlag, Regensburg.

– , 1997. Dating of geomorphological processes using dendrogeomorphological methods. *Catena* **31**, 137–151.

Swissphoto, 2000. *Aerial photo Täschgufer.* UP-Valais P-6040.015, Airway 86, Exposure 25, Slide 2352, Date, 06.07.2000.

T

Tianchi, L., 1983. A mathematical model for prediction the extent of a major rockfall. *Zeitschrift für Geomorphologie* **27(4)**, 473–482.

Toppe, R., 1987. Terrain models – a tool for natural hazard mapping. *IAHS Publication* **162**, 629–638.

U

Utelli, H. H., 1999. Die Möglichkeiten von GIS bei der Beurteilung der Steinschlaggefahr im alpinen Bereich. *Bulletin for Applied Geology* **4(1)**, 3–18.

V

Van Arsdale, R. B., Stahle, D. W., Cleaveland, M. K., Guccione, M. J., 1998. Earthquake signals in tree-ring data from the New Madrid seismic zone and implications for paleoseismicity. *Geology* **26(6)**, 515–518.

Van Dijke, J. J., van Westen, C. J., 1990. Rockfall hazard, a geomorphological application of neighbourhood analysis with ILWIS. *ITC Journal* **1**, 40–44.

Van Mantgem, P., Schwartz, M., 2003. Bark heat resistance of small trees in Californian mixed conifer forests: testing some model assumptions. *Forest Ecology and Management* **178**, 341–352.

Varnes, D. J., 1978. Slope movements: types and processes. In: Schuster, R. L., Krizek, R. J. (eds.), *Landslide analysis and control. Transportation Research Board,* Special Report 176, Washington D.C., pp. 11–33.

Vidrih, R., Ribièiè, M., Suhadolc, P., 2001. Seismogeological effects on rocks during the 12 April 1998 upper Soèa Territory earthquake (NW Slovenia). *Tectonophysics* **330 (3)**, 153–175.

Vittoz, P., Stewart, G. H., Duncan, R. P., 2001. Earthquake impacts in old-growth Nothofagus forests in New Zealand. *Journal of Vegetation Science* **12(3)**, 417–426.

W

Wasser, B., Frehner, M., 1996. *Minimale Pflegemassnahmen für Wälder mit Schutzfunktionen. Wegleitung.* Bundesamt für Umwelt, Wald und Landschaft (BUWAL), Bern.

Wegmann, M., Gudmundsson, G. H., Haeberli, W., 1998. Permafrost changes in rock walls and the retreat of Alpine glaciers: a thermal modelling approach. *Permafrost and Periglacial Processes* **9**, 27–38.

Wehrli, A., Weisberg, P.J., Schönenberger, W., Brang, P., Bugmann., H. subm. Improving the establishment of a forest patch model to predict the long-term protective effect of mountain forests. *European Journal of Forest Research*, in review.

Whalley, W. B., 1984. Rockfalls. In: Brundsen, D., Prior, D.B. (eds.), *Slope Instability*. Wiley, Chichester, pp. 217–256.

Wieczorek, G. F., Jäger, S., 1996. Triggering mechanisms and depositional rates of postglacial slope-movement processes in the Yosemite Valley. *Geomorphology* **15**, 17–31.

Wieczorek, G. F., Snyder, J. B., Waitt, R. B., Morrissey, M. M., Uhrhammer, R. A., Harp, E. L., Norris, R. D., Bursik, M. I., Finewood, L. G., 2000. Unusual July 10, 1996, rock fall at Happy Isles, Yosemite National Park, California. *Geological Society of America Bulletin* **112(1)**, 75–85.

Wieczorek, G. F., Nishenkod, S. P., Varnes, D. J., 1995. Analysis of rockfalls in the Yosemite Valley, California. In: Daemen, J. J. K., Schultz, R. A. (eds.), *Rock mechanics: Proceedings of the 35th US Symposium.* Balkema, Rotterdam, pp. 85–89.

Wiles, G. C., Calkin, P. E., Jacoby, G. C., 1996. Tree-ring analysis and Quaternary geology: Principles and recent applications. *Geomorphology* **16**, 259–272.

Wilson, B. G., Witkowski, E. T. F., 2003. Seed banks, bark thickness and change in age and size structure (1978-1999) of the African savanna tree, *Burkea africana*. *Plant Ecology* **167**, 151–162.

WSL, BUWAL (eds.), 2001. *Lothar. Der Orkan 1999. Ereignisanalyse.* Eidg. Forschungsanstalt WSL und Bundesamt für Umwelt, Wald und Landschaft BUWAL, Birmensdorf, Bern.

Wullschleger, E., 1982. Die Erfassung der Waldfunktionen. *Eidgenössische Anstalt für das forstliche Versuchswesen EAFV* **238**.

Y

Yamaguchi, D. K., 1985. Tree-ring evidence for a two-year interval between recent prehistoric eruptions of Mount St. Helens. *Geology* **13**, 554–557.

Z

Zinggeler, A., Krummenacher, B., Kienholz, H., 1991. Steinschlagsimulation in Gebirgswäldern. *Berichte und Forschungen des Geographischen Instituts der Universität Fribourg* **3**, 61-70.

Zurbriggen, J., 1952. *Täsch. Familienstatistik, Chronik und Kirche.* Buchdruckerei Tscherrig-Tröndle, Brig-Glis.

Internet sources

Air Zermatt, 2003. http://www.air-zermatt.ch/air_zermatt_new/index.php?content=00010 (as seen on 24 September 2003).

Briffa, K. R., Osborn, T. J., Schweingruber, F., Harris, I. C., Jones, P. D., Shiyatov, S. G., Vaganov, E. A., 2001b. Raw data for the low-frequency temperature variations paper cited above. ftp://ftp.ncdc.noaa.gov/pub/data/paleo/treering/reconstructions/n_hem_temp/briffa2001jgr3.txt (as seen on 31 August 2003).

CFL, 2003. http://www.cfl.scf.mcan.gc.ca/collections-cfl/ficheinsecte_e.asp?id=11213 (as seen on 10 May 2003)

Cipra, 2005. Protokoll zur Durchführung der Alpenkonvention von 1991, Bereich "Bergwald". http://www.cipra.org/d/alpenkonvention/offizielle_texte/Protokoll_d_Bergwald.pdf (as seen on 17 February 2005)

Erdas Imagine, 2005. http://www.geosystems.de/produkte/erdas_imagine/index.html (as seen on 11 March 2005)

Esri, 2003a. http://www.esri.com/software/arcgis/arcgisextensions/geostatistical/ (as seen on 14 July 2003)

– , 2003b. http://www.esri.com/software/arcgis/arcview. (as seen on 14 July 2003)

– , 2005a. http://www.esri.com/software/arcgis/arcview/index.html (as seen on 6 March 2005).

– , 2005b http://www.esri.com/software/arcgis/extensions/spatialanalyst/index.html (as seen on 11 February 2005).

Forestry Suppliers, 2005. http://www.forestry-suppliers.com/t01_pages/tt_pdf/1031_Increment.pdf (as seen on 1 March 2005)

Geology, 2005. http://geology.about.com/library/bl/blmsk64scale.htm (as seen on 18 March 2005).

Hoek, E., 1998a, Factor of safety and probability of failure. http://rockeng.utoronto.ca/hoekcorner. htm (as seen on 4 March 2005).

Hoek, E., 1998b, Analysis of rockfall hazards. http://rockeng.utoronto.ca/hoekcorner.htm (as seen on 4 March 2005).

MeteoSwiss, 2005. http://www.meteoswiss.ch/en/ (as seen on 6 March 2005)

NaiS, 2005. *Nachhaltigkeit im Schutzwald.* Report of the Swiss Forest Agency, SAEFL (working paper). http://www.gebirgswald.ch (as seen on 18 January 2005).

Quanterra, 2005. http://www.quanterra.org/guide/guide1_17.htm (as seen on 1 February 2005)

Rinntech, 2003. *LINTAB – Precision ring by ring*.http://www.rinntech.com/Products/Lintab.htm. (as seen on 31 August 2003)

Rro, 2003. http://www.rro.ch/ (as seen in the homepage of Radio Rottu Oberwallis (Rro) on 30 November 2003; texts and images are no longer available on the internet site)

Schoch, W., Heller, I., Schweingruber, F. H., Kienast, F., 2004. Wood anatomy of central European species. Online version: http://www.woodanatomy.ch (as seen on 4 March 2005).

Schwitter, 2000. *FAN-Tagung 1998. Zusammenfassung und Schlussfolgerungen. Waldwirkungen und Steinschlag.* http://www.gebirgswald.ch (as seen on 20 October 2001)

Swisstopo, 2005. http://www.swisstopo.ch/de/vd/lwn_etat.htm (as seen on 11 February 2005).

20Min, 2003. http://www.20min.ch/ (as seen in the online version of the newspaper on 5 May 2003; texts and images are no longer available on the internet site).

Unpublished sources

Baumgartner, M., 2002. *Detaillierte Ersterhebungen in einem steinschlaggeschädigtem Wald im Diemtigtal.* Diploma thesis. Geographisches Institut, Universität Bern, Bern.

Bonnard & Gardel SA, 1997. *CONSECRU – Evaluation des bassins versants en fonction de l'aménagement des cours d'eau.* Département des travaux publics du Canton du Valais, Service des Routes et des Cours d'Eau. Sion.

Gsteiger, P. 1989. *Steinschlag, Wald, Relief. Empirische Grundlagen zur Steinschlagmodellierung.* Diploma thesis. Geographisches Institut, Universität Bern, Bern.

Hopfmüller, M. W., 1997. *Datierung und räumliche Erfassung von Steinschlag- und Felssturzereignissen mit dendrochronologischen Methoden.* Diploma thesis. Institut für Geographie, Universität Regensburg, Regensburg.

Keller, F., 2003. *Kurzbericht über die Steinschlagereignisse im heissen Sommer 2003 im Bergell. Institut für Tourismus und Landschaft.* Academia Engiadina, Samedan.

Kläger, P., 2003. *Naturgefahren Stotzigwald*. Amt für Wald Kanton Uri, Altdorf.

Kühne, R., 2005. *Steinschlagsimulation in Gebirgswäldern – Validierung und Anwendung des 3D Modells ROCKYFOR in drei Testgebieten zur Analyse der Wirkung von Schutzwald.* Diploma thesis. Geographisches Institut, Universität Bern, Bern.

Lauber, T., 1995. *Bergsturz und Steinschlag im Täschgufer, Täsch.* Geologischer Bericht 95-525.1, Naters, Switzerland.

Marro, C., 1994. *Täschgufer, Westhang der Leiterspitzen (Gemeinde Täsch). Etude structu-rale et géomécanique expéditive.* CRSFA/94.35B, Sion, Switzerland.

Schneuwly, D., 2003. *500-jährige Rekonstruktion der Steinschlagfrequenz im Täschgufer anhand dendrogeomorphologischer Methoden.* Diploma thesis. University of Fribourg, Fribourg, Switzerland.

Stand Montafon, 1990. *Forest Inventory Results.* Internal Report. Stand Montafon Forstfonds, Schruns, Austria.

Stoffel, M., 1996. *Der Felssturz im Wassergraben.* Research report. Departement für Geowissenschaften, Geographie, Universität Fribourg.

– , 1999. *Klimawandel als Herausforderung für die Raumplanung der Vispertäler. NF-Projekt 4031-43826 des Nationalen Forschungsprogrammes (Nfp) 31 „Klimaänderungen und Naturkatastrophen".* Diploma thesis. Departement für Geowissenschaften, Geographie, Universität Fribourg.

Thali, U., 1997. *Waldbauprojekt Stotzigwald, Gurtnellen.* Ingenieurbüro U. Thali, Göschenen.

Wicht, J. M., Joris, C. L., 1985. *Felssturz Grosse Wang – Taeschbaerg. Geologischer Vorbericht.* Mandat 357. Odilo Schmid – Büro für beratende Geologie & Bureau d'études géotechniques Félicien Clavien, Brig and Sion.

Zinggeler, A., 1989. *Steinschlagsimulation in Gebirgswäldern. Modellierung der relevanten Teilprozesse.* Diploma thesis. Geographisches Institut, Universität Bern, Bern.

*****

Curriculum vitae

Markus Stoffel
Egghölzlistrasse 65
3006 Bern

born on April 28, 1974 in Visp, Switzerland
citizen of Visperterminen (VS)

1981-1989	Primary and secondary school in Visp, Valais.
1989-1994	Kollegium Spiritus Sanctus, Brig. Matura Typus B
1994-1999	Studies of Geography at the Department of Geosciences, University of Fribourg (dipl. Geogr.). Diploma thesis (M.Sc.): "Klimawandel als Herausforderung für die Raumplanung der Vispertäler" under the supervision of Prof. M. Monbaron.
1997-1999	Undergraduate assistant in the group of Prof. M. Monbaron, at the Department of Geosciences, Geography, University of Fribourg (teaching, excursions, fieldtrips).
1998-2003	Studies of Media and Communication Sciences at the Institute of Journalism and Communication Sciences, University of Fribourg (lic. phil. I). Licenciate thesis (M.Sc.): "Der Umgang der Schweizer Zeitungen mit Klimawandel und Naturkatastrophen" under the supervision of Prof. L. Bosshart and PD L. Schlapp
2000-2005	Diploma assistant, scientific collaborator and PhD student in the group of Prof. M. Monbaron, at the Department of Geosciences, Geography, University of Fribourg (teaching, guidance and care of geography students within the scope of their diploma thesis, excursions, fieldtrips).

PRINCIPAL PUBLICATIONS

Stoffel, M., Lièvre, I., Monbaron, M., Perret, S., 2005a. Seasonal timing of rockfall activity on a forested slope at Täschgufer (Swiss Alps) – a dendrochronological approach. *Zeitschrift für Geomorphologie* **49(1)**, 89–106.

Stoffel, M., Schneuwly, D., Bollschweiler, M., Lièvre, I., Delaloye, R., Myint, M., Monbaron, M., 2005b. Analyzing rockfall activity (1600-2002) in a protection forest – a case study using dendrogeomorphology. *Geomorphology* **68(3-4)**, 224–241.

Stoffel, M., Lièvre, I., Conus, D., Grichting, M., Raetzo, H., Gärtner, H., Monbaron, M., 2005c. 400 years of debris flow activity and triggering weather conditions: Ritigraben VS, Switzerland. *Arctic, Antarctic and Alpine Research* **37(3)**, 387–395.

Stoffel, M., 2005. A review of studies dealing with tree rings and rockfall activity: Where and how can dendrogeomorphology help natural hazard research? *Natural Hazards*, in press.

Stoffel, M., Perret, S., subm. Reconstructing past rockfall activity with tree rings: some methodological considerations. *Dendrochronologia*, in review.

Stoffel, M., Wehrli, A., Kühne, R., Dorren, L. K. A., Perret, S., Kienholz, H., 2005. Quantifying the protective effect of mountain forests against rockfall using a 3D simulation model. *Forest Ecology and Management*, in press.

Perret, S., Stoffel, M., Kienholz, H., 2005. Spatial and temporal rockfall activity in a forest stand in the Swiss Prealps – a dendrogeomorphological case study. *Geomorphology*, in press.

OTHER PUBLICATIONS

Bollschweiler, M., Stoffel, M., Schneuwly, D., 2005. Entwicklung der Murrinnen im Täschgufer seit 1936. *wasser, energie luft* **97(7–8)**, 218–223.

Bloetzer, W., Egli, T., Petrascheck, A., Sauter, J., Stoffel, M., 1998. *Klimaänderungen und Naturgefahren in der Raumplanung.* Synthesebericht NFP31. vdf Zürich, 200 pp. (ISBN 3-7281261-0-1)

Cabernard, V., Stoffel, M., Monbaron, M., 2004. Der Fidazer Felssturz von 1939: Analyse und Simulation. *Mitteilungen der VAW* **184**: 1–12.

Gärtner, H., Stoffel, M., 2002. Detailed mapping and dendrogeomorphological analysis of a debris flow torrent in Switzerland. *Proceedings INTERPRAEVENT 2002*: 199–207.

Stoffel, M., 2000. Impacts of climate change and natural hazards on land use in the Saas and Zermatt Valleys (Switzerland). In: Singh, R. B., Fox, J., Himiyama, Y., (eds.), *Land Use and Cover Change.* Science Publishers Inc., Enfield, 269–277.

Stoffel, M., 2005. Assessing the vertical distribution and visibility of rockfall scars in trees. *Schweizerische Zeitschrift für Forstwesen* **156(6)**, 195–199.

Stoffel, M., Monbaron, M., Maselli, D., 2002a. *Mountains and Lowlands: Enemies or Partners? Example of the High Atlas, Morocco. A contribution to the "Johannesburg Summit 2002 – The World Summit on Sustainable Development" and the International "Year of Mountains 2002".* Schlaefli & Maurer AG, Interlaken, 32 pp. (ISBN 3-9522536-2-6)

Stoffel, M., Monbaron, M., Maselli, D., 2002b. *Montagne et plaines: adversaires ou partenaires? Exemple du Haut Atlas, Maroc. Une contribution au "Sommet de Johannesburg 2002 – Sommet mondial sur le développement durable" et à l' "Année internationale de la montagne 2002".* Schlaefli & Maurer AG, Interlaken, 32 pp. (ISBN 3-9522536-1-8)

Stoffel, M., Gärtner, H., Lièvre, I., Monbaron, M., 2003. Comparison of reconstructed debris flow event years (Ritigraben, Switzerland) and existing flooding data in neighboring rivers. In: Rickenmann D. & Chen, C. (eds.): *Debris Flow Hazard Mitigation: Mechanics, Prediction, and Assessment* **1**, 243–253.

Stoffel, M., Lièvre, I., Conus, D., Grichting, M., Gärtner, H., Monbaron, M., 2004. Rekonstruktion der Muraktivität im Ritigraben (VS) und Vergleich mit Chronikdaten benachbarter Gewässer. *Mitteilungen der VAW* **184**, 25–40.

*****